

7.5

7-02-125-09
DWW-2002-106

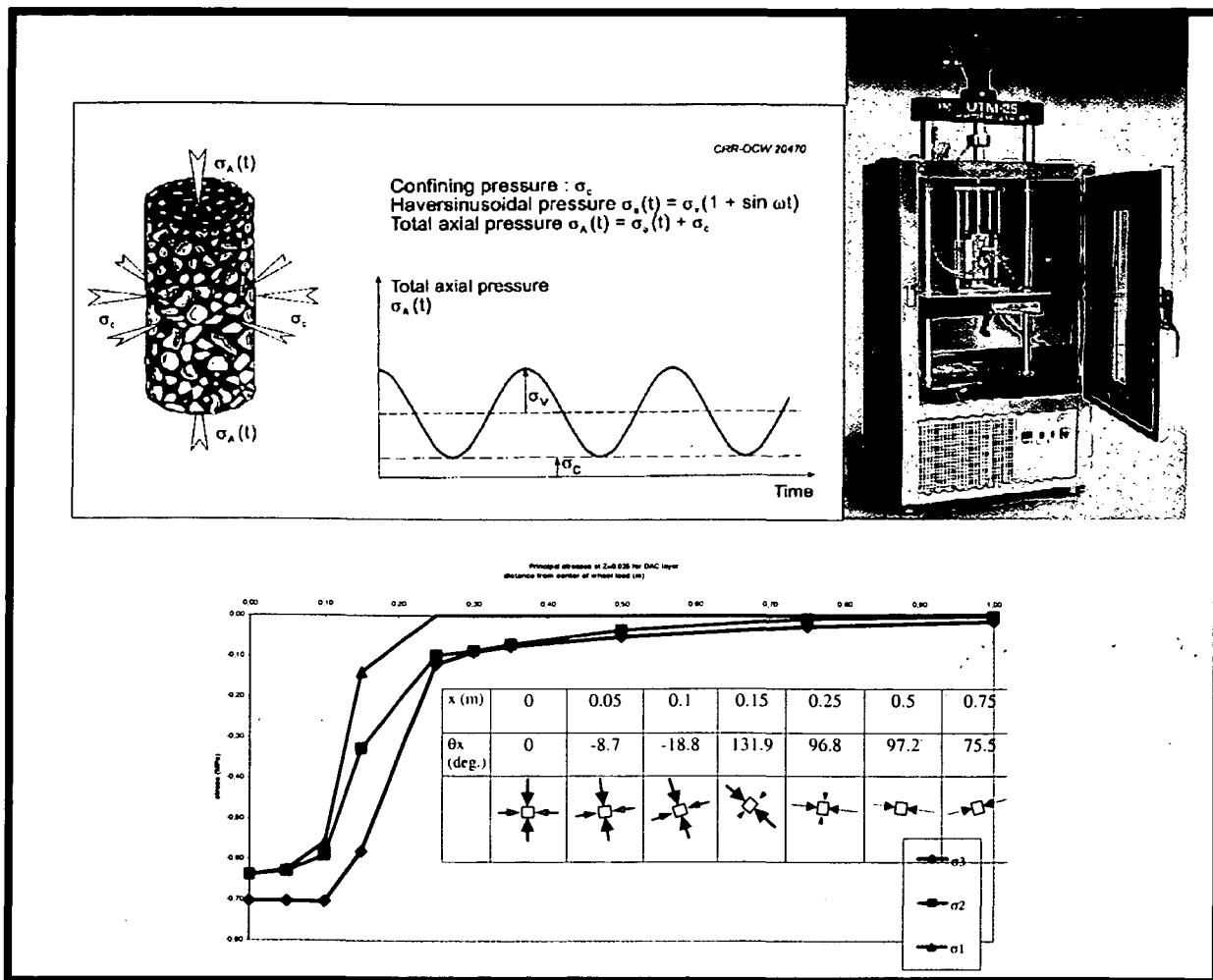
NOV 2002

Loading Conditions in the Triaxial Test for the Characterisation of the Resistance to Permanent Deformation of Asphalt

NOV 2002

August 2002

Hailu Shume



B I D O C
 (bibliotheek en documentatie)



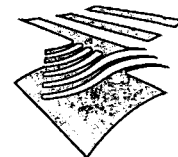
Dienst Weg- en Waterbouwkunde
 Postbus 5044, 2600 GA DELFT
 Tel. 015 - 2518 363/364

Rapport
 in opdracht van
DWW

28 (3)

TU Delft
 Delft University of Technology

Faculty of Civil Engineering and Geosciences



RWS-DWW

7.5 - 28
(3)

Final Report

**Loading Conditions in the Triaxial Test for the
Characterisation of the Resistance to Permanent
Deformation of Asphalt Mixtures**

**Rapport
in opdracht van
DWW**

**RWS, Dienst Weg- en
Waterbouwkunde (DWW) is
participant**

By: Hailu Shume
August 2002

Contactperson:

Prof.dr.ir. A.A.A. Molenaar

ing. B. Oosterbaan


TU Delft
Delft University of Technology



RWS-DWW

Summary

Permanent deformation (rutting) is among the major causes of road maintenance costs in the Netherlands. Due to the sharp increase in truck traffic, introduction of new tyre concepts and European regulations, it is expected that permanent deformation might become more important in the near future than it is currently. By studying the permanent deformation characteristics of a pavement material and development of rutting prediction models one can set permanent deformation related specifications. These permanent deformation related specifications can be used by contractors and consultants to control the degree of rutting.

With respect to characterisation of resistance to permanent deformation of asphalt mixtures, a study on loading conditions for the triaxial test has been conducted using the BISAR program. The study begins by making an insight of the triaxial test through a literature review; and performs stress analysis for standard Dutch pavement structures using the BISAR program, applying three kinds of loading arrangements. The variation of temperature and stiffness property of the pavement materials was considered by dividing the DAC and STAC layers into sublayers. From the BISAR outputs the variation of the principal stresses at each stress analysis point has been analysed.

Through the BISAR analysis the compressive, tensile and shear stresses in the points of interest are identified with respect to distance from load centre and depth of stress point by magnitude and direction. By plotting the principal stresses on the Mohr circle the stress combinations for the triaxial test are selected for DAC and STAC layers.

The study discusses the simulation of the stress conditions into the triaxial test. It is observed that:

- a. rotation of principal stresses in the reality is not considered in the triaxial test due to difficulty in rotation of specimens;
- b. the pulse time in the lab is longer than the reality;
- c. the load pulse in the reality is a half-sine curve than a block which is commonly used in the lab;
- d. it is not only the vertical stresses but the horizontal stresses also vary with distance to load centre.

Finally, it is concluded that without significant modification of the triaxial test, it will be difficult to model accurately the permanent deformation behaviour of asphalt mixes. However, the triaxial test in its current shape is useful in ranking of asphalt mixtures.

Acknowledgement

I would like to express my sincere gratitude for the valuable supervision and contribution during this study: to Prof. A.A.A. Molenaar, Ir. M.F.C. van de Ven and Ir. S.M.J.G. Erkens. I am grateful for their constructive suggestions and guidance. I would also like to thank Dr. R. Hofman, Ir. L.J.M. Houben, Ir. A.E. van Dommelen, Ir. B. Oostrebaan and other IL staff of DWW for their direct and indirect supports. God bless you all.

Table of Contents

<u>Contents</u>	<u>Pages</u>
Summary	i
Acknowledgement	ii
Table of Contents	iii
List of Figures	v
List of Tables	vi
1 INTRODUCTION	1
1.1 GENERAL	1
1.2 BACKGROUND	2
1.3 OBJECTIVES	2
1.4 METHODOLOGY	3
2 LITERATURE REVIEW	4
2.1 FLEXIBLE PAVEMENT DESIGN	4
2.1.1 <i>Empirical design</i>	4
2.1.2 <i>Mechanistic design</i>	4
2.2 VISCO-ELASTIC BEHAVIOUR OF PAVEMENT	5
2.3 PERMANENT DEFORMATION TESTING	6
2.4 TRIAXIAL TEST	6
2.4.1 <i>Stresses in triaxial test</i>	6
2.4.2 <i>Factors affecting triaxial test</i>	8
2.5 STRESSES IN AN ELASTIC LAYERED SYSTEM	14
2.6 CONCLUSIONS	15
3 STRESS ANALYSIS BY BISAR	16
3.1 PAVEMENT STRUCTURE	16
3.1.1 <i>Pavement structures in Netherlands</i>	16
3.2 WHEEL LOADS	17
3.2.1 <i>Simple super single</i>	17
3.2.2 <i>Double wheel</i>	17
3.2.3 <i>Extended Super single</i>	18
3.3 ASPHALT CONCRETE CHARACTERISTICS	19
3.3.1 <i>Volumetric compositions</i>	19
3.4 TEMPERATURE DISTRIBUTION IN PAVEMENT	20
3.5 LOADING TIME	27
3.6 POISSON'S RATIO	27
3.7 MIX STIFFNESS	28
3.7.1 <i>Mix stiffness for Asphalt concrete</i>	28
3.7.2 <i>Subgrade modulus</i>	29
3.7.3 <i>Base modulus</i>	29
3.8 STRESS ANALYSIS BY BISAR	29
3.8.1 <i>BISAR inputs</i>	29
3.8.2 <i>Co-ordinate system in BISAR</i>	31
3.8.3 <i>Strategy of analysis</i>	31
3.8.4 <i>Stress distribution</i>	31
3.8.5 <i>Effect of thickness of structure on stresses</i>	37

3.8.6	<i>Re-calculation of stresses</i>	38
3.9	STRESS CONDITIONS FOR TRIAXIAL TEST	42
3.9.1	<i>Stress combinations</i>	42
3.9.2	<i>Rotation of stresses</i>	43
3.9.3	<i>Stress pulse time</i>	48
3.10	CONCLUSIONS	49
4	REFERENCES	50

List of Tables

TABLE 2-1: SPECIMEN SIZE EFFECTS..... 12

TABLE 2-2: COORDINATES (R, Z) OF THE POINTS FOR MAXIMUM PRINCIPAL AND SHEAR STRESSES ... 15

TABLE 3-1: EXTENDED SUPER SINGLE LOAD 18

TABLE 3-2: MIX COMPOSITIONS 19

TABLE 3-3: AGGREGATE AND BITUMEN PROPERTIES 19

TABLE 3-4: VOLUMETRIC COMPOSITIONS 20

TABLE 3-5: PULSE TIMES 40

TABLE 3-6: SUMMARY OF BISAR INPUTS FOR SECOND ROUND.....40

TABLE 3-7: SELECTED STRESS COMBINATIONS..... 43

TABLE 3-8: SELECTED STRESS COMBINATIONS.....47

List of Figures

FIGURE 1-1: FLOW CHART.....	3
FIGURE 2-1: VISCO ELASTIC BEHAVIOUR OF AN ASPHALTIC MATERIAL	5
FIGURE 2-2: RHEOLOGICAL MODEL.....	5
FIGURE 2-3: STRESS CONDITIONS IN HAVERSINE LOADING	7
FIGURE 2-4: STRESSES IN BLOCK-PULSE LOADING	7
FIGURE 2-5: TYPICAL CREEP CURVES FOR DAC.....	9
FIGURE 2-6: CREEP CURVES WITH CONFINING STRESS AND VERTICAL STRESS.....	10
FIGURE 2-7: FRICTION REDUCTION TESTS.....	13
FIGURE 2-8: LINES OF EQUAL PRINCIPAL STRESS AS % OF UNIFORMLY DISTRIBUTE LOAD.....	14
FIGURE 3-1: EXTENDED SUPERSINGLE LOAD.....	18
FIGURE 3-2: PAVEMENT TEMPERATURE ESTIMATION BY SHRP METHOD.....	22
FIGURE 3-3: TEMPERATURE DISTRIBUTION IN PAVEMENT.....	23
FIGURE 3-4: PAVEMENT TEMPERATURE BY BELLS3 METHOD.....	24
FIGURE 3-5: COMPARISON OF THE DIFFERENT METHODS WITH MEASUREMENTS.....	25
FIGURE 3-6A: PAVEMENT SURFACE TEMPERATURE BY MEVA-3 TU DELFT, JULY 1989.....	26
FIGURE 3-6B: AIR TEMPERATURE ZESTIENHOVEN, EELDE, DEELEN, JULY 1989	26
FIGURE 3-7: LOADING TIME.....	27
FIGURE 3-8: POISSON'S RATIO WITH FREQUENCY AND TEMPERATURE.....	28
FIGURE 3-9: VERTICAL STRESS DUE TO EXTENDED SUPER SINGLE LOAD.....	32
FIGURE 3-10: VERTICAL STRESS DUE TO SIMPLE SUPERSINGLE LOAD.....	32
FIGURE 3-11: VERTICAL STRESS DUE TO DOUBLE WHEEL LOAD.....	33
FIGURE 3-12: TRANSVERSE (TANGENTIAL) STRESS DUE TO EXTENDED SUPERSINGLE LOAD	33
FIGURE 3-13: LONGITUDINAL (RADIAL) STRESS DUE TO EXTENDED SUPER SINGLE LOAD.....	34
FIGURE 3-13B: PRINCIPAL STRESSES.....	34
FIGURE 3-14: PRINCIPAL STRESS RATIOS	35
FIGURE 3-15: DEVIATOR STRESSES DUE TO WHEEL LOAD TYPES.....	35
FIGURE 3-16: PRINCIPAL STRESS RATIOS FOR EXTENDED SUPER SINGLE LOAD.....	36
FIGURE 3-17: PRINCIPAL STRESS RATIOS FOR DOUBLE WHEEL LOAD.....	36
FIGURE 3-18: PRINCIPAL STRESS RATIOS FOR SIMPLE SUPERSINGLE LOAD.....	37
FIGURE 3-19: PRINCIPAL STRESS RATIOS SIMPLE SUPER SINGLE LOAD STANDARD I.....	37
FIGURE 3-20: PRINCIPAL STRESS RATIOS SIMPLE SUPER SINGLE LOAD STANDARD II	38
FIGURE 3-21: PRINCIPAL STRESS RATIOS SIMPLE SUPER SINGLE LOAD STANDARD III	38
FIGURE 3-22: LOADING RADIUS.....	39
FIGURE 3-23: LOADING RADIUS.....	39
FIGURE 3-24: PULSE TIME ESTIMATION	40
FIGURE 3-25: VERTICAL STRESSES, SIMPLE SUPERSINGLE LOAD 1 ST ANALYSIS.....	41
FIGURE 3-26: VERTICAL STRESSES SIMPLE SUPER SINGLE LOAD, 2 ND ANALYSIS	41
FIGURE 3-27: PRINCIPAL STRESSES FOR DAC	42
FIGURE 3-28: PRINCIPAL STRESSES FOR STAC	43
FIGURE 3-29: PRINCIPAL STRESSES AND THEIR ROTATION ANGLE.....	44
FIGURE 3-30: STRESSES FOR DAC LAYER AT DEPTH OF 25MM.....	45
FIGURE 3-31: PRINCIPAL STRESSES FOR STAC.....	45
FIGURE 3-32: STRESSES IN STAC LAYER.....	46
FIGURE 3-33: COMPARISON OF DEVIATOR STRESSES FOR DAC	46
FIGURE 3-34: COMPARISON OF DEVIATOR STRESSES FOR STAC.....	4
FIGURE 3-35: VERTICAL AND RADIAL STRESSES AT Z=0.025.....	4

1 Introduction

1.1 General

Road transportation is an important aspect of the Dutch economy. 80% of the freight and 90% of the people are transported via roads [36]. As such, maintenance of the major highways in the Netherlands should interrupt traffic flow as little as possible. Together with the high costs of pavement maintenance, this results in a demand for low-maintenance roads. To provide low maintenance and good performing roads, one has to characterise and control the various distress types.

Permanent deformation (rutting) is among the types of distresses that occur in flexible pavements. Rutting can be predicted by estimating the permanent deformation resistance of the material in each layer of the pavement. The accuracy of the prediction depends on the quality of the models that are used to characterise the response and performance of asphalt mixtures. By studying the permanent deformation characteristics of a pavement material and development of rutting prediction models one can set permanent deformation related specifications. These permanent deformation related specifications can be used by contractors and consultants to control the degree of rutting.

In the past, flexible pavement design approaches to control permanent deformations (rutting) were:

- **Empirical design procedures:** They assume that primary source of deformation occurs in the subgrade. Deformations are controlled by adjusting the overlying pavement thickness and material quality to reduce the resulting subgrade strain to a level that yields permanent deformation below the allowable limit. These designs are based on material characterisation by means of empirical tests, for example the CBR test. These methods even though they are easy to use, however, cannot be used for conditions other than for which they have been developed [26].
- **Mechanistic design approaches:** They are based on the fundamental concept that the plastic strain is related to the elastic strain and the number of load repetitions. The permanent deformation of the pavement is obtained as a summation of the permanent deformation of the sub layers in which the structure is divided. This approach is used, for example in the VESYS method. This method is more rational, can predict over a wider range of conditions and provides the cumulative deformation of the entire pavement. However, the methods are not refined to the point so that they can be applied into more practical solutions with a sufficient level of confidence. [15,26].

Road authorities realise that a good performance of a pavement is what they really desire instead of asphalt mixtures that fulfil certain requirements with respect to their recipe, which in itself is not a guarantee for a good performance. With respect to permanent deformation this implies amongst others that the test procedures need to be developed which, together with adequate models, allow to design mixtures with a light resistance to rutting. One of the important aspects of such test procedures are the loading conditions that need to be used to characterise the asphalt mixture. The determination of the load conditions to be used in the triaxial tests for the characterisation of the resistance to permanent deformation of asphalt mixtures, is the topic of the report.

1.2 Background

Permanent deformation characterisation using the triaxial test is a means for mechanistic flexible pavement design as well as for developing performance based specifications. By developing rutting prediction models which can utilise results of triaxial tests, specifications for different pavement layer characteristics can be set. The triaxial test has been used in the past for the evaluation of mechanical properties of soils and granular materials [11]. However, the use of triaxial test for asphalt mixes, which have analogous composition to soils and granular materials, is slow in acceptance due to the complexity of the test and lack of standard procedures. There is limited published material on the use of the triaxial test for analysing mechanical properties of asphalt concrete mixes [11].

Currently, there is a draft European Standard (EN) for the triaxial cyclic compression test for bituminous mixtures, prEN 12967-25B. It is based on French, British and Belgian and Dutch experiences [20]. However, the draft standard procedures need exercising by users through further research and applications to testing conditions before it is utilised as a standard. This implies for example that the question which stress combinations should be used to characterise asphalt mixtures should be solved. Is only one combination of vertical and horizontal stress sufficient, or should several combinations be used. Are the stress levels to be applied independent of the type of structures or should they be related to the position in the structure at which the material is to be used. With respect to temperature one should ask the question whether the test should be done at only one temperature and if so, should this temperature be the same in all structures independent of the position in the structure at which the mixture under consideration is to be applied.

In addition, the sensitivity of the triaxial test on asphalt mixes to the boundary conditions needs further examining. This has been observed from a recent study on the effect of friction reduction methods used at different laboratories. The observed results using various friction reduction methods showed different trends of the creep curves. This clearly shows the need for specification of new test conditions [23].

1.3 Objectives

The objectives of this study is mainly:

- making an insight of the triaxial test through a literature review;
- to analyse the stress conditions in a few Dutch standard pavement structures by using the BISAR computer programme; and
- to obtain more insight in the behaviour of asphalt mixtures at high temperatures by means of the triaxial test.

1.4 Methodology

The method of the study is shown on a flow chart in figure 1-1 .

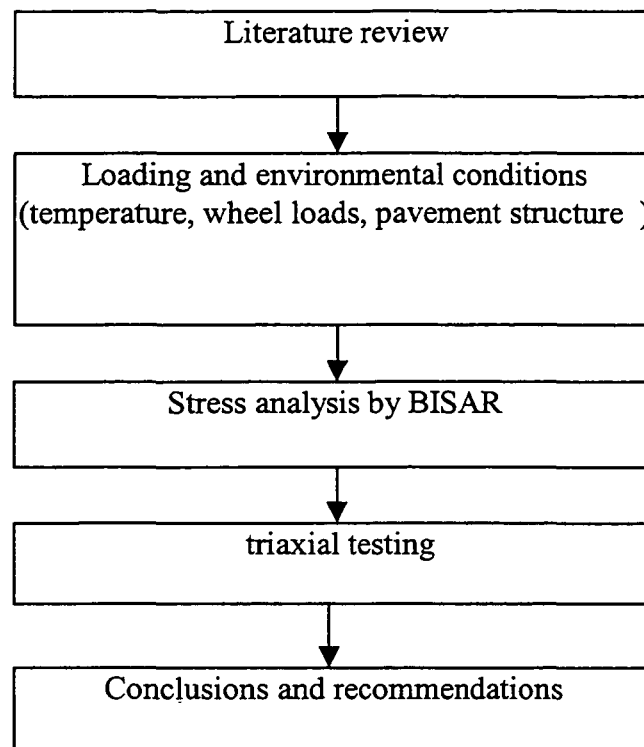


Figure 1-1 : Flow Chart

2 Literature review

In this literature review, a background study on flexible pavement design process and visco-elastic behaviour of asphalt is made. The triaxial test as means of permanent deformation characterisation is discussed; factors that may affect the triaxial test are reviewed. Problems are identified from previous studies.

2.1 *Flexible pavement design*

In the Netherlands, flexible pavements for the main highways consist of a number of asphalt layers with a total thickness up to approximately 300 mm built over layers of granular base and subbase, which rest upon a subgrade to protect the subgrade from being overstressed. A flexible pavement is required to have the following qualities:

- resistance to distress resulting from repeated load applications,
- non-skidding and less noisy riding surface,
- water proofing to the underlying layers.

Flexible pavement design involves structural design and material characterisation to fulfil the above mentioned requirements. Empirical and mechanistic pavement design procedures have been practised in the past as explained hereafter.

2.1.1 Empirical design

Empirical design methods are developed from long term experiences with the performance of in-service roads, supplemented from studies of specially constructed test pavements. Empirical design procedures are developed from empirical correlations of material properties to pavement characteristics under loading. The CBR method, AASHTO Design Guide for design of pavement structures, TRL Road Note 29 and TRL Road Note 31 are good examples of empirical design procedures [4,26]. The major advantage of empirical design procedures is that they are known widely as design tools. However, they can not be used to predict outside the conditions for which they have been developed. They are limited to a set of loading and environmental conditions, construction materials and construction techniques. Furthermore, an empirical pavement design is not based on a real understanding of pavement behaviour (analysis of stress and strain). For these reasons, empirical methods are not applied in the Netherlands.

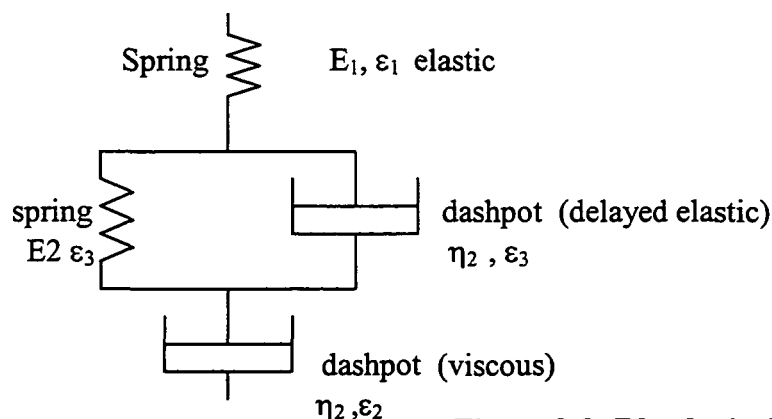
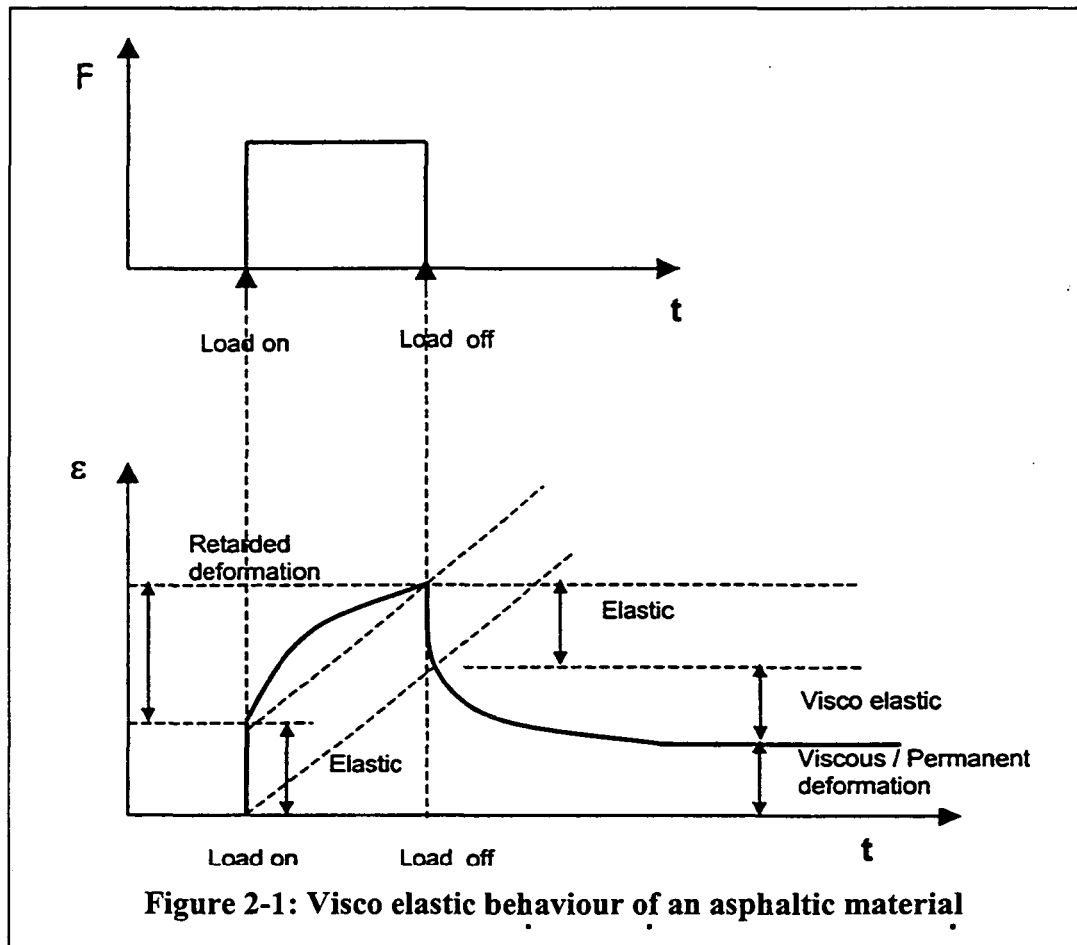
2.1.2 Mechanistic design

The continuous increase in traffic loads and tyre pressure, and the need to use new pavement materials urged the development of mechanistic or analytical design procedures. These methods are required to be adaptable and comprehensive in their nature. Mechanistic design methods are based on the fundamental analysis of pavement response and behaviour due to traffic loads and environmental conditions. Stress, strain and displacements of pavement layers are analysed through linear elastic multi layer theory or visco-elastic analysis. Several design guides and computer programs have been developed for mechanistic design procedures. The Shell Design manual, and BISAR, KENLAYER and VERODAD computer programs are among the best known examples [4, 24]. The thickness design manual used in the Netherlands for motorways is an example of a method based on a mechanistic approach. The method concentrates on limiting the tensile strain at the bottom of the asphalt layer in order to limit the chance on fatigue cracking. Subgrade deformation is not an issue because, as stated above, the pavement structures in the Netherlands for motorways are rather thick. Although the method has proven to be successful, one of the disadvantages

is that it does not take into account permanent deformation of the asphalt mixtures used. In fact the resistance to permanent deformation is controlled by means of the currently used recipe type of specifications.

2.2 Visco-elastic Behaviour of pavement

Asphalt concrete is a non-linear visco-elastic material. Its behaviour depends on temperature and loading time. At low temperature and short loading times it behaves as linear elastic material and at high temperatures and long loading times it shows viscous behaviour. This behaviour is well represented by visco-elastic diagram and rheological model as shown in figures 2-1 and 2-2.



2.3 Permanent Deformation Testing

Due to the sharp increase in truck traffic, introduction of new tire concepts and European regulations, it is expected that permanent deformation might become more important in the near future than it is currently [4]. Rutting is a significant cause of the road maintenance costs in the Netherlands [36].

Tests to determine the permanent deformation of pavement materials include:

- the incremental static test,
- the creep test,
- the triaxial test,
- the wheel track test,
- the Lintrack analysis.

As the purpose of this study is mainly to focus on triaxial testing the advantages and disadvantages of the other tests with respect to simulating the real field conditions are not included at this stage.

2.4 Triaxial test

The cyclic load triaxial test is a laboratory test performed on cylindrical specimens in order to determine the permanent deformation characteristics of asphalt mixes under various loading and temperature conditions. It is an axi-symmetric apparatus in which a cylindrical, laboratory compacted or field cored specimen is subjected to two independently controlled stress components. The resulting non recoverable axial strain is used as an indication of the resistance of the material to permanent deformation (rutting).

2.4.1 Stresses in triaxial test

Haversine or block-pulse cyclic loading can be used for axial stresses in triaxial test. Existing literature shows that block-pulse and haversine cyclic stresses are commonly used [2,7,28]. The draft European Standard also allows the use of a haversinusoidal pressure or a block-pulse pressure [20].

2.4.1.1 The haversine

The haversinusoidal cyclic loading is shown in figure 2-3. A vertical stress (σ_1), is applied through loading platen at the top of the specimen. A horizontal stress (σ_2, σ_3), is applied through an all around confining fluid or air pressure.

$$p = (\sigma_A(t) + 2\sigma_c)/3 = (\sigma_1 + \sigma_2 + \sigma_3)/3$$

$$q = \sigma_a(t) = \sigma_1 - \sigma_3, \sigma_2 = \sigma_3$$

Where:

p =bulk stress (MPa)

q = deviator stress (MPa)

$\sigma_1 = \sigma_A(t)$ = vertical stress(MPa)

$\sigma_2 = \sigma_3 = \sigma_c$ = horizontal confining stress(MPa)

CRR-OCW 20470

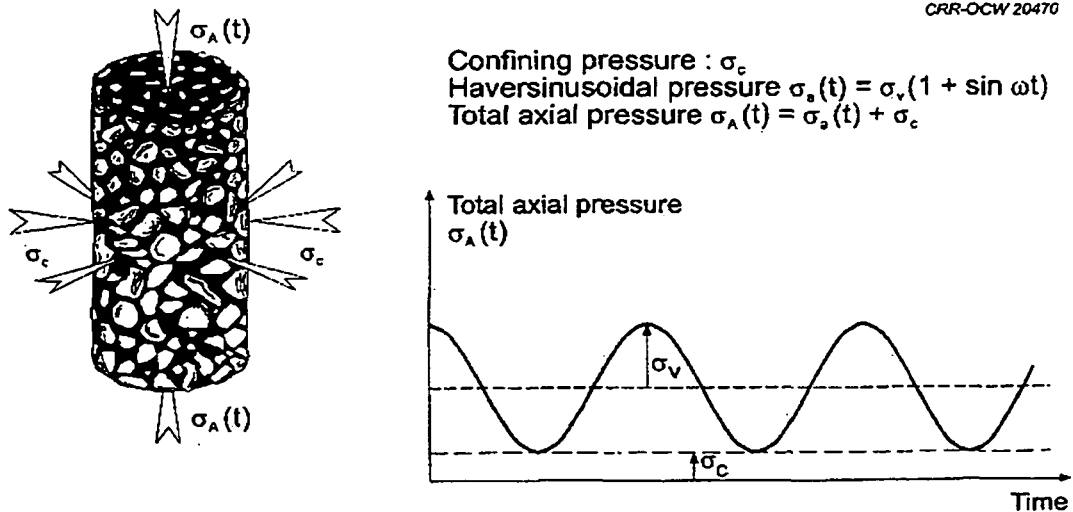


Figure 2-3: Stress conditions in haversine loading [20]

2.4.1.2 Block-Pulse load

In the block-pulse method an axial cyclic stress σ_B (block-pulse) is applied for a pulse duration of T_1 and a rest period of T_0 , as shown in fig 2-4. Furthermore an all around confining stress σ_c is applied.

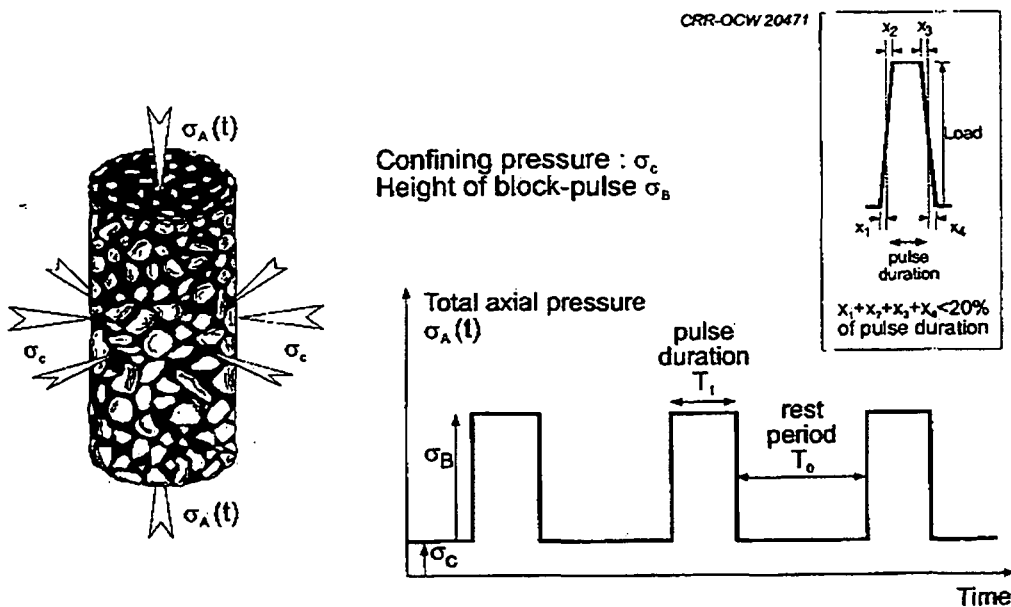


Figure 2-4: Stresses in block-pulse loading[20]

2.4.2 Factors affecting triaxial test

Deformation characteristics of different types of pavement materials are dependent on the loading conditions (stress combinations), temperature, mix composition, specimen size, friction reduction system and LVDT arrangement. Researches were carried out in the past to characterise the permanent deformation behaviour of asphalt mixes by means of repeated load triaxial test. In this section the influence factors mentioned above will be discussed in more detail.

2.4.2.1 Stress combinations

Permanent deformation studies through cyclic triaxial testing on DAC, OAC, STAC were done within the LINTRACK laboratory project at the TU Delft [7]. Specimens were obtained from cores of LINTRACK test sections. The tests were conducted with the UTM equipment of the Road and Railway Research Laboratory of the TU Delft. A constant horizontal confining stress and cyclic vertical stress having haversine load pulse with a duration of 0.2 sec followed by a rest period of 0.8 sec were used. Dual confining membrane was used to cover the samples. The end surfaces of the specimens were treated with a *coat of liquid soap-plastic foil- liquid soap* to reduce friction and reduce barrelling. A vertical stress range of 0.4 to 1.2 MPa and a horizontal stress range of 0.1 to 0.6 MPa were applied at 40 °C and 50 °C [7]. The criteria set for termination of the test was 7200 load cycles or 8 % of cumulative strain. Generally, an increase in creep deformation was observed from the study as the vertical stress increased with constant horizontal confining stress. However, in some cases, as is seen from figure 2-5, the deformation does not increase as the vertical pressure increases from 0.55 to 0.70 MPa with constant horizontal confining stress of 0.10 MPa [7]. This was also indicated by Parajuli [24], he mentioned that , perhaps due to initial densification, increasing vertical stress has decreasing effect on permanent deformation up to a certain limit of vertical stress for constant confining stress at 30 °C and 40 °C on DAC.

A big disadvantage of the triaxial test is that the direction of the principal stresses remain constant (horizontal and vertical) through out the duration of the test. In reality however this condition is only true if the stresses are considered under the center of the wheel load. During the passage of a wheel , the principal stresses will not only vary in magnitude but also in direction. This rotation of the direction of the principal stresses can not be simulated in a triaxial test. Section 3-9 discusses this in more detail.

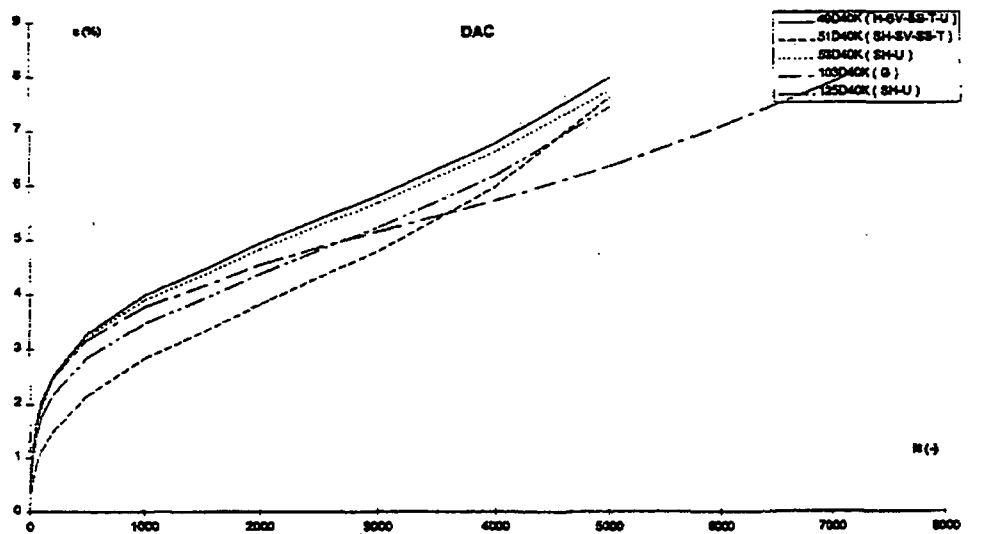
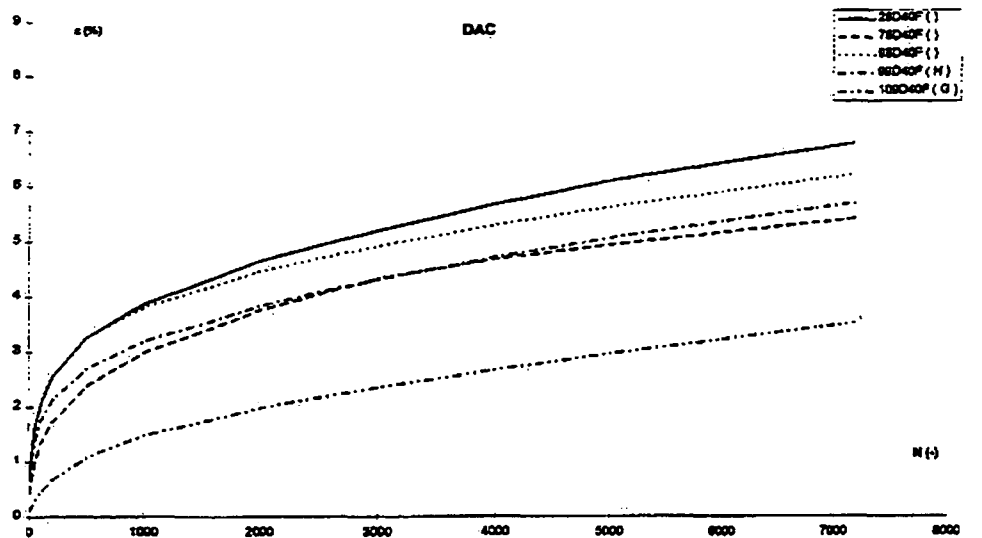


Figure 2-5: Typical creep curves for DAC[7]

Another study, done by Francken [19] shows similar relationships of permanent deformation with confining stress and variable vertical stress. This is as shown in fig 2-6.

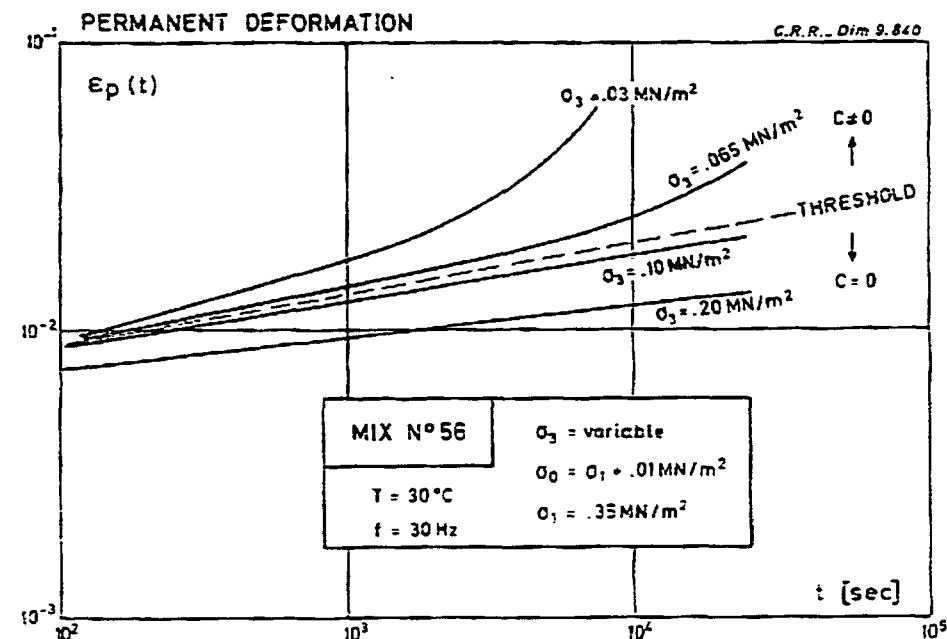
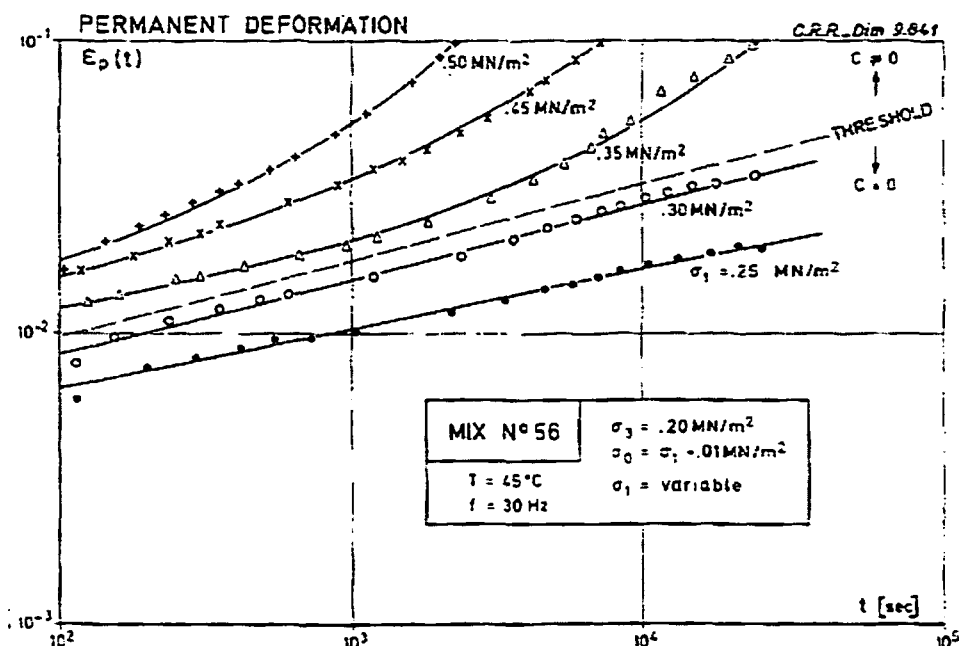
Creep curves for different values of the confining stress σ_3 .Creep curves for different values of the amplitude σ_1 .

Figure 2-6: Creep curves with confining stress and vertical stress[19]

The creep curves in fig 2-6 a show linear and parabolic relationship between deformation and loading time.

2.4.2.2 Temperature

The surface and internal temperature of asphalt concrete in a pavement vary depending on the air temperature, cloudiness, solar radiation, wind velocity and thermal characteristics of the pavement[9,30]. Further evaluation of the temperature distribution in the pavement shows that the temperature decreases with increasing depth. It is also shown in another study [10] that the stiffness of the asphalt mix decreases as the temperature increases.

To analyse the effect of temperature on the pavement distress the pavement temperature has to be simulated in the triaxial test by maintaining the temperature of the specimen at the temperature level of interest. This is monitored by keeping the specimen and cell temperature to the test condition temperature.

2.4.2.3 Mix properties

An asphalt mix is composed of granular material, bitumen, filler and voids. The properties of an asphalt mix are dependent on the mix composition. Different mixes show variability in resistance to deformation. A study done by Georgia Institute of Technology [8] to evaluate the effects of mix gradation on the rutting resistance of asphalt mixes using a repetitive wheel load test shows that aggregate gradation can significantly affect the rutting potential of asphalt mixes. In that study six aggregate gradations from three aggregate sources were selected and studied for their effect on rutting resistance. The maximum size of aggregates studied were 1 to 1 ½ in. Results of the study show that having the same content of fines, higher sizes of aggregates show less rutting.

Mix composition effects on the rutting resistance of OAC, STAC and DAC from cyclic triaxial loading test were studied in LINTRACK project [7]. Relationships between deformation and material properties show a high scatter between predicted and measured results. The study was not able to indicate a clear relationship between various characteristics of the mixes and test results. It was shown that a higher bitumen content and a high degree of filling results in high permanent deformation ; however, this has not been always the case. In any case however it was clear that use of a softer bitumen(higher penetration) resulted in a larger permanent deformation.

Higher air void contents in asphalt mixtures appear to have reducing effect on the permanent deformation characteristics of asphalt mixes. This was observed by researches of the Belgian Centre for Road Research. They also found that a high bitumen content has an increasing effect on permanent deformation. The positive effect of a higher void content should not be misunderstood. This is because a higher void content can be reached by decreasing the compaction effort or by decreasing the amount of bitumen in the voids of the aggregate skeleton. In order to have an asphalt mixture with a sufficient resistance to permanent deformation, good compaction is a must. This implies that the observation of the Belgian researchers with respect to the void content should in fact be related to the degree of filling rather than to the compaction level.

2.4.2.4 LVDT system

The most common method of measuring axial deformation in a triaxial test is by using external transducers, mounted directly on the specimens. At least two LVDTs (linear variable differential transformers) are needed to measure the axial deformation at different positions using on-specimen-measuring technique, to provide an average deformation. On-specimen LVDT systems are complex with respect of arranging and measurement. A single displacement transducer measurement technique, with less electronic instrumentation and water as a confining medium, was also tested by Monash University [16]. The effect of LVDT arrangement system needs further study. It should however be noted that only measurement of the axial deformation is not sufficient to fully understand the permanent deformation behaviour of asphalt mixtures. Measurements of the radial deformation are essential in order to capture effects like dilation, volume change etc.

2.4.2.5 Friction Reduction System

In a triaxial test the specimen deforms in a radial as well as axial direction. In the absence of friction reduction system, the radial deformation is restrained by the frictional resistance between loading platen and the specimen. The confinement of the top and bottom of the specimen by the friction causes a barrel-shape on the specimen [25]. To avoid this friction effect on the specimen a friction reduction system is required.

The following friction reduction systems have been used in Netherlands[23]:

- rubber membrane –silicon grease- rubber membrane (DWW)
- coat of liquid soap-plastic foil-coat of liquid soap (TU Delft)
- glycerine/graphite powder (KOAC/NPC)

To study the effects of the above three friction reduction systems with most often used stress combinations a triaxial test was carried out at DWW on STAC for certain specimen dimensions. In the study two tests were performed with the DWW friction reduction system, one test with the TU Delft system, one test with the KOAC/NPC systems and one test without friction reduction. The test results reveal that use of the *membrane –silicon grease- membrane (DWW)* or *plastic foil-soap-plastic foil (TU Delft)* friction reduction system give results that are very different from the result if such a system is not used; this is shown in figure 2-7. Friction reduction systems of DWW and TU Delft end up with high deformations before reaching 1000-1200 number of load cycles (see curves DWW1, DWW2 and TU Delft). However, use of the *glycerine/graphite powder (KOAC/NPC)* friction reduction system, produced a creep curve which is fairly close to the creep curve without friction reduction [23]. Thus, there is the need to examine the effect of friction reduction system in more detail.

2.4.2.6 Specimen height

Although the thickness of the total asphalt package might be large, the thickness of each layer is somewhere between 30 and 80 mm, depending on the maximum aggregate size. This implies that specimen with only limited height can be obtained from pavement by means of coring. Size effects might therefore influence the triaxial test. A size effect study on permanent deformation using UTM equipment was conducted by Makanga [22]. The study was conducted on three specimen heights of 40mm, 120 mm and 3x40 mm. It concludes that permanent deformation does not only increase with height of asphalt specimens, but either increases or decreases depending on stress combination, number of load cycles, specimen arrangement and temperature. A tabular summary of this conclusion is shown in table 2-1 for specimen heights of 40mm and 120 mm.

Table 2-1: Specimen size effects

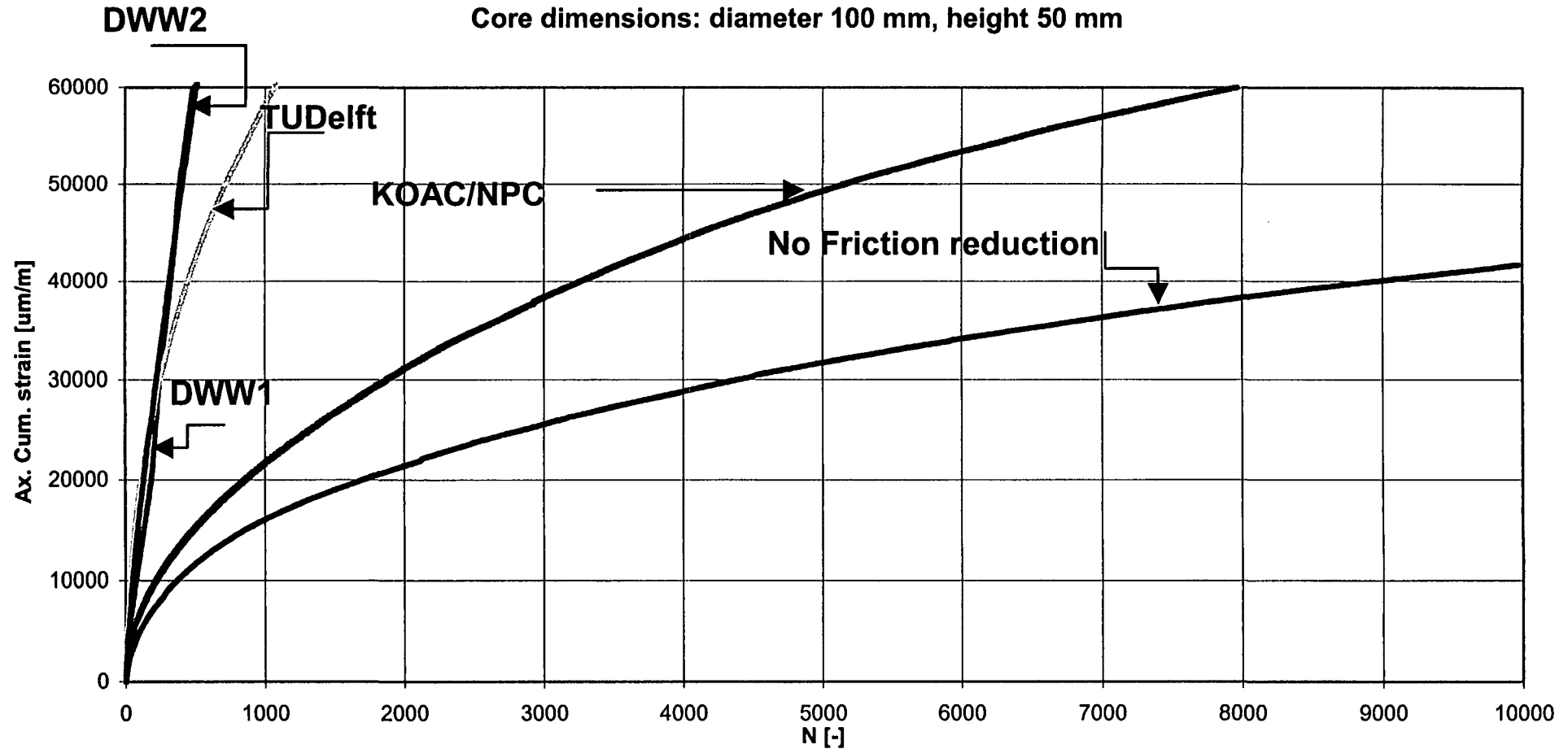
Temperature °C	Mix Type	Stress Combination	Load cycle ranges for $\Delta\epsilon_{120} > \Delta\epsilon_{40}$	Load cycle ranges $\Delta\epsilon_{120} < \Delta\epsilon_{40}$
40	DAC	700/100 1050/600 400/100	101-7200 101-2095 101-7200	2096-7200
40	STAC	700/100 1050/600 400/100	101-7200 101-543 101-772	544-7200 773-7200
50	STAC	700/100 1050/600 400/100	106-7200 122-7200 101-7200	101-105 101-121

Figure 2-7: Friction reduction tests

STAC 0/22 (Lintrack testtrack)

Confining pressure 50 kPa, deviator stress 450 kPa, Temperature 50°C

Core dimensions: diameter 100 mm, height 50 mm



2.5 Stresses in an elastic layered system

Stress combinations at a point in an asphalt layer can vary due to temperature variation, wheel load distributions and material properties. In order to capture the critical combination of principal stresses for the triaxial test, it is important to know the real nature and variation of these stresses. This can be done by means of stress analysis of layered systems. A research of this kind was done by Verstraten [37] performing numerical stress calculations in four-layered systems with continuous interfaces for varying moduli values. He did a great deal of effort to determine the physical and mechanical properties of road materials.

In this work, Verstraten considered the following types of loadings on a circular area of radius 'a':

- a uniformly distributed vertical stress;
- a uniformly distributed shear stress, directed towards the centre of circular area named as "uniform centripetal shear stress";
- a uniformly distributed shear stress, parallel to a single direction named as "uniform one-directional shear stress".

By solving systems of differential equations stresses and displacements were obtained at points of cylindrical coordinates (r , θ , z). From the analysis Verstraten made lines of equal principal stresses (P_1 , P_2 , P_3) as a percentage of the uniformly distributed load and lines of maximum shear stress ($|\tau|_{\max}$). A typical example of his lines of equal principal stresses for 'P2' is shown in figure 2-8.

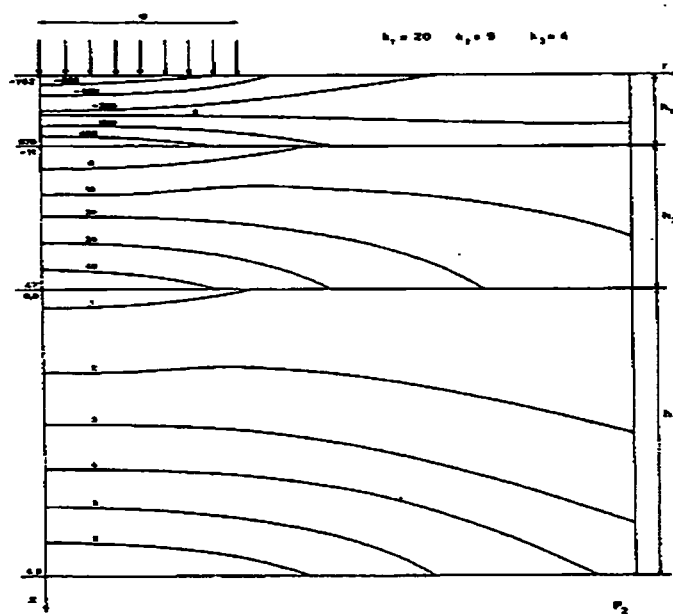


Figure 2-8: Lines of equal principal stress as % of uniformly distributed load [37]

From his analysis of the uniformly distributed vertical stress, he states that the points where the principal and shear stresses are largest are generally (but not always) found on a vertical axis passing through the centre of the loaded area. The summary of his analysis with coordinates of the points where the principal stresses and the shear stress are maximum is shown in table 2-2. However, he also states that if shear loads on the surface are neglected, important errors can be made on the values and types of distributions of the stresses likely to be developed in the upper areas of the surfacing course of an asphaltic structure. He indicates that in contra-distinction to the vertical load, shear loads induce tensions at the upper surface of the surfacing course.

Table 2-2: Coordinates (r, z) of the points for maximum principal and shear stresses [37]

Stresses	Surfacing course (thickness h_1)	Base (thickness h_2)	Subbase (thickness h_3)	Soil
P_1 and P_2 Compression Tension	(0,0) (0, h_1)	(0, h_1) (0, h_1+h_2)	(0, h_1+h_2) 0, $h_1+h_2+h_3$)	upper surface no tension
P_3 Compression Tension	($0 \leq r \leq a$) (r, z)	(0, h_1) no tension	(0, h_1+h_2) no tension	(0, $h_1+h_2+h_3$) no tension
$ \tau _{\max.}$	(0,0) *	(0, h_1+h_2)	(0, h_1+h_2)	

* the maximum may sometimes be found under the edge of the loaded area.

The work of Vanstraten has shown the complexity of the mechanical behaviour of elastic layered systems by particularly showing the variation of principal stresses, and the effect of superposition of vertical stress with horizontal shear loads. However, it does not consider the effect of temperature variation throughout the layers. It also does not consider a broad range of moduli variations .

2.6 Conclusions

- Because rotation of the principal stresses can not be achieved in a triaxial test, this test is not capable of fully capturing the permanent deformation resistance of asphalt mixtures.
- In spite of this drawback, the triaxial test is by far the best suited to analyse the permanent deformation resistance of asphaltic mixes when compared to other commonly available tests .
- A large number of factors, such as specimen height, friction reduction, LVDT placement, influence the test result. A significant amount of work should still be done to fully understand the magnitude of these influences.
- Given the large variation of stresses and temperatures over the height of an asphaltic layer, characterisation of the permanent deformation resistance at only one temperature and one stress combination does not seem the right thing to do.
- Although there should be a significant influence of the mix composition on the resistance to permanent deformation, results obtained until now do not show these influences to the extent expected.

3 Stress Analysis by BISAR

Stresses in pavements are generated due to traffic and environmental loads. These stresses vary in the three dimension of the pavement structure depending on the degree of loading, temperature and material characteristics. To determine stress conditions within the asphalt layers of typical Dutch standard pavement structures for highways, a linear elastic stress analysis using the BISAR model is performed. In the analysis the following conditions are assumed.

- full friction is assumed between layers,
- multi layer linear elastic theory is considered,
- layers are infinite horizontally,
- specific elastic modulus and Poisson's ratio are assigned to a layer,
- uniformly distributed tyre contact pressure is considered,
- infinite depth of subgrade layer is assumed.

In this analysis the variation of the stresses in various locations in the pavement in relation to the distance to the load will be studied. However, before coming to these stresses, the type of pavement structures and wheel loads used in the analysis are explained in the sections 3.1 to 3.2. The temperature distribution and how the different modulus values for the various layers are arrived are discussed in the sections 3.3 to 3.7.

3.1 Pavement structure

3.1.1 Pavement structures in Netherlands

Three pavement structures taken from the DWW manual [10] as shown below are analysed to see the stress conditions at different depths.

50 mm DAC 0/16
60 mm STAC 0/22
60 mm GAC 0/32
250 mm Mix granulate

Structure (standard) I

50 mm DAC 0/16
60 mm STAC 0/22
60 mm GAC 0/32
50 mm GAC 0/32
250 mm Mix granulate

Structure (standard) II

50 mm DAC 0/16
60 mm STAC 0/22
60 mm STAC 0/22
60 mm STAC 0/22
70 mm STAC 0/22
250 mm Mix granulate

Structure (standard) III

The abbreviations for the standard mixes in the pavement structures I to III and in other sections of this report stand for:

DAC- dense asphalt concrete

STAC-stone asphalt concrete

OAC- open asphalt concrete

PAC- porous asphalt concrete

GAC- gravel asphalt concrete

SMA- stone mastic asphalt

It is common to use PAC as wearing surface. However, since the analysis in this study is limited to DAC and STAC mixes only, PAC layers are not used. STAC 0/22 layers for this analysis also replace the GAC 0/32 layers. In the above mentioned structures the mix granulate layers are used as base course. In the western parts of the Netherlands, structures standard I to III are normally built on a sand subbase. This subbase is there because of the very low bearing capacity of the natural soil. Normally the sand subbase is constructed as embankment and several metres of sand are usually needed to get the pavement surface at the right level. In such a case, the subbase can actually be considered as the subgrade because of the large thickness of the applied sand layer. In the eastern and southern part of the Netherlands the natural subsoil is of much better quality and in such cases a sand subbase is not needed or only to a limited height.

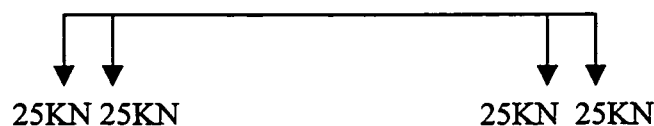
3.2 Wheel Loads

The following standard wheel loads are used for the stress analysis by BISAR[3]:

3.2.1 Simple super single



3.2.2 Double wheel



Type	Axle Load	Radius of contact area	Distance between wheels
super single	100 KN	0.15	-----
Double wheel	100 KN	0.105	0.105

3.2.3 Extended Super single

The extended super single load contains not only vertical load but also radial and tangential stresses. This can represent possible shear and breaking forces on the highway. The vertical stresses are equal to a vertical wheel load of 50KN.

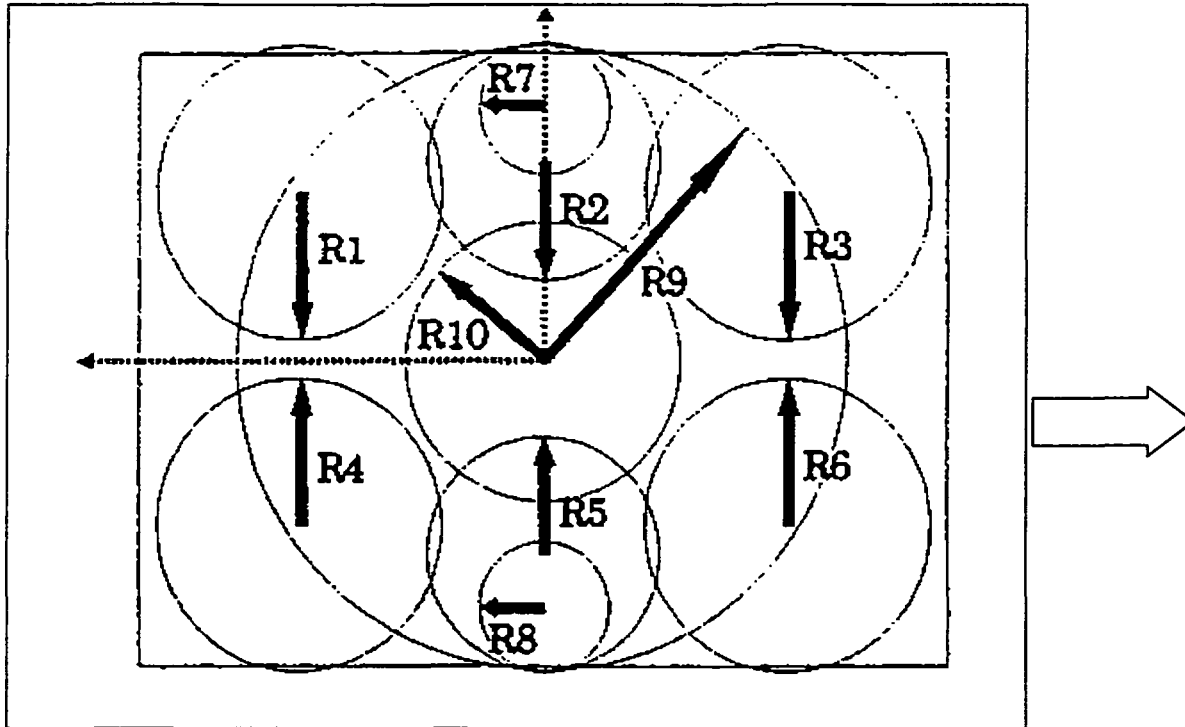


Figure 3-1: Extended super single load

Table 3-1: Extended super single load

Load No.	Position(mm)		Radius(mm)	Stress(KPa)		
	X	Y		X	Y	Z
R1	+60	+90	52.57	-200	0	+400
R2	+70	0	42.57	-200	0	0
R3	+60	-90	52.57	-200	0	+400
R4	-60	+90	52.57	-200	0	+400
R5	-70	0	42.57	-200	0	0
R6	-60	-90	52.57	-200	0	+400
R7	+90	0	22.57	-180	0	0
R8	-90	0	22.57	-180	0	0
R9	0	0	112.57	0	+150	+750
R10	0	0	50	0	-60	+750

Total vertical load = 50KN

3.3 Asphalt concrete characteristics

The mix characteristics for six types of Dutch Standard mixes have been studied. The mix properties are summarised in tables 3-2,3-3,3-4. The mix compositions shown in table 3-2 are taken from CROW standard specifications[17].

Table 3-2: Mix compositions

Mix Type	DAC	OAC	STAC	PAC	SMA	GAC
coarse aggregate (2mm-22mm)	60.0	72	57	85	77.5	77.5
63µm- 2mm	36.9	23	36	10	14.5	14.5
Filler < 63µm	3.1	5	7	5	8	8
Bitumen*	6.2	4.5	4.5	4.5	7	7
Void content	6	10	7	20	5	7

* on 100% of mineral aggregate by mass

Table 3-3: Aggregate and bitumen properties

specific gravity of coarse aggregate (2mm-22mm)	2.65
specific gravity of 63µm	2.7
specific gravity of filler	2.45
specific gravity of bitumen	1.025
pen800 (softening point)	51 °C
penetration including ageing	31 (0.1 mm)
softening point after ageing	55 °C

3.3.1 Volumetric compositions

The mix property of the mixes is affected by the volumetric composition. The volumetric compositions are obtained as follows:

$$Gsb = \frac{P_1 + P_2 + \dots + P_i}{\frac{P_1}{G_1} + \frac{P_2}{G_2} + \dots + \frac{P_i}{G_i}}$$

Where:

Gsb = bulk specific gravity of the mineral aggregate

P₁ mass of aggregate g₁, with bulk specific gravity G₁

P₂ mass of aggregate g₂, with bulk specific gravity G₂

P_i mass of aggregate g_i, with bulk specific gravity G_i

P_b% by mass of bitumen with specific gravity G_b

The maximum specific gravity of the mix is:

$$Gmm = \frac{100}{\frac{100 - P_b}{Gsb} + \frac{P_b}{G_b}}$$

The bulk specific gravity of the compacted mix is:

Gmb (determined by water displacement method)

Can be estimated as:

$$Gmb = Gmm (1 - Va/100)$$

The bulk specific gravity of the compacted aggregate is:

$$G_{sc} = G_{mb} \frac{(100 - P_b)}{100}$$

From the above values the volume percentages are:

$$\text{Aggregates: } V_g = 100 \frac{G_{sc}}{G_{sb}}$$

$$\text{Bitumen: } V_b = 100 \frac{G_{mb}}{G_{mm}} - V_g$$

$$\text{Air } V_a = 100 \left(1 - \frac{G_{mb}}{G_{mm}} \right)$$

A typical calculation of the volumetric composition for DAC is shown as follows:

$$G_{sb} = (60 + 36.9 + 3.1) / (60.0/2.65 + 36.9/2.7 + 3.1/2.45) = 2.66$$

$$G_{mm} = 100 / ((100 - 6.2)/2.66 + 6.2/1.025) = 2.43$$

$$G_{mb} = 2.43 (1 - 6/100) = 2.29$$

$$G_{sc} = 2.29 (100 - 6.2) / 100 = 2.15$$

$$V_g = 100 (2.15 / 2.66) = 80.7$$

$$V_b = 100 (2.29 / 2.43) - 80.7 = 13.3$$

$$V_a = 100 (1 - 2.29 / 2.43) = 6$$

Summaries of volumetric compositions for all other mixes are shown in table 3-4.

Table 3-4: Volumetric compositions

	DAC	OAC	STAC	PAC	SMA	GAC
Gsb	2.66	2.65	2.65	2.64	2.64	2.64
Gmm	2.43	2.48	2.48	2.48	2.39	2.39
Gmb	2.29	2.33	2.31	1.98	2.27	2.23
Gsc	2.15	2.23	2.21	1.89	2.11	2.07
Vg	80.7	84.0	83.1	71.5	80.1	78.4
Vb	13.3	10.0	9.9	8.5	14.9	14.6
Va	6.0	6.0	7.0	20.0	5.0	7.0
VFB	0.69	0.62	0.59	0.30	0.75	0.68

3.4 Temperature distribution in pavement

Temperature is one of the environmental factors that affect the stiffness of an asphalt concrete mix. Higher temperatures reduce the mix stiffness as the asphalt concrete shows viscous behaviour. At lower temperatures the mix stiffness of asphalt concrete becomes higher due to the more rigid behaviour of the bitumen. To study relationships of the stiffness with the variation of temperature, the temperature at the different depths has been evaluated using three methods and was compared with actual measurements from MEVA-3 project[38] . These methods are:

- SHRP method,
- Finite element program WEGTEM,
- BELLS3 model.

3.4.1.1 SHRP method

SHRP method is based on measurements of air temperature to predict pavement surface temperatures. In this method, average consecutive 7-day maximum temperatures are calculated for each year. All the average 7-day maximum temperatures are determined for all the years from which records are available. For example, if there are 30 years of data, 30 maximum 7-day temperatures will be obtained. The average value of the 30 maximum 7-day temperatures will be used as the mean highest average temperature for the determination of pavement temperature. The pavement surface temperature is calculated using the equation 3-1, which was developed, based on energy balance at the surface [30].

$$422 \alpha \tau_{\alpha}^{1/\cos Z} \cos Z + 0.7 \sigma T_a^4 - h_c(T_s - T_a) - 90k - \epsilon \sigma T_s^4 = 0 \dots\dots\dots \text{eqn 3-1}$$

Where:

- Z = zenith angle (approximately $z = \text{latitude} - 20$ for may through august)
- τ_{α} = sunshine factor (0.81) for perfectly sunny conditions)
- α = solar absorptivity (default: 0.9)
- σ = Stefan-Boltzman constant $0.1714 \text{ E-}8 \text{ Btu}/(\text{hr} \cdot \text{ft}^2 \cdot \text{R}^4)$
- h_c = surface coefficient of heat transfer (default = $3.5 \text{ Btu}/(\text{hr} \cdot \text{ft}^2 \cdot \text{F})$)
- k = thermal conductivity (default : $0.8 \text{ Btu}/(\text{hr} \cdot \text{ft}^2 \cdot \text{F})/\text{ft}$)
- ϵ = surface emissivity (default: 0.9)
- T_a = maximum air temperature (*Rankine)
- T_s = maximum pavement surface temperature (*Rankine)

*The absolute zero version of the Fahrenheit scale is the Rankine scale. Add 460 degrees to Fahrenheit temperatures to obtain the Rankine temperature.

After determining the surface temperature from the above formula, the maximum pavement temperature to a depth of 200mm is estimated using equation 3-2 [30].

$$T_d = T_s (1 - 0.063d + 0.007d^2 - 0.0004d^3) \dots\dots\dots \text{eqn 3-2}$$

- T_d = temperature at depth 'd' (°F)
- T_s = The maximum surface temperature (°F)

For the estimation of the pavement temperature by the SHRP method, air temperature measurements from the meteorological stations at Deelen, Eelde, Zestienhoven in Netherlands for the years 1981-1989 were taken[38]. Taking 9 years average maximum 7-days temperature for the three stations as 25.5°C , the pavement surface temperature by SHRP method is estimated to be 47.91°C from equation 3-1. Using this surface temperature and equation 3-2 the temperature gradient for the pavement depth is estimated as shown in figure 3-2 together with gradients for surface temperatures of 45°C and 50°C .

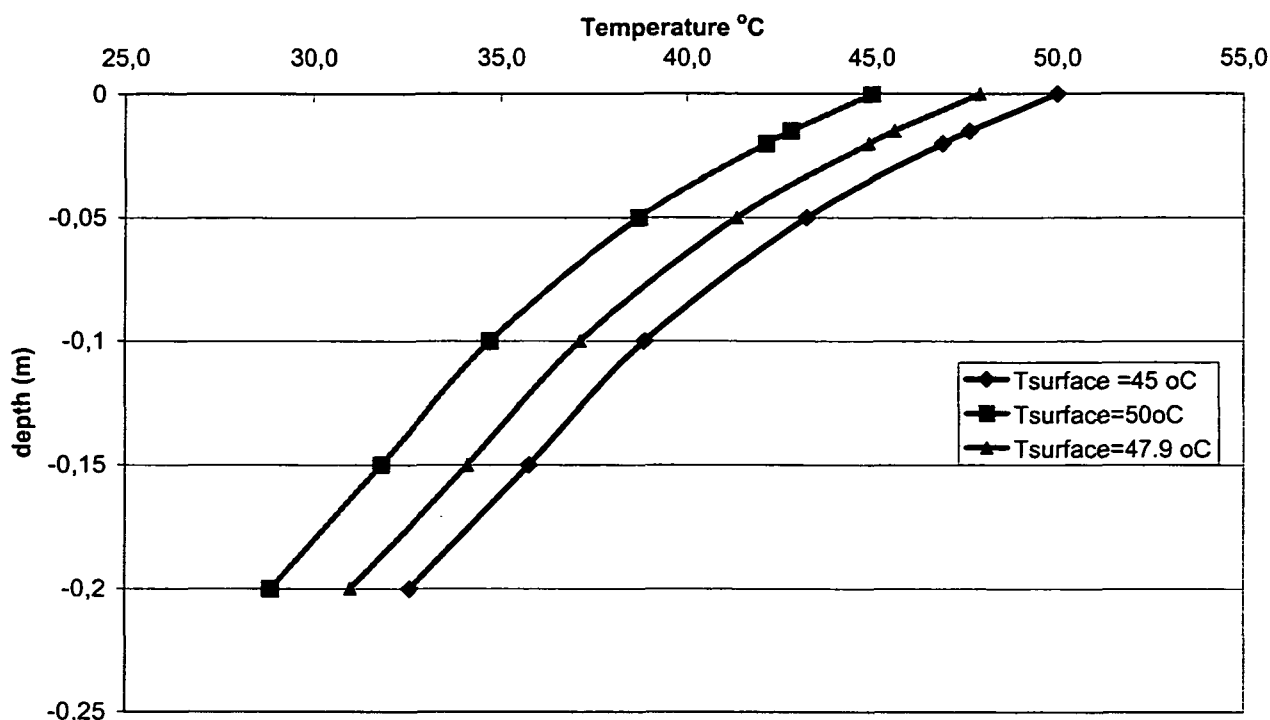


Figure 3-2: Pavement temperature estimation by SHRP method

From SHRP method of pavement temperature estimation one can see that pavement temperatures at a depth of 0.2m can reach a value between 28 to 33 °C, for surface temperature of 45°C and 50 °C respectively.

3.4.1.2 Finite element program WEGTEM

WEGTEM is a finite element program, which uses a multilayer pavement system and climatic data as input to determine the temperature distribution within a pavement. It is developed based on heat transfer analogy, where heat transfer is dependent on the thermal conductivity of the pavement material, density and heat capacity per unit of volume [29]. It solves the Fourier's partial differential equation expressed on eqn.3-3 for defined boundary conditions.

$$\rho \cdot c \cdot \frac{dT}{dt} = \lambda \cdot \frac{d^2T}{dz^2} \quad [\text{W/m}^3] \dots \dots \dots \text{eqn. 3-3}$$

Where:

- ρ = density (kg/m³)
- c = specific heat of material (J/kg.K)
- λ = thermal conductivity of material (W/m.K)
- T = temperature (K)
- Z = depth below surface of pavement (m)

One-dimensional calculations of temperature distribution within the asphalt pavement structures with sand sub-base and an EPS (expanded polystyrene foam) sub-base were carried out by Duskov, using WEGTEM [29]. The calculation used climatic data measurements from a meteorological station in Den Helder, in the Netherlands for year 1981. 54 pavement structures, half of them with sand sub-base and half of them with EPS sub-base, were analysed. The asphalt layers consisted of DAC, OAC, and GAC.

The goal of the analysis was to determine the length of time at which the temperature in a layer has a value within defined classes. Even though the main purpose of the study was to analyse the distribution of pavement temperature with and without EPS sub base, it has shown that the duration of a certain temperature in the asphalt layer is almost the same with and without EPS sub base. Typical output of the WEGTEM analysis for absolute warmest period of August 1981 is shown in fig 3-3. The pavement structure had 50mm DAC, 50 mm GAC, 150 mm road base, and 100 mm sand and 2000 mm EPS/sand sub base. The value of the maximum surface temperature is 45 °C.

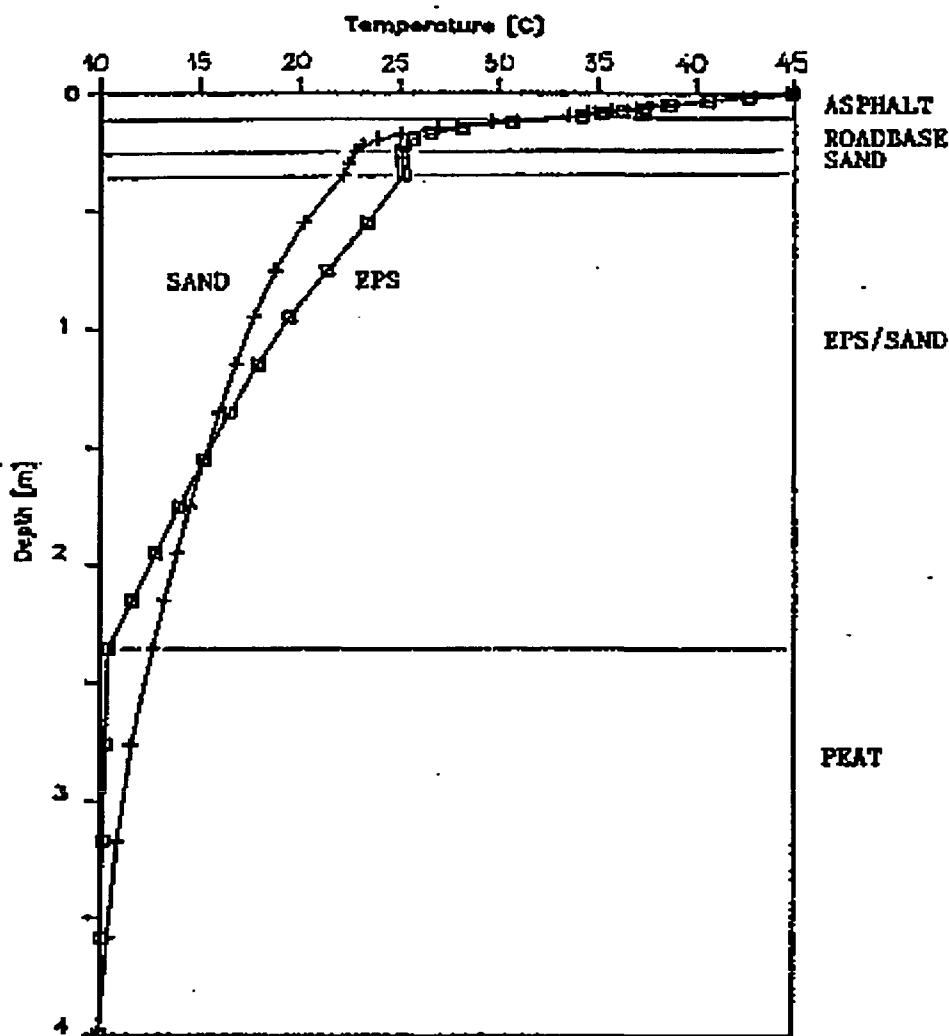


Figure 3-3: Temperature distribution in pavement [29]

3.4.1.3 BELLS3 model

A spreadsheet has been developed by CROW to predict pavement temperature at different depths by means of the BELLS3 model [31]. The formula in the spreadsheet and the factors used are expressed in eqn.3-4.

$$T_d = 1.4 + 0.907 \cdot T_{opp} + \{\log d - 1.25\} \{-0.54 \cdot T_{opp} + 0.764 \cdot T_{vd} + 2.39 \cdot \sin(hr_{18} - 15.5)\} + 0.060 \cdot T_{opp} \cdot \sin(hr_{18} - 13.5) \dots \text{eqn. 3-4}$$

Where:

T_d = asphalt temperature at depth 'd' (°C)

T_{opp} = temperature at asphalt surface (°C)

d = depth in asphalt (mm)

T_{vd} = average air temperature on previous day (°C)

\sin = sine function in 18-hours system where 2π radians equals 18-hr cycles

hr_{18} = time of the day in 24-hours system (summer time) adapted for 18-hours system

For calculation of the pavement temperature using BELLS3 method the asphalt surface temperatures were taken from measurements of MEVA-3 at TU Delft for July 1989 which is shown in figure 3-6a[38]. By selecting the surface temperature measurements for the 3rd of July and 6th of July as T_d , values of 45°C and 50°C are picked respectively. The temperatures on previous day (T_{vd}) for the BELLS3 model is taken from the mean air temperature records of Zestienhoven, Eelde and Deelen for 2nd and 5th of July 1989 (see figure 3-6b). By taking the average mean temperatures of the three stations, the ' T_{vd} ' for the surface temperatures of 45°C and 50°C will be 15.5°C and 21.3°C. With these average air temperature values and surface temperatures of 45°C and 50°C, the temperature under the pavement is estimated as shown in figure 3-4. From the BELLS3 method one can see that the pavement temperature at a depth of 200mm can reach values between 28-33°C for surface temperatures of 45°C and 50°C respectively.

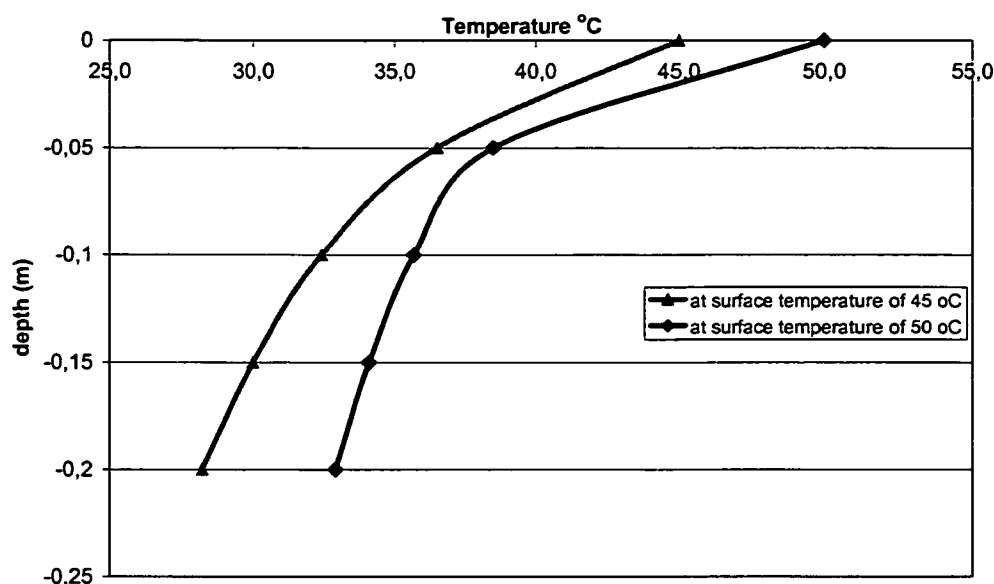


Figure 3-4: Pavement temperature by BELLS3 method

Among the three methods discussed above the SHRP method and the finite element program WEGTEM have taken the conductivity of the pavement material into consideration. The WEGTEM calculations are based on single station and one-year record considered as average climatic conditions for Netherlands. The calculations based on SHRP method have a better number of climatic record years and are based on maximum temperature records. The three methods of temperature analysis are compared with each other by plotting the predicted temperature distributions together with an actual measurement done by MEVA-3 at TU Delft in 1989. The result is shown in figure 3-5 for surface temperature of 45 °C. As can be seen from figure 3-5 estimations with the SHRP method are closer to actual pavement temperature measurements. The BELLS3 method predictions and the WEGTEM analysis are lower by 10-15 °C from the actual measurements. For this reasons the calculations based on SHRP method are considered more suitable for this study.

The surface temperature prediction by SHRP approach discussed in section 3.4.1.1 has obtained a value of 47.9 °C using maximum 7-day consecutive temperatures. Typical pavement temperature measurements at TU Delft for the surface and 5cm below the surface have also proven that peak surface temperatures can reach a value up to 50 °C (see figure 3-6a). Thus, the SHRP method seems closer in predicting surface temperatures.

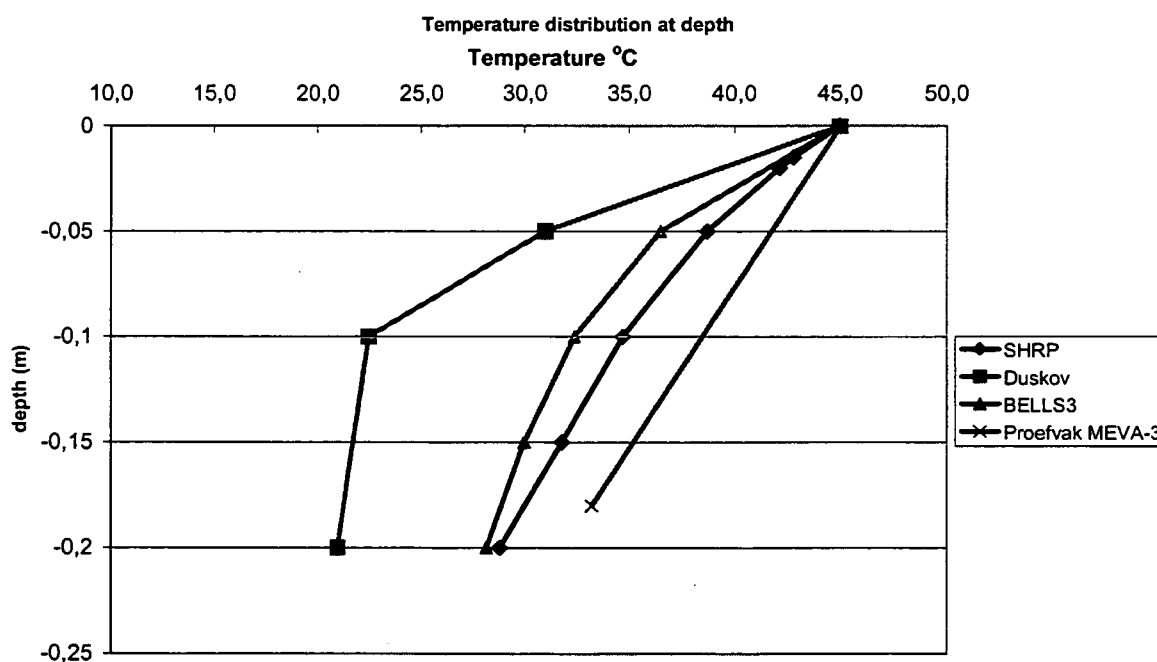


Figure 3-5: Comparison of the different methods with measurements

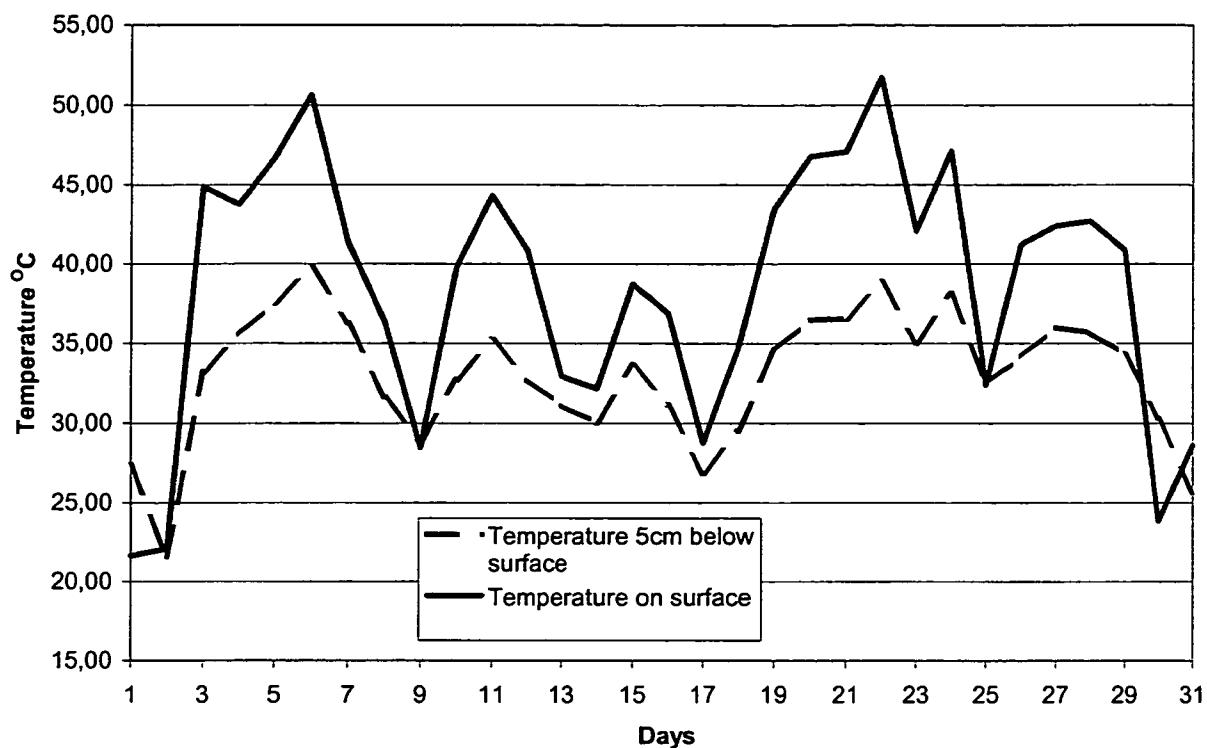


Figure 3-6a: Pavement surface temperature by MEVA-3 TU Delft, July 1989 [38]

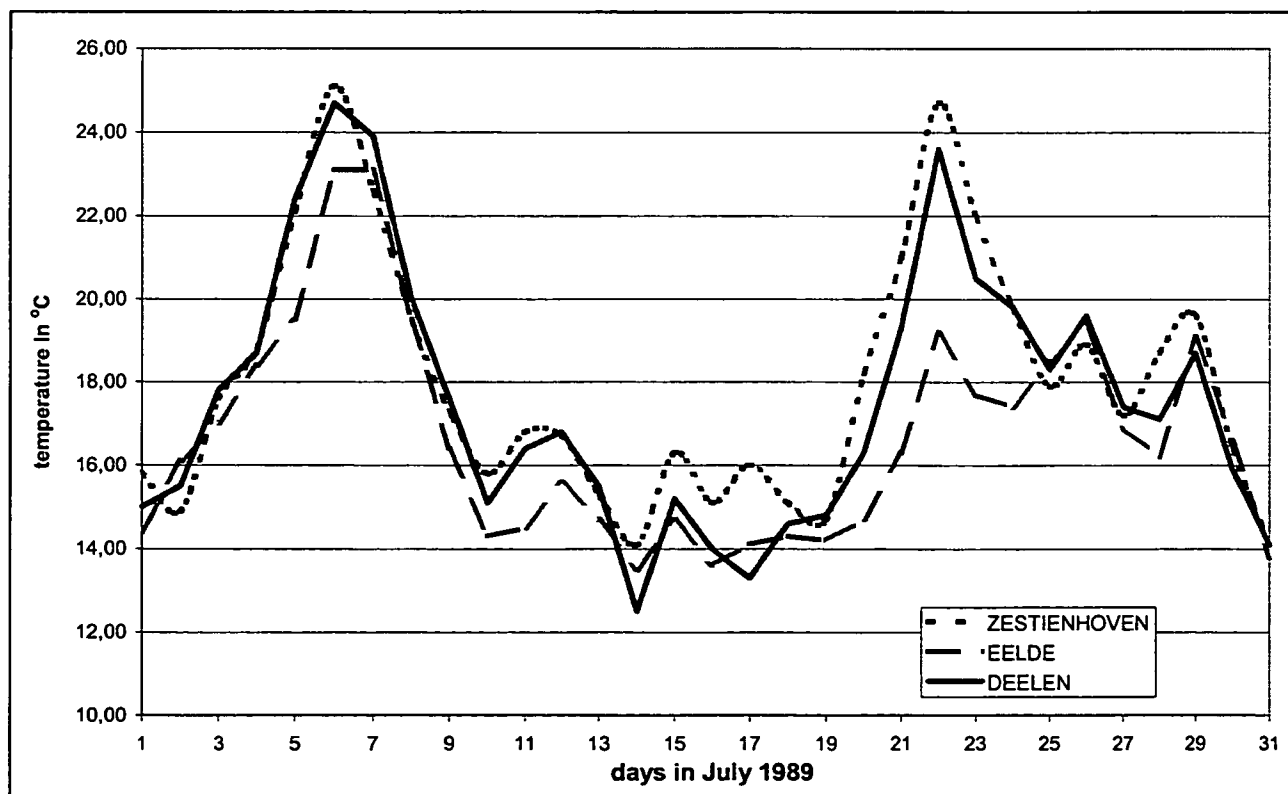


Figure 3-6b: Air temperature Zestienhoven, Eelde, Deelen, July 1989 [38]

3.5 Loading time

The loading time is defined as:

$$t = D/V$$

Where: t = loading time (s)

V = vehicle speed (m/s)

D = diameter of the contact area (m)

At different depths of the pavement 'D' changes due to load spreading [4]. The loading time for the first round of stress calculations was done by means of figure 3-7. A speed of 60km/h was assumed.

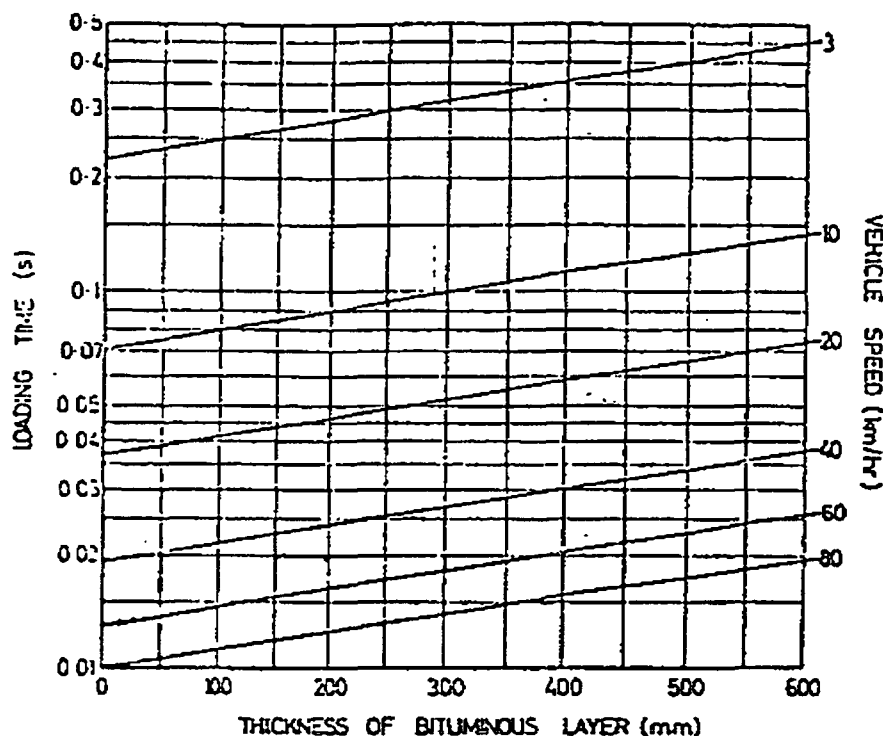


Figure 3-7: Loading time

The loading time can also be calculated from equation 3-5 [39].

$$\log t = 0.5 h - 0.2 - 0.94 \log V \dots \dots \dots \text{eqn 3-5}$$

Where:

t = time in seconds,

h = layer thickness in meters,

V = vehicle speed in km/hr.

3.6 Poisson's ratio

Poisson's ratio is the ratio of horizontal strain to vertical strain. Poisson's ratio of asphalt concrete mixes depends on temperature and loading frequency. This is shown in fig 3-8. The maximum Poisson ratio is 0.5[21].

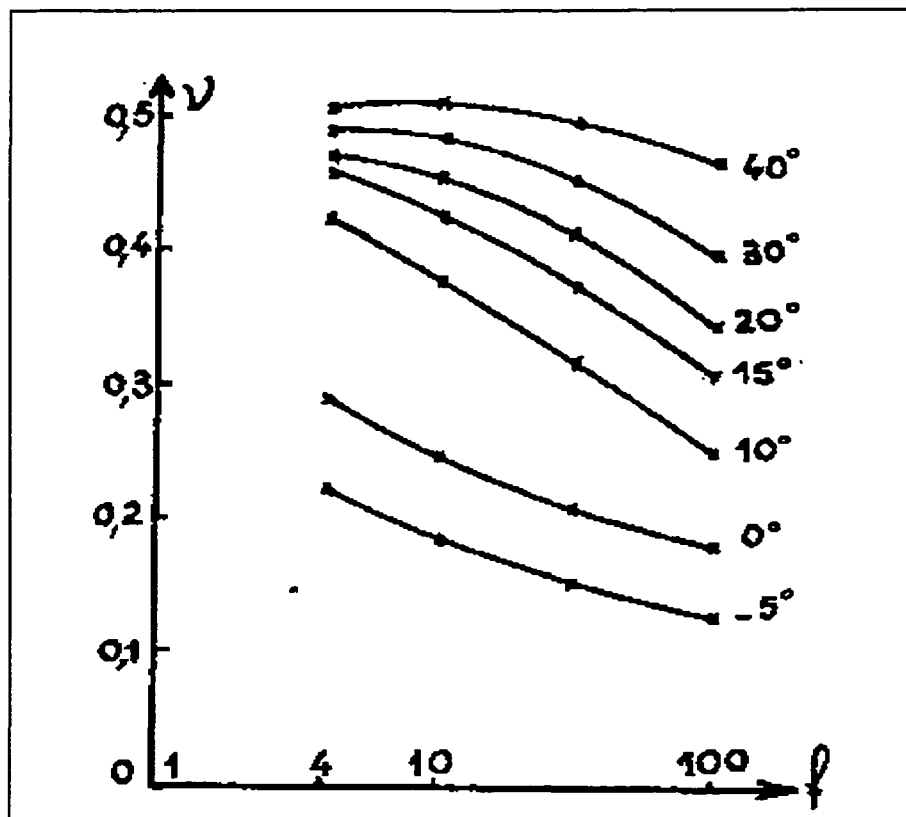


Figure 3-8: Poisson's ratio with frequency and temperature [21]

3.7 Mix stiffness

3.7.1 Mix stiffness for Asphalt concrete

The Asphalt concrete mix stiffness is affected by the mix property, pavement temperature and loading time. With longer loading time and higher temperatures, the mix stiffness becomes lower and with shorter loading times and low temperatures the mix becomes stiffer.

The BANDS model, one of the Shell pavement design packages, is used to calculate mix stiffness for bitumen stiffness values higher than 5 MPa. At higher temperatures where bitumen stiffness values could be lower than 5 MPa, the Francken formula shown on equation 3-6 is used [32].

$$E_{\infty}(V_b, V_a) = 3.56 \cdot 10^4 (V_b + V_a) / V_b \cdot e^{(-0.1 V_a)} \dots \dots \dots \text{eqn 3-6}$$

Where:

$E_{\infty}(V_b, V_a)$: maximum mix modulus at maximum bitumen stiffness
(both values are true elastic modulus values)(MPa)

V_b : volume percentage of bitumen

V_a : volume percentage of air voids

V_g : volume percentage of aggregates.

This equation is valid for the conditions:

$1.5\% < V_a < 32\%$,

$3 < V_g / V_b < 12$,

$0.3 \text{ Mpa} < S_{bit} < 3000 \text{ Mpa}$

The SMIX of the BANDS is based on a method to predict the stiffness of bituminous mixes from the stiffness modulus of the bituminous binder and the volumetric composition of the mix. The stiffness modulus of the bituminous binder (S_{bit}) is obtained from the Van der Poel nomograph.

3.7.2 Subgrade modulus

The subgrade modulus assumed for a subgrade CBR of 5 as:

$$E=10 \text{ CBR} = 50 \text{ MPA}$$

It is understood that 50 MPa is a low value for a sand subgrade (natural soil or embankment) but it was considered important not to arrive to too optimistic predictions with respect to the stresses in the asphalt layer.

3.7.3 Base modulus

It is assumed by following Australian procedure as shown below [4]. The subbase is divided into two sublayers.

$$R = (E_b/E_s)^{1/n} \dots\dots\dots \text{eqn. 3-7}$$

R = modulus ratio taken maximum as 2

E_b = Maximum modulus of the base material

E_s = modulus of subgrade

n = number of sublayers of the base

In order not to obtain a too optimistic picture of the stresses in the asphalt layer the maximum base modulus was estimated as 100 MPa. Again it is understood that this is a conservative value.

3.8 Stress Analysis by BISAR

In the early 1970 Shell Research developed the BISAR computer program to develop design charts for the Shell Design Manual. Currently it is possible to calculate stresses, strains and displacements by using the BISAR 3 PC based program for a pavement structure and loading arrangements[34].

The BISAR program allows loading with one or more circular loads located at defined coordinate positions. The following data input are required:

- number and location of loads
- number of layers
- Young's modulus, poisson ratio, thickness of each layer
- coordinate location of data output

Each of the layers in the standard pavement structures I to III were divided into sublayers keeping the total number of layers including the subgrade to 10 at a time, to make them suitable for analysis in BISAR. The BISAR calculations at a time will allow only for ten loads/stresses, ten layers and ten stress points. The BISAR also allows for horizontal loads applied as shear stresses. The principal stresses have been analyzed looking at their behavior at each stress analysis point.

3.8.1 BISAR inputs

The following layer characteristics have been defined as an initial inputs for the BANDS model for determining S_{bit} and S_{mix} , and for BISAR to determine the three dimensional stresses. As was expressed in section 3.7.1, the mix stiffness values for S_{bit} lower than 5MPa are obtained from

equation 3-5. It is understood that the values for the DAC layer are too low when compared to resilient modulus values of triaxial test obtained by Parajuli [24] at the same temperature and frequency. Nevertheless it was decided to carry on with the values obtained.

3.8.1.1 Standard I

Thickness(mm)	Loading time (sec)	frequency (Hz)	temp(Duskov)	poisson ratio	Type of mix	Vb	Vg	Sbit	Smix
12.5	0.0125	8	45	0.5	DAC	13.2	80.8	0.468	200
12.5	0.0133	8	40	0.47	DAC	13.2	80.8	2.7	825
15	0.0135	8	38	0.46	DAC	13.2	80.8	4.01	1110
30	0.014	8	35	0.45	STAC	12.1	81.0	6.93	1200
30	0.015	8	33	0.45	STAC	12.1	81.0	9.82	1520
30	0.0152	8	30	0.45	STAC	12.1	81.0	17.4	2240
30	0.016	8	27	0.44	STAC	12.1	81.0	27.8	3070
125	0.0165	8	26	0.35	subbase				100
125				0.35	subbase				100
				0.5	subgrade				50

3.8.1.2 Standard II

thickness(mm)	Loading time (sec)	frequency (Hz)	temp(Duskov)	poisson ratio	Type of mix	Vb	Vg	Sbit	Smix
12.5	0.0125	8	45	0.5	DAC	13.2	80.8	0.468	200
12.5	0.0133	8	40	0.47	DAC	13.2	80.8	2.7	825
15	0.0135	8	38	0.46	DAC	13.2	80.8	4.01	1110
30	0.014	8	35	0.45	STAC	12.1	81.0	6.93	1200
30	0.015	8	33	0.45	STAC	12.1	81.0	9.82	1520
30	0.0152	8	30	0.45	STAC	12.1	81.0	17.4	2240
30	0.016	8	27	0.44	STAC	12.1	81.0	27.8	3070
70	0.0165	8	26	0.43	STAC	12.1	81.0	31.8	3700
250				0.35	subbase				100
				0.5	subgrade				50

3.8.1.3 Standard III

thickness(mm)	Loading time (sec)	frequency (Hz)	temp	poisson ratio	Type of mix	Vb	Vg	Sbit	Smix
12.5	0.0125	8	45	0.5	DAC	13.2	80.8	0.468	300
12.5	0.0133	8	40	0.47	DAC	13.2	80.8	2.7	500
15	0.0135	8	38	0.46	DAC	13.2	80.8	4.01	800
30	0.014	8	35	0.45	STAC	12.1	81.0	6.93	1200
30	0.015	8	33	0.45	STAC	12.1	81.0	9.82	1520
30	0.016	8	27	0.45	STAC	12.1	81.0	27.8	3070
70	0.0167	8	25	0.44	STAC	12.1	81.0	36.8	3700
70	0.018	8	25	0.43	STAC	12.1	81.0	35.2	3600
250				0.35	subbase				100
				0.5	subgrade				50

3.8.2 Co-ordinate system in BISAR

Inputs of the BISAR are expressed in terms of X, Y, Z Cartesian co-ordinate system. However, actual calculations are carried out also in a cylindrical co-ordinate system (r, θ, z). The BISAR co-ordinate system is shown on figure 3-8.

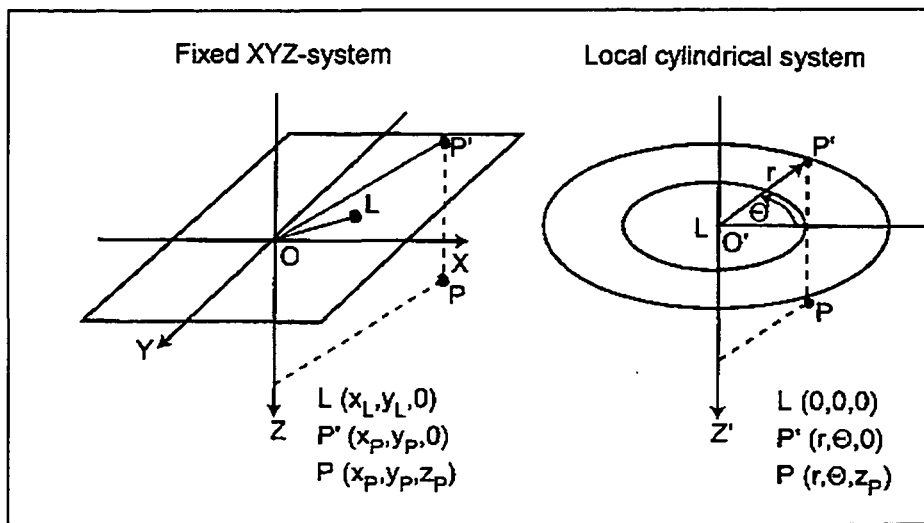


Figure 3-8: Outline of coordinate systems within BISAR [34]

3.8.3 Strategy of analysis

The BISAR analysis is done for the three structures and for the three loadings in section 3.2. However analysis of the BISAR outputs is done for structure III and compared with structures I and II. The output due to extended super single load is analysed and compared with simple super single and double wheel loads. The results of the analysis are interpreted graphically. The numerical values are attached in the appendices.

3.8.4 Stress distribution

3.8.4.1 Vertical stress (σ_{zz})

In this section the variation of the vertical stress with depth and distance from centre of loading in the transverse direction due to three types of loads is discussed for structure III. The three stress variations within the asphalt layer are shown on figures 3-9 to 3-11. As can be seen from these figures the maximum vertical stress at the surface ($Z=0$) due to extended super single load (1.5Mpa) is almost double to that of simple and double wheel loads. The maximum vertical stress at the surface due to double wheel load (0.722MPa) is slightly higher to that of simple supersingle load (0.707MPa). From this one can conclude that the vertical stress is largely affected by non-uniform distribution of the wheel loads distributed over many circular areas than over two or a single circular area.

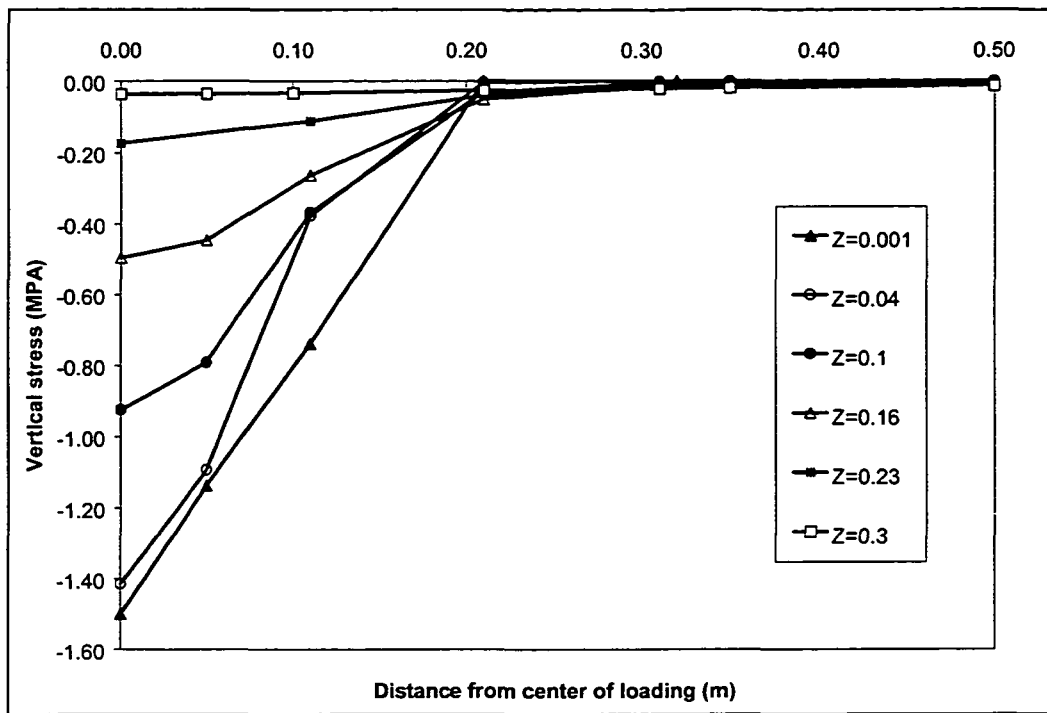


Figure 3-9: Vertical stress due to extended super single load

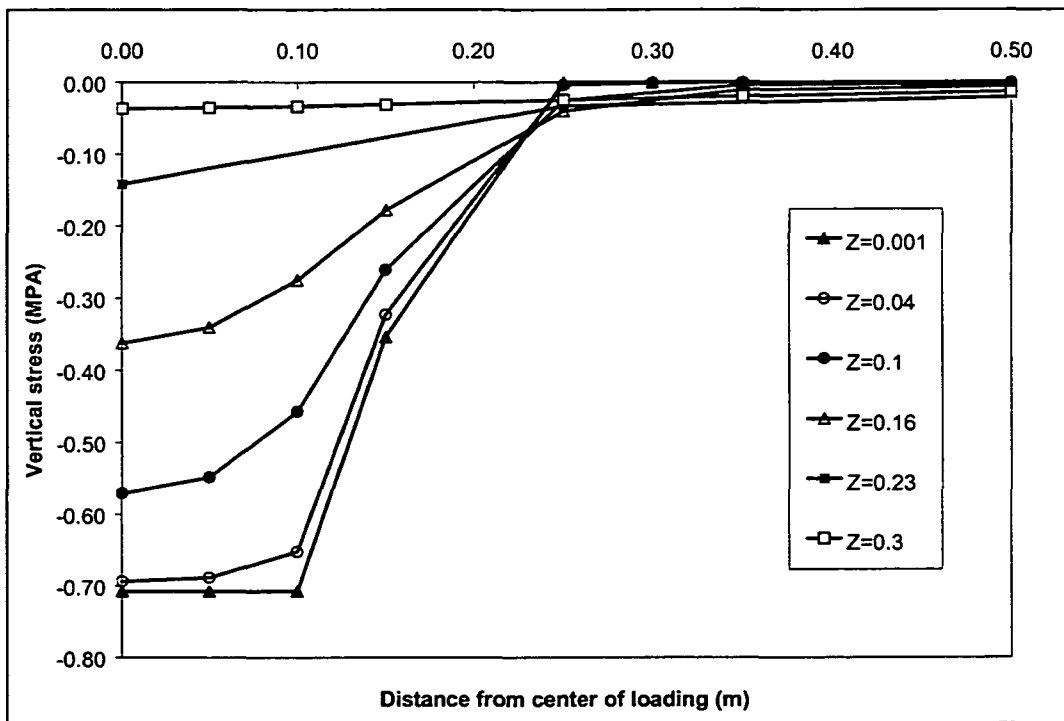


Figure 3-10: Vertical stress due to simple supersingle load

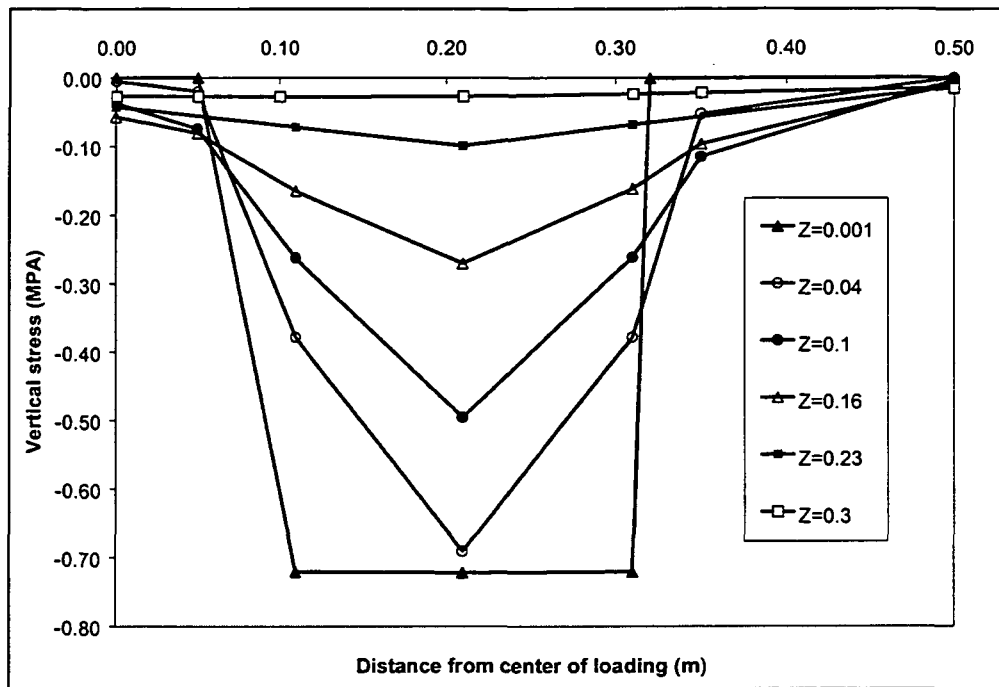


Figure 3-11: Vertical stress due to Double wheel load

3.8.4.2 Tangential stress (σ_{yy}) and radial stress (σ_{xx})

These stresses for structure III are shown on figures 3-12 to 3-13. As can be seen from the figures the radial and tangential stresses vary between compressive and tensile stresses depending on the point in the pavement. For the asphalt layer in this analysis the radial and tangential stresses below depth of about 180mm are tensile. The radial and tangential stresses have nearly equal magnitudes. This could be due to symmetry of loading along the radial and tangential directions.

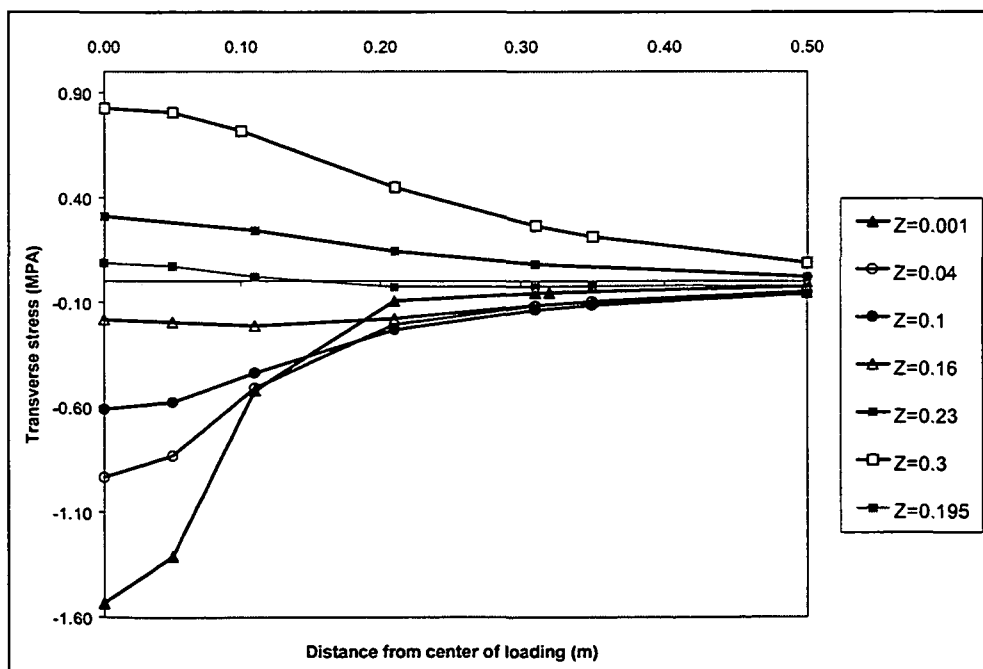


Figure 3-12: Transverse (tangential) stress due to extended supersingle load

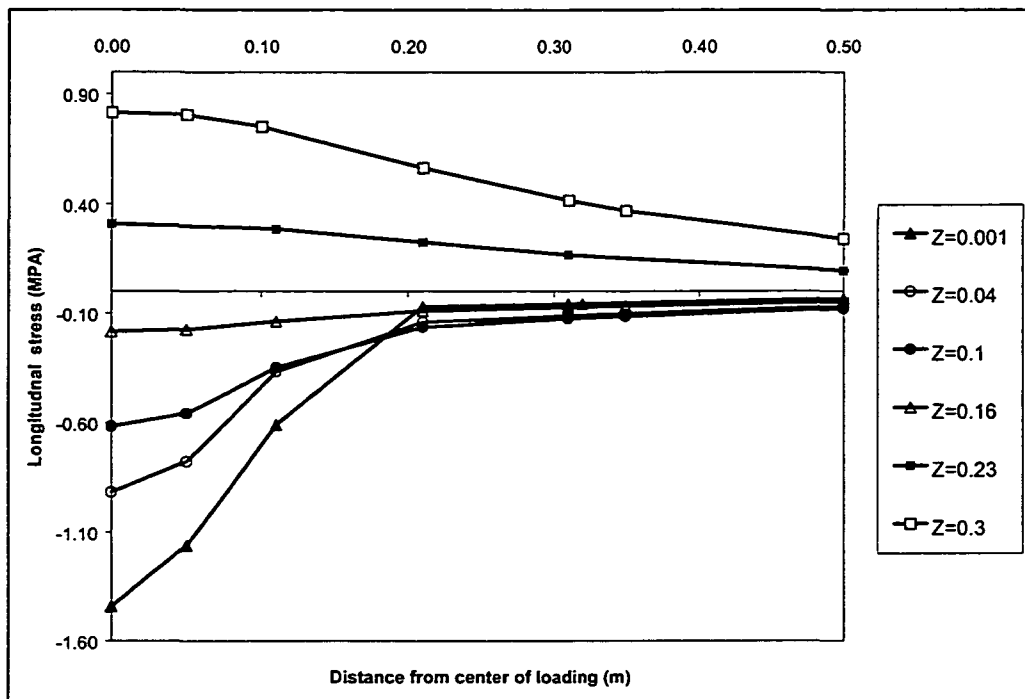


Figure 3-13: Longitudinal (radial) stress due to Extended super single load

3.8.4.3 Principal stresses (σ_1 , σ_2 , σ_3)

The principal stresses are the stresses where the shear stresses at a location are zero. σ_3 is always the largest compressive stress where as σ_1 can be either the smallest compressive or largest tensile stress. σ_2 is an intermediate value. They are defined diagrammatically on Mohr circle in figure 3-13b:

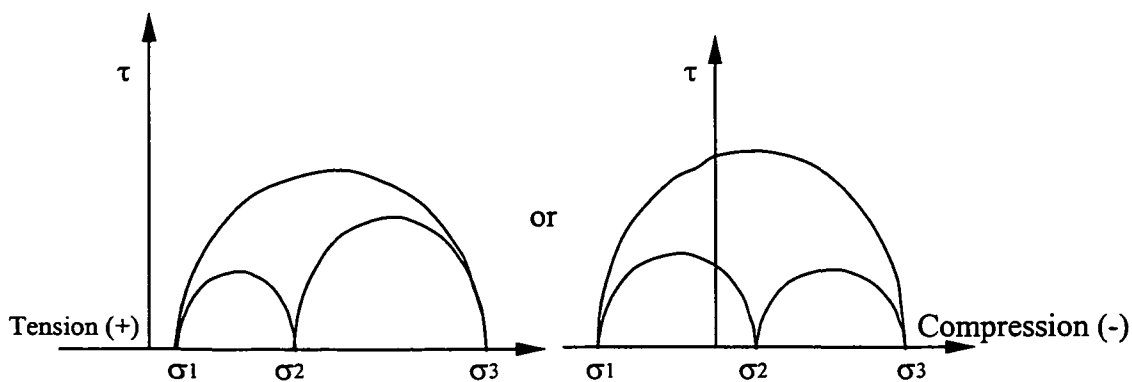


Figure 3- 13b: Principal stresses

The magnitudes of the principal stresses are shown on the appendix. The principal stress ratios (σ_1/σ_3) for structure III were analysed for the three load cases as shown on figures 3-14 to 3-18. From the outputs of the BISAR it is observed that the principal stress ratios (σ_1/σ_3) varies with depth. The principal stress ratios are positive until reaching a depth of 170-180mm within the asphalt layer. This indicates that σ_1 change from compressive to tensile at that depth. From figure 3-14 we can also see that tensile stresses increase at higher rate as compressive stresses decrease at depths lower than 230mm.

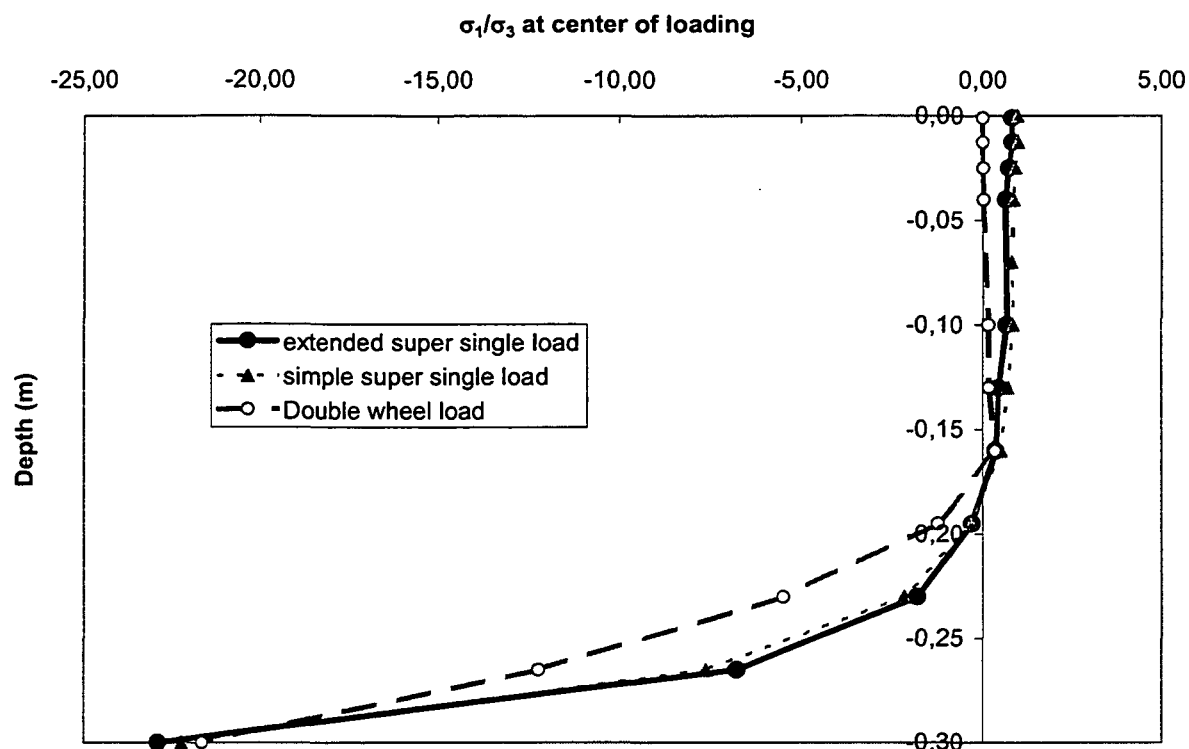


Figure 3-14: Principal stress ratios

The behaviour of the deviator stresses was also studied by looking at the differences between compressive values of σ_1 and σ_3 . The deviator stresses are higher for the extended supersingle load throughout the asphalt layer, than the simple supersingle and the double wheel loads. Below a depth of 150mm it is also seen that the deviator stresses due to simple supersingle load are even higher than the double wheel load. From this one can learn that it needs greater care in considering the type of load for better simulation of σ_1 and σ_3 in the triaxial test.

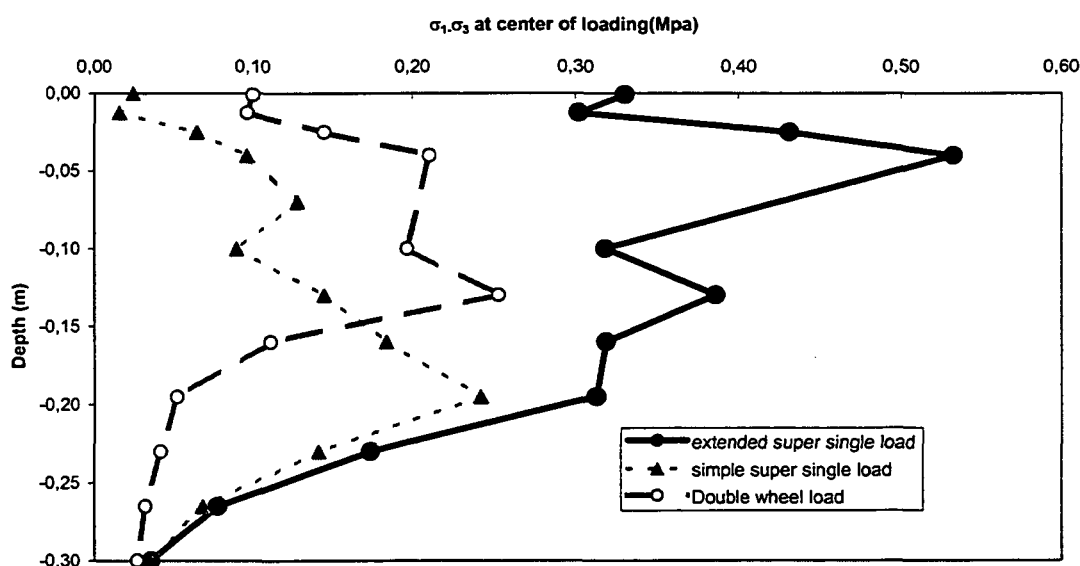


Figure 3-15: Deviator stresses due to wheel load types

The variation of the principal stresses σ_1 and σ_3 is determined in relation with the distance from the load centre. As can be seen from figures 3-16 to 3-18 the principal stress ratios change with distance from load centre. For all load types tensile stresses are not observed at 150mm from load centre for a depth of 160mm. This extends further to a distance of 300 mm for double wheel load.

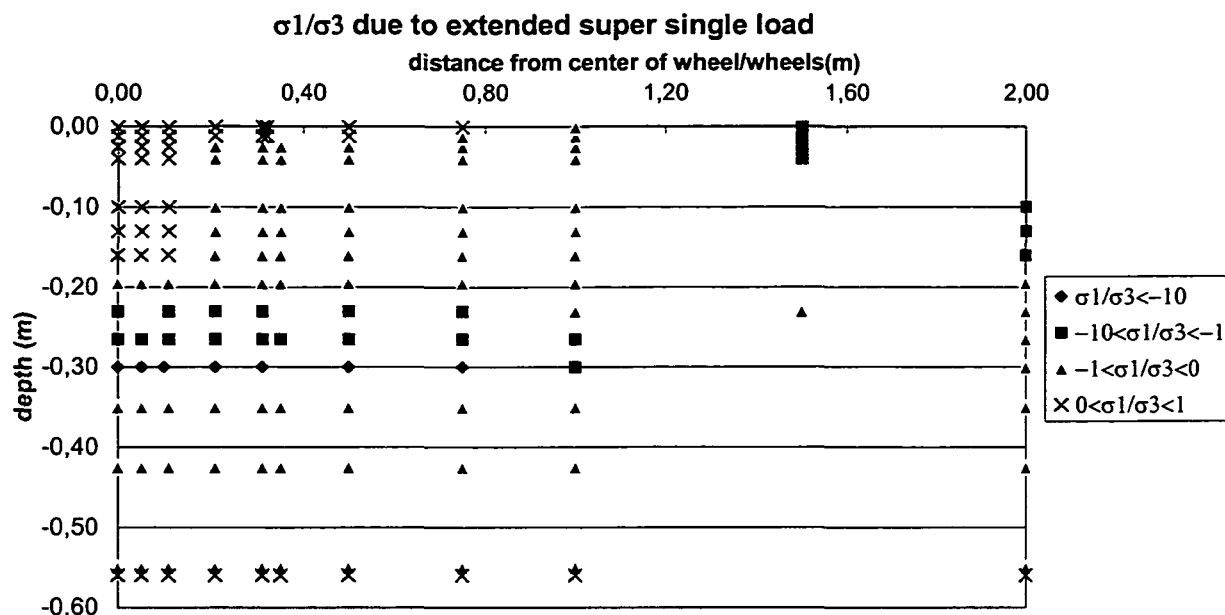


Figure 3-16: Principal stress ratios for extended super single load

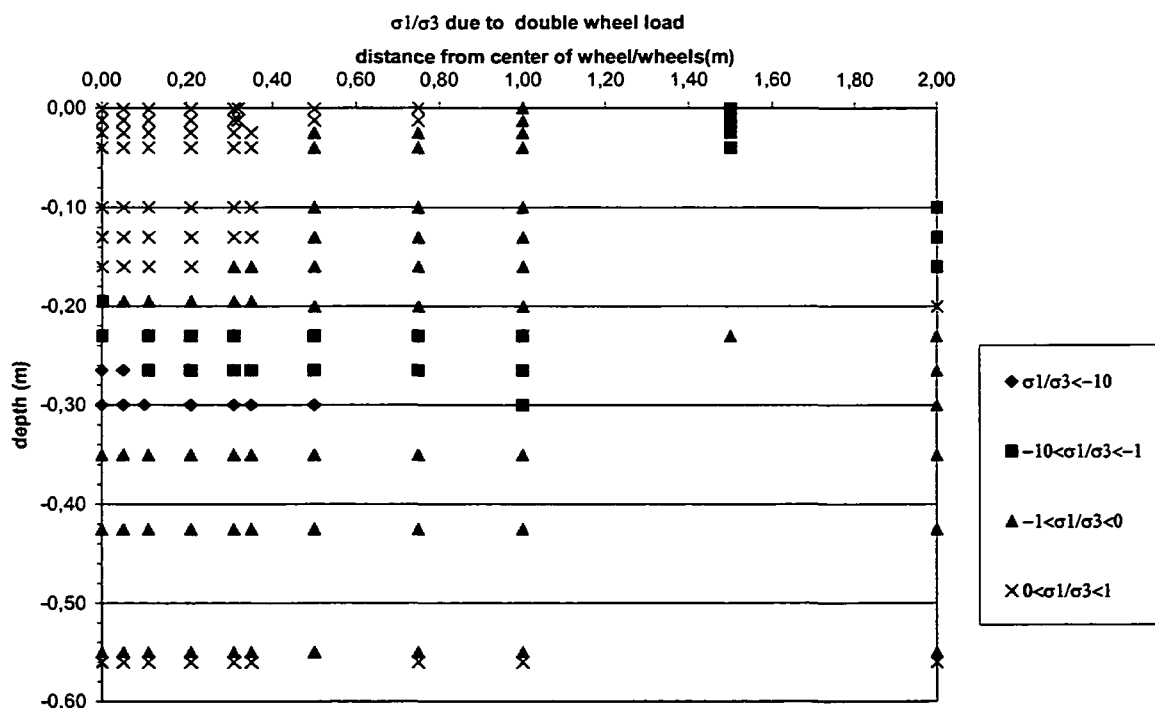


Figure 3-17: Principal stress ratios for double wheel load

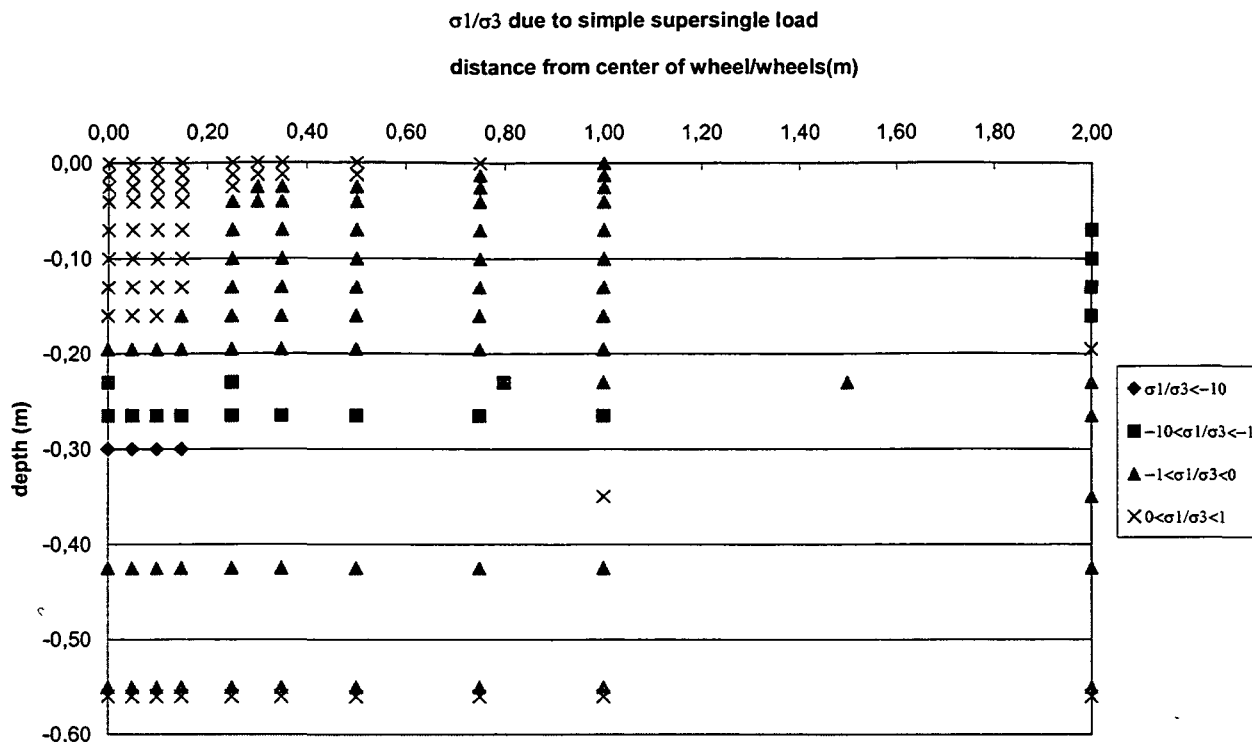


Figure 3-18: Principal stress ratios for simple supersingle load

3.8.5 Effect of thickness of structure on stresses

The three Dutch standard structures have been analysed to see the effect of thickness on the stress distribution due to the simple supersingle load. The variation of principal stress ratios with depth for the three structures are shown in figures 3-19 to 3-21. In these figures one can see that the stress ratios are positive in the top 3/4 of the asphalt layer. This means that tensile principal stresses start being developed at the bottom 1/4 of the asphalt layer.

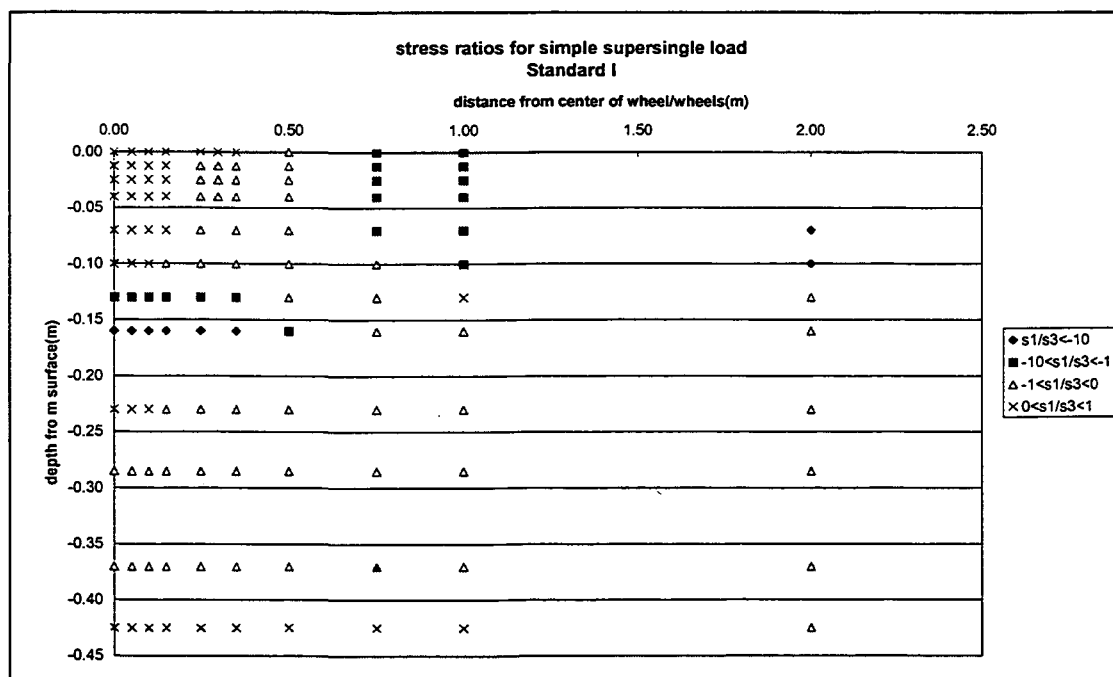


Figure 3-19: Principal stress ratios simple super single load standard I

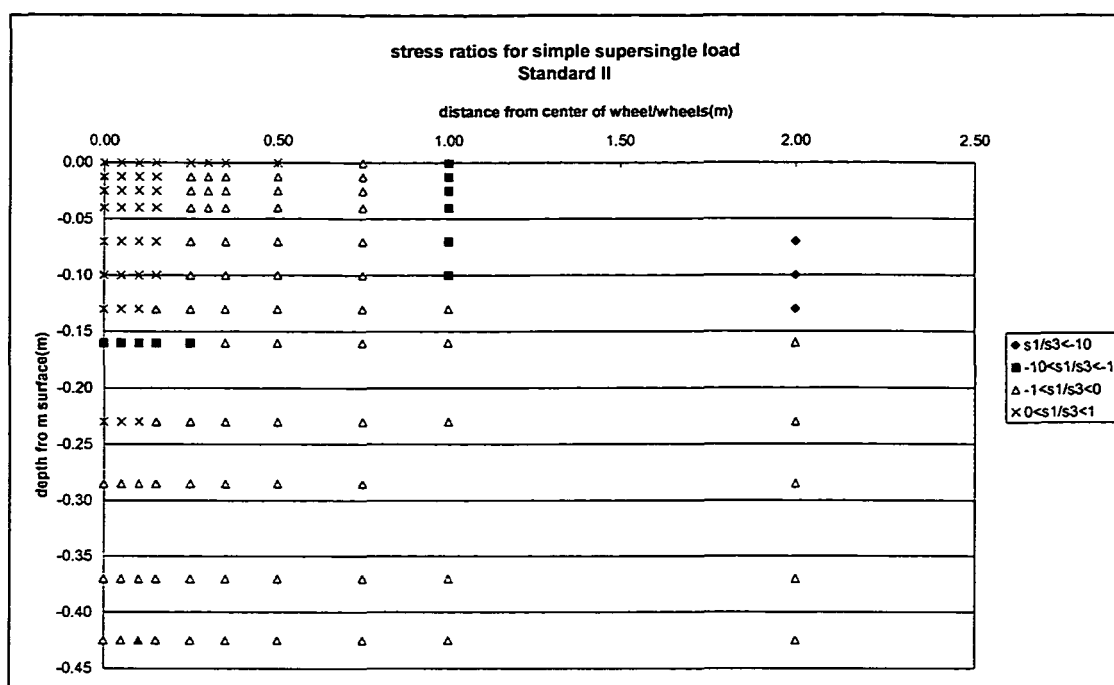


Figure 3-20: Principal stress ratios simple super single load standard II

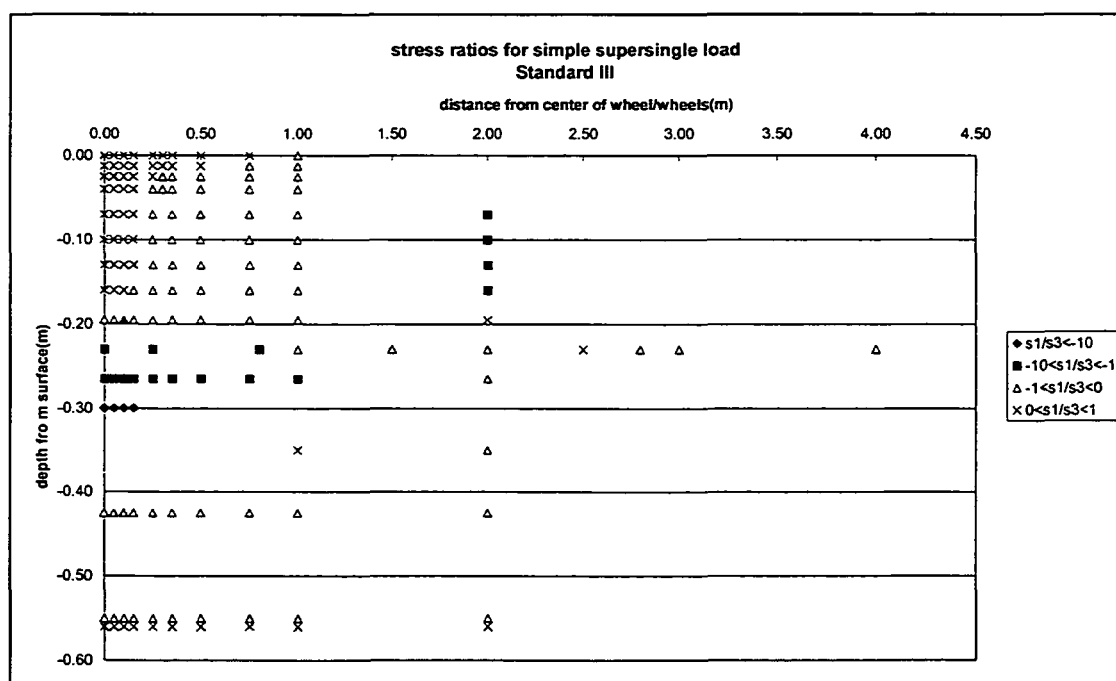


Figure 3-21: Principal stress ratios simple super single load standard III

3.8.6 Re-calculation of stresses

The initial analysis of stresses by BISAR was based on reading of the pulse times from figure 3-7 and on assumptions with respect to stiffness values. Final stress values have to be confirmed by using actual load pulses due to the applied load. This is done by iterating until there is consistency in the stiffness values. Loading times are recalculated from stress contact diameters of BISAR outputs for a speed of 60 km/hr. The iteration process is done only for the simple supersingle load applied on structure III for the purpose of simplicity. It is assumed that the results will not be very much different for structures I and II or for the other loadings.

The radius of contact area is considered as the distance from centre of wheel up to where the vertical stresses is nearly “zero” when compared to the maximum stress. In this study Barksdale’s approach of visually fitting an equivalent sinusoidal curve to each calculated stress curve is used, as it seems a good procedure to estimate the duration of the real stress pulse in triaxial testing [35]. Typical pulse time radius estimations are shown in figures 3-22 and 3-23. It is seen that the BISAR analysis as performed does not result in the same diameter as the diameter of the loaded area at the surface (see figure 3-23 at $z = 0.0$). The resulting diameter where the vertical stress becomes “zero” is higher than the diameter of the loaded area.

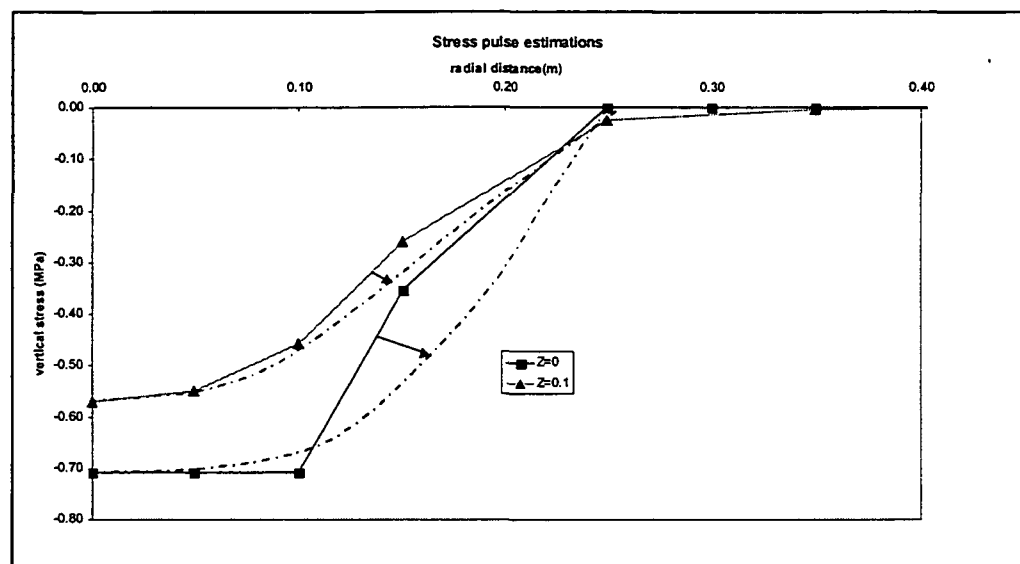


Figure 3-22: Loading radius

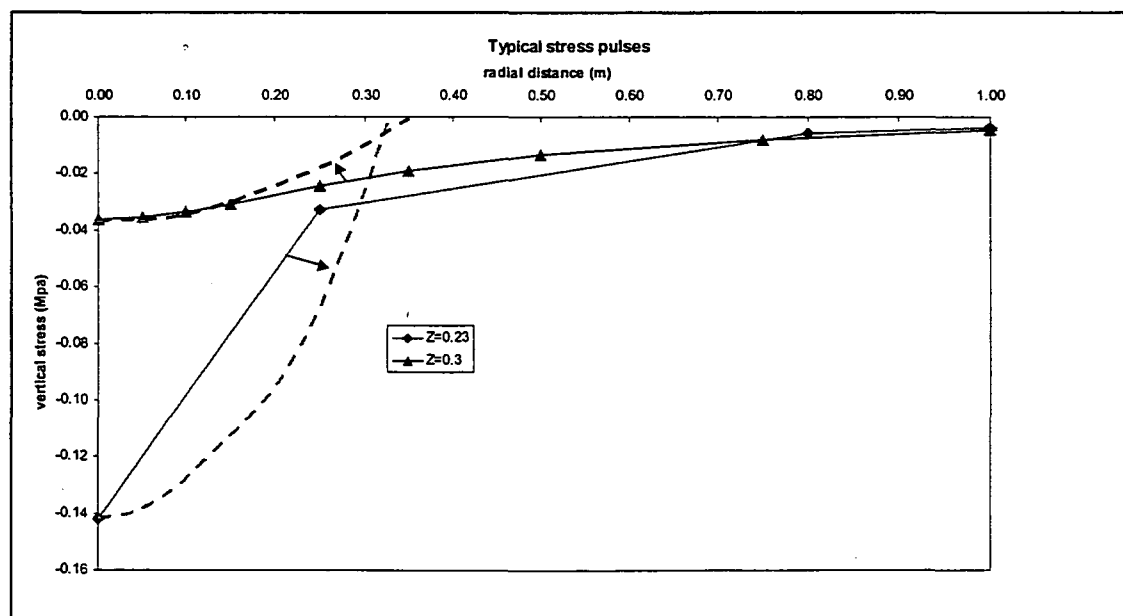
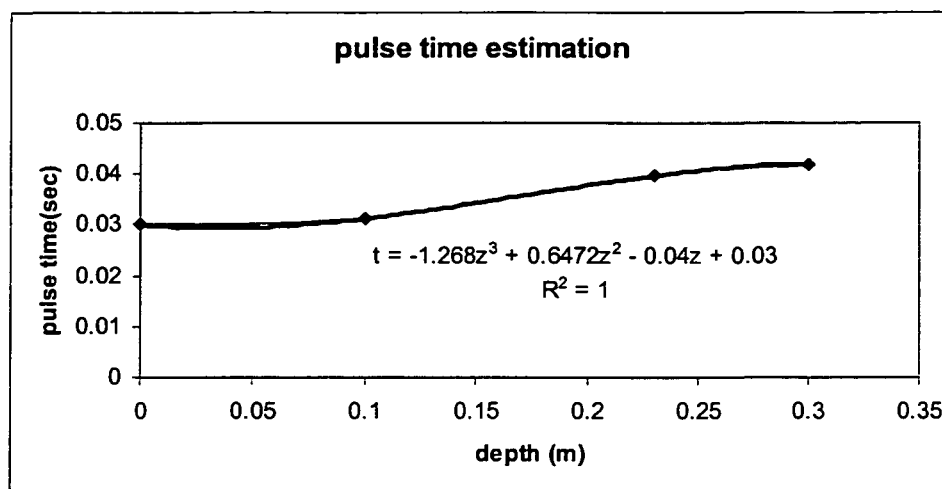


Figure 3-23: Loading radius

Using the typical pulse radiuses in figures 3-22 to 3-23 and speed of 60km/hr the pulse times as shown in table 3-5 are estimated. The pulse times for other depths are estimated by a trend line shown in figure 3-24.

Table 3-5: Pulse times

Depth (m)	contact radius(m)	(pulse time)
0	0.25	0.03
0.1	0.26	0.0312
0.23	0.33	0.0396
0.3	0.35	0.042

**Figure 3-24: Pulse time estimation**

By replacing the loading times of the first round of BISAR analysis with loading times from figure 3-24 the mix stiffness values shown in table 3-6 are obtained for the second round of BISAR calculations for the simple super single load.

Table 3-6: Summary of BISAR inputs for second round

thickness (mm)	Temp (°C)	Poisson's ratio	Type of mix	Vb (%)	Vg (%)	First round BISAR			Second round BISAR		
						Loading time 1 (sec)	Sbit 1 (MPa)	Smix 1 (MPa)	Loading time 2 (sec)	Sbit 2 (MPa)	Smix 2 (MPa)
12,5	45	0,5	DAC	13,2	80,8	0,0125	0,468	300	0,03	0,511	209
12,5	40	0,47	DAC	13,2	80,8	0,0133	2,7	500	0,03	1,35	480
15	38	0,46	DAC	13,2	80,8	0,135	4,01	800	0,029	2,07	676
30	35	0,45	STAC	12,1	81,0	0,014	6,93	1200	0,03	3,69	1317
30	33	0,45	STAC	12,1	81,0	0,015	9,82	1520	0,031	5,56	1040
30	27	0,45	STAC	12,1	81,0	0,016	27,8	3070	0,033	17,4	2240
70	25	0,44	STAC	12,1	81,0	0,0167	36,8	3700	0,035	23,7	2760
70	25	0,43	STAC	12,1	81,0	0,018	35,2	3600	0,037	22,9	2690
250		0,35	subbase					100			100
		0,5	subgrade					50			50

To determine Mix stiffnesses for Sbit < 5 Mpa the Francken formula, on equation 3-6 is used. Where as mix stiffnesses for Sbit > 5 Mpa are estimated by the BANDS model (Van der Poel nomograph). If the stiffness of an upper layer estimated by the Francken formula is higher than the lower layer of the same material, then the lower stiffness value is considered. A second round of BISAR analysis with the recalculated mix stiffnesses was performed. The vertical stress plots were compared with the initial analysis. However, the vertical stresses haven't changed significantly as can be seen from the figures 3-25 and 3-26.

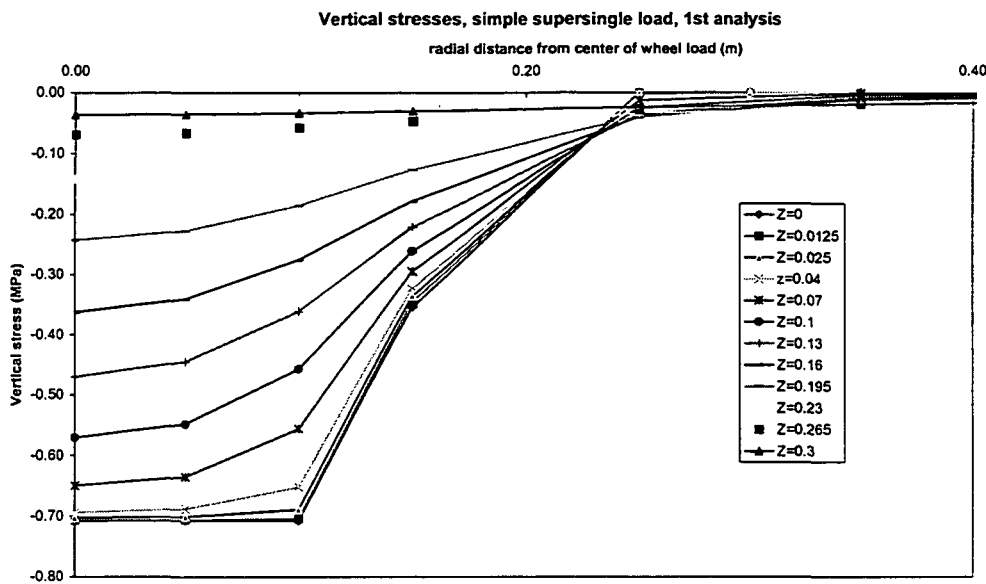


Figure 3-25: Vertical stresses, simple supersingle load 1st analysis

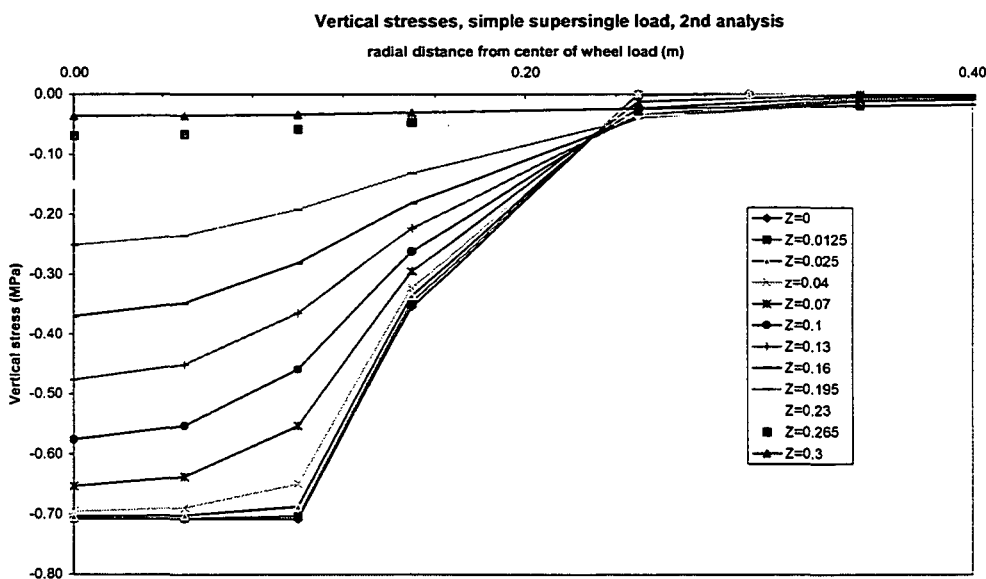


Figure 3-26: Vertical stresses simple super single load, 2nd analysis

If one tries to estimate the pulse time for each depth of the asphalt layer by modifying the stress curves to a half sine curve, as shown on figures 3-23 and 3-24 there would not be significant difference on the loading times. Thus, third round of BISAR analysis is not necessary, as the mix stiffness would be consistent due to same values of pulse times. The final conclusions on stresses that can happen due to wheel loading on the standard III pavement structure can be made at this stage.

3.9 Stress conditions for triaxial test

Potential loading conditions for the triaxial test can be derived from outputs of the BISAR stress analysis. The BISAR analysis provides a complete picture of the compressive, tensile and shear stresses in any point of the pavement and, it also gives the magnitude of the principal stresses and their direction. These stresses are compressive and tensile. Because axial and radial compressive stresses are used in triaxial testing (axial tension is however also a possibility) only the compressive stresses are considered for the testing conditions. This can also be supported by the fact that rutting and permanent deformation calculations, for which triaxial test results are the basis, are mainly based on compressive stresses.

However, to simulate the stress conditions under the pavement into the triaxial test as realistic as possible, one has to consider the variation and magnitude of the stresses due to a load passage. It is important to select those critical stress conditions for the triaxial test that have a great effect on the distress type considered. In the following subsections this is discussed further.

3.9.1 Stress combinations

Stress combinations are selected first by plotting the principal stresses of each point on the Mohr circle; and then the principal stresses with Mohr circles closer to Mohr-Coulomb yield line of the material are selected as the critical stress combinations. With this approach the Mohr circles due to principal stresses of the extended super single load on standard III for the DAC and STAC layers are shown in figures 3-27 and 3-28. The Mohr-Coulomb yield lines for DAC and STAC are assumed at 40° with the horizontal line of ' σ '. The typical stress combinations selected for DAC and STAC layers of structure III are shown in table 3-7. For the STAC layer the stresses in the top 160 mm are considered since they have higher compressive stress values.

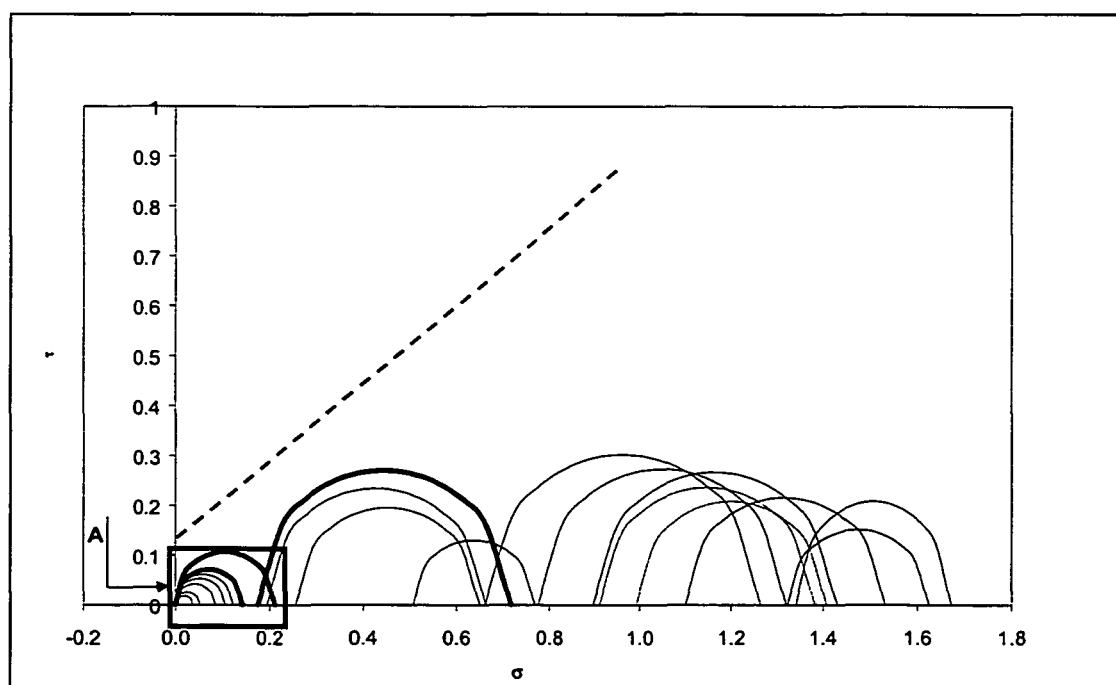


Figure 3-27: Principal stresses for DAC

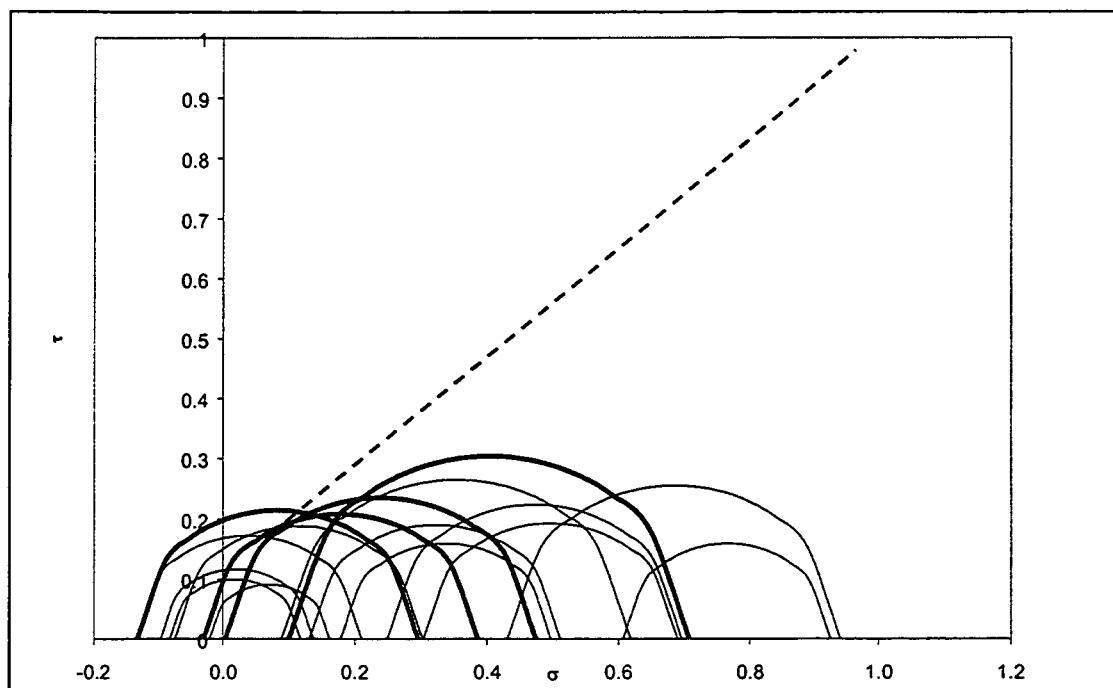


Figure 3-28: Principal stresses for STAC

Table 3-7: Selected stress combinations

DAC				STAC			
Distance from load centre (m)	Depth (m)	σ_1 (kPa)	σ_3 (kPa)	Distance from load centre (m)	Depth (m)	σ_1 (kPa)	σ_3 (kPa)
0.21	0.025	0	150	0.11	0.16	0	300
0.21	0.04	0	220	0.21	0.10	0	390
0.11	0.04	200	720	0.11	0.13	0	480
				0.11	0.04	100	710

In figures 3-27 and 3-28 the stress circles which are considered to be relevant for the triaxial tests are indicated by bold lines. The location at which these stresses occur and their magnitude are tabulated in table 3-7. With respect to the stress circles in figures 3-27 it is noted that in fact all stress circles in area 'A' are close to the Mohr-Coulomb failure line. The small stress circles however are not being considered as important for two reasons:

- The stresses indicated by those circles are small,
- Figure 3-27 only gives the stresses due to the wheel load; in reality one should add the dead weight stresses to the stresses shown. Adding these dead weight stresses means that all circles move to the right resulting in less critical conditions; this effect is the largest on the small circles.

3.9.2 Rotation of stresses

As mentioned in section 2.4.2 triaxial tests are done on vertically placed specimens loaded with vertical dynamic load and constant horizontal confinement. The triaxial test however is not capable of simulating shear stresses and rotation of principal stresses. In the pavement the principal stresses are only vertical and horizontal under the centre of the wheel load. When simulating outside the centre of the wheel load shear stresses have to be considered for better simulation of reality.

However in the triaxial test this is simplified by neglecting the shear stresses. If one wants to take into account the rotation of the principal stresses one must:

- know the rotation of the stresses,
- modify the triaxial test to cater for this rotation.

In order to obtain information on the rotation of the principal stresses, figure 3-29 was made. As one can observe from fig. 3-29, significant rotation takes place. In order to obtain information on the magnitude of the shear stresses that have to be applied on the specimen in order to allow rotation of the principal stresses to be made, figure 3-30 was made. These figure shows a number of interesting things:

- the vertical and horizontal stresses have a different duration (distance to load centre can be transformed in time) which indicates kneading takes place.
- the equipment should be capable of developing shear stresses with a maximum magnitude of about 0.2 MPa.
- the shear stresses are out of phase with the horizontal and vertical stresses.

Modification of the triaxial test to take into account the shear stresses makes the test very complicated and not suitable at all for mixture design, quality control and quality assurance procedures. Therefore, it was decided to analyse only the change in vertical and horizontal stresses as a result of a wheel passage and at those stress levels as representative for triaxial test conditions. The disadvantage of course is that the effect of the shear stresses is neglected but it is important to see the consequences there of.

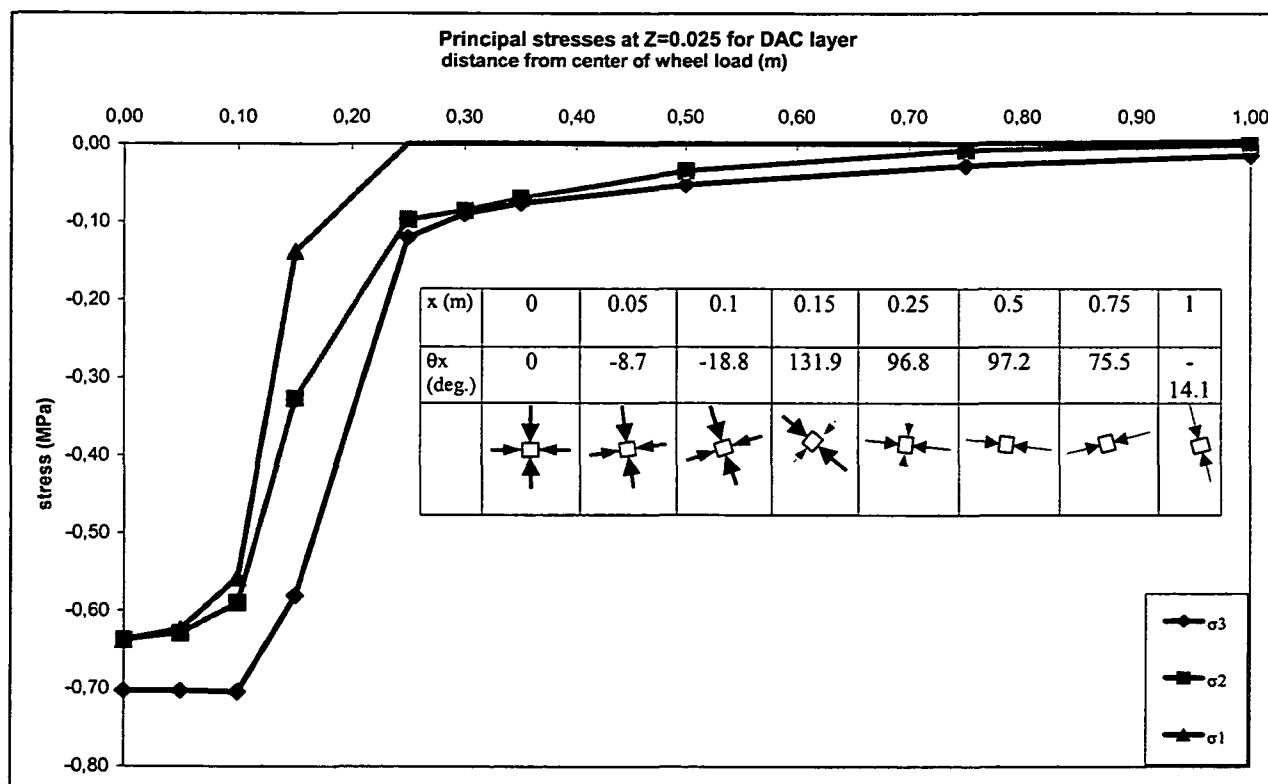


Figure 3-29: Principal stresses and their rotation angle

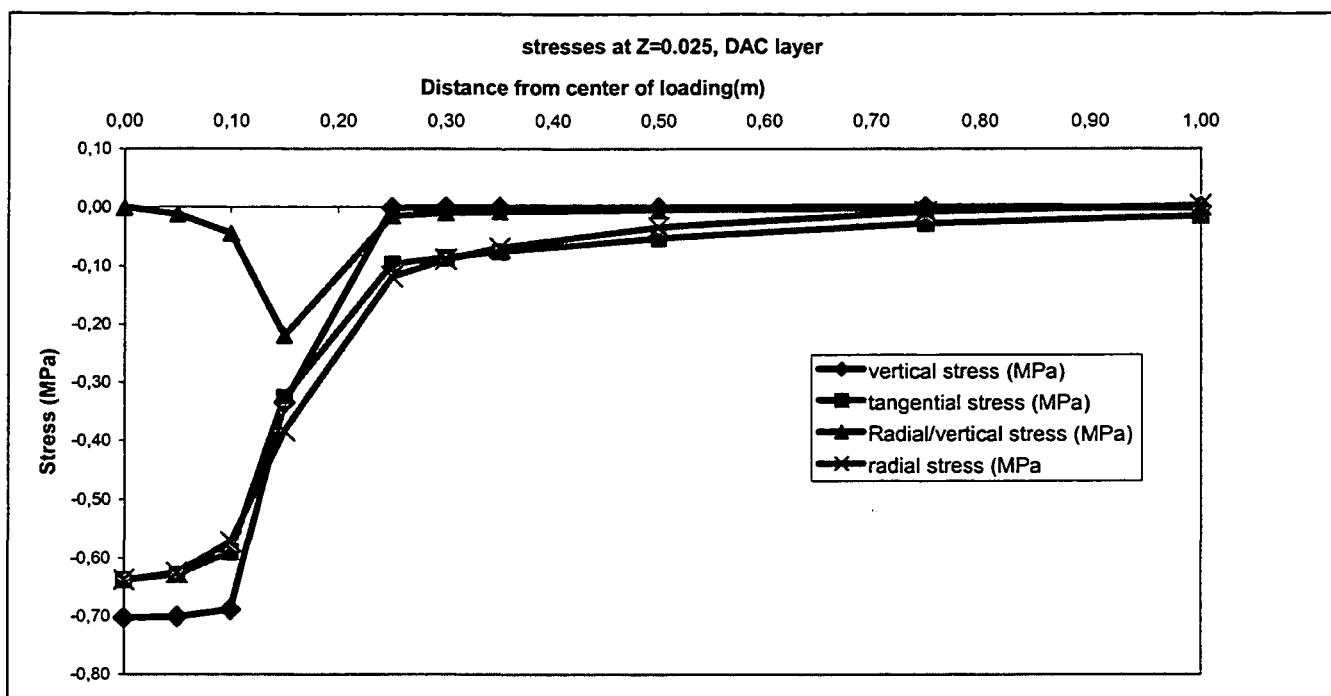


Figure 3-30: Stresses for a DAC layer at depth of 25mm

To see the effect of neglecting the shear stresses, a comparison is made with the principal stresses and their rotation angle for DAC and STAC. In similar way to the DAC, the stresses for STAC layer are shown in figures 3-31 and 3-32. By taking the smallest and largest stresses among radial, tangential and vertical stresses for distances of 0, 0.05, 0.10 and 0.15m from load centre, and the principal stresses for the same points the values of deviator stresses shown in figure 3-33 and 3-34 are obtained.

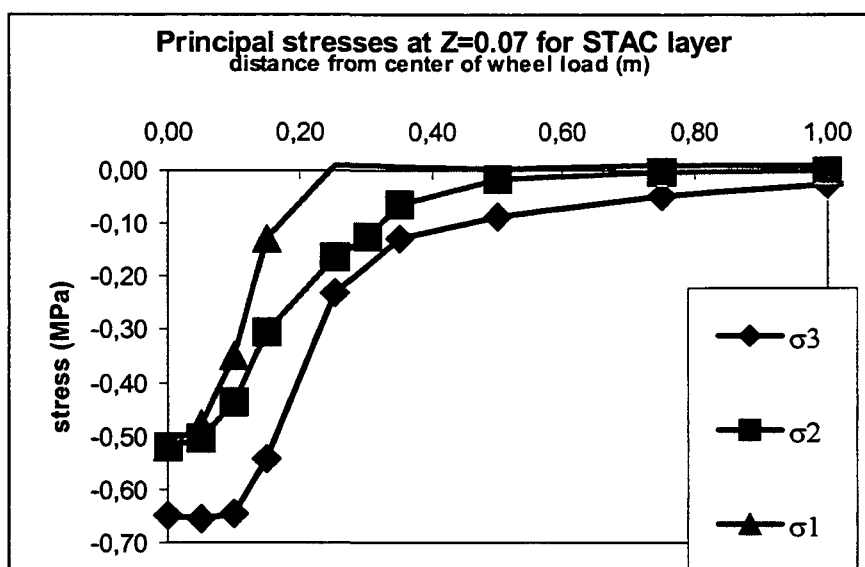


Figure 3-31: Principal stresses for STAC

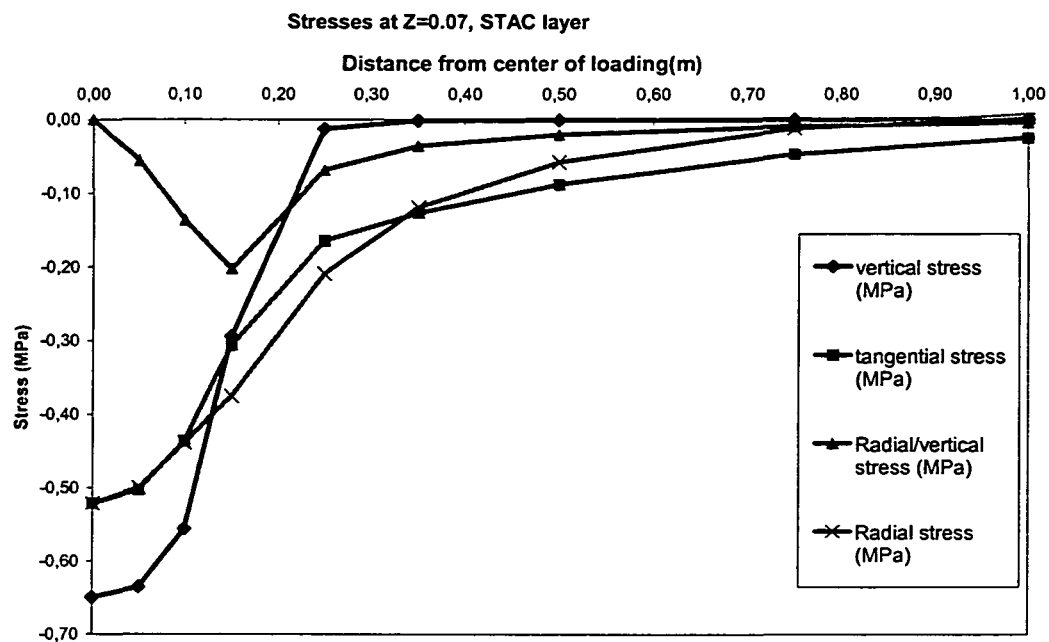


Figure 3-32: Stresses in STAC layer

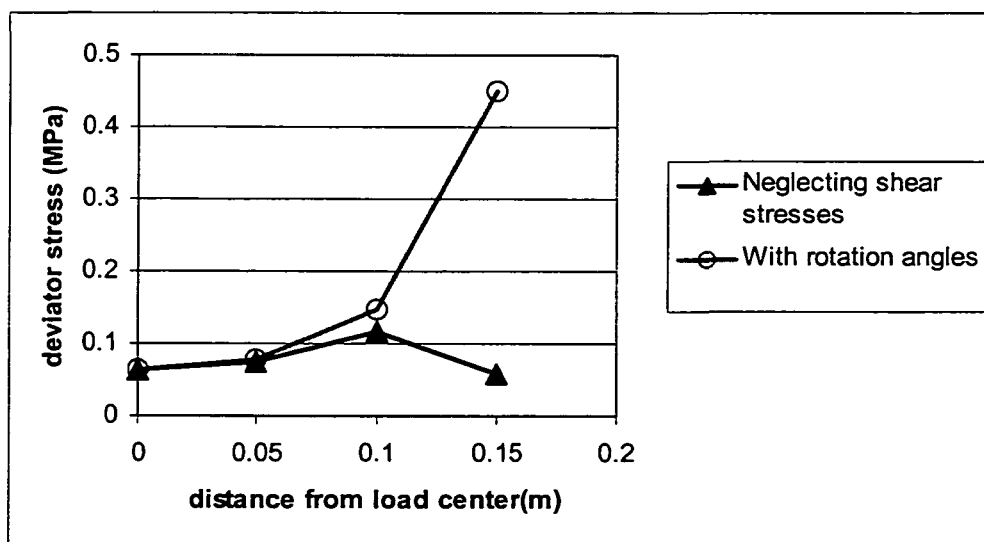


Figure 3-33: Comparison of deviator stresses for DAC

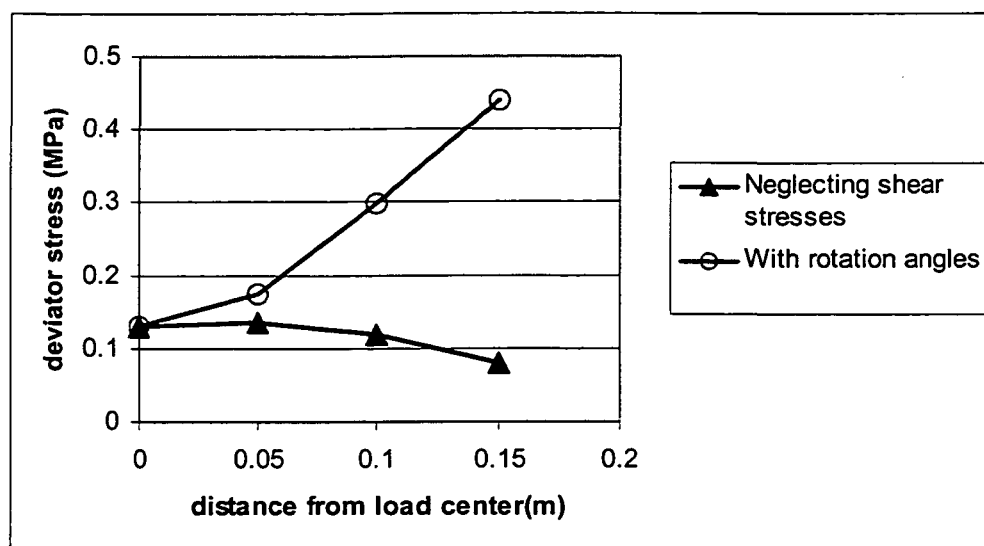


Figure 3-34: Comparison of deviator stresses for STAC

As we can see from figures 3-33 and 3-34 the deviator stresses derived from the vertical and horizontal stresses, thus by neglecting the shear stresses, are lower than the deviator stresses derived from the principal stresses. It implies that if one considers the vertical and horizontal stresses without the shear stresses, one ignores the significant effect of the shear stress that could have produced higher deviator stress. On the other hand if one wants to apply the principal stresses by rotating the specimen, one will have deviator stresses higher than neglecting the shear stresses. From this argument it seems that rotating specimens with rotation angles of the principal stresses is a better simulation of reality. However, rotating the specimen with rotation angle of the principal stresses in the triaxial test by itself is a difficult scenario.

Based on this information the following option to arrive to stress conditions for the triaxial test was derived.

- consider the vertical stresses at 0, 0.05, 0.10 and 0.15m from the load centre which are given in figures 3-30 and 3-32,
- use the deviator stress given in figures 3-33 and 3-34; using this approach one arrives to the stress combinations shown on table 3-8.

Table 3-8: Selected stress combinations

DAC			STAC		
Distance from load centre (m)	deviator stress (kPa)	Vertical stress (kPa)	Distance from load centre (m)	deviator stress (kPa)	Vertical stress (kPa)
0	65.5	703	0	130	650
0.05	80.0	703	0.05	176	636
0.10	146.5	690	0.10	298	556
0.15	442.0	380	0.15	414	375

3.9.3 Stress pulse time

In the tradition of DWW and TU Delft there is a usage of '0.2 sec' stress pulse time and '0.8 sec' rest time in the simulation of reality by means of the triaxial test. However if one observes the real situation which is simulated by the BISAR stress analysis it seems that specimens in the lab are loaded for a longer time than the reality. If we take e.g. a contact radius of 0.25m (this can be derived from the stress Vs distance diagram of figure 3-35) and assuming a speed of 60 km/hr (16.7 m/s), the pulse time can be calculated as:

$$t = d/v = 2 \cdot 0.25 / 16.7 = 0.03 \text{ sec}$$

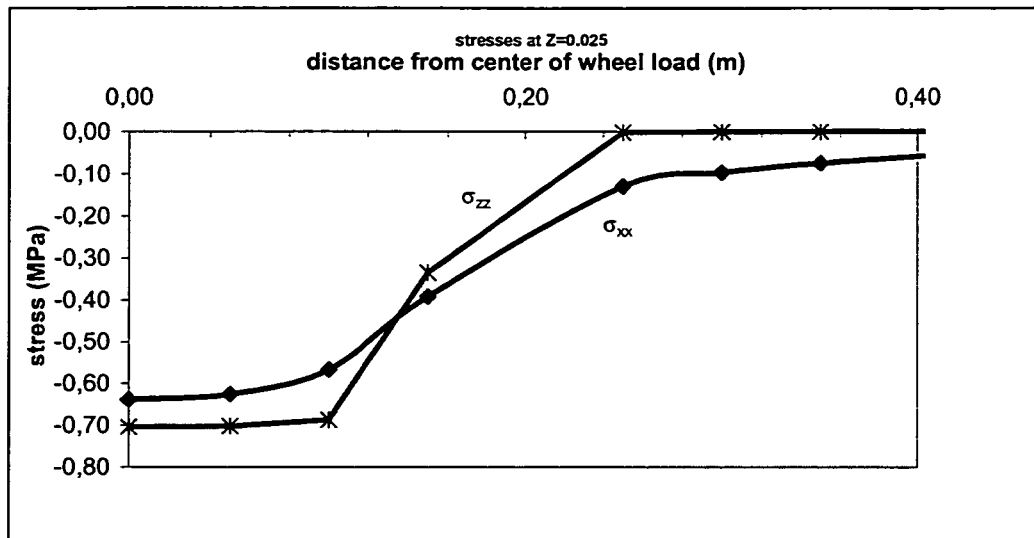


Figure 3-35: Vertical and radial stresses at $Z=0.025$

Not only the duration of the stress pulse time is of importance also the shape of the stress pulse on the triaxial test should be considered. From the stress curve in figure 3-35, we observe that the load pulse is more of a half-sine curve than a block, which is commonly used in the lab.

Another area of interest in the triaxial test is the simulation of the horizontal stresses. As we can see from figure 3-35, both the vertical and horizontal stresses are varying with distance to the load centre. However, horizontal stresses in the lab are kept constant while applying a dynamic vertical stress.

3.10 Conclusions

Based on the analysis presented in this study, the following conclusions can be drawn.

- a. Stress analyses by means of the BISAR program are an excellent way to obtain information on the complex way of the stress field as particular points of interest are changing as a result of wheel passage.
- b. The results of the stress analyses are strongly influenced by the quality of the input. Especially accurate modelling of the stiffness and the load is of higher importance.
- c. Given the complexity of the stress field and the fact that rotation of the principal stresses takes place in reality, it is not simple to derive stress conditions which can be used in the triaxial test.
- d. Given 'c' one can also conclude that without significant modification of the triaxial test as it is commonly used, accurate modelling of the permanent deformation behaviour will be difficult.
- e. Given 'd' one can conclude that the triaxial test in its current shape is useful for ranking of asphalt mixtures but great care should be given to the use of the test results for permanent deformation predictions.

4 References

1. Houben, L.J.M., A.F.H.M. Visser and A. E. van Dommelen , INTRACK Research into Rutting of Asphalt Concrete Test Pavement 1999/2000, Report 7-00-200-28M, TU Delft, June 2000.
2. Miradi, A., L.J.M. Houben and A. E. van Dommelen , *Cyclic Loading Triaxial Tests 1999/2000 on Asphaltic Materials of LINTRACK Test Pavements*, Measuring Report 7-00-200-30M, TU Delft, July 2000.
3. Molenaar, A.A.A., Road Materials Part III-Asphaltic Materials , Lecture Notes, IHE Delft & TU Delft, 1993.
4. Molenaar, A.A.A., *Structural Design of Pavements Part III-Design of Flexible Pavements*, Lecture Notes, IHE Delft & TU Delft, 1998.
5. Molenaar, A.A.A., *Structural Design of Flexible Pavements Design II*, Lecture Notes, IHE Delft & TU Delft, 2000.
6. Molenaar, A.A.A., *Stresses, Strains and Failure Pavement Design II*, Lecture Notes, IHE Delft & TU Delft, 2000.
7. Miradi, A., L.J.M. Houben and A. E. van Dommelen , *Analysis of Triaxial Test Results at 40 °C on Asphalt Samples from LINTRACK Test Section with DAC 80/100 Wearing Course*, Report 7-01-200-36M, TU Delft & DWW, May 2001.
8. Lai, J.S., *Evaluation of the Effect of Gradation of Aggregate on Rutting Characteristics of Asphalt Mixes*, Final Report, School of Civil Engineering, Georgia Institute of Technology, Atlanta, Georgia, August 1998.
9. Witczak, M.W., *Design of Full-Depth Asphalt Airfield Pavements* , RR 72-2, The Asphalt Institute, College Park, 1972.
10. Road and Hydraulic Engineering Division, Ministry of Transport, *Pavement Design Guide* (in Dutch), Delft, 1991.
11. Low, B.H., S.A.Tan, and T.F.Fwa, *Analysis of Marshall Test Behaviour with Triaxial Test Determined Material Properties*, Journal of Testing and Evaluation, vol. 21, No. 3, pp 192-198, May 1993.
12. Scullion, T., J. Uzan, S. Nazarian and B. Briggs, *Future Directions in Characterising Strength and Deformation Properties of Pavement Layers*, TRB Millennium Paper, Committee Report, A2BO5, <http://www.nas.edu/trb/publications/millennium/00017.pdf> .
13. Molenaar, J.M.M., H.A. Verburg and G.E. Westera, *Characterisation of Permanent Deformation Behaviour of Asphalt Mixtures*, W-Dww-95.535, DWW, Delft, 1995.
14. Southgate, H.F. , *An Evaluation of Temperature Distribution within Asphalt Pavements and its relationship to Pavement deflection*, Kentucky Department of Highways, April 1968.
15. Huang, Y. H., *Pavement Analysis and Design*, Prentice-Hall Inc., Englewood Cliffs, New Jersey, 1993.
16. Nataatmadja, A ., and A. K. Parkin , *Axial Deformation Measurement in Repeated Load Triaxial Testing*, Technical Note, Geotechnical Testing Journal, GTJODJ, vol. 13, No. 1, pp 45-48, March 1990.
17. CROW, *RAW Standard Conditions of Contract for Works of Civil Engineering Construction*, Ede, 2000.
18. Alavi, S.H. and C.L. Monismith, *Time and Temperature Dependent Properties of Asphalt Concrete Mixes Tested as Hollow Cylinders and Subjected to Dynamic Axial and Shear Loads*, Proceedings, Journal of AAPT from Proceedings of the Technical Sessions, vol. 63, St Louis, Missouri, March 21-23, 1994.
19. Francken, L., *Permanent Deformation Law of Bituminous Road Mixes in Repeated Triaxial Compression*, Proceedings, Fourth International Conference Structural Design of Asphalt Pavements, vol. 1, University of Michigan, Ann Arbor, August 1977.

20. CEN., *Bituminous Mixtures – Test Methods for Hot Mix Asphalt-Part 25: Cyclic Compression Test*, Draft European Standard, Brussels, December 2001.
21. Sayegh G., *Visco Elastic Properties of Bituminous Mixtures*, Proceedings, 2nd International Conference on Structural Design of Asphalt Pavements, Proceedings, pp 743-745, ICSDAP, University of Michigan, Ann Arbor, 1967
22. Makanga, D.S. , *Size Effects on Permanent Deformation of Asphalt at High Temperatures*, Msc. Thesis, IHE Delft, March 2002.
23. DWW, *Eindrapportage Inleidend Landelijk Vergelijkend Onderzoek van de Triaxial Proef*, Concept, DWW, Reprot No. 072, 2001.
24. Parajuli, U. , *Stress Dependent Analysis of Asphalt Concrete*, Msc. Thesis, IHE Delft, March 2002.
25. Erkens, S.M.J.G. and M.R. Poot, *The Uniaxial Compression Test –Asphalt Concrete Response (ACRe)*, Report, TU Delft, Report 7-98-117-4, 2000.
26. Yoder, E.J. and M.W. Witczak, *Principles of Pavement Design*, second edition, John Wiley & Sons, Inc. , New York, 1975.
27. Lekarp, F., U. Isacsson and A. Dawson, *State of the Art. II: Permanent Strain Response of Unbound Aggregates*, Paper, Journal of Transportation Engineering, Vol. 126, No. 1, pp 76-83, January/ February 2000.
28. Houben, L.J.M and J.A.M. Kalf, *Cyclic Loading Triaxial Tests on Swiss Asphaltic Material*, Report 7-99-114-11M, TU Delft, March 1999.
29. Duskov, M , *One Dimensional Final Element Calculations of the Temperature Distribution in Road Pavement Structures with and with out EPS*, Report 7-90-211-1, TU delft, august 1990.
30. Sousa, J.B., M. Solaimanian and S.L.Weissman, *Development and Use of the Repeated Shear Test (Constant Height) : An Optional Superpave Mix Design Tool*, SHRP-A-698, SHRP, Washington, DC, 1994.
31. CROW, *Bepaling Asfalttemperatuur met BELLS3-Model*, Bijlage VII, <http://www.crow.nl/> , 1992.
32. Francken, L., *Complex Modulus of Bituminous Mixes* (in French); Bulletin de Liaison des Laboratoires des Ponts et Chaussées, Special Volume, LCPC, pp. 181-198 , Paris, December 1977.
33. Groenendijk, J., *Accelerated Testing and Surface Cracking of Asphaltic Concrete Pavements*, Ph.D. Thesis, Delft, 1988.
34. SHELL, *BISAR 3 User Manual*, Bitumen Business Group, The Hague, May 1998.
35. Barksdale, R. D., *Compressive Stress Pulse Times in Flexible Pavements for Use in Pavement Design*, Highway Research Record, No. 345, pp 32-44, HRB, Washington, D.C., 1971.
36. Jacobs, M.M.J. , *Crack Growth in Asphaltic Mixes*, Delft, 1995.
37. Verstraeten, J., *Stresses and Displacements in Elastic Layered Systems, General Theory –Numerical Stress Calculations in Four Layered Systems with Continuous Surfaces*, Proceedings, 2nd International conference in Structural Design of Asphalt Pavements, pp 277-290, Ann Arbor, 1967.
38. DWW, *Temperatuurmetingen Mei t/m Augustus 1989 t/m 1989*, Deelrapport, MAO-R-90033, MEVA3 TU Delft, 1990.
39. Brown, S.F. , *Determination of Young's Modulus for Bituminous Materials in Pavement Design*, Highway Research Record, No. 431, pp 38-49, Washington, D.C., 1973.

APPENDIX A

Draft European Standard for the Triaxial Cyclic Compression Test

PART B : TRIAXIAL CYCLIC COMPRESSION TEST

Foreword

The present draft is based on the existing French standard for the triaxial cyclic compression test (NF P 98253-2), on a draft British standard (DD 226) and on Belgian and Dutch experiences with characterising bituminous mixtures by this method.

CONTENTS	Page
1. SCOPE	B-2
2. NORMATIVE REFERENCES	B-2
3. DEFINITIONS	B-3
4. SYMBOLS AND ABBREVIATIONS	B-3
5. PRINCIPLE OF THE TEST	B-4
6. APPARATUS	B-5
7. SPECIMEN PREPARATION	B-6
8. CONDITIONING	B-8
9. TEST PROCEDURE	B-8
10. CALCULATION AND EXPRESSION OF RESULTS	B-10
11. REPORT	B-11
12. PRECISION	B-12
INFORMATIVE ANNEX	B-13
FIGURES	B-14

1. SCOPE

This Standard describes the method for determining the creep characteristics of bituminous mixtures by means of the triaxial cyclic compression test. In this test a cylindrical specimen is subjected to a static confining stress and a cyclic axial stress.

The purpose of this test is to determine the resistance to permanent deformation of a bituminous mixture. The test is most often used for the purpose of evaluation and development of new types of mixtures.

Specimens prepared in the laboratory or cored from the road can be used. The maximum size of the aggregates is 32 mm.

2. NORMATIVE REFERENCES

This European Standard incorporates by dated or undated reference, provisions from other publications. These normative references are cited at the appropriate places in the text and the publications are listed hereafter. For dated references, subsequent amendments to or revisions of any of these publications apply to this European Standard only when incorporated in it by amendment or revision. For undated references the latest edition of the publication referred to applies.

- | | |
|---------------|--|
| prEN 12697-6 | Bituminous mixtures - Test methods for hot mix asphalt - Part 6: Determination of bulk density of bituminous specimens by hydro-static method or by dimensions |
| prEN 12697-9 | Bituminous mixtures - Test methods for hot mix asphalt - Part 9: Determination of reference density |
| prEN 12697-29 | Bituminous mixtures - Test methods for hot mix asphalt - Part 29: Determination of the dimensions of bituminous specimen |
| prEN 12697-30 | Bituminous mixtures - Test methods for hot mix asphalt. Specimen preparation by impact compactor. |
| prEN 12697-31 | Bituminous mixtures - Test methods for hot mix asphalt. Specimen preparation by gyratory compactor. |
| prEN 12697-33 | Bituminous mixtures - Test methods for hot mix asphalt. Specimen preparation by slab compactor. |
| prEN 12697-38 | Bituminous mixtures - Test methods for hot mix asphalt - Part 38: Test equipment & calibration |

3. DEFINITIONS

For the purposes of this standard, the following definitions apply:

Contact area: The contact area is the portion of the upper loading platen that is in contact with the specimen.

Haversine: A haversine is a sine offsetted by a static signal equal to the amplitude of the sine (see fig. B-2a).

Permanent deformation : The permanent deformation of the specimen is here defined as the cumulative axial deformation after a given number of load applications.

Creep curve: The creep curve gives the cumulative axial strain (expressed in %) of the specimen as a function of the number of load applications. Generally the following stages can be distinguished (see figure B-1) :

- stage 1: the (initial) part of the deformation curve, where the slope of the curve decreases with increasing number of loading cycles;
- stage 2: the (middle) part of the deformation curve, where the slope of the curve is quasi constant;
- stage 3: the (last) part of the deformation curve, where the slope increases with increasing number of loading cycles.

Depending on the testing conditions and on the mix, one or more stages may be absent.

Accuracy class:

The permissible measuring error, expressed as a percentage, in the output signal of a transducer.

Measuring error:

The difference between the true value of the physical quantity and the value indicated on the measuring instrument, expressed as a percentage of the true value.

4. SYMBOLS AND ABBREVIATIONS

N	:	number of load applications;
h_0	:	original height after preload of the specimen [mm]
h_N	:	height of the sample [mm] after N load applications;
Δh_N	:	cumulative axial deformation [mm] of the specimen after N load applications
ε_N	:	cumulative axial strain of the specimen after N load applications:
		Can be expressed in
		[mm/mm] : $\varepsilon_N = (h_0 - h_N)/h_0$;
		[%] : $\varepsilon_N = 100 \times (h_0 - h_N)/h_0$;
		[μ strain] : $\varepsilon_N = (h_0 - h_N)/h_0 \times 10^6$;
σ_c	:	static confining stress [kPa] (all around the specimen);
σ_v	:	amplitude of the haversinusoidal pressure [kPa];
σ_B	:	height of the block-pulse [kPa];
f	:	the frequency of the haversinusoidal load [Hz];
T_0	:	rest period [s], in case of block-pulse loading;
T_1	:	pulse duration [s], in case of block-pulse loading;

- $\sigma_a(t)$: cyclic axial pressure [kPa], as a function of time;
 In case of haversinusoidal pressure, $\sigma_a(t)$ is defined by:

$$\sigma_a(t) = \sigma_v \cdot (1 + \sin(2\pi \cdot f \cdot t)).$$
- f_c : creep rate [microstrain/loading pulse]

5. PRINCIPLE OF THE TEST

This method determines the resistance to permanent deformation of a cylindrical specimen of bituminous mixture. The specimen may be either prepared in the laboratory or be cored from the road.

A cylindrical test specimen, maintained at elevated conditioning temperature, is placed between two planparallel loading platens. The specimen is subjected to a static confining pressure, σ_c , on which a cyclic axial pressure $\sigma_a(t)$ is superposed. The cyclic axial pressure can be :

- a haversinusoidal pressure $\sigma_a(t)$, with amplitude σ_v , as represented in figure B-2a. The resulting total axial pressure is: $\sigma_c + \sigma_a(t) = \sigma_c + \sigma_v (1 + \sin(2\pi \cdot f \cdot t))$. Rest periods can applied.
- a block-pulse pressure $\sigma_a(t)$, with height σ_B , as represented in figure B-2b. The resulting total pressure is: $\sigma_c + \sigma_a(t)$.

In both cases, a small dead load of maximum $0,02 \cdot \sigma_v$ (for haversine loading) and $0,02 \cdot \sigma_B$ (for block-pulse loading) is allowed.

During the test the change in height of the specimen is measured at specified numbers of load applications. From this, the cumulative axial strain ϵ_N (permanent deformation) of the test specimen is determined as a function of the number of load applications. The results are represented in a creep curve as given in figure B-1. From this, the creep characteristics of the specimen are computed.

NOTE 1: The outcome of the test is dependent on the stress conditions, on the testing temperature, the frequency and rest period and on the dimensions of the test specimens. Results obtained with a haversinusoidal loading cannot be quantitatively compared to those obtained with block-pulse loading, because of the presence of rest periods and the different shape of the signal. Results of triaxial compression tests can only be fully compared, if they are obtained under the same testing conditions. Also, in case that the outcome of the test is used to check on the acceptability of a given mixture, the results are to be evaluated with respect to specific requirements related to well-defined testing conditions.

6. APPARATUS

6.1 Measuring instruments and accessories needed

- Test system, as described in 6.2;
- Balance and other equipment required to determine the bulk density in accordance with prEN12697-6;
- Vernier callipers or other suitable apparatus to determine the specimen dimensions in accordance with prEN12697-29;
- Drying cabinet, temperature between 15 and 25 °C;
- Storage area, temperature between 0 and 10 °C.

6.2 Test system

6.2.1 General

The axial loading system consists of two steel loading platens between which the specimen is placed. The static confining pressure and the axial cyclic pressure are applied by means of a servo-hydraulic, pneumatic, electro-magnetic or other suitable system, able to generate the required pressures with an accuracy of $\pm 1.0\%$ at least.

The specimen shall be put in a rubber foil to separate the specimen from the confining medium. A direct contact between confining gases (air) or liquids (water, oil) on one hand and the specimen on the other hand must be prevented.

Depending on the way of applying the confining stress, three types of triaxial test systems exist. They are represented in figures B-3a to B-3c.

- a) In the test system represented in figure B-3a, the whole specimen, including the upper and lower platens, is put in a rubber socket (or foil). The rubber socket must seal the circumference of the platens, to ensure that ingress of water, oil or air does not occur. This may be achieved by using O-rings. The whole set-up is mounted in the test rig, and a pressure cell is placed around the specimen. Then the confining pressure is applied by pressurising the cell (by water, oil or air as medium). The axial cyclic load is subsequently applied.
- b) In the test system represented in figure B-3b, a lateral confining pressure is applied to the specimen by placing it in a "pressure ring". This may be achieved by mounting an inner tube of an appropriate sized tyre around the specimen and inflating this tyre. Before applying the desired lateral confining pressure, the specimen is mounted in the set-up and the loading platens are brought into contact with the specimen. After applying the lateral confining pressure, a constant axial stress (equal to the inflation pressure) is applied via the platens, to create a confining stress all around the specimen. The axial cyclic load is subsequently applied.
- c) In the test system represented in figure B-3c, the confining pressure is realised by applying a partial vacuum to the specimen. The specimen is sealed within a rubber membrane. This is secured at either end by two O-rings which rest in purpose cut grooves around the perimeter of two specially designed platens. In addition, the lower platen is hollow and has a series of drainage holes arranged in a radial pattern on its top surface. It also has an outlet pipe fitted in the base which connects via a pressure regulator and gauge to a vacuum pump.

Hence, by extracting air from the specimen, an effective confining stress of typically 50 - 70 kPa, and at maximum 100 kPa can be realised on the specimen. The axial cyclic load is subsequently applied.

6.2.2 Loading platens

The loading platens shall deform less than 2 μm when a stress of 250 kPa is applied. This can be verified by means of a dummy specimen which deforms less than 0,1 μm on application of a 250 kPa stress or by pressing the two loading platens directly onto each other.

The surfaces of the platens must be flat and smooth. The clearance between the two platens should be such that test specimens can be accommodated.

6.2.3 Control system

The apparatus should be provided with a system to control the confining and cyclic axial stresses separately.

6.2.4 Load cell

The load cell shall have a measuring range capable of measuring the required stresses and shall comply with the specification for transducers of accuracy class 0,2. Resonance frequencies of the load cell, as mounted, should be at least 10 times as high as the test frequency.

6.2.5 Displacement transducers

The apparatus shall be provided with displacement transducers to measure the change in height of the specimen during the test. The measures are taken between the platens or directly on the specimen. The transducers shall comply with accuracy class 0,2. Resonance frequencies of the mounted transducers should be at least 10 times higher than the test frequency. The measuring range of the transducers must be 10 mm at least.

6.2.6 Data registration equipment

Data-acquisition system for controlling and collecting the signals from the load and displacement transducers.

Measuring instruments, including amplification, must be such that forces and displacements can be read with a resolution of 1 N and 1 μm , respectively.

Any system for graphical follow-up of the creep curve during testing is recommended.

6.2.7 Temperature conditioning

The accuracy of the temperature control is $\pm 1\text{ }^{\circ}\text{C}$ or better.

To apply the chosen temperature to the specimen, either the whole test apparatus shall be placed in a thermostatic chamber, or the test apparatus must be equipped with a temperature chamber in which the specimen is mounted.

7. SPECIMEN PREPARATION

7.1 At least two test specimens shall be prepared for testing.

7.2 Each test specimen shall have the shape of a cylinder. The end of the test specimen shall be even and plan-parallel, which is achieved by sawing both ends of the specimen. A diamond tipped masonry saw equipped with parallel blades is recommended. It should be aimed that the ends are parallel and perpendicular to the cylinder axis (i.e a right-angle not more than about 2-3°). For a rough control of evenness: brush the hand over the surface. If it feels even without

blemishes it is considered adequate, otherwise it must be polished. After sawing/polishing the specimen shall be dried at a temperature not exceeding 25 °C. A test specimen is considered to be dry when two weighings performed 2 h apart differ by less than 0,1 %.

7.3 Different specimen dimensions can be used. The following minimum dimensions have to be respected:

- if the nominal maximum aggregate size is less than or equal to 16 mm, the minimum diameter is 50 mm and the minimum height is 50 mm;
- if the nominal maximum aggregate size is greater than 16 mm, the minimum diameter is 80 mm and the minimum height is 80 mm.

NOTE 1: Some equipment makes use of the minimum specimen dimensions. It makes the test less complex. Other equipment uses a height-to-diameter-ratio of 1.25 to 2 in order to obtain a homogeneous state of stress and hence much higher specimens. It makes the test heavier to carry out and, for some specimen dimensions, impossible to perform on cores taken from the road.

NOTE 2 : It is known that the creep parameters depend on the height-to-diameter-ratio of the sample. Test results obtained on specimens having different dimensions cannot therefore generally be quantitatively compared. Hence, in case that the outcome of the test is used to check on the acceptability of a given mixture, the results are to be evaluated with respect to specific requirements related to specimens with well-defined dimensions.

- For the product standards, a height-to-diameter-ratio of 0.5 is chosen, because it allows the use of smaller samples, making the test easier to perform.

Measure the dimensions on the dry test specimen according to PrEN 12697-6, Procedure D (prEN 12697-29, using a vernier calliper). The height of the specimen shall not vary by more than 1,0 mm and the diameter not by more than 2 mm.

7.4 The test can be performed on:

- test specimens prepared in the laboratory by gyratory compaction (prEN 12697 part 31)
- test specimens drilled from laboratory-prepared slab of asphalt (prEN 12697 part 33)
- test specimens prepared from drilled core specimen taken from the road (prEN 12697 part 27)
- test specimens prepared in the laboratory by impact compactor (prEN 12697 part 30)

The laboratory specimens shall be compacted to obtain a bulk density corresponding to (97 ± 1) % of the reference density as determined in accordance with prEN 12697-9.

NOTE : The way of compaction has a considerable impact on the results.

7.5 The bulk density of the test specimen shall be measured in accordance with prEN 12697-6. Laboratory prepared specimens with a bulk density outside the specified range in 7.4 should be discarded.

NOTE: Results from specimens obtained from cores showing differences in bulk density larger than specified in 7.4 will generally show larger differences between each other, than specimens satisfying 7.4.

7.6 Damage to the test specimen shall be avoided in all stages of sampling, transport and preparation before testing. During transport and storage the slab and drilled core specimen should be fully supported to prevent deformation or damage.

8. CONDITIONING

8.1 The specimens shall be stored at a temperature between 0 and 25 °C. Test specimens shall be fully supported and not be stacked on top of each other. Any damage must be prevented.

8.2 Testing shall start not before 7 days after compaction in the laboratory or on the road.

8.3 Specimens shall be cleaned if necessary by brushing or washing, as required.

8.4 The specimens shall be dried at ambient temperature to constant mass, at a relative air humidity of less than 80% .

NOTE: Constant mass is obtained when the change of mass between two determinations at an interval of at least two hours is less than 0,1 % (m/m).

8.5 To minimise the friction between the loading platens and the test specimen, the end faces of the specimen must be smooth and plain. Brush the hand over the specimens' surface. If it feels even without blemishes, it is considered adequate, otherwise it must be polished.

To minimise the friction between the loading platens and the test specimen, a membrane-silicon-membrane – system shall be used between the loading platens and the specimen. The membrane consists of a disk, cut out of typical geotechnical latex rubber membranes e.g. ELE P/N EL-25-7621 or WFI P/N 11091 or equivalent, of the same diameter as the specimen. A small amount of silicon grease is applied between both disks.

NOTE: The amount of friction between the loading platens and the specimen is known to have a large impact on the results.

8.6 Test specimens shall be conditioned, before mounting, at the test temperature. The temperature may not vary more than 1°C over the specimen. This conditioning period shall be at least 4 h and not more than 7 h.

9. TEST PROCEDURE

To evaluate the resistance to permanent deformation of a given mixture under given test conditions, at least two specimens shall be tested.

9.1 Preparation of the test

- a) Ensure that the temperature of the testing chamber has reached the specified temperature within ± 1.0 °C before installing the test specimen.

NOTE 1: Test temperatures are generally between 30 and 50 °C.

NOTE 2: It is recommended to monitor the temperature of a dummy core during pre-conditioning.

- b) The test specimen shall be positioned coaxially with the loading platens. In case of self-aligning platens : before locking the self-aligning loading platen, the specimen shall be pre-loaded carefully in order to adjust the self-aligning loading platen such that any slight deviation in the parallelism of the end faces of the specimen is corrected. This pre-loading stress shall not exceed $0,02 \cdot (2 \cdot \sigma_v + \sigma_c)$ in the case of haversinusoidal loading and $0,02 \cdot (\sigma_B + \sigma_c)$ in the case of block-pulse loading. The time of pre-loading shall not exceed $120 \text{ s} \pm 6 \text{ s}$. Then, lock the self-aligning platen.
- c) Mount the displacement transducers.
- d) Before starting the test, make sure that the temperature of the specimen is at the specified temperature within $\pm 1,0 \text{ }^\circ\text{C}$. Allow sufficient time between the fixing of the specimen and the start-up of the test, for relaxation of the stresses due to the clamping of the specimen.

9.2 Application of the loads

- a) Before the test loads are applied, the specimen shall be pre-loaded again for 120 seconds with a static load equal to $0,02 \cdot (2 \cdot \sigma_H + \sigma_c)$ in the case of haversinusoidal loading and $0,02 \cdot (\sigma_B + \sigma_c)$ in the case of block-pulse loading. This load shall be applied gradually and smoothly.
- b) Immediately after preloading, the confining stress shall be applied. A minimum confining stress of 25 kPa is required.

NOTE: Confining stresses in the range 50 kPa to 200 kPa are most often applied.

- c) Within 10 seconds after that, the cyclic axial load shall be applied.

NOTE 1: Frequencies in the range of 1 to 5 Hz are most often applied for the axial haversinusoidal loading. To simulate slow traffic, a lower frequency may be appropriate.

NOTE 2: Examples of pulse duration in use for block-pulse loading are : pulse duration of 1 second with 1 second rest period and pulse duration of 0,2 second with rest period 0,8 second.

NOTE 3: For the amplitude of the haversinusoidal pressure, values ranging from 100 to 200 kPa are most often used. For haversinusoidal loading, the amplitude of the haversinusoidal load is usually taken two to three times larger than the confining stress. For block-pulse loading, pressures σ_B of 100 kPa up to 700 kPa are used.

NOTE 4: Some examples of stress combinations applied in tests on asphalt concrete for underlayers (for block pulse loading with 0.8s rest period and 0.2 s loading time)

Temperature (°C)	Confining stress (kPa)	Total axial stress (kPa)
40	100	700
40	100	550
40	250	850

NOTE 5: The results and the shape of the creep curve depend largely on the testing conditions: temperature, axial and confining stress. However, preferably the combination should be such that stage 2 of the creep curve (see figure B-3.5) exists and that the creep characteristics (see 10.2) can be determined.

9.3 Measurements during the test

Measure the change in height of the specimen as the test progresses using the displacement transducers and a data acquisition system. As a minimum, readings shall be taken after every 10th load applications up to 100 load applications, every 100th load applications up to 1000 load applications and thereafter every 500 load applications. Each measurement should be taken at the moment that the axial strain is minimal. At each measurement, the corresponding load application number should be known.

NOTE 1: More measurements may be necessary, e.g. depending on the type of representation of the creep curve.

During the test, it should be checked that the static confining stress and the amplitude of the haversinusoidal axial stress or the height of the block-pulse remain constant within 5 % of the required value.

The test is either ended if the permanent deformation is 6 % of the height of the sample or after 10000 loading cycles. It may happen that stage two of the creep curve is measured during a too short period to determine the creep parameters. In that case the duration of the test can be extended.

10. CALCULATION AND EXPRESSION OF RESULTS

10.1 Calculate the cumulative strain ε_N [%] of the specimen for each measured load application as follows:

$$\varepsilon_N = 100 \times (h_0 - h_N) / h_0$$

in which h_0 [in mm] is the average height after preload of the specimen and h_N [in mm] the average height after N load applications.

10.2 Determine the resistance to permanent deformation of the mixture by interpreting the creep curve. One of the following methods is used and can be requested :

a) Determination of the creep rate f_c

Represent the creep curve on a linear scale. Determine the slope B_1 from the least square linear fit of the (quasi) linear part of the creep curve (stage 2), if stage 2 is present :

$$\varepsilon_N = A_1 + B_1 \cdot N$$

Determine the creep rate f_c in the (quasi)linear part of the creep curve. This is the slope B_1 ,

but expressed in (μ strain/loading cycle) :

$$f_c = 10^6 \cdot B_1$$

The parameter f_c is used to characterise the resistance to permanent deformation of a given mixture.

NOTE 1: This method is simple, but has the disadvantage that it is only a poor representation of the deformation curve. Furthermore, the slope f_c depends highly on the selected interval used for curve fitting, because there is generally no part with real constant slope in the creep curve.

b) Determination of the parameters B and $\epsilon_{1000, \text{calc.}}$

Represent the creep curve on a log-log – scale. Determine the following least square fit of the (quasi) linear part of the creep curve is:

$$\epsilon_N = A \cdot N^B$$

or equivalent, determine the least square linear fit on the ($\log \epsilon_N - \log N$) values:

$$\log \epsilon_N = \log A + B \cdot \log N$$

Determine the calculated permanent deformation after 1000 loading cycles, $\epsilon_{1000, \text{calc.}}$:

$$\epsilon_{1000, \text{calc.}} = A \cdot 1000^B$$

The parameters B and $\epsilon_{1000, \text{calc.}}$ are used to characterise the resistance to permanent deformation of a given mixture.

NOTE: This method seems more complex than method 10.2.a), but has the advantage that in many cases a clear linear part is observed in the creep curve.

10.3 If only stage 1 and stage 3 of the creep curve are present, or if the deformation is so large that the 6 % deformation limit to stop the test is already reached after a short number of loading cycles so that only phase 1 is observed, the mixture is to be considered as very sensitive to permanent deformation for the test conditions considered. Values of the permanent deformation corresponding to a well-defined number of load applications can be used to compare such mixtures; e.g. ϵ_{1000} and ϵ_{10000} .

11. TEST REPORT

With reference to this standard the test method shall include the following :

11.1. Information on the specimens

For each specimen:

- a) Type and origin of material tested.
- b) Specimen identification number.

- c) Specimen preparation method: laboratory made (refer to relevant EN standard) or cored from the road.
- a) Average diameter, in millimetre.
- b) Initial height, in millimetre.
- c) Bulk density, in gram per cubic centimetre to the nearest 0,001 g/cm³.
- d) Particulars (including the number of discarded samples).

11.2 Information on the test conditions

For each specimen:

- a) Test temperature,
- b) Confining stress, in kilopascals,
- c) Shape of the cyclic signal : haversine or block-pulse,
- d) Amplitude of the haversinusoidal stress, or height of the block pulse, in kilopascals,
- e) Frequency, in Hertz (in case of haversinoidal axial load) ; pulse duration and rest period (in case of block-pulse loading).

11.3 Test results

For each specimen:

- a) Creep curve,
- b) Creep characteristics, if requested, with representation of the fit on the creep curve.

Mean creep characteristics

12. PRECISION

Precision data are estimated from a precision study with the Vacuum Repeated Load Axial Test (VRLAT) involving 7 laboratories testing 6 replicate specimens of 3 materials, led to the values of repeatability and reproducibility given in table 1.

Table 1: Repeatability (r) and reproducibility (R) for the strain at the end of the test and for the strain rate over the last 600 cycles

Cumulative strain at end of test (µstrain)			
	SMA	HRA	AC
Average	7400	14300	3553
Repeatability (r)	1710	4130	841
Reproducibility (R)	1710	7290	1640
Strain rate over last 600 cycles (µstrain/100 cycles)			
	SMA	HRA	AC
Average	44.1	70.9	13.1
Repeatability (r)	13,2	29,9	4,6
Reproducibility (R)	18,9	34,7	10,5

INFORMATIVE ANNEX

Cyclic versus static confining stress

The actual stress conditions in the road cannot be simulated in the laboratory with simple test equipment. They depend on time (position of the wheel), the road structure, the depth in the structure, the stiffness of other layers, ... Therefore, the applied load conditions are only an approximation of the loads that occur in reality. One might suggest that application of a cyclic confining stress is to be preferred over a static confining stress. However, given the considerations just mentioned above and the fact that cyclic confining stresses require advanced and expensive equipment, it is usually not applied.

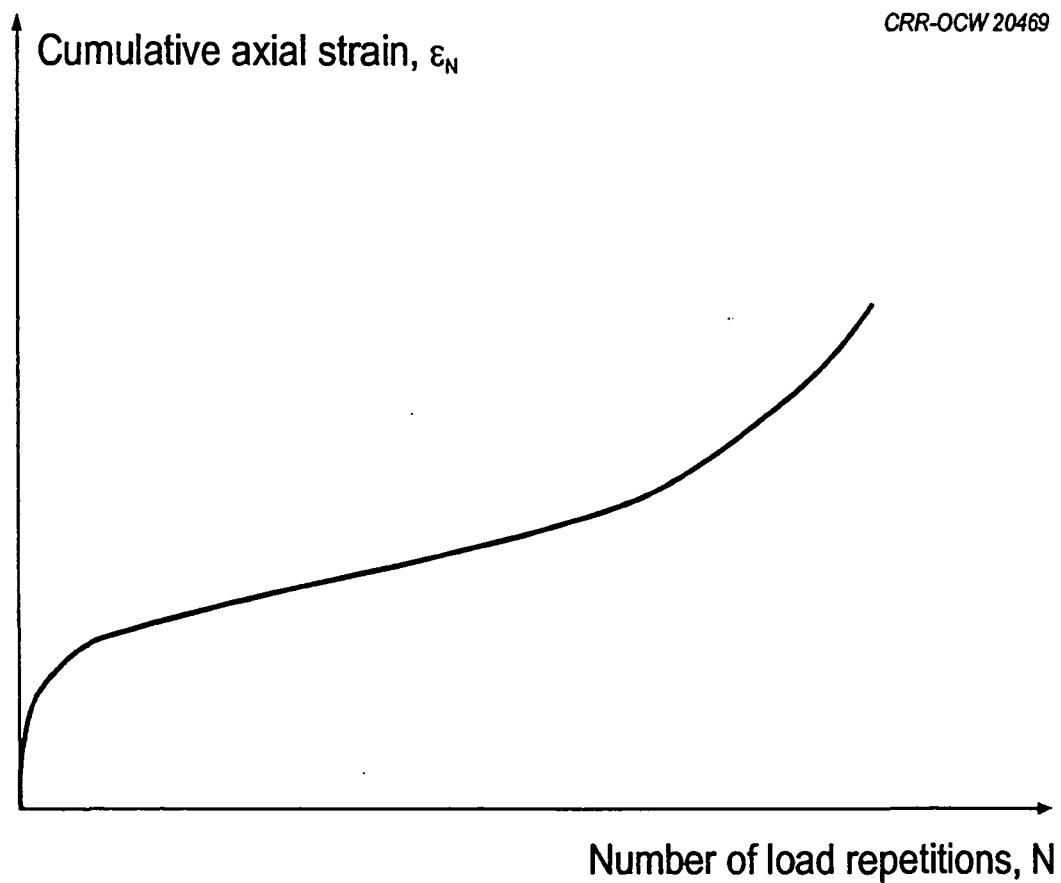
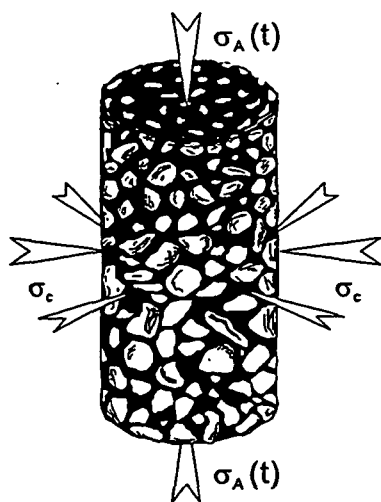


Figure B-1:
Example of a creep curve



Confining pressure : σ_c
 Haversinusoidal pressure $\sigma_a(t) = \sigma_v(1 + \sin \omega t)$
 Total axial pressure $\sigma_A(t) = \sigma_a(t) + \sigma_c$

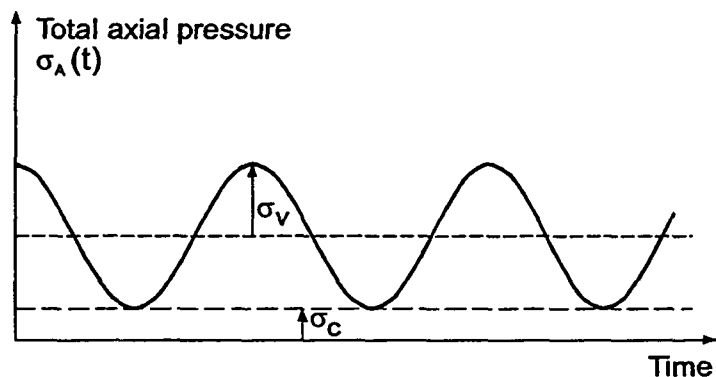
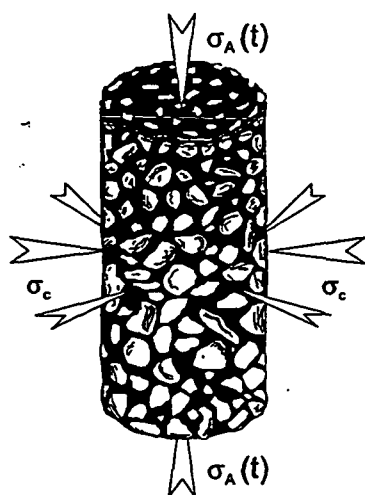


Figure B-2a

Representation of the pressures exerted on the specimen,
 in case of haversinusoidal cyclic loading



Confining pressure : σ_c
 Height of block-pulse σ_B

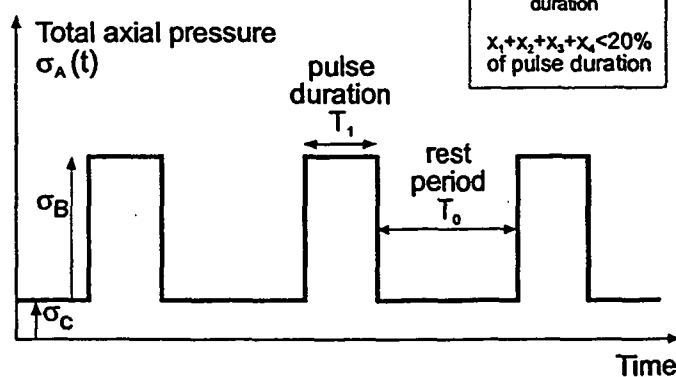


Figure B-2b

Representation of the pressures exerted on the specimen,
 in case of bloc-pulse cyclic loading

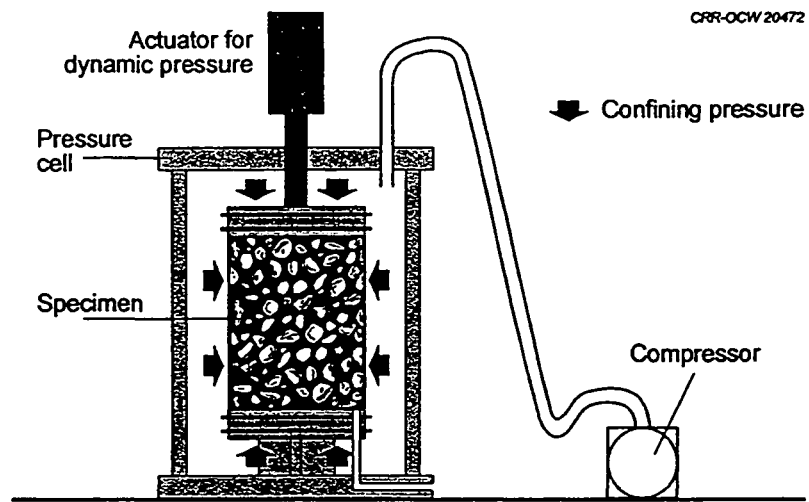


Figure B-3a
Schematic representation of a triaxial cyclic compression test device with pressure cell

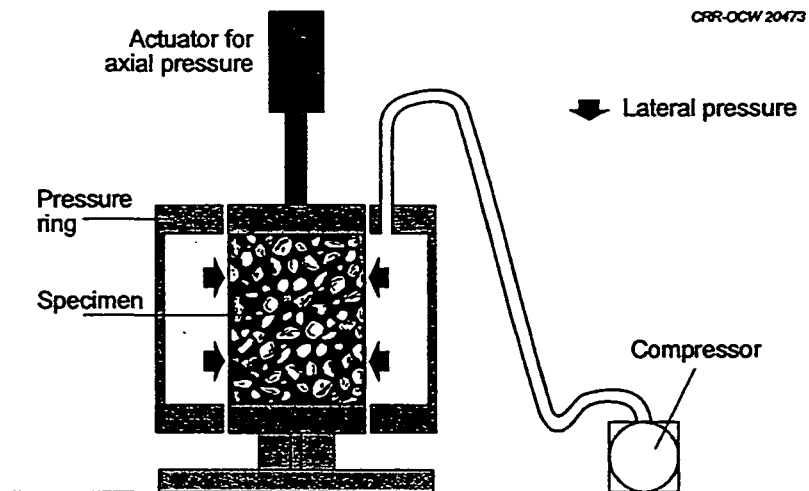


Figure B-3b
Schematic representation of a triaxial cyclic compression test device with pressure ring

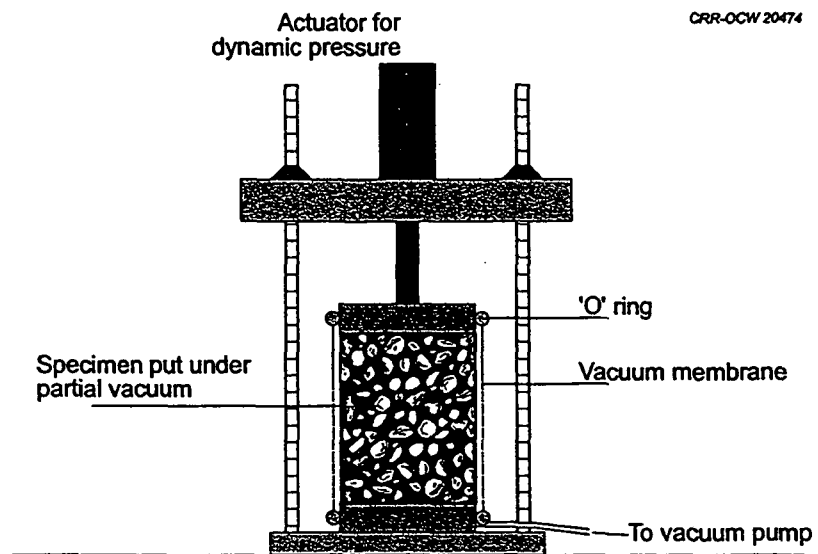


Figure B-3c
Schematic representation of a triaxial cyclic compression test device
making use of a partial vacuum as confining pressure

APPENDIX B

BISAR Outputs

Principal stresses due to Super super single load on Standard III

x(m)	y	z	σ_1	σ_2	$\sigma_3(\text{Pa})$	$\sigma_1 - \sigma_3$	$(\sigma_1 - \sigma_3)/10 \cdot \sigma_1/\sigma_3$		
0,00	0,00	0,30	826400,00	816800,00	-36090,00	-0,3000	862490,00	0,86	-22,90
0,00	0,05	0,30	808800,00	802000,00	-35660,00	-0,3000	844460,00	0,84	-22,68
0,00	0,10	0,30	751400,00	717000,00	-33540,00	-0,3000	784940,00	0,78	-22,40
0,00	0,21	0,30	564300,00	449000,00	-26360,00	-0,3000	590660,00	0,59	-21,41
0,00	0,31	0,30	368900,00	214600,00	-18760,00	-0,3000	387660,00	0,39	-19,66
0,00	0,50	0,30	240900,00	89990,00	-13650,00	-0,3000	254550,00	0,25	-17,65
0,00	0,75	0,30	123600,00	392,00	-11640,00	-0,3000	135240,00	0,14	-10,62
0,00	2,00	0,10	8490,00	-59,95	-920,30	-0,1000	9410,30	0,01	-9,23
0,00	2,00	0,13	10410,00	-93,41	-1218,00	-0,1300	11628,00	0,01	-8,55
0,00	0,31	0,27	284300,00	197100,00	-40390,00	-0,2650	324690,00	0,32	-7,04
0,00	0,35	0,27	252600,00	160800,00	-36260,00	-0,2650	288860,00	0,29	-6,97
0,00	0,21	0,27	381100,00	319600,00	-55260,00	-0,2650	436360,00	0,44	-6,90
0,00	0,00	0,27	533000,00	529000,00	-78460,00	-0,2650	611460,00	0,61	-6,79
0,00	0,05	0,27	524300,00	520200,00	-77690,00	-0,2650	601990,00	0,60	-6,75
0,00	0,11	0,27	484600,00	463100,00	-72310,00	-0,2650	556910,00	0,56	-6,70
0,00	0,50	0,27	164900,00	71480,00	-26830,00	-0,2650	191730,00	0,19	-6,15
0,00	2,00	0,16	3697,00	-165,90	-654,00	-0,1600	4351,00	0,00	-5,65
0,00	0,75	0,27	84290,00	10480,00	-23820,00	-0,2650	108110,00	0,11	-3,54
0,00	1,50	0,01	4591,00	-2,14	-1994,00	-0,0125	6585,00	0,01	-2,30
0,00	1,50	0,00	4885,00	0,03	-2138,00	-0,0010	7023,00	0,01	-2,28
0,00	1,50	0,03	7028,00	11,45	-3311,00	-0,0250	10339,00	0,01	-2,12
0,00	0,31	0,23	166700,00	144900,00	-81020,00	-0,2300	247720,00	0,25	-2,06
0,00	1,50	0,04	10040,00	-15,14	-4944,00	-0,0400	14984,00	0,01	-2,03
0,00	0,50	0,23	94060,00	59610,00	-48330,00	-0,2300	142390,00	0,14	-1,95
0,00	0,21	0,23	227000,00	219900,00	-118400,00	-0,2300	345400,00	0,35	-1,92
0,00	0,11	0,23	291600,00	284000,00	-161600,00	-0,2300	453200,00	0,45	-1,80
0,00	0,00	0,23	312600,00	308200,00	-174100,00	-0,2300	486700,00	0,49	-1,80
0,00	1,00	0,30	64280,00	-4099,00	-37840,00	-0,3000	102120,00	0,10	-1,70
0,00	0,75	0,23	46780,00	16140,00	-32620,00	-0,2300	79400,00	0,08	-1,43
0,00	1,00	0,27	43680,00	-1352,00	-31380,00	-0,2650	75060,00	0,08	-1,39
0,00	1,00	0,23	23690,00	2511,00	-26970,00	-0,2300	50660,00	0,05	-0,88
0,00	0,31	0,20	96200,00	40530,00	-137200,00	-0,1950	233400,00	0,23	-0,70
0,00	0,35	0,20	81950,00	33840,00	-117800,00	-0,1950	199750,00	0,20	-0,70
0,00	0,21	0,20	134900,00	61900,00	-210200,00	-0,1950	345100,00	0,35	-0,64
0,00	0,50	0,20	45040,00	17690,00	-72670,00	-0,1950	117710,00	0,12	-0,62
0,00	0,00	0,55	10540,00	10500,00	-17440,00	-0,5500	27980,00	0,03	-0,60
0,00	0,05	0,55	10490,00	10400,00	-17430,00	-0,5500	27920,00	0,03	-0,60
0,00	0,11	0,55	10180,00	9993,00	-17150,00	-0,5500	27330,00	0,03	-0,59
0,00	0,21	0,55	9356,00	8446,00	-16200,00	-0,5500	25556,00	0,03	-0,58
0,00	0,31	0,55	8235,00	6458,00	-14850,00	-0,5500	23085,00	0,02	-0,55
0,00	0,35	0,55	7759,00	5651,00	-14260,00	-0,5500	22019,00	0,02	-0,54
0,00	1,00	0,16	8661,00	-15280,00	-16250,00	-0,1600	24911,00	0,02	-0,53
0,00	0,50	0,55	6015,00	2981,00	-12040,00	-0,5500	18055,00	0,02	-0,50
0,00	0,75	0,20	17300,00	6652,00	-38320,00	-0,1950	55620,00	0,06	-0,45
0,00	0,11	0,20	132500,00	81270,00	-296000,00	-0,1950	428500,00	0,43	-0,45
0,00	0,75	0,55	3720,00	151,80	-8820,00	-0,5500	12540,00	0,01	-0,42
0,00	0,75	0,16	15320,00	-28520,00	-38220,00	-0,1600	53540,00	0,05	-0,40
0,00	0,50	0,16	30980,00	-50120,00	-89350,00	-0,1600	120330,00	0,12	-0,35
0,00	1,00	0,55	2235,00	-1041,00	-6468,00	-0,5500	8703,00	0,01	-0,35
0,00	0,35	0,16	51670,00	-67810,00	-156800,00	-0,1600	208470,00	0,21	-0,33
0,00	1,00	0,10	7499,00	-5884,00	-22940,00	-0,1000	30439,00	0,03	-0,33
0,00	0,31	0,16	59460,00	-72980,00	-185900,00	-0,1600	245360,00	0,25	-0,32
0,00	0,05	0,20	98570,00	86740,00	-314900,00	-0,1950	413470,00	0,41	-0,31
0,00	1,00	0,13	9197,00	-10680,00	-30770,00	-0,1300	39967,00	0,04	-0,30
0,00	0,00	0,20	91620,00	84890,00	-313000,00	-0,1950	404620,00	0,40	-0,29
0,00	1,00	0,20	6149,00	2569,00	-22120,00	-0,1950	28269,00	0,03	-0,28
0,00	1,50	0,23	5719,00	-852,70	-21030,00	-0,2300	26749,00	0,03	-0,27
0,00	0,21	0,16	74260,00	-90360,00	-302300,00	-0,1600	376560,00	0,38	-0,25
0,00	0,00	0,43	5041,00	4742,00	-23500,00	-0,4250	28541,00	0,03	-0,21
0,00	0,05	0,43	4979,00	4755,00	-23460,00	-0,4250	28439,00	0,03	-0,21
0,00	0,11	0,43	4717,00	4671,00	-22930,00	-0,4250	27647,00	0,03	-0,21
0,00	1,00	0,04	4111,00	-829,70	-20060,00	-0,0400	24171,00	0,02	-0,20
0,00	0,21	0,43	4316,00	3973,00	-21200,00	-0,4250	25516,00	0,03	-0,20

Principal stresses due to Super super single load on Standard III

x(m)	y	z	σ_1	σ_2	$\sigma_3(\text{Pa})$	$\sigma_1 - \sigma_3$	$(\sigma_1 - \sigma_3)/10 \cdot \sigma_1/\sigma_3$		
0,00	0,31	0,43	3737,00	3127,00	-18970,00	-0,4250	22707,00	0,02	-0,20
0,00	0,35	0,43	3477,00	2798,00	-18050,00	-0,4250	21527,00	0,02	-0,19
0,00	1,00	0,03	2618,00	-308,60	-13850,00	-0,0250	16468,00	0,02	-0,19
0,00	0,75	0,13	10500,00	-37460,00	-57260,00	-0,1300	67760,00	0,07	-0,18
0,00	0,50	0,43	2614,00	1601,00	-14800,00	-0,4250	17414,00	0,02	-0,18
0,00	0,75	0,10	7535,00	-23630,00	-43060,00	-0,1000	50595,00	0,05	-0,17
0,00	0,50	0,13	17270,00	-103400,00	-106700,00	-0,1300	123970,00	0,12	-0,16
0,00	1,00	0,01	1406,00	-93,01	-9014,00	-0,0125	10420,00	0,01	-0,16
0,00	1,00	0,00	1434,00	-0,58	-9633,00	-0,0010	11067,00	0,01	-0,15
0,00	0,75	0,43	1525,00	191,90	-10400,00	-0,4250	11925,00	0,01	-0,15
0,00	0,50	0,10	11600,00	-70900,00	-79950,00	-0,1000	91550,00	0,09	-0,15
0,00	0,35	0,13	26990,00	-147500,00	-196100,00	-0,1300	223090,00	0,22	-0,14
0,00	0,35	0,10	17970,00	-114700,00	-134200,00	-0,1000	152170,00	0,15	-0,13
0,00	0,31	0,13	30420,00	-160800,00	-234500,00	-0,1300	264920,00	0,26	-0,13
0,00	2,00	0,55	306,50	-432,10	-2369,00	-0,5500	2675,50	0,00	-0,13
0,00	0,31	0,10	20680,00	-126100,00	-161500,00	-0,1000	182180,00	0,18	-0,13
0,00	1,00	0,43	863,10	-510,00	-7226,00	-0,4250	8089,10	0,01	-0,12
0,00	2,00	0,30	3200,00	-402,40	-32390,00	-0,3000	35590,00	0,04	-0,10
0,00	0,21	0,10	28600,00	-165900,00	-290400,00	-0,1000	319000,00	0,32	-0,10
0,00	2,00	0,27	2213,00	-364,10	-23180,00	-0,2650	25393,00	0,03	-0,10
0,00	0,00	0,35	2757,00	2563,00	-29930,00	-0,3500	32687,00	0,03	-0,09
0,00	0,05	0,35	2705,00	2535,00	-29810,00	-0,3500	32515,00	0,03	-0,09
0,00	0,11	0,35	2438,00	2412,00	-28770,00	-0,3500	31208,00	0,03	-0,08
0,00	0,21	0,35	2006,00	1804,00	-25660,00	-0,3500	27666,00	0,03	-0,08
0,00	0,21	0,13	29810,00	-198100,00	-386000,00	-0,1300	415810,00	0,42	-0,08
0,00	2,00	0,23	1071,00	-298,50	-14490,00	-0,2300	15561,00	0,02	-0,07
0,00	2,00	0,43	131,80	-332,70	-1846,00	-0,4250	1977,80	0,00	-0,07
0,00	0,31	0,35	1494,00	1261,00	-22150,00	-0,3500	23644,00	0,02	-0,07
0,00	0,35	0,35	1320,00	1070,00	-20830,00	-0,3500	22150,00	0,02	-0,06
0,00	0,50	0,35	777,00	518,50	-16500,00	-0,3500	17277,00	0,02	-0,05
0,00	2,00	0,20	148,00	-215,40	-5057,00	-0,1950	5205,00	0,01	-0,03
0,00	0,75	0,04	1055,00	-12750,00	-38120,00	-0,0400	39175,00	0,04	-0,03
0,00	0,75	0,35	255,00	-113,20	-11150,00	-0,3500	11405,00	0,01	-0,02
0,00	0,31	0,04	2151,00	-113700,00	-120200,00	-0,0400	122351,00	0,12	-0,02
0,00	0,35	0,04	1854,00	-99110,00	-103900,00	-0,0400	105754,00	0,11	-0,02
0,00	2,00	0,35	26,86	-264,70	-1522,00	-0,3500	1548,86	0,00	-0,02
0,00	0,50	0,04	1237,00	-50180,00	-71610,00	-0,0400	72847,00	0,07	-0,02
0,00	0,750	0,025	392,60	-8501,00	-26490,00	-0,0250	26882,60	0,03	-0,01
0,00	2,500	0,230	106,40	-10,47	-9198,00	-0,2300	9304,40	0,01	-0,01
0,00	0,500	0,025	457,90	-34410,00	-50090,00	-0,0250	50547,90	0,05	-0,01
0,00	0,350	0,025	653,30	-67990,00	-72990,00	-0,0250	73643,30	0,07	-0,01
0,00	0,210	0,040	1892,00	-142500,00	-211400,00	-0,0400	213292,00	0,21	-0,01
0,00	0,310	0,025	732,10	-79940,00	-82240,00	-0,0250	82972,10	0,08	-0,01
0,00	1,000	0,350	40,71	-450,00	-7468,00	-0,3500	7508,71	0,01	-0,01
0,00	0,750	0,013	92,73	-5978,00	-17670,00	-0,0125	17762,73	0,02	-0,01
0,00	0,210	0,025	728,20	-99480,00	-140900,00	-0,0250	141628,20	0,14	-0,01
0,00	0,310	0,013	207,50	-54610,00	-55530,00	-0,0125	55737,50	0,06	0,00
0,00	0,320	0,013	167,00	-52430,00	-53890,00	-0,0125	54057,00	0,05	0,00
0,00	0,500	0,013	90,06	-23520,00	-33930,00	-0,0125	34020,06	0,03	0,00
0,00	0,210	0,013	202,70	-68480,00	-91740,00	-0,0125	91942,70	0,09	0,00
0,00	0,210	0,001	12,25	-72420,00	-94100,00	-0,0010	94112,25	0,09	0,00
0,00	0,750	0,001	0,65	-6086,00	-18790,00	-0,0010	18790,65	0,02	0,00
0,00	0,500	0,001	-0,20	-24650,00	-36190,00	-0,0010	36189,80	0,04	0,00
0,00	0,320	0,001	-7,20	-55120,00	-57500,00	-0,0010	57492,80	0,06	0,00
0,00	0,310	0,001	-9,42	-57570,00	-59010,00	-0,0010	59000,58	0,06	0,00
0,00	0,110	0,160	-3607,00	-138200,00	-473700,00	-0,1600	470093,00	0,47	0,01
0,00	0,110	0,100	-99930,00	-349300,00	-707600,00	-0,1000	607670,00	0,61	0,14
0,00	0,110	0,130	-89010,00	-261900,00	-618500,00	-0,1300	529490,00	0,53	0,14
0,00	2,000	0,560	-348,00	-450,30	-1860,00	-0,5600	1512,00	0,00	0,19
0,00	0,110	0,040	-174600,00	-367600,00	-716200,00	-0,0400	541600,00	0,54	0,24
0,00	0,050	0,560	-4351,00	-4399,00	-17160,00	-0,5600	12809,00	0,01	0,25
0,00	0,000	0,560	-4358,00	-4389,00	-17170,00	-0,5600	12812,00	0,01	0,25
0,00	0,110	0,560	-4335,00	-4379,00	-16970,00	-0,5600	12635,00	0,01	0,26

Principal stresses due to Super super single load on Standard III

x(m)	y	z	σ_1	σ_2	$\sigma_3(\text{Pa})$	$\sigma_1 - \sigma_3$	$(\sigma_1 - \sigma_3)/10 \cdot \sigma_1/\sigma_3$		
0,00	0,050	0,160	-131400,00	-175700,00	-511700,00	-0,1600	380300,00	0,38	0,26
0,00	0,210	0,560	-4270,00	-4285,00	-16230,00	-0,5600	11960,00	0,01	0,26
0,00	0,310	0,560	-4100,00	-4161,00	-15150,00	-0,5600	11050,00	0,01	0,27
0,00	0,350	0,560	-4015,00	-4092,00	-14660,00	-0,5600	10645,00	0,01	0,27
0,00	0,500	0,560	-3641,00	-3737,00	-12720,00	-0,5600	9079,00	0,01	0,29
0,00	0,110	0,025	-193800,00	-365800,00	-662600,00	-0,0250	468800,00	0,47	0,29
0,00	0,750	0,560	-2911,00	-2958,00	-9642,00	-0,5600	6731,00	0,01	0,30
0,00	1,000	0,560	-2168,00	-2189,00	-7105,00	-0,5600	4937,00	0,00	0,31
0,00	0,050	0,130	-248600,00	-307200,00	-696100,00	-0,1300	447500,00	0,45	0,36
0,00	0,000	0,160	-178200,00	-187300,00	-496900,00	-0,1600	318700,00	0,32	0,36
0,00	0,110	0,013	-257200,00	-423200,00	-648800,00	-0,0125	391600,00	0,39	0,40
0,00	0,000	0,130	-303400,00	-319800,00	-689200,00	-0,1300	385800,00	0,39	0,44
0,00	0,050	0,100	-430300,00	-557500,00	-940100,00	-0,1000	509800,00	0,51	0,46
0,00	0,050	0,040	-660000,00	-780000,00	-1264000,00	-0,0400	604000,00	0,60	0,52
0,00	0,050	0,025	-775300,00	-909100,00	-1321000,00	-0,0250	545700,00	0,55	0,59
0,00	0,000	0,040	-897600,00	-939200,00	-1430000,00	-0,0400	532400,00	0,53	0,63
0,00	0,000	0,100	-606600,00	-620400,00	-924800,00	-0,1000	318200,00	0,32	0,66
0,00	0,050	0,013	-911500,00	-1097000,00	-1383000,00	-0,0125	471500,00	0,47	0,66
0,00	0,110	0,001	-506700,00	-598700,00	-767500,00	-0,0010	260800,00	0,26	0,66
0,00	0,050	0,001	-992100,00	-1209000,00	-1408000,00	-0,0010	415900,00	0,42	0,70
0,00	0,000	0,025	-1100000,00	-1155000,00	-1532000,00	-0,0250	432000,00	0,43	0,72
0,00	0,000	0,001	-1342000,00	-1463000,00	-1672000,00	-0,0010	330000,00	0,33	0,80
0,00	0,000	0,013	-1323000,00	-1421000,00	-1625000,00	-0,0125	302000,00	0,30	0,81

Project: ST_III/SS Due to the Etended super single load
Calculated: #####

System: 1: sys31

Layer Number	Thickness (m)	Young's Modulus (Pa)	Poisson's Ratio	Shear Spring Compliance (m ³ /N)	Load Number	Normal Stress (Pa)	Shear Stress (Pa)	Radius of Loaded Area (m)	Load Position X (m)	Load Position Y (m)	Shear Direction (°)
1	0,013	3,00E+08	0,5	0,00E+00	1	4,00E+05	2,00E+05	5,28E-02	9,00E-02	6,00E-02	2,70E+02
2	0,013	5,00E+08	0,47	0,00E+00	2	1,75E+02	2,00E+05	4,26E-02	0,00E+00	7,00E-02	2,70E+02
3	0,015	8,00E+08	0,46	0,00E+00	3	4,00E+05	2,00E+05	5,28E-02	-9,00E-02	6,00E-02	2,70E+02
4	0,03	1,20E+09	0,45	0,00E+00	4	4,00E+05	2,00E+05	5,28E-02	9,00E-02	-6,00E-02	9,00E+01
5	0,03	1,52E+09	0,45	0,00E+00	5	1,75E+02	2,00E+05	4,26E-02	0,00E+00	-7,00E-02	9,00E+01
6	0,06	3,07E+09	0,45	0,00E+00	6	1,15E+02	2,00E+05	5,28E-02	-9,00E-02	-6,00E-02	9,00E+01
7	0,07	3,70E+09	0,44	0,00E+00	7	6,23E+02	1,80E+05	2,26E-02	0,00E+00	9,00E-02	1,80E+02
8	0,07	3,80E+09	0,43	0,00E+00	8	6,23E+02	1,80E+05	2,26E-02	0,00E+00	-9,00E-02	1,80E+02
9	0,25	1,00E+08	0,35	0,00E+00	9	7,50E+05	1,50E+05	1,13E-01	0,00E+00	0,00E+00	4,50E+01
10		5,00E+07	0,5		10	7,50E+05	6,00E+04	5,00E-02	0,00E+00	0,00E+00	1,35E+02

Position Number 1 Layer Number: 1 X Coordinate (m): 0,00E+00 Y Coordinate (m): 0,00E+00 Z Coordinate (m): 1,00E-03

Load No.	Distance to Load Axis (m)	Theta (°)	Radial Displacement (m)	Tangential Displacement (m)	Vertical Displacement (m)	Radial Stress (Pa)	Tangential Stress (Pa)	Vertical Stress (Pa)	Rad./Tang. Stress (Pa)	Rad./Vert. Stress (Pa)	Tang./Vert. Stress (Pa)	Radial Strain	Tangential Strain	Vertical Strain	Rad./Tang. Strain	Rad./Vert. Strain	Tang./Vert. Strain
1	1,08E-01	-4,16E+02	6,53E-06	3,96E-06	3,38E-05	-4,00E+04	-9,25E+03	-1,00E+01	6,92E+02	-6,35E+02	8,98E+00	-1,18E-04	3,59E-05	8,21E-05	3,46E-06	-3,17E-06	4,49E-08
2	7,00E-02	-3,80E+02	1,17E-05	1,03E-11	-1,21E-08	-8,24E+04	-1,23E+04	-4,92E+01	4,01E-02	-2,32E+03	1,25E-03	-2,54E-04	9,63E-05	1,58E-04	2,01E-10	-1,16E-05	6,24E-12
3	1,08E-01	-3,04E+02	6,53E-06	-3,96E-06	3,38E-05	-4,00E+04	-9,25E+03	-1,00E+01	-6,92E+02	-6,35E+02	-8,98E+00	-1,18E-04	3,59E-05	8,21E-05	-3,46E-06	-3,17E-06	-4,49E-08
4	1,08E-01	5,63E+01	6,53E-06	-3,96E-06	3,38E-05	-4,00E+04	-9,25E+03	-1,00E+01	-6,92E+02	-6,35E+02	-8,98E+00	-1,18E-04	3,59E-05	8,21E-05	-3,46E-06	-3,17E-06	-4,49E-08
5	7,00E-02	-3,67E-05	1,17E-05	3,16E-12	-1,21E-08	-8,24E+04	-1,23E+04	-4,92E+01	1,23E-02	-2,32E+03	3,83E-04	-2,54E-04	9,63E-05	1,58E-04	6,16E-11	-1,16E-05	1,92E-12
6	1,08E-01	-5,63E+01	5,39E-06	3,96E-06	-2,58E-07	-2,14E+04	-3,07E+03	-5,97E+00	6,92E+02	-4,09E+02	8,98E+00	-6,81E-05	2,54E-05	4,07E-05	3,48E-06	-2,05E-06	4,49E-08
7	9,00E-02	-2,70E+02	5,86E-10	-8,10E-07	9,93E-09	-7,07E+00	-1,55E+00	-1,04E-03	-6,79E+02	-9,87E-02	-9,82E+00	-2,10E-08	6,81E-09	1,44E-08	-3,40E-06	-4,94E-10	-4,91E-08
8	9,00E-02	-9,00E+01	5,91E-10	8,10E-07	9,93E-09	-7,06E+00	-1,56E+00	-1,04E-03	6,79E+02	-9,86E-02	9,82E+00	-2,10E-08	6,88E-09	1,44E-08	3,40E-06	-4,93E-10	4,91E-08
9	0,00E+00	-4,50E+01	4,25E-05	4,25E-05	3,44E-04	-7,15E+05	-7,15E+05	-7,50E+05	0,00E+00	-1,08E+05	-1,06E+05	5,88E-05	5,88E-05	-1,18E-04	0,00E+00	-5,27E-04	-5,27E-04
10	0,00E+00	-1,33E+02	-9,53E-06	9,53E-06	1,04E-04	-5,93E+05	-5,93E+05	-7,50E+05	0,00E+00	4,16E+04	-4,16E+04	2,62E-04	2,62E-04	-5,23E-04	0,00E+00	2,08E-04	-2,08E-04

Total Stresses F XX: -1,44E+06 YY: -1,54E+06 ZZ: -1,50E+06 YZ: -1,47E+05 XZ: -6,38E+04 XY: 5,76E+03
Total Strains XX: 2,50E-04 YY: -2,12E-04 ZZ: -3,82E-05 YZ: -7,35E-04 XZ: -3,19E-04 XY: 2,88E-05
Total Displacement UX: 3,04E-05 UY: 5,14E-05 UZ: 5,47E-04

Principal Value and Direction of Total Stresses and Strains

	Normal Stress (Pa)	Normal Strain	Shear Stress (Pa)	Shear Strain	X Comp.	Y Comp.	Z Comp.
Maximum:	-1,34E+06	7,53E-04			-0,472	-0,543	0,6948
Minimum:	-1,46E+06	1,45E-04			0,8651	-0,4389	0,2463
Minimum:	-1,67E+06	-8,98E-04			0,1697	0,7172	0,8759
Maximum:			1,65E+05	8,25E-04	-0,4537	-0,891	0,0132
MiniMax:	-1,51E+06				-0,2137	0,1232	0,9691
			1,04E+05	5,21E-04	0,4917	-0,816	-0,3038
	-1,57E+06				0,7317	0,1982	0,6521
Minimum:			6,08E+04	3,04E-04	-0,9455	-0,075	0,317
	-1,40E+06				0,278	-0,6929	0,6853

Strain Energy (J) 1,39E+02
Strain Energy of 1,39E+02

Position Number 2 Layer Number: 1 X Coordinate (m): 0,00E+00 Y Coordinate (m): 5,00E-02 Z Coordinate (m): 1,00E-03

Load No.	Distance to Load Axis (m)	Theta (°)	Radial Displacement (m)	Tangential Displacement (m)	Vertical Displacement (m)	Radial Stress (Pa)	Tangential Stress (Pa)	Vertical Stress (Pa)	Rad./Tang. Stress (Pa)	Rad./Vert. Stress (Pa)	Tang./Vert. Stress (Pa)	Radial Strain	Tangential Strain	Vertical Strain	Rad./Tang. Strain	Rad./Vert. Strain	Tang./Vert. Strain
1	9,06E-02	-4,44E+02	3,65E-06	5,71E-06	3,46E-05	-3,42E+04	-7,11E+03	2,36E+00	-8,22E+02	-5,40E+02	-7,83E+01	-1,02E-04	3,33E-05	6,88E-05	-4,11E-06	-2,70E-06	-3,92E-07
2	2,00E-02	-3,60E+02	3,78E-05	7,74E-11	-1,30E-06	-8,91E+04	-3,63E+04	-2,82E+02	1,16E-02	-1,93E+05	5,23E-03	-2,36E-04	2,80E-05	2,08E-04	5,81E-11	-9,66E-04	2,61E-11
3	9,06E-02	-2,76E+02	3,65E-06	-5,71E-06	3,46E-05	-3,42E+04	-7,11E+03	2,36E+00	8,22E+02	-5,40E+02	7,83E+01	-1,02E-04	3,33E-05	6,88E-05	4,11E-06	-2,70E-06	3,92E-07
4	1,42E-01	3,93E+01	5,24E-06	-2,54E-06	3,34E-05	-2,49E+04	-7,91E+03	-1,01E+01	-4,86E+02	-2,69E+02	-1,11E+01	-6,88E-05	1,51E-05	5,46E-05	-2,43E-06	-1,35E-06	-5,54E-08
5	1,20E-01	-3,87E-05	5,52E-06	1,80E-12	-1,32E-07	-1,79E+04	-2,18E+03	-3,37E+00	2,88E-03	-2,87E+02	5,24E-05	-5,59E-05	2,25E-05	3,34E-05	1,44E-11	-1,43E-06	2,62E-13
6	1,42E-01	-3,93E+01	5,39E-06	2,54E-06	1,00E-07	-1,35E+04	-1,91E+03	-2,12E+00	4,86E+02	-1,83E+02	1,11E+01	-4,18E-05	1,61E-05	2,57E-05	2,43E-06	-9,14E-07	5,54E-08
7	4,00E-02	-2,70E+02	3,26E-09	-2,43E-06	1,17E-08	-3,04E+01	9,27E+00	9,88E-02	2,35E+03	7,55E-01	4,05E+02	-1,17E-07	8,14E-08	3,56E-08	1,17E-05	3,77E-09	2,02E-06

8	1,40E-01	-9,00E+01	-4,05E-11	6,48E-07	9,60E-09	-3,21E+00	-1,69E+00	-1,43E-03	2,02E+02	-2,41E-02	3,39E+00	-7,88E-09	-2,83E-10	8,17E-09	1,01E-06	-1,20E-10	1,70E-08
9	5,00E-02	4,50E+01	4,43E-05	-4,08E-05	3,42E-04	-7,28E+05	-7,18E+05	-7,50E+05	7,34E+03	-1,06E+05	1,05E+05	2,03E-05	7,05E-05	-9,08E-05	3,67E-05	-5,30E-04	5,27E-04
10	5,00E-02	-4,50E+01	2,04E-05	4,67E-06	7,99E-05	-4,35E+05	-3,16E+05	-3,86E+05	-4,03E+04	-2,49E+05	-1,95E+04	-2,78E-04	3,14E-04	-3,60E-05	-2,02E-04	-1,24E-03	-9,77E-05
Total Stresses (F XX:		-1,16E+06	YY:	-1,31E+06	ZZ:	-1,14E+06	YZ:	-1,82E+05	XZ:	-8,53E+04	XY:	3,31E+04					
Total Strains XX:		2,05E-04	YY:	-5,38E-04	ZZ:	3,33E-04	YZ:	-8,07E-04	XZ:	-4,27E-04	XY:	1,65E-04					
Total Displacement UX:		3,31E-05	UY:	3,17E-05	UZ:	5,23E-04											

Principal Value and Direction of Total Stresses and Strains

	Normal Stress (Pa)	Normal Strain	Shear Stress (Pa)	Shear Strain	X Comp.	Y Comp.	Z Comp.	
Maximum:	-9,92E+05	1,06E-03				-0,47	-0,4374	0,7666
Minimax:	-1,21E+06	-2,97E-05				0,88	-0,2995	0,3686
Minimum:	-1,41E+06	-1,03E-03				0,0684	0,8479	0,5257
Maximum:			2,08E+05	1,04E-03	-0,3807	-0,9089	0,1704	
	-1,20E+06				-0,284	0,2902	0,9138	
MiniMax:			1,08E+05	5,42E-04	-0,9546	-0,0975	0,2614	
	-1,10E+06				0,2899	-0,5211	0,8027	
Minimum:			9,95E+04	4,98E-04	0,5739	-0,8113	-0,1111	
	-1,31E+06				0,6706	0,3878	0,6324	
Strain Energy (J)	2,16E+02							
Strain Energy of	2,16E+02							

Position Number 3 Layer Number: 1 X Coordinate (m): 0,00E+00 Y Coordinate (m): 1,10E-01 Z Coordinate (m): 1,00E-03

Load No.	Distance to Load Axis (m)	Theta (°)	Radial Displacement (m)	Tangential Displacement (m)	Vertical Displacement (m)	Radial Stress (Pa)	Tangential Stress (Pa)	Vertical Stress (Pa)	Rad./Tang. Stress (Pa)	Rad./Vert. Stress (Pa)	Tang./Vert. Stress (Pa)	Radial Strain	Tangential Strain	Vertical Strain	Rad./Tang. Strain	Rad./Vert. Strain	Tang./Vert. Strain
1	1,03E-01	-1,19E+02	-3,61E-06	4,35E-06	3,45E-05	9,88E+02	-2,99E+03	-1,50E+00	5,42E+02	1,70E+02	1,73E+00	8,28E-06	-1,16E-05	3,33E-06	2,71E-06	8,52E-07	8,63E-09
2	4,00E-02	-1,80E+02	-2,85E-05	-4,77E-11	1,84E-06	3,39E+05	1,40E+05	8,33E+03	-4,54E-02	1,54E+05	-8,49E-03	8,83E-04	-1,14E-04	-7,70E-04	-2,27E-10	7,68E-04	-4,25E-11
3	1,03E-01	-2,41E+02	-3,61E-06	-4,35E-06	3,45E-05	9,88E+02	-2,99E+03	-1,50E+00	-5,42E+02	1,70E+02	-1,73E+00	8,28E-06	-1,16E-05	3,33E-06	-2,71E-06	8,52E-07	-8,63E-09
4	1,92E-01	2,79E+01	3,39E-06	-1,68E-06	3,31E-05	-1,44E+04	-8,85E+03	1,37E+00	-1,34E+02	-9,67E+01	-4,03E+00	-3,65E-05	1,12E-06	3,54E-05	-6,68E-07	-4,84E-07	-2,02E-08
5	1,80E-01	-3,67E-05	3,59E-06	1,53E-12	3,52E-07	-5,91E+03	-9,53E+02	-4,53E-01	8,55E-04	-5,56E+01	1,28E-05	-1,81E-05	6,68E-06	1,14E-05	4,28E-12	-2,78E-07	6,39E-14
6	1,92E-01	-2,79E+01	4,57E-06	1,68E-06	5,54E-07	-6,85E+03	-1,24E+03	-5,02E-01	1,34E+02	-5,89E+01	4,03E+00	-2,08E-05	7,29E-06	1,35E-05	6,68E-07	-2,95E-07	2,02E-08
7	2,00E-02	-9,00E+01	5,73E-09	1,42E-05	3,13E-08	-4,07E+02	-4,26E+02	-6,17E+02	-9,50E+04	-1,73E+01	-1,48E+05	3,81E-07	2,87E-07	-6,68E-07	-4,75E-04	-8,67E-08	-7,41E-04
8	2,00E-01	-9,00E+01	-3,84E-10	5,85E-07	9,35E-09	-2,04E+00	-1,60E+00	-2,43E-03	4,81E+01	-2,10E-02	1,82E+00	-4,14E-09	-1,92E-09	6,06E-09	2,41E-07	-1,05E-10	9,07E-09
9	1,10E-01	4,50E+01	4,23E-05	-2,60E-05	3,19E-04	-7,96E+05	-7,27E+05	-7,47E+05	8,38E+04	-1,03E+05	9,21E+04	-1,97E-04	1,48E-04	4,94E-05	4,19E-04	-5,16E-04	4,61E-04
10	1,10E-01	-4,50E+01	3,55E-06	8,91E-07	5,75E-05	-3,72E+04	-1,13E+04	4,14E-01	2,11E+02	-4,89E+02	2,35E+00	-1,05E-04	2,42E-05	8,09E-05	1,05E-06	-2,45E-06	1,18E-08
Total Stresses (F XX:		-8,10E+05 YY:		-5,24E+05 ZZ:		-7,39E+05 YZ:		4,99E+04 XZ:		5,60E+04 XY:		1,17E+04					
Total Strains XX:		7,02E-05 YY:		5,03E-04 ZZ:		-5,73E-04 YZ:		2,50E-04 XZ:		2,80E-04 XY:		5,86E-05					
Total Displacement UX:		1,09E-05 UY:		1,85E-05 UZ:													

Principal Value and Direction of Total Stresses and Strains

	Normal Stress (Pa)	Normal Strain	Shear Stress (Pa)	Shear Strain	X Comp.	Y Comp.	Z Comp.	
Maximum:	-5,07E+05	5,88E-04				0,2462	0,9337	0,26
Minimax:	-5,99E+05	1,28E-04				0,9153	-0,3122	0,2543
Minimum:	-7,68E+05	-7,16E-04				-0,3186	-0,1754	0,9315
Maximum:			1,30E+05	6,52E-04	0,3994	0,7842	-0,4748	
	-6,37E+05				-0,0512	0,5362	0,8425	
MiniMax:			8,44E+04	4,22E-04	0,8726	-0,0967	-0,4788	
	-6,83E+05				0,4219	-0,3448	0,8385	
Minimum:			4,60E+04	2,30E-04	-0,4731	0,881	0,004	
	-5,53E+05				0,8213	0,4395	0,3637	
Strain Energy (J)	8,75E+01							
Strain Energy of	8,75E+01							

Position Number 4 Layer Number: 1 X Coordinate (m): 0,00E+00 Y Coordinate (m): 2,10E-01 Z Coordinate (m): 1,00E-03

Load No.	Distance to Load Axis (m)	Theta (°)	Radial Displacement (m)	Tangential Displacement (m)	Vertical Displacement (m)	Radial Stress (Pa)	Tangential Stress (Pa)	Vertical Stress (Pa)	Rad./Tang. Stress (Pa)	Rad./Vert. Stress (Pa)	Tang./Vert. Stress (Pa)	Radial Strain	Tangential Strain	Vertical Strain	Rad./Tang. Strain	Rad./Vert. Strain	Tang./Vert. Strain
1	1,75E-01	-1,49E+02	-5,73E-06	1,90E-06	3,24E-05	-7,91E+00	-4,39E+03	6,90E+00	2,15E+02	4,31E+01	7,43E+00	7,28E-06	-1,48E-05	7,36E-06	1,07E-06	2,16E-07	3,72E-08

2	1.40E-01	-1.80E+02	-4.62E-06	-5.20E-12	-5.46E-08	1.16E+04	1.48E+03	1.87E+00	-5.72E-03	1.56E+02	-9.27E-05	3.61E-05	-1.43E-05	-2.17E-05	-2.86E-11	7.79E-07	-4.63E-13
3	1.75E-01	-2.11E+02	-5.73E-06	-1.90E-08	3.24E-05	-7.93E+00	-4.39E+03	6.90E+00	-2.15E+02	4.31E+01	-7.43E+00	7.28E-08	-1.46E-05	7.36E-08	-1.07E-06	2.16E-07	-3.72E-08
4	2.85E-01	1.84E+01	1.43E-06	-1.02E-06	3.22E-05	-7.84E+03	-5.55E+03	-1.87E+00	2.60E+01	-3.36E+01	-1.68E+00	-1.62E-05	-5.76E-06	2.20E-05	1.30E-07	-1.68E-07	-8.38E-09
5	2.80E-01	-3.67E-05	2.54E-06	1.36E-12	7.31E-07	-2.20E+03	-6.64E+02	5.27E-02	1.86E-04	-1.12E+01	3.58E-06	-6.22E-06	1.45E-06	4.77E-06	9.28E-13	-5.59E-08	1.79E-14
6	2.85E-01	-1.84E+01	3.63E-06	1.02E-06	1.07E-06	-3.09E+03	-9.52E+02	-1.36E-01	-2.60E+01	-1.30E+01	1.68E+00	-8.70E-06	1.97E-06	6.73E-06	-1.30E-07	-6.52E-08	8.38E-09
7	1.20E-01	-9.00E+01	1.38E-10	6.89E-07	9.71E-09	-4.08E+00	-1.69E+00	2.04E-03	3.21E+02	-4.02E-02	6.40E+00	-1.08E-08	1.16E-09	9.62E-09	1.61E-06	-2.01E-10	3.20E-08
8	3.00E-01	-9.00E+01	-6.69E-10	5.31E-07	8.90E-09	-1.24E+00	-1.29E+00	-4.44E-04	-1.75E+01	-6.33E-03	-1.75E-01	-1.98E-09	-2.23E-09	4.20E-09	-8.76E-08	-3.16E-11	-8.73E-10
9	2.10E-01	4.50E+01	4.37E-07	-8.79E-06	2.79E-04	-7.78E+04	-5.08E+04	3.00E+00	3.07E+02	-5.13E+02	-1.64E+01	-1.75E-04	-3.98E-05	2.14E-04	1.53E-06	-2.57E-06	-6.21E-08
10	2.10E-01	-4.50E+01	-1.53E-06	6.71E-07	5.49E-05	-1.26E+04	-9.46E+03	-6.32E+00	3.47E+01	-7.24E+01	2.28E+00	-2.63E-05	-1.05E-05	3.68E-05	1.73E-07	-3.62E-07	1.14E-08

Total Stresses (F XX: -7.24E+04 YY: -9.41E+04 ZZ: 1.04E+01 YZ: -4.18E+02 XZ: 1.44E+01 XY: -6.58E+02
Total Strains XX: -8.47E-05 YY: -1.93E-04 ZZ: 2.78E-04 YZ: -2.09E-06 XZ: 7.20E-08 XY: -3.29E-06
Total Displacement UX: 7.60E-06 UY: -9.50E-06 UZ: 4.32E-04

Principal Value and Direction of Total Stresses and Strains

	Normal Stress (Pa)	Normal Strain	Shear Stress (Pa)	Shear Strain	X Comp.	Y Comp.	Z Comp.	
Maximum:	1.23E+01	2.78E-04			0.0002	-0.0044	1	
Minimum:	-7.24E+04	-8.46E-05			0.9995	-0.0303	-0.0004	
Maximum:	-9.41E+04	-1.93E-04			0.0303	0.9995	0.0044	
Maximum:			4.71E+04	2.35E-04	-0.0213	-0.7099	0.704	
	-4.71E+04				0.0216	0.7036	0.7102	
MiniMax:			3.62E+04	1.81E-04	-0.7066	0.0183	0.7074	
	-3.62E+04				0.707	-0.0246	0.7068	
Minimum:			1.08E+04	5.42E-05	0.6853	-0.7282	-0.0034	
	-8.33E+04				0.7282	0.6853	0.0029	
Strain Energy (J)	1.22E+01							
Strain Energy of	1.22E+01							

Position Number 5 Layer Number: 1 X Coordinate (m): 0.00E+00 Y Coordinate (m): 3.10E-01 Z Coordinate (m): 1.00E-03

Load No.	Distance to Load Axis (m)	Theta (°)	Radial Displacement (m)	Tangential Displacement (m)	Vertical Displacement (m)	Radial Stress (Pa)	Tangential Stress (Pa)	Vertical Stress (Pa)	Rad./Tang. Stress (Pa)	Rad./Vert. Stress (Pa)	Tang./Vert. Stress (Pa)	Radial Strain	Tangential Strain	Vertical Strain	Rad./Tang. Strain	Rad./Vert. Strain	Tang./Vert. Strain
1	2.66E-01	-1.60E+02	-5.83E-06	1.12E-06	3.05E-05	-1.49E+03	-3.83E+03	-2.50E+00	-1.47E+01	-7.63E+00	2.77E+00	1.42E-06	-1.03E-05	8.85E-06	-7.33E-08	-3.82E-08	1.39E-08
2	2.40E-01	-1.80E+02	-2.84E-06	-4.42E-12	-5.96E-07	3.02E+03	7.33E+02	3.29E-02	-1.03E-03	1.61E+01	-1.72E-05	8.83E-06	-2.58E-06	-6.25E-06	-5.15E-12	8.04E-08	-8.80E-14
3	2.66E-01	-2.00E+02	-5.83E-06	-1.12E-06	3.05E-05	-1.49E+03	-3.83E+03	-2.50E+00	1.47E+01	-7.63E+00	-2.77E+00	1.42E-06	-1.03E-05	8.85E-06	7.33E-08	-3.82E-08	-1.39E-08
4	3.81E-01	1.37E+01	3.86E-07	-7.06E-07	3.09E-05	-4.74E+03	-4.37E+03	-5.85E-01	4.40E+01	-2.31E+01	-7.92E-01	-8.51E-06	-6.67E-06	1.52E-05	2.20E-07	-1.15E-07	-3.96E-09
5	3.80E-01	-3.67E-05	2.09E-06	1.26E-12	9.10E-07	-1.25E+03	-5.25E+02	3.97E-02	4.28E-05	-5.74E+00	1.25E-06	-3.29E-06	3.33E-07	2.96E-06	2.14E-13	-2.87E-08	6.25E-15
6	3.81E-01	-1.37E+01	3.09E-06	7.06E-07	1.34E-06	-1.84E+03	-7.74E+02	-8.16E-02	-4.40E+01	-9.33E+00	7.92E-01	-4.85E-06	4.91E-07	4.36E-06	-2.20E-07	-4.67E-08	3.96E-09
7	2.20E-01	-9.00E+01	-4.59E-10	5.72E-07	9.26E-09	-1.82E+00	-1.54E+00	-1.65E-03	2.72E+01	-9.33E-03	1.45E+00	-3.51E-09	-2.09E-09	5.59E-09	1.36E-07	-4.67E-11	7.24E-09
8	4.00E-01	-9.00E+01	-8.02E-10	4.89E-07	8.40E-09	-7.60E-01	-9.81E-01	-1.27E-04	-3.20E+01	-1.36E-03	1.39E+00	-8.99E-10	-2.00E-09	2.90E-09	-1.60E-07	-6.78E-12	8.96E-09
9	3.10E-01	4.50E+01	-1.10E-05	-7.72E-06	2.66E-04	-4.21E+04	-3.92E+04	-3.22E+00	3.62E+02	-2.09E+02	-1.29E+01	-7.51E-05	-8.05E-05	1.36E-04	1.81E-06	-1.05E-06	-6.43E-08
10	3.10E-01	-4.50E+01	-3.34E-06	6.07E-07	5.23E-05	-7.35E+03	-7.49E+03	-1.96E+00	-2.41E+01	-3.06E+01	9.57E-01	-1.20E-05	-1.27E-05	2.47E-05	-1.21E-07	-1.53E-07	4.79E-09

Total Stresses (F XX: -5.88E+04 YY: -5.78E+04 ZZ: -1.08E+01 YZ: -2.77E+02 XZ: 1.23E+01 XY: -4.94E+02
Total Strains XX: -9.98E-05 YY: -9.45E-05 ZZ: 1.94E-04 YZ: -1.38E-06 XZ: 6.15E-08 XY: -2.47E-06
Total Displacement UX: 6.70E-06 UY: -2.31E-05 UZ: 4.12E-04

Principal Value and Direction of Total Stresses and Strains

	Normal Stress (Pa)	Normal Strain	Shear Stress (Pa)	Shear Strain	X Comp.	Y Comp.	Z Comp.	
Maximum:	-9.42E+00	1.94E-04			0.0002	-0.0048	1	
Minimum:	-5.76E+04	-9.35E-05			-0.3673	0.9301	0.0045	
Maximum:	-5.90E+04	-1.01E-04			0.9301	0.3673	0.0015	
Maximum:			2.95E+04	1.48E-04	-0.6575	-0.2631	0.708	
	-2.95E+04				0.6579	0.2563	0.7082	
MiniMax:			2.88E+04	1.44E-04	0.2599	-0.6611	0.7039	
	-2.88E+04				-0.2596	0.6543	0.7103	
Minimum:			7.22E+02	3.61E-06	-0.9174	0.3979	0.0021	
	-5.83E+04				0.3979	0.9174	0.0043	
Strain Energy (J)	5.68E+00							
Strain Energy of	5.68E+00							

Position Number	6	Layer Number:	1	X Coordinate (m):	0,00E+00	Y Coordinate (m):	3,20E-01	Z Coordinate (m):	1,00E-03								
Load No.	Distance to Load Axis (m)	Theta (°)	Radial Displacement (m)	Tangential Displacement (m)	Vertical Displacement (m)	Radial Stress (Pa)	Tangential Stress (Pa)	Vertical Stress (Pa)	Rad./Tang. Stress (Pa)	Rad./Vert. Stress (Pa)	Tang./Vert. Stress (Pa)	Radial Strain	Tangential Strain	Vertical Strain	Rad./Tang. Strain	Rad./Vert. Strain	Tang./Vert. Strain
1	2,75E-01	-1,61E+02	-5,83E-06	1,07E-06	3,03E-05	-1,48E+03	-3,73E+03	-1,67E+00	-2,14E+01	-6,22E+00	2,17E+00	1,31E-06	-9,98E-06	8,67E-06	-1,07E-07	-3,11E-08	1,08E-08
2	2,50E-01	-1,80E+02	-2,75E-06	-4,38E-12	-6,29E-07	2,76E+03	7,13E+02	1,12E-01	-8,88E-04	1,68E+01	-1,49E-05	8,02E-06	-2,23E-06	-5,79E-06	-4,44E-12	8,40E-08	-7,44E-14
3	2,75E-01	-1,99E+02	-5,83E-06	-1,07E-06	3,03E-05	-1,48E+03	-3,73E+03	-1,67E+00	2,14E+01	-6,22E+00	-2,17E+00	1,31E-06	-9,98E-06	8,67E-06	1,07E-07	-3,11E-08	-1,08E-08
4	3,91E-01	1,33E+01	2,97E-07	-6,84E-07	3,07E-05	-4,54E+03	-4,26E+03	-3,52E-01	4,38E+01	-2,08E+01	-1,76E-01	-8,04E-06	-6,63E-06	1,47E-05	2,19E-07	-1,04E-07	-8,82E-10
5	3,90E-01	-3,67E-05	2,06E-06	1,25E-12	9,21E-07	-1,19E+03	-5,11E+02	-7,20E-02	3,63E-05	-6,27E+00	1,11E-06	-3,12E-06	2,82E-07	2,84E-06	1,82E-13	-3,14E-08	5,54E-15
6	3,91E-01	-1,33E+01	3,05E-06	6,84E-07	1,36E-06	-1,77E+03	-7,59E+02	8,36E-02	-4,38E+01	-4,30E+00	1,76E-01	-4,63E-06	4,19E-07	4,21E-08	-2,19E-07	-2,15E-08	8,82E-10
7	2,30E-01	-9,00E+01	-4,94E-10	5,66E-07	9,22E-09	-1,72E+00	-1,51E+00	-1,37E-03	1,65E+01	-7,91E-03	1,39E+00	-3,24E-09	-2,14E-09	5,38E-09	8,23E-08	-3,96E-11	6,94E-09
8	4,10E-01	-9,00E+01	-8,10E-10	4,85E-07	8,35E-09	-7,40E-01	-9,62E-01	-1,14E-04	-3,25E+01	-3,35E-03	1,23E+00	-8,64E-10	-1,97E-09	2,84E-09	-1,63E-07	-1,68E-11	6,13E-09
9	3,20E-01	4,50E+01	-1,18E-05	-7,65E-06	2,65E-04	-4,01E+04	-3,82E+04	-3,23E+00	3,82E+02	-1,91E+02	-1,08E+01	-6,99E-05	-6,06E-05	1,31E-04	1,91E-06	-9,55E-07	-5,41E-08
10	3,20E-01	-4,50E+01	-3,44E-06	6,02E-07	5,20E-05	-7,03E+03	-7,30E+03	-1,66E+00	-2,68E+01	-4,46E+01	8,24E-01	-1,13E-05	-1,26E-05	2,39E-05	-1,34E-07	-2,23E-07	4,12E-09

Total Stresses (F XX: -5,74E+04 YY: -5,52E+04 ZZ: -8,46E+00 YZ: -2,63E+02 XZ: 1,12E+01 XY: -5,03E+02
Total Strains XX: -9,92E-05 YY: -8,84E-05 ZZ: 1,88E-04 YZ: -1,31E-08 XZ: 5,60E-08 XY: -2,51E-06
Total Displacement UX: 6,63E-06 UY: -2,40E-05 UZ: 4,10E-04

Principal Value and Direction of Total Stresses and Strains

	Normal Stress (Pa)	Normal Strain	Shear Stress (Pa)	Shear Strain	X Comp.	Y Comp.	Z Comp.
Maximum:	-7,20E+00	1,88E-04			0,0002	-0,0048	1
Minimax:	-5,51E+04	-8,79E-05			-0,2162	0,9763	0,0047
Minimum:	-5,75E+04	-9,98E-05			0,9763	0,2162	0,0008
Maximum:			2,88E+04	1,44E-04	-0,6902	-0,1563	0,7065
	-2,88E+04				0,6905	0,1495	0,7077
MiniMax:			2,76E+04	1,38E-04	0,1531	-0,6937	0,7038
	-2,76E+04				-0,1527	0,687	0,7104
Minimum:			1,19E+03	5,95E-06	-0,8433	0,5375	0,0028
	-5,63E+04				0,5375	0,8433	0,0039

Strain Energy (J) 5,29E+00

Strain Energy of 5,29E+00

Position Number	7	Layer Number:	1	X Coordinate (m):	0,00E+00	Y Coordinate (m):	5,00E-01	Z Coordinate (m):	1,00E-03								
Load No.	Distance to Load Axis (m)	Theta (°)	Radial Displacement (m)	Tangential Displacement (m)	Vertical Displacement (m)	Radial Stress (Pa)	Tangential Stress (Pa)	Vertical Stress (Pa)	Rad./Tang. Stress (Pa)	Rad./Vert. Stress (Pa)	Tang./Vert. Stress (Pa)	Radial Strain	Tangential Strain	Vertical Strain	Rad./Tang. Strain	Rad./Vert. Strain	Tang./Vert. Strain
1	4,49E-01	-1,68E+02	-5,75E-06	5,68E-07	2,69E-05	-7,18E+02	-2,35E+03	-1,35E-01	-4,02E+01	-7,64E+00	5,87E-01	1,52E-06	-6,62E-06	5,11E-06	-2,01E-07	-3,82E-08	2,94E-09
2	4,30E-01	-1,80E+02	-1,94E-06	-3,76E-12	-9,44E-07	1,01E+03	4,63E+02	-4,66E-02	-5,25E-05	1,48E+00	-4,29E-06	2,58E-06	-1,34E-07	-2,45E-06	-2,62E-13	7,40E-09	-2,15E-14
3	4,49E-01	-1,92E+02	-5,75E-06	-5,68E-07	2,69E-05	-7,18E+02	-2,35E+03	-1,35E-01	4,02E+01	-7,64E+00	-5,87E-01	1,52E-06	-6,62E-06	5,11E-06	2,01E-07	-3,82E-08	-2,94E-09
4	5,67E-01	9,13E+00	-5,23E-07	-4,13E-07	2,77E-05	-2,11E+03	-2,69E+03	-5,61E-02	3,01E+01	-1,35E+01	-8,35E-02	-2,55E-06	-5,45E-06	8,00E-06	1,51E-07	-6,77E-08	-4,18E-10
5	5,70E-01	-3,67E-05	1,67E-06	1,09E-12	1,01E-06	-6,18E+02	-3,29E+02	3,15E-02	-8,28E-06	5,95E-01	-2,84E-07	-1,51E-06	-6,63E-08	1,58E-06	-4,14E-14	2,98E-09	-1,42E-15
6	5,67E-01	-9,13E+00	2,52E-06	4,13E-07	1,52E-06	-9,37E+02	-4,97E+02	3,17E-02	-3,01E+01	-4,54E+00	8,35E-02	-2,30E-06	-9,58E-06	2,39E-06	-1,51E-07	-2,27E-08	4,18E-10
7	4,10E-01	-9,00E+01	-8,10E-10	4,85E-07	8,35E-09	-7,40E-01	-9,62E-01	-1,14E-04	-3,25E+01	-3,35E-03	1,23E+00	-8,64E-10	-1,97E-09	2,84E-09	-1,63E-07	-1,68E-11	6,13E-09
8	5,90E-01	-9,00E+01	-8,71E-10	4,26E-07	7,42E-09	-3,03E-01	-5,94E-01	-2,24E-05	-3,10E+01	2,09E-03	7,53E-01	-1,99E-11	-1,47E-09	1,49E-09	-1,55E-07	1,05E-11	3,77E-09
9	5,00E-01	4,50E+01	-1,88E-05	-6,63E-06	2,39E-04	-1,74E+04	-2,40E+04	-7,67E-01	4,81E+02	-1,13E+02	-5,55E+00	-1,81E-05	-5,09E-05	6,90E-05	2,41E-06	-5,65E-07	-2,77E-08
10	5,00E-01	-4,50E+01	-4,55E-06	5,23E-07	4,67E-05	-3,05E+03	-4,57E+03	-2,41E-01	-3,78E+01	-2,19E+01	6,14E-01	-2,55E-06	-1,01E-05	1,27E-05	-1,89E-07	-1,09E-07	3,07E-09

Total Stresses (F XX: -3,62E+04 YY: -2,47E+04 ZZ: -1,32E+00 YZ: -1,66E+02 XZ: 4,38E+00 XY: -5,40E+02
Total Strains XX: -7,94E-05 YY: -2,20E-05 ZZ: 1,01E-04 YZ: -8,29E-07 XZ: 2,19E-08 XY: -2,70E-06
Total Displacement UX: 5,68E-06 UY: -3,30E-05 UZ: 3,68E-04

Principal Value and Direction of Total Stresses and Strains

	Normal Stress (Pa)	Normal Strain	Shear Stress (Pa)	Shear Strain	X Comp.	Y Comp.	Z Comp.
Maximum:	-2,02E-01	1,01E-04			0,0002	-0,0067	1
Minimax:	-2,47E+04	-2,19E-05			-0,0468	0,9989	0,0067
Minimum:	-3,62E+04	-7,95E-05			0,9989	0,0468	0,0001
Maximum:			1,81E+04	9,05E-05	-0,7062	-0,0379	0,707
	-1,81E+04				0,7065	0,0283	0,7072
MiniMax:			1,23E+04	6,16E-05	0,0333	-0,7111	0,7023
	-1,23E+04				-0,0329	0,7016	0,7118

Minimum: -3,04E+04 5,77E+03 2,89E-05 -0,7394 0,6732 0,0047
0,6732 0,7394 0,0048

Strain Energy (J) 1,71E+00
Strain Energy of 1,71E+00

Position Number 8 Layer Number: 1 X Coordinate (m): 0,00E+00 Y Coordinate (m): 7,50E-01 Z Coordinate (m): 1,00E-03

Load No.	Distance to Load Axis (m)	Theta (°)	Radial Displacement (m)	Tangential Displacement (m)	Vertical Displacement (m)	Radial Stress (Pa)	Tangential Stress (Pa)	Vertical Stress (Pa)	Rad./Tang. Stress (Pa)	Rad./Vert. Stress (Pa)	Tang./Vert. Stress (Pa)	Radial Strain	Tangential Strain	Vertical Strain	Rad./Tang. Strain	Rad./Vert. Strain	Tang./Vert. Strain
1	6,96E-01	-1,73E+02	-5,28E-06	3,10E-07	2,24E-05	1,08E+02	-1,20E+03	-9,14E-02	-2,10E+01	-7,55E+00	1,55E-01	2,36E-06	-4,18E-06	1,82E-06	-1,05E-07	-3,77E-08	7,77E-10
2	6,80E-01	-1,80E+02	-1,53E-06	-3,16E-12	-9,66E-07	4,47E+02	2,49E+02	-3,33E-02	3,37E-05	1,27E+00	-6,43E-07	1,08E-06	6,33E-08	-1,16E-06	1,68E-13	6,34E-09	-3,21E-15
3	6,96E-01	-1,87E+02	-5,28E-06	-3,10E-07	2,24E-05	1,08E+02	-1,20E+03	-9,14E-02	2,10E+01	-7,55E+00	-1,55E-01	2,36E-06	-4,18E-06	1,82E-06	1,05E-07	-3,77E-08	-7,77E-10
4	8,15E-01	6,34E+00	-7,40E-07	-2,46E-07	2,34E-05	-6,44E+02	-1,41E+03	-5,27E-02	1,50E+01	-6,42E+00	-1,46E-02	2,03E-07	-3,63E-06	3,42E-06	7,48E-08	-3,21E-08	-7,30E-11
5	8,20E-01	-3,67E-05	1,40E-06	9,33E-13	9,52E-07	-3,07E+02	-1,74E+02	-1,00E-02	-8,63E-06	-7,85E-01	8,86E-08	-7,34E-07	-6,85E-08	8,02E-07	-4,32E-14	-3,92E-09	4,43E-16
6	8,15E-01	-8,34E+00	2,13E-06	2,46E-07	1,44E-06	-4,69E+02	-2,66E+02	-3,68E-02	-1,50E+01	-1,04E+00	1,46E-02	-1,12E-06	-1,04E-07	1,23E-06	-7,48E-08	-5,20E-09	7,30E-11
7	6,60E-01	-8,00E+01	-8,84E-10	4,07E-07	7,06E-09	-2,01E-01	-4,93E-01	-1,34E-05	-2,78E+01	1,09E-03	7,04E-01	1,52E-10	-1,31E-09	1,16E-09	-1,39E-07	5,46E-12	3,52E-09
8	8,40E-01	-9,00E+01	-8,06E-10	3,65E-07	6,19E-09	-3,33E-02	-3,04E-01	-3,96E-06	-2,12E+01	9,09E-05	-9,15E-01	3,96E-10	-9,59E-10	5,63E-10	-1,06E-07	4,55E-13	-4,58E-09
9	7,50E-01	4,50E+01	-1,98E-05	-5,63E-06	2,01E-04	-4,58E+03	-1,25E+04	-1,25E-01	3,62E+02	-4,90E+01	-1,29E+00	5,51E-06	-3,39E-05	2,84E-05	1,81E-06	-2,45E-07	-6,43E-10
10	7,50E-01	-4,50E+01	-4,57E-06	4,44E-07	3,93E-05	-7,16E+02	-2,36E+03	-3,18E-02	-2,87E+01	-1,17E+01	1,58E-01	1,55E-06	-6,68E-06	5,13E-06	-1,43E-07	-5,83E-08	7,91E-10

Total Stresses (F XX: -1,88E+04 YY: -6,10E+03 ZZ: -4,72E-01 YZ: -8,26E+01 XZ: 1,93E+00 XY: -3,91E+02
Total Strains XX: -5,24E-05 YY: 1,10E-05 ZZ: 4,15E-05 YZ: -4,13E-07 XZ: 9,67E-09 XY: -1,95E-06
Total Displacement UX: 4,73E-06 UY: -3,36E-05 UZ: 3,10E-04

Principal Value and Direction of Total Stresses and Strains

	Normal Stress (Pa)	Normal Strain	Shear Stress (Pa)	Shear Strain	X Comp.	Y Comp.	Z Comp.
Maximum:	6,50E-01	4,15E-05			0,0004	-0,0136	0,9999
Minimum:	-6,09E+03	1,10E-05			-0,0307	0,9994	0,0136
Maximum:	-1,88E+04	-5,25E-05			0,9995	0,0307	0
Minimum:			9,40E+03	4,70E-05	-0,7065	-0,0313	0,707
Maximum:	-9,40E+03				0,707	0,0121	0,7071
Minimum:			6,35E+03	3,18E-05	-0,7285	0,685	0,0096
Maximum:	-1,24E+04				0,685	0,7285	0,0096
Minimum:			3,04E+03	1,52E-05	0,022	-0,7163	0,6974
Maximum:	-3,04E+03				-0,0215	0,6971	0,7166

Strain Energy (J) 4,60E-01
Strain Energy of 4,60E-01

Position Number 9 Layer Number: 1 X Coordinate (m): 0,00E+00 Y Coordinate (m): 1,00E+00 Z Coordinate (m): 1,00E-03

Load No.	Distance to Load Axis (m)	Theta (°)	Radial Displacement (m)	Tangential Displacement (m)	Vertical Displacement (m)	Radial Stress (Pa)	Tangential Stress (Pa)	Vertical Stress (Pa)	Rad./Tang. Stress (Pa)	Rad./Vert. Stress (Pa)	Tang./Vert. Stress (Pa)	Radial Strain	Tangential Strain	Vertical Strain	Rad./Tang. Strain	Rad./Vert. Strain	Tang./Vert. Strain
1	9,44E-01	-1,75E+02	-4,68E-06	1,98E-07	1,86E-05	4,40E+02	-6,09E+02	-1,26E-02	-1,07E+01	9,50E-02	1,44E-02	2,48E-06	-2,76E-06	2,82E-07	-5,32E-08	4,75E-10	7,19E-11
2	9,30E-01	-1,80E+02	-1,33E-06	-2,74E-12	-8,80E-07	2,40E+02	1,33E+02	-1,70E-02	1,85E-05	3,19E-01	-1,36E-07	5,76E-07	4,56E-08	-6,22E-07	9,26E-14	1,80E-09	-6,79E-16
3	9,44E-01	-1,86E+02	-4,68E-06	-1,98E-07	1,86E-05	4,40E+02	-6,09E+02	-1,26E-02	1,07E+01	9,50E-02	-1,44E-02	2,48E-06	-2,76E-06	2,82E-07	5,32E-08	4,75E-10	-7,19E-11
4	1,06E+00	4,85E+00	-5,56E-07	-1,66E-07	1,94E-05	-4,04E+01	-7,29E+02	1,14E-02	8,11E+00	-9,38E-01	-5,59E-03	1,08E-06	-2,36E-06	1,28E-06	4,05E-08	-4,69E-09	-2,80E-11
5	1,07E+00	-3,67E-05	1,28E-06	8,23E-13	8,20E-07	-1,75E+02	-9,37E+01	1,18E-02	-2,62E-06	-2,14E-01	1,38E-08	-4,26E-07	-2,11E-08	4,47E-07	-1,31E-14	-1,07E-09	6,92E-17
6	1,06E+00	-4,85E+00	1,92E-06	1,66E-07	1,24E-06	-2,70E+02	-1,45E+02	1,43E-02	-8,11E+00	-3,49E-01	5,59E-03	-6,59E-07	-3,30E-08	6,92E-07	-4,05E-08	-1,75E-09	2,80E-11
7	9,10E-01	-9,00E+01	-8,00E-10	3,52E-07	5,88E-09	1,28E-02	-2,57E-01	-2,66E-06	-2,00E+01	-4,29E-05	-7,47E-01	4,71E-10	-8,78E-10	4,07E-10	-9,98E-08	-2,14E-13	-3,74E-09
8	1,09E+00	-9,00E+01	-7,11E-10	3,23E-07	5,14E-09	7,46E-02	-1,58E-01	-7,57E-07	-1,55E+01	1,69E-04	-4,70E-01	5,13E-10	-6,52E-10	1,39E-10	-7,77E-08	-8,45E-13	-2,35E-09
9	1,00E+00	4,50E+01	-1,74E-05	-4,92E-06	1,67E-04	5,92E+02	-6,39E+03	-9,50E-03	2,51E+02	-2,63E+01	6,34E-01	1,26E-05	-2,23E-05	9,66E-06	1,26E-06	-1,32E-07	3,17E-09
10	1,00E+00	-4,50E+01	-4,01E-06	3,86E-07	3,26E-05	2,23E+02	-1,21E+03	-1,23E-02	-1,96E+01	-8,90E-01	5,88E-02	2,76E-06	-4,40E-06	1,64E-06	-9,82E-08	-4,45E-09	2,93E-10

Total Stresses (F XX: -9,63E+03 YY: 1,43E+03 ZZ: -2,66E-02 YZ: -2,82E+01 XZ: 5,74E-01 XY: -2,65E+02
Total Strains XX: -3,45E-05 YY: 2,08E-05 ZZ: 1,37E-05 YZ: -1,41E-07 XZ: 2,87E-09 XY: -1,32E-06
Total Displacement UX: 4,07E-06 UY: -2,94E-05 UZ: 2,58E-04

Principal Value and Direction of Total Stresses and Strains

	Normal Stress (Pa)	Normal Strain	Shear Stress (Pa)	Shear Strain	X Comp.	Y Comp.	Z Comp.
Maximum:	1,43E+03	2,08E-05			-0,0239	0,9995	-0,0197

Minimax: -5,81E-01 1,37E-05 -0,0005 0,0197 0,9998
Minimum: -9,63E+03 -3,45E-05 0,9997 0,0239 0
Maximum: 5,53E+03 2,77E-05 -0,7238 0,6899 -0,0139
MiniMax: -4,10E+03 4,82E+03 2,41E-05 -0,7072 -0,003 0,707
-4,82E+03 0,7066 0,0308 0,707
Minimum: 7,17E+02 7,17E+02 3,59E-06 -0,0166 0,6929 -0,7209
-0,0172 0,7207 0,6931
Strain Energy (J) 1,81E-01
Strain Energy of 1,81E-01

Position Number 10 Layer Number: 1 X Coordinate (m): 0,00E+00 Y Coordinate (m): 1,50E+00 Z Coordinate (m): 1,00E-03

Load No.	Distance to Load Axis (m)	Theta (°)	Radial Displacement (m)	Tangential Displacement (m)	Vertical Displacement (m)	Radial Stress (Pa)	Tangential Stress (Pa)	Vertical Stress (Pa)	Rad./Tang. Stress (Pa)	Rad./Vert. Stress (Pa)	Tang./Vert. Stress (Pa)	Radial Strain	Tangential Strain	Vertical Strain	Rad./Tang. Strain	Rad./Vert. Strain	Tang./Vert. Strain
1	1,44E+00	-1,76E+02	-3,56E-06	1,06E-07	1,29E-05	5,17E+02	-1,31E+02	1,04E-02	-3,27E+00	-1,89E-01	-3,32E-02	1,94E-06	-1,30E-06	-6,44E-07	-1,63E-08	-9,43E-10	-1,66E-10
2	1,43E+00	-1,80E+02	-1,15E-06	-2,22E-12	-6,09E-07	8,69E+01	3,52E+01	-2,79E-03	-1,08E-05	1,29E+00	2,73E-08	2,31E-07	-2,74E-08	-2,04E-07	-5,38E-14	6,45E-09	1,36E-16
3	1,44E+00	-1,84E+02	-3,56E-06	-1,06E-07	1,29E-05	5,17E+02	-1,31E+02	1,04E-02	3,27E+00	-1,89E-01	3,32E-02	1,94E-06	-1,30E-06	-6,44E-07	1,63E-08	-9,43E-10	1,66E-10
4	1,56E+00	3,30E+00	6,20E-08	-9,36E-08	1,35E-05	2,76E+02	-1,62E+02	6,68E-04	2,65E+00	-9,87E-01	6,17E-02	1,19E-06	-9,99E-07	-1,92E-07	1,32E-08	-4,94E-09	3,08E-10
5	1,57E+00	-3,67E-05	1,12E-06	6,81E-13	5,32E-07	-6,93E+01	-2,34E+01	2,11E-03	4,85E-06	-9,70E-01	-1,01E-08	-1,92E-07	3,76E-08	1,55E-07	2,42E-14	-4,85E-09	-5,03E-17
6	1,56E+00	-3,30E+00	1,71E-06	9,36E-08	8,30E-07	-1,06E+02	-3,59E+01	-2,63E-04	-2,65E+00	-4,88E-01	-6,17E-02	-2,94E-07	5,70E-08	2,37E-07	-1,32E-08	-2,44E-09	-3,08E-10
7	1,41E+00	-9,00E+01	-5,46E-10	2,85E-07	4,06E-09	1,16E-01	-5,81E-02	1,62E-07	-1,02E+01	-1,63E-04	-2,37E-01	4,83E-10	-3,87E-10	-9,64E-11	-5,07E-08	-8,15E-13	-1,19E-09
8	1,59E+00	-9,00E+01	-4,63E-10	2,68E-07	3,57E-09	1,15E-01	-2,96E-02	2,90E-07	-8,16E+00	-1,41E-04	-1,71E-01	4,33E-10	-2,91E-10	-1,43E-10	-4,08E-08	-7,06E-13	-8,55E-10
9	1,50E+00	4,50E+01	-1,07E-05	-4,03E-06	1,16E-04	3,03E+03	-1,42E+03	1,42E-02	1,24E+02	-2,84E+00	-3,31E-01	1,25E-05	-9,79E-06	-2,67E-06	6,21E-07	-1,42E-08	-1,65E-09
10	1,50E+00	-4,50E+01	-2,63E-06	3,18E-07	2,26E-05	6,38E+02	-2,70E+02	2,77E-03	-9,80E+00	-1,02E+00	-2,30E-01	2,58E-06	-1,96E-06	-6,12E-07	-4,90E-08	-5,08E-09	-1,15E-09

Total Stresses (F XX: -2,14E+03 YY: 4,88E+03 ZZ: 3,75E-02 YZ: -5,39E+00 XZ: 9,97E-01 XY: -1,25E+02
Total Strains XX: -1,53E-05 YY: 1,98E-05 ZZ: -4,58E-06 YZ: -2,70E-08 XZ: 4,99E-09 XY: -6,27E-07
Total Displacement UX: 3,26E-06 UY: -1,87E-05 UZ: 1,78E-04

Principal Value and Direction of Total Stresses and Strains

	Normal Stress (Pa)	Normal Strain	Shear Stress (Pa)	Shear Strain	X Comp.	Y Comp.	Z Comp.
Maximum:	4,89E+03	1,98E-05			-0,0179	0,9998	-0,0011
Minimax:	3,19E-02	-4,58E-06			0,0004	0,0011	1
Minimum:	-2,14E+03	-1,53E-05			0,9998	0,0179	-0,0004
Maximum:			3,51E+03	1,76E-05	-0,7196	0,6944	-0,0005
	1,37E+03				0,6944	0,7196	-0,0011
MiniMax:			2,44E+03	1,22E-05	-0,0129	0,7062	-0,7079
	2,44E+03				-0,0123	0,7078	0,7063
Minimum:			1,07E+03	5,34E-06	-0,7067	-0,0118	0,7074
	-1,07E+03				0,7073	0,0134	0,7068

Strain Energy (J) 6,48E-02
Strain Energy of 6,48E-02

System: 2: sys32

Layer Number	Thickness (m)	Young's Modulus (Pa)	Poisson's Ratio	Shear Spring Compliance (m³/N)	Load Number	Normal Stress (Pa)	Shear Stress (Pa)	Radius of Loaded Area (m)	Load Position X (m)	Load Position Y (m)	Shear Direction (°)	
1	0,013	3,00E+08		0,5	0,00E+00	1	4,00E+05	2,00E+05	5,26E-02	9,00E-02	6,00E-02	2,70E+02
2	0,013	5,00E+08	0,47	0,00E+00	2	1,75E+02	2,00E+05	4,26E-02	0,00E+00	7,00E-02		2,70E+02
3	0,015	8,00E+08	0,46	0,00E+00	3	4,00E+05	2,00E+05	5,26E-02	-9,00E-02	6,00E-02		2,70E+02
4	0,03	1,20E+09	0,45	0,00E+00	4	4,00E+05	2,00E+05	5,26E-02	9,00E-02	-6,00E-02		9,00E+01
5	0,03	1,52E+09	0,45	0,00E+00	5	1,75E+02	2,00E+05	4,26E-02	0,00E+00	-7,00E-02		9,00E+01
6	0,06	3,07E+09	0,45	0,00E+00	6	1,15E+02	2,00E+05	5,26E-02	-9,00E-02	-6,00E-02		9,00E+01
7	0,07	3,70E+09	0,44	0,00E+00	7	6,23E+02	1,80E+05	2,26E-02	0,00E+00	9,00E-02		1,80E+02
8	0,07	3,60E+09	0,43	0,00E+00	8	6,23E+02	1,80E+05	2,26E-02	0,00E+00	-9,00E-02		1,80E+02
9	0,25	1,00E+08	0,35	0,00E+00	9	7,50E+05	1,50E+05	1,13E-01	0,00E+00	0,00E+00		4,50E+01
10		5,00E+07	0,5		10	7,50E+05	6,00E+04	5,00E-02	0,00E+00	0,00E+00		1,35E+02

Position Number 1 Layer Number: 1 X Coordinate (m): 0,00E+00 Y Coordinate (m): 0,00E+00 Z Coordinate (m): 1,25E-02

Load No.	Distance to Load Axis (m)	Theta (°)	Radial Displacement (m)	Tangential Displacement (m)	Vertical Displacement (m)	Radial Stress (Pa)	Tangential Stress (Pa)	Vertical Stress (Pa)	Rad./Tang. Stress (Pa)	Rad./Vert. Stress (Pa)	Tang./Vert. Stress (Pa)	Radial Strain	Tangential Strain	Vertical Strain	Rad./Tang. Strain	Rad./Vert. Strain	Tang./Vert. Strain
1	1.08E-01	-4.16E+02	6.30E-06	3.98E-06	3.47E-05	-3.77E+04	-9.42E+03	-1.36E+03	1.27E+02	-7.98E+03	5.70E+01	-1.08E-04	3.37E-05	7.41E-05	6.34E-07	-3.99E-05	2.85E-07
2	7.00E-02	-3.60E+02	9.96E-06	1.01E-11	3.44E-07	-6.13E+04	-1.23E+04	-7.10E+03	3.04E-02	-2.49E+04	1.36E-02	-1.72E-04	7.29E-05	9.91E-05	1.52E-10	-1.24E-04	6.89E-11
3	1.08E-01	-3.04E+02	6.30E-06	-3.98E-06	3.47E-05	-3.77E+04	-9.42E+03	-1.36E+03	-1.27E+02	-7.98E+03	-5.70E+01	-1.08E-04	3.37E-05	7.41E-05	-6.34E-07	-3.99E-05	-2.85E-07
4	1.08E-01	5.63E+01	6.30E-06	-3.98E-06	3.47E-05	-3.77E+04	-9.42E+03	-1.36E+03	-1.27E+02	-7.98E+03	-5.70E+01	-1.08E-04	3.37E-05	7.41E-05	-6.34E-07	-3.99E-05	-2.85E-07
5	7.00E-02	-3.67E-05	9.96E-06	3.10E-12	3.44E-07	-6.13E+04	-1.23E+04	-7.10E+03	9.33E-03	-2.49E+04	4.23E-03	-1.72E-04	7.29E-05	9.91E-05	4.67E-11	-1.24E-04	2.12E-11
6	1.08E-01	-5.63E+01	5.00E-06	3.98E-06	1.73E-07	-1.82E+04	-3.01E+03	-8.49E+02	1.27E+02	-4.64E+03	5.70E+01	-5.43E-05	2.18E-05	3.25E-05	6.34E-07	-2.32E-05	2.85E-07
7	9.00E-02	-2.70E+02	6.47E-10	-8.25E-07	1.01E-08	-7.42E+00	-1.67E+00	-2.16E-01	-4.22E+02	-1.40E+00	-1.18E+02	-2.16E-08	7.17E-09	1.44E-08	-2.11E-08	-6.99E-09	-5.91E-07
8	9.00E-02	-9.00E+01	6.42E-10	8.25E-07	1.01E-08	-7.42E+00	-1.67E+00	-2.16E-01	4.22E+02	-1.40E+00	1.18E+02	-2.16E-08	7.14E-09	1.44E-08	2.11E-08	-6.98E-09	5.91E-07
9	0.00E+00	-4.50E+01	3.07E-05	3.07E-05	3.43E-04	-7.06E+05	-7.06E+05	-7.48E+05	0.00E+00	-9.89E+04	-9.89E+04	7.04E-05	7.02E-05	-1.41E-04	0.00E+00	-4.95E-04	-4.95E-04
10	0.00E+00	-1.35E+02	-5.35E-06	5.35E-06	9.74E-05	-5.70E+05	-5.70E+05	-7.40E+05	0.00E+00	3.24E+04	-3.24E+04	2.84E-04	2.84E-04	-5.67E-04	0.00E+00	1.62E-04	-1.62E-04

Total Stresses (F XX: -1.40E+06 YY: -1.46E+06 ZZ: -1.51E+06 YZ: -1.30E+05 XZ: -6.39E+04 XY: 6.05E+03
Total Strains XX: 2.74E-04 YY: -1.90E-05 ZZ: -2.55E-04 YZ: -6.47E-04 XZ: -3.20E-04 XY: 3.02E-05
Total Displacement UX: 2.27E-05 UY: 3.54E-05 UZ: 5.45E-04

Principal Value and Direction of Total Stresses and Strains

	Normal Stress (Pa)	Normal Strain	Shear Stress (Pa)	Shear Strain	X Comp.	Y Comp.	Z Comp.
Maximum:	-1.32E+06	6.67E-04			0.5358	0.5921	-0.6019
Minimum:	-1.42E+06	1.76E-04			0.819	-0.5377	0.2002
Minimum:	-1.63E+06	-8.43E-04			0.2051	0.6003	0.7731
Maximum:			1.51E+05	7.55E-04	0.2338	-0.0058	-0.9723
	-1.47E+06				0.5239	0.8431	0.121
MiniMax:			1.02E+05	5.09E-04	0.4341	-0.8047	-0.4051
	-1.52E+06				0.7242	0.0443	0.6882
Minimum:			4.91E+04	2.45E-04	-0.2003	0.7989	-0.5672
	-1.37E+06				0.958	0.0385	-0.2841

Strain Energy (J) 1.19E+02
Strain Energy of 1.19E+02

Position Number 2 Layer Number: 1 X Coordinate (m): 0.00E+00 Y Coordinate (m): 5.00E-02 Z Coordinate (m): 1.25E-02

Load No.	Distance to Load Axis (m)	Theta (°)	Radial Displacement (m)	Tangential Displacement (m)	Vertical Displacement (m)	Radial Stress (Pa)	Tangential Stress (Pa)	Vertical Stress (Pa)	Rad./Tang. Stress (Pa)	Rad./Vert. Stress (Pa)	Tang./Vert. Stress (Pa)	Radial Strain	Tangential Strain	Vertical Strain	Rad./Tang. Strain	Rad./Vert. Strain	Tang./Vert. Strain
1	9.06E-02	-4.44E+02	3.73E-06	5.70E-06	3.54E-05	-3.62E+04	-8.63E+03	-1.63E+03	-1.64E+03	-8.71E+03	-8.43E+02	-1.03E-04	3.42E-05	6.92E-05	-8.21E-08	-4.35E-05	-4.21E-06
2	2.00E-02	-3.60E+02	1.97E-05	3.98E-11	6.25E-07	-6.08E+04	-2.79E+04	-1.43E+04	1.34E-02	-1.27E+05	5.68E-02	-1.32E-04	3.22E-05	1.00E-04	6.89E-11	-6.35E-04	2.84E-10
3	9.06E-02	-2.76E+02	3.73E-06	-5.70E-06	3.54E-05	-3.62E+04	-8.63E+03	-1.63E+03	1.64E+03	-8.71E+03	8.43E+02	-1.03E-04	3.42E-05	6.92E-05	8.21E-08	-4.35E-05	4.21E-06
4	1.42E-01	3.93E+01	5.16E-06	-2.53E-06	3.41E-05	-2.36E+04	-7.62E+03	-4.37E+02	-3.17E+02	-3.32E+03	-1.31E+02	-6.51E-05	1.46E-05	5.05E-05	-1.58E-06	-1.66E-05	-6.57E-07
5	1.20E-01	-3.67E-05	5.21E-06	1.80E-12	2.29E-07	-1.58E+04	-2.16E+03	-5.13E+02	2.55E-03	-3.32E+03	6.16E-04	-4.81E-05	2.00E-05	2.82E-05	1.28E-11	-1.66E-05	3.08E-12
6	1.42E-01	-3.93E+01	5.17E-06	2.53E-06	3.79E-07	-1.22E+04	-1.67E+03	-3.01E+02	3.17E+02	-2.15E+03	1.31E+02	-3.71E-05	1.46E-05	2.25E-05	1.58E-06	-1.08E-05	6.57E-07
7	4.00E-02	-2.70E+02	3.84E-09	-2.22E-06	1.27E-08	-5.93E+01	-6.14E+00	-1.06E+01	2.21E+03	-2.89E+01	2.85E+03	-1.70E-07	9.60E-08	7.36E-08	1.11E-05	-1.45E-07	1.43E-05
8	1.40E-01	-9.00E+01	-5.96E-12	6.47E-07	9.70E-09	-3.19E+00	-1.62E+00	-2.42E-02	1.54E+02	-2.84E-01	4.42E+01	-7.91E-09	-3.69E-11	7.94E-09	7.69E-07	-1.42E-09	2.21E-07
9	5.00E-02	4.50E+01	3.34E-05	-2.82E-05	3.40E-04	-7.13E+05	-7.06E+05	-7.48E+05	6.46E+03	-1.06E+05	9.68E+04	4.45E-05	8.41E-05	-1.29E-04	3.23E-05	-5.31E-04	4.84E-04
10	5.00E-02	-4.50E+01	1.90E-05	2.89E-06	7.78E-05	-3.45E+05	-2.57E+05	-3.62E+05	-7.41E+03	-2.35E+05	-1.23E+04	-1.17E-04	3.23E-04	-2.06E-04	-3.71E-05	-1.18E-03	-6.13E-05

Total Stresses (F XX: -1.08E+06 YY: -1.18E+06 ZZ: -1.13E+06 YZ: -2.18E+05 XZ: -8.10E+04 XY: 1.33E+03
Total Strains XX: 2.33E-04 YY: -2.38E-04 ZZ: 5.40E-06 YZ: -1.09E-03 XZ: -4.05E-04 XY: 6.64E-06
Total Displacement UX: 2.34E-05 UY: 3.70E-05 UZ: 5.24E-04

Principal Value and Direction of Total Stresses and Strains

	Normal Stress (Pa)	Normal Strain	Shear Stress (Pa)	Shear Strain	X Comp.	Y Comp.	Z Comp.
Maximum:	-9.12E+05	1.09E-03			-0.3461	-0.5953	0.7252
Minimum:	-1.10E+06	1.68E-04			0.9209	-0.3634	0.1412
Minimum:	-1.38E+06	-1.26E-03			0.1795	0.7167	0.6739
Maximum:			2.36E+05	1.18E-03	-0.3716	-0.9277	0.0363
	-1.15E+06				-0.1178	0.0859	0.9893
MiniMax:			1.43E+05	7.15E-04	0.5242	-0.7837	-0.3767
	-1.24E+06				0.7781	0.2498	0.5764
Minimum:			9.25E+04	4.63E-04	-0.8959	-0.1639	0.413
	-1.00E+06				0.4064	-0.6779	0.6126

Strain Energy (J) 2,82E+02
Strain Energy of 2,82E+02

Position Number	3	Layer Number:	1	X Coordinate (m):	0,00E+00	Y Coordinate (m):	1,10E-01	Z Coordinate (m):	1,25E-02								
Load No.	Distance to Load Axis (m)	Theta (")	Radial Displacement (m)	Tangential Displacement (m)	Vertical Displacement (m)	Radial Stress (Pa)	Tangential Stress (Pa)	Vertical Stress (Pa)	Rad./Tang. Stress (Pa)	Rad./Vert. Stress (Pa)	Tang./Vert. Stress (Pa)	Radial Strain	Tangential Strain	Vertical Strain	Rad./Tang. Strain	Rad./Vert. Strain	Tang./Vert. Strain
1	1,03E-01	-1,19E+02	-3,05E-06	4,36E-06	3,46E-05	-3,74E+03	-3,52E+03	3,35E+02	-1,15E+02	8,89E+02	-4,98E+01	-7,16E-06	-6,05E-06	1,32E-05	-5,75E-07	4,44E-06	-2,49E-07
2	4,00E-02	-1,80E+02	-1,62E-05	-2,49E-11	-1,72E-06	1,18E+05	6,35E+04	6,45E+04	-3,71E-02	8,56E+04	-5,51E-02	1,81E-04	-9,28E-05	-8,80E-05	-1,85E-10	4,28E-04	-2,76E-10
3	1,03E-01	-2,41E+02	-3,05E-06	-4,36E-06	3,46E-05	-3,74E+03	-3,52E+03	3,35E+02	1,15E+02	8,88E+02	4,98E+01	-7,16E-06	-6,05E-06	1,32E-05	5,75E-07	4,44E-06	2,49E-07
4	1,92E-01	2,79E+01	3,42E-06	-1,66E-06	3,35E-05	-1,37E+04	-6,47E+03	-8,68E+01	-9,87E+01	-1,19E+03	-6,23E+01	-3,48E-05	1,43E-06	3,33E-05	-4,93E-07	-5,95E-06	-3,12E-07
5	1,80E-01	-3,67E-05	3,50E-06	1,52E-12	4,79E-07	-5,53E+03	-9,24E+02	-6,80E+01	8,01E-04	-6,50E+02	1,51E-04	-1,68E-05	6,26E-06	1,05E-05	4,00E-12	-3,25E-06	7,57E-13
6	1,92E-01	-2,79E+01	4,46E-06	1,66E-06	7,06E-07	-6,43E+03	-1,19E+03	-6,91E+01	9,87E+01	-6,97E+02	6,23E+01	-1,93E-05	6,86E-06	1,25E-05	4,93E-07	-3,49E-06	3,12E-07
7	2,00E-02	-9,00E+01	6,88E-09	5,50E-06	2,31E-08	-2,30E+02	-1,86E+02	-3,49E+02	-1,46E+04	-1,54E+02	-3,80E+04	1,26E-07	3,44E-07	-4,70E-07	-7,31E-05	-7,70E-07	-1,90E-04
8	2,00E-01	-9,00E+01	-3,40E-10	5,79E-07	9,41E-09	-1,97E+00	-1,50E+00	-1,61E-03	3,90E+01	-1,22E-01	2,24E+01	-4,07E-09	-1,70E-09	5,77E-09	1,95E-07	-6,12E-10	1,12E-07
9	1,10E-01	4,50E+01	3,80E-05	-1,89E-05	3,17E-04	-5,13E+05	-4,57E+05	-5,06E+05	2,95E+04	-2,72E+05	4,88E+04	-1,06E-04	1,74E-04	-6,79E-05	1,47E-04	-1,36E-03	2,44E-04
10	1,10E-01	-4,50E+01	3,70E-06	8,94E-07	5,85E-05	-3,74E+04	-1,15E+04	-1,03E+03	8,35E+01	-6,58E+03	3,15E+01	-1,04E-04	2,55E-05	7,81E-05	4,18E-07	-3,29E-05	1,57E-07
Total Stresses (F XX:			-4,25E+05	YY:	-4,62E+05	ZZ:	-4,42E+05	YZ:	-1,95E+05	XZ:	-1,06E+04	XY:	-1,42E+04				
Total Strains XX:			9,25E-05	YY:	-9,70E-05	ZZ:	4,47E-06	YZ:	-9,74E-04	XZ:	-5,32E-05	XY:	-7,08E-05				
Total Displacement UX:			1,24E-05	UY:	2,70E-05	UZ:	4,78E-04										

Principal Value and Direction of Total Stresses and Strains

	Normal Stress (Pa)	Normal Strain	Shear Stress (Pa)	Shear Strain	X Comp.	Y Comp.	Z Comp.
Maximum:	-2,57E+05	9,28E-04			0,0122	-0,6888	0,7248
Minimax:	-4,23E+05	9,93E-05			0,9969	-0,0484	-0,0627
Minimum:	-6,49E+05	-1,03E-03			0,0782	0,7233	0,6861
Maximum:			1,96E+05	9,79E-04	-0,0467	-0,9985	0,0274
	-4,53E+05				0,0639	0,0244	0,9977
MiniMax:			1,13E+05	5,64E-04	0,6496	-0,5457	-0,5295
	-5,36E+05				0,7602	0,4773	0,4408
Minimum:			8,30E+04	4,15E-04	-0,6963	-0,4529	0,5569
	-3,40E+05				0,7135	-0,5213	0,4682
Strain Energy (J)	1,93E+02						
Strain Energy of	1,93E+02						

Position Number	4	Layer Number:	1	X Coordinate (m):	0,00E+00	Y Coordinate (m):	2,10E-01	Z Coordinate (m):	1,25E-02								
Load No.	Distance to Load Axis (m)	Theta (")	Radial Displacement (m)	Tangential Displacement (m)	Vertical Displacement (m)	Radial Stress (Pa)	Tangential Stress (Pa)	Vertical Stress (Pa)	Rad./Tang. Stress (Pa)	Rad./Vert. Stress (Pa)	Tang./Vert. Stress (Pa)	Radial Strain	Tangential Strain	Vertical Strain	Rad./Tang. Strain	Rad./Vert. Strain	Tang./Vert. Strain
1	1,75E-01	-1,49E+02	-5,45E-06	1,89E-06	3,25E-05	-3,94E+02	-4,11E+03	8,21E+01	1,60E+02	3,93E+02	7,93E+01	5,39E-06	-1,32E-05	7,77E-06	8,01E-07	1,97E-06	3,96E-07
2	1,40E-01	-1,80E+02	-4,43E-06	-5,19E-12	-2,93E-07	1,05E+04	1,46E+03	2,46E+02	-5,20E-03	1,80E+03	-1,10E-03	3,21E-05	-1,30E-05	-1,91E-05	-2,60E-11	9,00E-06	-5,50E-12
3	1,75E-01	-2,11E+02	-5,45E-06	-1,89E-06	3,25E-05	-3,94E+02	-4,11E+03	8,21E+01	-1,60E+02	3,93E+02	-7,93E+01	5,39E-06	-1,32E-05	7,77E-06	-8,01E-07	1,97E-06	-3,96E-07
4	2,85E-01	1,84E+01	1,56E-06	-1,01E-06	3,25E-05	-7,27E+03	-5,20E+03	-1,10E+01	2,74E+01	-4,46E+02	-2,35E+01	-1,56E-05	-5,18E-06	2,07E-05	1,37E-07	-2,23E-06	-1,18E-07
5	2,80E-01	-3,67E-05	2,50E-06	1,35E-12	7,84E-07	-2,09E+03	-6,21E+02	-4,07E+00	1,82E-04	-1,22E+02	4,36E-05	-5,93E-06	1,42E-06	4,51E-06	9,11E-13	-6,12E-07	2,18E-13
6	2,85E-01	-1,84E+01	3,58E-06	1,01E-06	1,14E-06	-2,94E+03	-8,93E+02	-7,39E+00	-2,74E+01	-1,73E+02	2,35E+01	-8,30E-06	1,94E-06	6,36E-06	-1,37E-07	-8,64E-07	1,18E-07
7	1,20E-01	-9,00E+01	1,88E-10	6,92E-07	9,82E-09	-4,16E+00	-1,65E+00	-7,22E-02	2,33E+02	-4,99E-01	6,54E+01	-1,10E-08	1,57E-09	9,44E-09	1,16E-06	-2,49E-09	3,27E-07
8	3,00E-01	-9,00E+01	-6,19E-10	5,24E-07	8,94E-09	-1,15E+00	-1,19E+00	4,24E-04	-1,79E+01	-7,27E-02	1,29E+01	-1,85E-09	-2,06E-09	3,91E-09	-8,97E-08	-3,84E-10	6,44E-08
9	2,10E-01	4,50E+01	1,43E-06	-8,70E-06	2,81E-04	-7,48E+04	-4,80E+04	-4,99E+02	4,21E+02	-6,51E+03	-1,81E+02	-1,68E-04	-3,46E-05	2,03E-04	2,11E-06	-3,26E-05	-9,05E-07
10	2,10E-01	-4,50E+01	-1,30E-06	6,63E-07	5,53E-05	-1,21E+04	-8,89E+03	-3,23E+01	2,47E+01	-8,16E+02	2,31E+01	-2,56E-05	-9,35E-06	3,49E-05	1,24E-07	-4,08E-06	1,16E-07
Total Stresses (F XX:		-6,85E+04	YY:	-9,14E+04	ZZ:	-1,44E+02	YZ:	-5,63E+03	XZ:	1,66E+02	XY:	-6,52E+02					
Total Strains XX:		-7,58E-05	YY:	-1,90E-04	ZZ:	2,66E-04	YZ:	-2,81E-05	XZ:	8,29E-07	XY:	-3,26E-06					
Total Displacement UX:		7,46E-06	UY:	-7,55E-06	UZ:	4,35E-04											

Principal Value and Direction of Total Stresses and Strains

	Normal Stress (Pa)	Normal Strain	Shear Stress (Pa)	Shear Strain	X Comp.	Y Comp.	Z Comp.
Maximum:	2,03E+02	2,68E-04			0,003	-0,0614	0,9981
Minimax:	-6,85E+04	-7,57E-05			0,9996	-0,0273	-0,0047
Minimum:	-9,17E+04	-1,92E-04			0,0276	0,9977	0,0613
Maximum:			4,60E+04	2,30E-04	-0,0174	-0,7489	0,6625

MiniMax: -4,58E+04 3,43E+04 1,72E-04 0,0218 0,6621 0,7491
-3,41E+04 0,7047 -0,0241 0,7091
Minimum: 1,16E+04 5,82E-05 0,709 -0,0627 0,7025
-8,01E+04 0,6874 -0,7248 -0,0466
0,7263 0,6862 0,04

Strain Energy (J) 1,14E+01
Strain Energy of 1,14E+01

Position Number 5 Layer Number: 1 X Coordinate (m): 0,00E+00 Y Coordinate (m): 3,10E-01 Z Coordinate (m): 1,25E-02

Load No.	Distance to Load Axis (m)	Theta (°)	Radial Displacement (m)	Tangential Displacement (m)	Vertical Displacement (m)	Radial Stress (Pa)	Tangential Stress (Pa)	Vertical Stress (Pa)	Rad./Tang. Stress (Pa)	Rad./Vert. Stress (Pa)	Tang./Vert. Stress (Pa)	Radial Strain	Tangential Strain	Vertical Strain	Rad./Tang. Strain	Rad./Vert. Strain	Tang./Vert. Strain
1	2,66E-01	-1,60E+02	-5,60E-06	1,10E-06	3,06E-05	-1,42E+03	-3,57E+03	1,05E+01	-1,79E+01	-8,13E+01	2,85E+01	1,19E-06	-8,54E-06	8,35E-06	-8,94E-06	-4,06E-07	1,42E-07
2	2,40E-01	-1,80E+02	-2,78E-06	-4,37E-12	-6,66E-07	2,87E+03	6,96E+02	1,69E+01	-9,91E-04	2,16E+02	-2,05E-04	8,37E-06	-2,49E-06	-5,88E-06	-4,96E-12	1,08E-06	-1,02E-12
3	2,68E-01	-2,00E+02	-5,60E-06	-1,10E-06	3,06E-05	-1,42E+03	-3,57E+03	1,05E+01	1,79E+01	-8,13E+01	-2,85E+01	1,19E-06	-8,54E-06	8,35E-06	8,94E-06	-4,06E-07	-1,42E-07
4	3,81E-01	1,37E+01	5,46E-07	-6,97E-07	3,10E-05	-4,51E+03	-4,08E+03	-3,92E-01	4,17E+01	-2,64E+02	-9,94E+00	-8,23E-06	-6,08E-06	1,43E-05	2,08E-07	-1,32E-06	-4,97E-08
5	3,80E-01	-3,67E-05	2,07E-06	1,24E-12	9,44E-07	-1,19E+03	-4,88E+02	-5,37E-01	4,63E-05	-4,86E+01	2,02E-05	-3,16E-06	3,60E-07	2,80E-06	2,32E-13	-2,43E-07	1,01E-13
6	3,81E-01	-1,37E+01	3,07E-06	6,97E-07	1,39E-06	-1,78E+03	-7,23E+02	-1,11E+00	-4,17E+01	-7,51E+01	9,94E+00	-4,67E-06	5,32E-07	4,14E-06	-2,08E-07	-3,75E-07	4,97E-08
7	2,20E-01	-9,00E+01	-4,16E-10	5,65E-07	9,32E-09	-1,75E+00	-1,44E+00	-1,61E-03	2,02E+01	-1,07E-01	1,91E+01	-3,42E-09	-1,89E-09	5,31E-09	1,01E-07	-5,34E-10	9,57E-08
8	4,00E-01	-9,00E+01	-7,52E-10	4,83E-07	8,43E-09	-7,17E-01	-9,22E-01	4,24E-04	-2,94E+01	-5,36E-02	6,24E+00	-8,55E-10	-1,88E-09	2,73E-09	-1,47E-07	-2,68E-10	3,12E-08
9	3,10E-01	4,50E+01	-9,62E-06	-7,63E-06	2,68E-04	-4,01E+04	-3,87E+04	-1,67E+01	3,62E+02	-2,49E+03	-1,42E+02	-7,23E-05	-5,56E-05	1,28E-04	1,81E-06	-1,25E-05	-7,09E-07
10	3,10E-01	-4,50E+01	-3,05E-06	5,99E-07	5,26E-05	-6,97E+03	-7,02E+03	-4,59E+00	-2,36E+01	-4,36E+02	1,19E+01	-1,15E-05	-1,18E-05	2,33E-05	-1,18E-07	-2,18E-06	5,95E-08

Total Stresses (F XX: -5,51E+04 YY: -5,49E+04 ZZ: 1,47E+01 YZ: -3,26E+03 XZ: 1,49E+02 XY: -4,71E+02
Total Strains XX: -9,20E-05 YY: -9,13E-05 ZZ: 1,83E-04 YZ: -1,63E-05 XZ: 7,46E-07 XY: -2,35E-06
Total Displacement UX: 8,57E-06 UY: -2,08E-05 UZ: 4,14E-04

Principal Value and Direction of Total Stresses and Strains

	Normal Stress (Pa)	Normal Strain	Shear Stress (Pa)	Shear Strain	X Comp.	Y Comp.	Z Comp.
Maximum:	2,08E+02	1,84E-04			0,0032	-0,059	0,9983
Minimum:	-5,46E+04	-8,98E-05			0,7203	-0,6923	-0,0432
Minimum:	-5,55E+04	-9,44E-05			0,6936	0,7192	0,0403
Maximum:			2,79E+04	1,39E-04	-0,4882	-0,5503	0,6774
	-2,77E+04				0,4927	0,4668	0,7344
MiniMax:			2,74E+04	1,37E-04	-0,5071	0,4478	0,7384
	-2,72E+04				0,5116	-0,5312	0,6753
Minimum:			4,61E+02	2,31E-06	0,0189	-0,9981	-0,0591
	-5,51E+04				0,9998	0,019	-0,0021

Strain Energy (J) 5,09E+00
Strain Energy of 5,09E+00

Position Number 6 Layer Number: 1 X Coordinate (m): 0,00E+00 Y Coordinate (m): 3,20E-01 Z Coordinate (m): 1,25E-02

Load No.	Distance to Load Axis (m)	Theta (°)	Radial Displacement (m)	Tangential Displacement (m)	Vertical Displacement (m)	Radial Stress (Pa)	Tangential Stress (Pa)	Vertical Stress (Pa)	Rad./Tang. Stress (Pa)	Rad./Vert. Stress (Pa)	Tang./Vert. Stress (Pa)	Radial Strain	Tangential Strain	Vertical Strain	Rad./Tang. Strain	Rad./Vert. Strain	Tang./Vert. Strain
1	2,75E-01	-1,81E+02	-5,61E-06	1,06E-06	3,04E-05	-1,40E+03	-3,48E+03	1,04E+01	-2,26E+01	-9,89E+01	2,46E+01	1,13E-06	-9,30E-06	8,17E-06	-1,13E-07	-4,95E-07	1,23E-07
2	2,50E-01	-1,80E+02	-2,71E-06	-4,32E-12	-6,94E-07	2,63E+03	6,71E+02	7,35E+00	-8,60E-04	1,85E+02	-1,83E-04	7,63E-06	-2,16E-06	-5,48E-06	-4,30E-12	9,25E-07	-9,14E-13
3	2,75E-01	-1,99E+02	-5,61E-06	-1,06E-06	3,04E-05	-1,40E+03	-3,48E+03	1,04E+01	2,26E+01	-9,89E+01	-2,46E+01	1,13E-06	-9,30E-06	8,17E-06	1,13E-07	-4,95E-07	-1,23E-07
4	3,91E-01	1,33E+01	4,70E-07	-6,75E-07	3,09E-05	-4,32E+03	-3,99E+03	-4,57E+00	4,21E+01	-2,44E+02	-9,38E+00	-7,73E-06	-6,09E-06	1,38E-05	2,11E-07	-1,22E-06	-4,89E-08
5	3,90E-01	-3,67E-05	2,04E-06	1,23E-12	9,54E-07	-1,14E+03	-4,79E+02	-5,14E-01	4,00E-05	-4,69E+01	1,90E-05	-3,01E-06	3,11E-07	2,70E-06	2,00E-13	-2,35E-07	9,49E-14
6	3,91E-01	-1,33E+01	3,03E-06	6,75E-07	1,41E-06	-1,69E+03	-7,08E+02	-1,86E+00	-4,21E+01	-7,09E+01	9,38E+00	-4,44E-06	4,59E-07	3,98E-06	-2,11E-07	-3,55E-07	4,69E-08
7	2,30E-01	-9,00E+01	-4,48E-10	5,59E-07	9,28E-09	-1,65E+00	-1,41E+00	-1,13E-03	1,32E+01	-1,06E-01	1,77E+01	-3,15E-09	-1,95E-09	5,09E-09	6,59E-08	-5,31E-10	8,84E-08
8	4,10E-01	-9,00E+01	-7,61E-10	4,79E-07	8,38E-09	-6,98E-01	-9,00E-01	9,36E-03	-3,08E+01	-4,84E-02	7,27E+00	-8,42E-10	-1,85E-09	2,70E-09	-1,54E-07	-2,42E-10	3,64E-08
9	3,20E-01	4,50E+01	-1,03E-05	-7,55E-06	2,66E-04	-3,81E+04	-3,58E+04	-3,54E+01	3,76E+02	-2,38E+03	-1,39E+02	-6,72E-05	-5,58E-05	1,23E-04	1,88E-06	-1,19E-05	-6,97E-07
10	3,20E-01	-4,50E+01	-3,16E-06	5,94E-07	5,23E-05	-6,65E+03	-6,85E+03	-8,32E+00	-2,68E+01	-4,04E+02	1,17E+01	-1,08E-05	-1,17E-05	2,25E-05	-1,34E-07	-2,02E-06	5,87E-08

Total Stresses (F XX: -5,37E+04 YY: -5,24E+04 ZZ: -2,25E+01 YZ: -3,15E+03 XZ: 1,43E+02 XY: -4,78E+02
Total Strains XX: -9,17E-05 YY: -8,51E-05 ZZ: 1,77E-04 YZ: -1,58E-05 XZ: 7,12E-07 XY: -2,39E-06
Total Displacement UX: 6,51E-06 UY: -2,17E-05 UZ: 4,12E-04

Principal Value and Direction of Total Stresses and Strains

	Normal Stress (Pa)	Normal Strain	Shear Stress (Pa)	Shear Strain	X Comp.	Y Comp.	Z Comp.
Maximum:	1,67E+02	1,78E-04			0,0032	-0,0599	0,9982
MinImax:	-5,24E+04	-8,52E-05			-0,3405	0,9385	0,0574
Minimum:	-5,39E+04	-9,25E-05			0,9403	0,34	0,0174
Maximum:			2,70E+04	1,35E-04	-0,6626	-0,2828	0,6935
	-2,69E+04				0,6671	0,1981	0,7181
MiniMax:			2,63E+04	1,32E-04	0,243	-0,706	0,6653
	-2,61E+04				-0,2385	0,6213	0,7464
Minimum:			7,31E+02	3,66E-06	-0,9056	0,4232	0,0283
	-5,32E+04				0,4241	0,9041	0,0529
Strain Energy (J)	4,74E+00						
Strain Energy of	4,74E+00						

Position Number 7 Layer Number: 1 X Coordinate (m): 0,00E+00 Y Coordinate (m): 5,00E-01 Z Coordinate (m): 1,25E-02

Load No.	Distance to Load Axis (m)	Theta (°)	Radial Displacement (m)	Tangential Displacement (m)	Vertical Displacement (m)	Radial Stress (Pa)	Tangential Stress (Pa)	Vertical Stress (Pa)	Rad./Tang. Stress (Pa)	Rad./Vert. Stress (Pa)	Tang./Vert. Stress (Pa)	Radial Strain	Tangential Strain	Vertical Strain	Rad./Tang. Strain	Rad./Vert. Strain	Tang./Vert. Strain
1	4,49E-01	-1,68E+02	-5,53E-06	5,61E-07	2,69E-05	-6,85E+02	-2,21E+03	-6,02E+00	-3,79E+01	-1,00E+02	5,64E+00	1,40E-06	-6,20E-06	4,80E-06	-1,90E-07	-5,01E-07	2,82E-08
2	4,30E-01	-1,80E+02	-1,93E-06	-3,72E-12	-9,70E-07	9,58E+02	4,29E+02	-1,88E+00	-6,50E-05	3,70E+01	-4,64E-05	2,48E-06	-1,65E-07	-2,32E-06	-3,25E-13	1,85E-07	-2,32E-13
3	4,49E-01	-1,92E+02	-5,53E-06	-5,61E-07	2,69E-05	-6,85E+02	-2,21E+03	-6,02E+00	3,79E+01	-1,00E+02	-5,64E+00	1,40E-06	-6,20E-06	4,80E-06	1,90E-07	-5,01E-07	-2,82E-08
4	5,67E-01	9,13E+00	-3,23E-07	-4,08E-07	2,78E-05	-2,02E+03	-2,52E+03	1,88E+00	2,86E+01	-1,27E+02	-2,39E+00	-2,53E-06	-5,05E-06	7,58E-06	1,43E-07	-6,34E-07	-1,19E-08
5	5,70E-01	-3,67E-05	1,67E-06	1,08E-12	1,03E-06	-5,92E+02	-3,07E+02	-1,81E+00	-4,25E-06	-1,82E+01	7,50E-06	-1,46E-06	-3,46E-08	1,49E-06	-2,12E-14	-9,09E-08	3,75E-14
6	5,67E-01	-9,13E+00	2,51E-06	4,08E-07	1,55E-06	-8,98E+02	-4,82E+02	2,07E+00	-2,86E+01	-3,04E+01	2,39E+00	-2,23E-06	-4,75E-08	2,27E-06	-1,43E-07	-1,52E-07	1,19E-08
7	4,10E-01	-9,00E+01	-7,61E-10	4,79E-07	8,38E-09	-6,98E-01	-9,00E-01	9,36E-03	-3,08E+01	-4,84E-02	7,27E+00	-8,42E-10	-1,85E-09	2,70E-09	-1,54E-07	-2,42E-10	3,64E-08
8	5,90E-01	-9,00E+01	-8,12E-10	4,21E-07	7,43E-09	-2,87E-01	-5,57E-01	-2,04E-03	-2,90E+01	-2,09E-02	2,42E+00	-2,41E-11	-1,38E-09	1,40E-09	-1,45E-07	-1,05E-10	1,21E-08
9	5,00E-01	4,50E+01	-1,71E-05	-6,55E-06	2,39E-04	-1,65E+04	-2,25E+04	-1,67E+01	4,55E+02	-1,16E+03	-5,80E+01	-1,76E-05	-4,73E-05	6,49E-05	2,27E-06	-5,79E-06	-2,90E-07
10	5,00E-01	-4,50E+01	-4,21E-06	5,17E-07	4,68E-05	-2,87E+03	-4,27E+03	-6,14E+00	-3,66E+01	-2,18E+02	3,78E+00	-2,43E-06	-9,45E-06	1,19E-05	-1,83E-07	-1,09E-06	1,89E-08
Total Stresses (F XX:		-3,39E+04 YY:		-2,34E+04 ZZ:		-3,46E+01 YZ:		-1,71E+03 XZ:		5,99E+01 XY:		-5,05E+02					
Total Strains XX:		-7,39E-05 YY:		-2,15E-05 ZZ:		9,54E-05 YZ:		-8,55E-06 XZ:		2,99E-07 XY:		-2,53E-06					
Total Displacem UX:		5,58E-06 UY:		-3,04E-05 UZ:		3,70E-04											

Principal Value and Direction of Total Stresses and Strains

	Normal Stress (Pa)	Normal Strain	Shear Stress (Pa)	Shear Strain	X Comp.	Y Comp.	Z Comp.
Maximum:	9,01E+01	9,61E-05			0,0028	-0,0726	0,9974
MinImax:	-2,35E+01	-2,20E-05			-0,0481	0,9962	0,0727
Minimum:	-3,39E+04	-7,40E-05			0,9988	0,0482	0,0007
Maximum:			1,70E+04	8,50E-05	-0,7043	-0,0854	0,7048
	-1,69E+04				0,7083	-0,0173	0,7057
MiniMax:			1,18E+04	5,90E-05	0,036	-0,7558	0,6539
	-1,17E+04				-0,032	0,6531	0,7568
Minimum:			5,20E+03	2,60E-05	-0,7403	0,6704	0,0509
	-2,87E+04				0,6723	0,7385	0,0518
Strain Energy (J)	1,52E+00						
Strain Energy of	1,52E+00						

Position Number 8 Layer Number: 1 X Coordinate (m): 0,00E+00 Y Coordinate (m): 7,50E-01 Z Coordinate (m): 1,25E-02

Load No.	Distance to Load Axis (m)	Theta (°)	Radial Displacement (m)	Tangential Displacement (m)	Vertical Displacement (m)	Radial Stress (Pa)	Tangential Stress (Pa)	Vertical Stress (Pa)	Rad./Tang. Stress (Pa)	Rad./Vert. Stress (Pa)	Tang./Vert. Stress (Pa)	Radial Strain	Tangential Strain	Vertical Strain	Rad./Tang. Strain	Rad./Vert. Strain	Tang./Vert. Strain
1	6,96E-01	-1,73E+02	-5,09E-06	3,06E-07	2,24E-05	9,17E+01	-1,14E+03	-4,66E+00	-2,02E+01	-4,32E+01	1,20E+00	2,21E-06	-3,95E-06	1,73E-06	-1,01E-07	-2,16E-07	6,00E-09
2	6,80E-01	-1,80E+02	-1,53E-06	-3,13E-12	-1,00E-06	4,28E+02	2,29E+02	-4,27E+00	2,28E-05	1,54E+01	-1,47E-05	1,05E-06	5,60E-08	-1,11E-06	1,14E-13	7,68E-08	-7,36E-14
3	6,96E-01	-1,87E+02	-5,09E-06	-3,06E-07	2,24E-05	9,17E+01	-1,14E+03	-4,66E+00	2,02E+01	-4,32E+01	-1,20E+00	2,21E-06	-3,95E-06	1,73E-06	1,01E-07	-2,16E-07	-6,00E-09
4	8,15E-01	6,34E+00	-5,50E-07	-2,44E-07	2,34E-05	-6,13E+02	-1,32E+03	-2,08E-02	1,41E+01	-6,12E+01	-6,56E-01	1,53E-07	-3,37E-06	3,22E-06	7,03E-08	-3,06E-07	-3,28E-09
5	8,20E-01	-3,67E-05	1,41E-06	9,25E-13	9,61E-07	-2,97E+02	-1,64E+02	-2,31E+00	-5,85E-06	-8,24E+00	1,61E-06	-7,14E-07	-4,67E-08	7,61E-07	-2,93E-14	-4,12E-08	8,02E-15
6	8,15E-01	-6,34E+00	2,14E-06	2,44E-07	1,46E-06	-4,56E+02	-2,49E+02	1,44E+00	-1,41E+01	-1,43E+01	6,56E-01	-1,11E-06	-7,11E-08	1,18E-06	-7,03E-08	-7,15E-08	3,28E-09
7	6,60E-01	-9,00E+01	-8,24E-10	4,02E-07	7,07E-09	-1,85E-01	-4,67E-01	-1,22E-03	-2,65E+01	-1,79E-02	3,73E-01	1,65E-10	-1,25E-09	1,08E-09	-1,33E-07	-8,93E-11	1,87E-09
8	8,40E-01	-9,00E+01	-7,56E-10	3,62E-07	6,20E-09	-3,74E-02	-2,89E-01	-3,58E-04	-2,06E+01	-1,01E-02	2,10E+00	3,57E-10	-9,00E-10	5,43E-10	-1,03E-07	-5,03E-11	1,05E-08
9	7,50E-01	4,50E+01	-1,82E-05	-5,57E-06	2,01E-04	-4,42E+03	-1,17E+04	1,25E+01	3,45E+02	-5,09E+02	-1,86E+01	4,76E-06	-3,17E-05	2,69E-05	1,73E-06	-2,55E-06	-9,32E-08
10	7,50E-01	-4,50E+01	-4,25E-06	4,40E-07	3,93E-05	-6,78E+02	-2,22E+03	-3,44E+00	-2,76E+01	-1,03E+02	1,66E+00	1,44E-06	-6,25E-06	4,81E-06	-1,38E-07	-5,14E-07	8,30E-09

Total Stresses (F XX: -1,77E+04 YY: -5,89E+03 ZZ: -5,46E+00 YZ: -7,66E+02 XZ: 1,97E+01 XY: -3,70E+02
Total Strains XX: -4,90E-05 YY: 9,80E-06 ZZ: 3,92E-05 YZ: -3,83E-06 XZ: 9,84E-08 XY: -1,85E-06
Total Displacem UX: 4,67E-06 UY: -3,11E-05 UZ: 3,10E-04

Principal Value and Direction of Total Stresses and Strains

	Normal Stress (Pa)	Normal Strain	Shear Stress (Pa)	Shear Strain	X Comp.	Y Comp.	Z Comp.
Maximum:	9,27E+01	3,97E-05			0,0038	-0,1271	0,9919
Minimax:	-5,98E+03	9,38E-08			-0,0312	0,9914	0,1272
Minimum:	-1,77E+04	-4,91E-05			0,9995	0,0315	0,0002
Maximum:			8,88E+03	4,44E-05	-0,7041	-0,1121	0,7012
	-8,78E+03				0,7094	-0,0878	0,7015
MiniMax:			5,84E+03	2,92E-05	-0,7288	0,6788	0,0897
	-1,18E+04				0,6847	0,7233	0,0901
Minimum:			3,04E+03	1,52E-05	0,0247	-0,7909	0,6114
	-2,94E+03				-0,0194	0,6111	0,7913
Strain Energy (J)	4,07E-01						
Strain Energy of	4,07E-01						

Position Number 9 Layer Number: 1 X Coordinate (m): 0,00E+00 Y Coordinate (m): 1,00E+00 Z Coordinate (m): 1,25E-02

Load No.	Distance to Load Axis (m)	Theta (°)	Radial Displacement (m)	Tangential Displacement (m)	Vertical Displacement (m)	Radial Stress (Pa)	Tangential Stress (Pa)	Vertical Stress (Pa)	Rad./Tang. Stress (Pa)	Rad./Vert. Stress (Pa)	Tang./Vert. Stress (Pa)	Radial Strain	Tangential Strain	Vertical Strain	Rad./Tang. Strain	Rad./Vert. Strain	Tang./Vert. Strain
1	9,44E-01	-1,75E+02	-4,52E-06	1,97E-07	1,86E-05	4,20E+02	-5,72E+02	5,82E-01	-1,02E+01	-2,13E+01	1,03E-01	2,35E-08	-2,61E-08	2,55E-07	-5,08E-08	-1,08E-07	5,16E-10
2	9,30E-01	-1,80E+02	-1,34E-06	-2,72E-12	-8,93E-07	2,27E+02	1,21E+02	-1,53E+00	1,13E-05	5,99E+00	-4,55E-08	5,58E-07	2,76E-08	-5,86E-07	5,86E-14	3,00E-08	-2,28E-14
3	9,44E-01	-1,88E+02	-4,52E-06	-1,97E-07	1,86E-05	4,20E+02	-5,72E+02	5,82E-01	1,02E+01	-2,13E+01	-1,03E-01	2,35E-08	-2,61E-08	2,55E-07	5,08E-08	-1,08E-07	-5,16E-10
4	1,06E+00	4,85E+00	-3,76E-07	-1,65E-07	1,95E-05	-3,31E+01	-6,71E+02	1,04E+00	7,85E+00	-3,03E+01	-3,39E-01	1,01E-08	-2,18E-08	1,18E-08	3,92E-08	-1,52E-07	-1,70E-09
5	1,07E+00	-3,67E-05	1,27E-08	8,17E-13	8,15E-07	-1,66E+02	-8,50E+01	3,55E-01	-7,86E-07	-4,09E+00	8,44E-07	-4,13E-07	-6,76E-09	4,20E-07	-3,93E-15	-2,05E-08	4,22E-15
6	1,06E+00	-4,85E+00	1,93E-06	1,65E-07	1,28E-06	-2,58E+02	-1,32E+02	1,25E+00	-7,85E+00	-7,97E+00	3,39E-01	-6,43E-07	-1,14E-08	6,54E-07	-3,92E-08	-3,98E-08	1,70E-09
7	9,10E-01	-9,00E+01	-7,29E-10	3,48E-07	5,88E-09	3,24E-04	-2,40E-01	-2,20E-04	-1,89E+01	-8,53E-03	1,06E+00	4,02E-10	-8,01E-10	3,98E-10	-9,46E-08	-4,26E-11	5,32E-09
8	1,09E+00	-9,00E+01	-6,49E-10	3,21E-07	5,14E-09	6,73E-02	-1,45E-01	-4,28E-05	-1,47E+01	-8,30E-03	7,69E-01	4,68E-10	-5,95E-10	1,29E-10	-7,34E-08	-4,15E-11	3,85E-09
9	1,00E+00	4,50E+01	-1,59E-05	-4,89E-06	1,67E-04	5,10E+02	-5,98E+03	5,73E+00	2,39E+02	-2,52E+02	-6,83E+00	1,17E-05	-2,08E-05	9,14E-06	1,20E-06	-1,26E-06	-3,41E-08
10	1,00E+00	-4,50E+01	-3,73E-06	3,85E-07	3,26E-05	1,99E+02	-1,14E+03	-1,76E-01	-1,86E+01	-4,54E+01	1,12E+00	2,56E-08	-4,12E-08	1,56E-08	-9,28E-08	-2,27E-07	5,61E-09

Total Stresses (F XX: -9,01E+03 YY: 1,30E+03 ZZ: 7,79E+00 YZ: -3,75E+02 XZ: 5,76E+00 XY: -2,52E+02
Total Strains XX: -3,22E-05 YY: 1,93E-05 ZZ: 1,29E-05 YZ: -1,88E-06 XZ: 2,88E-08 XY: -1,26E-06
Total Displacem UX: 4,03E-06 UY: -2,72E-05 UZ: 2,58E-04

Principal Value and Direction of Total Stresses and Strains

	Normal Stress (Pa)	Normal Strain	Shear Stress (Pa)	Shear Strain	X Comp.	Y Comp.	Z Comp.
Maximum:	1,41E+03	1,99E-05			-0,0235	0,9655	-0,2593
Minimax:	-9,30E+01	1,24E-05			-0,0067	0,2592	0,9658
Minimum:	-9,01E+03	-3,22E-05			0,9997	0,0244	0,0004
Maximum:			5,21E+03	2,61E-05	-0,7235	0,6855	-0,1836
	-3,80E+03				0,6903	0,7	-0,1831
MiniMax:			4,46E+03	2,23E-05	-0,7118	0,1881	0,6827
	-4,55E+03				0,7022	0,2005	0,6832
Minimum:			7,50E+02	3,75E-06	-0,0119	0,4994	-0,8663
	6,57E+02				-0,0213	0,868	0,4996
Strain Energy (J)	1,59E-01						
Strain Energy of	1,59E-01						

Position Number 10 Layer Number: 1 X Coordinate (m): 0,00E+00 Y Coordinate (m): 1,50E+00 Z Coordinate (m): 1,25E-02

Load No.	Distance to Load Axis (m)	Theta (°)	Radial Displacement (m)	Tangential Displacement (m)	Vertical Displacement (m)	Radial Stress (Pa)	Tangential Stress (Pa)	Vertical Stress (Pa)	Rad./Tang. Stress (Pa)	Rad./Vert. Stress (Pa)	Tang./Vert. Stress (Pa)	Radial Strain	Tangential Strain	Vertical Strain	Rad./Tang. Strain	Rad./Vert. Strain	Tang./Vert. Strain
1	1,44E+00	-1,76E+02	-3,48E-06	1,05E-07	1,29E-05	4,89E+02	-1,30E+02	2,62E-01	-3,07E+00	-7,38E-01	8,22E-02	1,85E-08	-1,25E-08	-5,97E-07	-1,54E-08	-3,69E-09	4,11E-10
2	1,43E+00	-1,80E+02	-1,16E-06	-2,21E-12	-6,09E-07	8,56E+01	3,22E+01	-2,54E-01	-1,38E-05	1,67E+00	-5,41E-07	2,32E-07	-3,50E-08	-1,97E-07	-6,92E-14	8,35E-09	-2,70E-15
3	1,44E+00	-1,84E+02	-3,48E-06	-1,05E-07	1,29E-05	4,89E+02	-1,30E+02	2,62E-01	3,07E+00	-7,38E-01	-8,23E-02	1,85E-08	-1,25E-08	-5,97E-07	1,54E-08	-3,69E-09	-4,11E-10
4	1,56E+00	3,30E+00	1,74E-07	-9,33E-08	1,35E-05	2,62E+02	-1,47E+02	-1,26E+00	2,54E+00	-4,05E+00	-6,84E-02	1,12E-08	-9,23E-07	-1,97E-07	1,27E-08	-2,03E-08	-3,32E-10

5	1,57E+00	-3,67E-05	1,13E-06	6,78E-13	5,47E-07	-7,08E+01	-2,30E+01	-1,45E+00	5,63E-06	-3,12E+00	1,34E-06	-1,95E-07	4,37E-08	1,52E-07	2,82E-14	-1,56E-08	6,67E-15
6	1,56E+00	-3,30E+00	1,72E-06	9,33E-08	8,32E-07	-1,08E+02	-3,47E+01	-1,42E+00	-2,54E+00	-1,06E+00	6,64E-02	-2,99E-07	6,61E-08	2,33E-07	-1,27E-08	-5,30E-09	3,32E-10
7	1,41E+00	-9,00E+01	-5,01E-10	2,83E-07	4,06E-09	1,04E-01	-5,44E-02	4,42E-05	-9,66E+00	-1,93E-03	5,95E-01	4,38E-10	-3,55E-10	-8,29E-11	-4,83E-08	-9,84E-12	2,97E-09
8	1,59E+00	-9,00E+01	-4,25E-10	2,67E-07	3,57E-09	1,01E-01	-2,99E-02	2,85E-05	-6,42E+00	-2,59E-04	-7,96E-01	3,85E-10	-2,67E-10	-1,18E-10	-3,21E-08	-1,30E-12	-3,98E-09
9	1,50E+00	4,50E+01	-9,72E-06	-4,02E-06	1,16E-04	2,85E+03	-1,32E+03	2,18E+00	1,16E+02	-4,66E+01	5,57E-01	1,17E-05	-9,16E-06	-2,53E-06	5,78E-07	-2,33E-07	2,79E-09
10	1,50E+00	-4,50E+01	-2,40E-06	3,17E-07	2,26E-05	6,02E+02	-2,42E+02	3,71E-01	-9,52E+00	-7,54E+00	-2,23E-01	2,41E-06	-1,81E-06	-5,98E-07	-4,76E-08	-3,77E-08	-1,12E-09

Total Stresses (F XX: -1,99E+03 YY: 4,59E+03 ZZ: -1,30E+00 YZ: -6,21E+01 XZ: 3,96E-02 XY: -1,18E+02
Total Strains XX: -1,43E-05 YY: 1,86E-05 ZZ: -4,33E-06 YZ: -3,11E-07 XZ: 1,98E-10 XY: -5,88E-07
Total Displacement UX: 3,24E-06 UY: -1,72E-05 UZ: 1,78E-04

Principal Value and Direction of Total Stresses and Strains

	Normal Stress (Pa)	Normal Strain	Shear Stress (Pa)	Shear Strain	X Comp.	Y Comp.	Z Comp.
Maximum:	4,59E+03	1,86E-05			-0,0179	0,9997	-0,0135
Minimax:	-2,14E+00	-4,34E-06			-0,0008	0,0135	0,9999
Minimum:	-1,99E+03	-1,43E-05			0,9998	0,0179	0,0005
Maximum:			3,29E+03	1,65E-05	-0,7196	0,6943	-0,0099
	1,30E+03				0,6944	0,7196	-0,0092
MiniMax:			2,30E+03	1,15E-05	-0,0121	0,6974	-0,7166
	2,30E+03				-0,0132	0,7165	0,6975
Minimum:			9,96E+02	4,98E-06	-0,7075	-0,0031	0,7067
	-9,98E+02				0,7064	0,0222	0,7074

Strain Energy (J) 5,70E-02
Strain Energy of 5,70E-02

System: 3: sys33

Layer Number	Thickness (m)	Young's Modulus (Pa)	Poisson's Ratio	Shear Spring Compliance (m ³ /N)	Load Number	Normal Stress (Pa)	Shear Stress (Pa)	Radius of Loaded Area (m)	Load Position X (m)	Load Position Y (m)	Shear Direction (°)
1	0,013	3,00E+08	0,5	0,00E+00	1	4,00E+05	2,00E+05	5,26E-02	9,00E-02	6,00E-02	2,70E+02
2	0,013	5,00E+08	0,47	0,00E+00	2	1,75E+02	2,00E+05	4,26E-02	0,00E+00	7,00E-02	2,70E+02
3	0,015	8,00E+08	0,46	0,00E+00	3	4,00E+05	2,00E+05	5,26E-02	-9,00E-02	6,00E-02	2,70E+02
4	0,03	1,20E+09	0,45	0,00E+00	4	4,00E+05	2,00E+05	5,26E-02	9,00E-02	-6,00E-02	9,00E+01
5	0,03	1,52E+09	0,45	0,00E+00	5	1,75E+02	2,00E+05	4,26E-02	0,00E+00	-7,00E-02	9,00E+01
6	0,06	3,07E+09	0,45	0,00E+00	6	1,15E+02	2,00E+05	5,26E-02	-9,00E-02	-6,00E-02	9,00E+01
7	0,07	3,70E+09	0,44	0,00E+00	7	6,23E+02	1,80E+05	2,26E-02	0,00E+00	9,00E-02	1,80E+02
8	0,07	3,60E+09	0,43	0,00E+00	8	6,23E+02	1,80E+05	2,26E-02	0,00E+00	-8,00E-02	1,80E+02
9	0,25	1,00E+08	0,35	0,00E+00	9	7,50E+05	1,50E+05	1,13E-01	0,00E+00	0,00E+00	4,50E+01
10		5,00E+07	0,5		10	7,50E+05	6,00E+04	5,00E-02	0,00E+00	0,00E+00	1,35E+02

Position Number 1 Layer Number: 2 X Coordinate (m): 0,00E+00 Y Coordinate (m): 0,00E+00 Z Coordinate (m): 2,50E-02

Load No.	Distance to Load Axis (m)	Theta (°)	Radial Displacement (m)	Tangential Displacement (m)	Vertical Displacement (m)	Radial Stress (Pa)	Tangential Stress (Pa)	Vertical Stress (Pa)	Rad./Tang. Stress (Pa)	Rad./Vert. Stress (Pa)	Tang./Vert. Stress (Pa)	Radial Strain	Tangential Strain	Vertical Strain	Rad./Tang. Rad./Vert. Strain	Tang./Vert. Strain
1	1,08E-01	-4,16E+02	5,82E-06	3,91E-06	3,55E-05	-5,26E+04	-1,26E+04	-5,77E+03	-3,75E+02	-1,82E+04	-1,30E+02	-8,79E-05	2,97E-05	4,97E-05	-1,10E-06	-5,34E-05
2	7,00E-02	-3,60E+02	7,88E-06	9,31E-12	1,06E-06	-5,93E+04	-1,25E+04	-1,90E+04	3,45E-02	-3,75E+04	2,50E-02	-8,91E-05	4,87E-05	2,96E-05	1,01E-10	-1,10E-04
3	1,08E-01	-3,04E+02	5,82E-06	-3,91E-06	3,55E-05	-5,26E+04	-1,26E+04	-5,77E+03	3,75E+02	-1,82E+04	1,30E+02	-8,79E-05	2,97E-05	4,97E-05	1,10E-06	-5,34E-05
4	1,08E-01	5,83E+01	5,82E-06	-3,91E-06	3,55E-05	-5,26E+04	-1,26E+04	-5,77E+03	3,75E+02	-1,82E+04	1,30E+02	-8,79E-05	2,97E-05	4,97E-05	1,10E-06	-5,34E-05
5	7,00E-02	-3,67E-05	7,88E-06	2,86E-12	1,06E-06	-5,93E+04	-1,25E+04	-1,90E+04	1,06E-02	-3,75E+04	7,68E-03	-8,91E-05	4,87E-05	2,96E-05	3,11E-11	-1,10E-04
6	1,08E-01	-5,83E+01	4,49E-06	3,91E-06	4,72E-07	-2,25E+04	-3,30E+03	-3,04E+03	-3,75E+02	-9,21E+03	-1,30E+02	-3,91E-05	1,74E-05	1,82E-05	-1,10E-06	-2,71E-05
7	9,00E-02	-2,70E+02	6,42E-10	-8,22E-07	1,03E-08	-1,15E+01	-2,35E+00	-1,13E+00	-3,49E+02	-3,71E+00	-1,57E+02	-1,96E-08	7,12E-09	1,07E-08	-1,03E-06	-1,09E-08
8	9,00E-02	-9,00E+01	6,37E-10	8,22E-07	1,03E-08	-1,14E+01	-2,36E+00	-1,13E+00	3,49E+02	-3,70E+00	1,57E+02	-1,96E-08	7,09E-09	1,07E-08	1,03E-06	-1,09E-08
9	0,00E+00	-4,50E+01	2,35E-05	2,35E-05	3,38E-04	-5,85E+05	-5,85E+05	-7,41E+05	0,00E+00	-8,91E+04	-8,91E+04	7,63E-05	7,62E-05	-3,82E-04	0,00E+00	-2,62E-04
10	0,00E+00	-1,35E+02	-3,20E-06	3,20E-06	8,84E-05	-3,79E+05	-3,79E+05	-6,94E+05	0,00E+00	2,22E+04	-2,22E+04	2,50E-04	2,50E-04	-6,74E-04	0,00E+00	6,53E-05

Total Stresses (F XX: -1,13E+06 YY: -1,17E+06 ZZ: -1,49E+06 YZ: -1,06E+05 XZ: -5,98E+04 XY: 9,59E+03
Total Strains XX: 2,51E-04 YY: 1,24E-04 ZZ: -8,30E-04 YZ: -3,13E-04 XZ: -1,76E-04 XY: 2,82E-05
Total Displacement UX: 1,75E-05 UY: 2,60E-05 UZ: 5,36E-04

Principal Value and Direction of Total Stresses and Strains

	Normal Stress (Pa)	Normal Strain	Shear Stress (Pa)	Shear Strain	X Comp.	Y Comp.	Z Comp.
Maximum:	-1,10E+06	3,26E-04			0,8106	0,5225	-0,2645

Minimax:	-1,16E+06	1,64E-04			-0,5702	0,8071	-0,1532
Minimum:	-1,53E+06	-9,44E-04			0,1335	0,275	0,9521
Maximum:			2,16E+05	6,35E-04	0,4788	0,175	-0,8603
	-1,32E+06				0,6675	0,5639	0,4862
MiniMax:			1,89E+05	5,54E-04	-0,4976	0,3762	-0,7816
	-1,34E+06				-0,3088	0,7652	0,5649
Minimum:			2,77E+04	8,13E-05	0,9764	-0,2013	-0,0787
	-1,13E+06				0,17	0,9401	-0,2954
Strain Energy (J)	4,49E+02						
Strain Energy of	1,63E+02						

Position Number	2	Layer Number:	2	X Coordinate (m):	0,00E+00	Y Coordinate (m):	5,00E-02	Z Coordinate (m):	2,50E-02								
Load No.	Distance to Load Axis (m)	Theta (°)	Radial Displacement (m)	Tangential Displacement (m)	Vertical Displacement (m)	Radial Stress (Pa)	Tangential Stress (Pa)	Vertical Stress (Pa)	Rad./Tang. Stress (Pa)	Rad./Vert. Stress (Pa)	Tang./Vert. Stress (Pa)	Radial Strain	Tangential Strain	Vertical Strain	Rad./Tang. Strain	Rad./Vert. Strain	Tang./Vert. Strain
1	9,08E-02	-4,44E+02	3,43E-06	5,48E-06	3,61E-05	-5,19E+04	-1,29E+04	-8,67E+03	-2,79E+03	-2,25E+04	-2,01E+03	-8,36E-05	3,12E-05	4,35E-05	-8,19E-06	-6,61E-05	-5,92E-06
2	2,00E-02	-3,60E+02	1,14E-05	2,25E-11	1,12E-06	-4,70E+04	-2,23E+04	-3,04E+04	1,99E-02	-7,84E+04	8,72E-02	-4,44E-05	2,81E-05	4,34E-06	5,84E-11	-2,31E-04	2,56E-10
3	9,06E-02	-2,76E+02	3,43E-06	-5,48E-06	3,61E-05	-5,19E+04	-1,29E+04	-8,67E+03	2,79E+03	-2,25E+04	2,01E+03	-8,36E-05	3,12E-05	4,35E-05	8,19E-06	-6,61E-05	5,92E-06
4	1,42E-01	3,93E+01	4,97E-06	-2,51E-06	3,46E-05	-3,45E+04	-1,04E+04	-1,80E+03	-2,79E+02	-7,73E+03	-2,24E+02	-5,75E-05	1,34E-05	3,85E-05	-8,21E-07	-2,27E-05	-6,58E-07
5	1,20E-01	-3,67E-05	4,81E-06	1,79E-12	5,01E-07	-2,08E+04	-2,35E+03	-1,97E+03	3,64E-03	-8,99E+03	1,37E-03	-3,76E-05	1,87E-05	1,79E-05	1,07E-11	-2,06E-05	4,02E-12
6	1,42E-01	-3,93E+01	4,87E-06	2,51E-06	6,02E-07	-1,68E+04	-2,12E+03	-1,19E+03	2,78E+02	-4,70E+03	2,24E+02	-3,06E-05	1,27E-05	1,54E-05	8,21E-07	-1,38E-05	6,58E-07
7	4,00E-02	-2,70E+02	2,89E-09	-1,77E-06	1,30E-08	-6,80E+01	-1,44E+01	-4,13E+01	1,79E+03	-5,46E+01	3,36E+03	-7,97E-08	7,21E-08	-7,01E-09	5,27E-06	-1,60E-07	9,88E-06
8	1,40E-01	-9,00E+01	3,06E-11	6,44E-07	9,78E-09	-5,00E+00	-2,30E+00	-1,38E-01	1,83E+02	-7,62E-01	8,78E+01	-7,70E-09	2,25E-10	6,59E-09	5,36E-07	-2,24E-09	2,58E-07
9	5,00E-02	4,50E+01	2,66E-05	-2,22E-05	3,36E-04	-5,91E+05	-5,80E+05	-7,39E+05	8,81E+03	-1,11E+05	8,48E+04	5,76E-05	8,96E-05	-3,76E-04	2,59E-05	-3,25E-04	2,49E-04
10	5,00E-02	-4,50E+01	1,29E-05	2,01E-06	7,42E-05	-2,57E+05	-1,68E+05	-3,32E+05	-4,27E+03	-2,12E+05	-8,26E+03	-4,47E-05	2,17E-04	-2,63E-04	-1,26E-05	-6,24E-04	-2,43E-05
Total Stresses (F XX:		-9,03E+05	YY:	-9,79E+05	ZZ:	-1,12E+06	YZ:	-2,52E+05	XZ:	-7,14E+04	XY:	-1,91E+03					
Total Strains XX:		1,70E-04	YY:	-5,39E-05	ZZ:	-4,77E-04	YZ:	-7,40E-04	XZ:	-2,10E-04	XY:	-5,63E-06					
Total Displacement UX:		1,77E-05	UY:	3,21E-05	UZ:	5,19E-04											

Principal Value and Direction of Total Stresses and Strains

	Normal Stress (Pa)	Normal Strain	Shear Stress (Pa)	Shear Strain	X Comp.	Y Comp.	Z Comp.
Maximum:	-7,75E+05	5,48E-04			0,3225	0,7342	-0,5975
Minimax:	-9,09E+05	1,52E-04			0,9363	-0,3401	0,0876
Minimum:	-1,32E+06	-1,06E-03			0,1389	0,5877	0,7971
Maximum:			2,73E+05	8,02E-04	0,1299	0,1036	-0,9861
	-1,05E+06				0,3263	0,9347	0,1411
MiniMax:			2,06E+05	6,05E-04	0,5639	-0,656	-0,5017
	-1,12E+06				0,7603	0,1751	0,6256
Minimum:			6,69E+04	1,97E-04	-0,434	0,7596	-0,4844
	-8,42E+05				0,8901	0,2787	-0,3605
Strain Energy (J)	4,18E+02						
Strain Energy of	2,38E+02						

Position Number	3	Layer Number:	2	X Coordinate (m):	0,00E+00	Y Coordinate (m):	1,10E-01	Z Coordinate (m):	2,50E-02								
Load No.	Distance to Load Axis (m)	Theta (°)	Radial Displacement (m)	Tangential Displacement (m)	Vertical Displacement (m)	Radial Stress (Pa)	Tangential Stress (Pa)	Vertical Stress (Pa)	Rad./Tang. Stress (Pa)	Rad./Vert. Stress (Pa)	Tang./Vert. Stress (Pa)	Radial Strain	Tangential Strain	Vertical Strain	Rad./Tang. Strain	Rad./Vert. Strain	Tang./Vert. Strain
1	1,03E-01	-1,19E+02	-2,53E-06	4,28E-06	3,48E-05	-1,17E+04	-6,31E+03	-2,11E+02	-7,89E+02	-1,48E+03	-4,07E+02	-1,72E-05	-1,44E-06	1,65E-05	-2,32E-06	-4,36E-06	-1,20E-06
2	4,00E-02	-1,80E+02	-1,03E-05	-1,60E-11	-1,85E-06	7,47E+04	3,52E+04	6,09E+04	-3,87E-02	6,75E+04	-6,79E-02	5,90E-05	-5,70E-05	1,86E-05	-1,14E-10	1,99E-04	-2,00E-10
3	1,03E-01	-2,41E+02	-2,53E-06	-4,28E-06	3,48E-05	-1,17E+04	-6,31E+03	-2,11E+02	7,89E+02	-1,48E+03	4,07E+02	-1,72E-05	-1,44E-06	1,65E-05	2,32E-06	-4,36E-06	1,20E-06
4	1,92E-01	2,79E+01	3,42E-06	-1,64E-06	3,39E-05	-2,06E+04	-9,04E+03	-3,66E+02	-1,08E+02	-2,90E+03	-1,39E+02	-3,23E-05	1,62E-06	2,71E-05	-3,17E-07	-8,53E-06	-4,09E-07
5	1,80E-01	-3,67E-05	3,37E-06	1,50E-12	5,90E-07	-8,14E+03	-1,10E+03	-2,79E+02	1,24E-03	-1,50E+03	3,61E-04	-1,50E-05	5,72E-06	8,12E-06	3,66E-12	-4,41E-06	1,06E-12
6	1,92E-01	-2,79E+01	4,32E-06	1,64E-06	8,36E-07	-9,52E+03	-1,45E+03	-2,85E+02	1,08E+02	-1,63E+03	1,39E+02	-1,74E-05	6,31E-06	9,74E-06	3,17E-07	-4,80E-06	4,09E-07
7	2,00E-02	-9,00E+01	3,53E-09	2,89E-06	1,80E-08	-1,20E+02	-8,32E+01	-2,46E+02	-4,67E+03	-1,09E+02	-1,62E+04	6,97E-08	1,77E-07	-3,00E-07	-1,37E-05	-3,19E-07	-4,75E-05
8	2,00E-01	-9,00E+01	-3,01E-10	5,73E-07	9,48E-09	-2,98E+00	-2,16E+00	-1,07E-02	5,15E+01	-3,24E-01	5,03E+01	-3,93E-09	-1,50E-09	4,81E-09	1,51E-07	-9,52E-10	1,48E-07
9	1,10E-01	4,50E+01	2,96E-05	-1,54E-05	3,15E-04	-4,37E+05	-3,49E+05	-4,43E+05	2,30E+04	-2,75E+05	3,79E+04	-1,30E-04	1,30E-04	-1,47E-04	6,77E-05	-8,07E-04	1,11E-04
10	1,10E-01	-4,50E+01	3,60E-06	8,83E-07	5,93E-05	-5,60E+04	-1,63E+04	-4,94E+03	-1,16E+01	-1,66E+04	1,11E+01	-9,20E-05	2,47E-05	5,81E-05	-3,46E-08	-4,87E-05	3,27E-08
Total Stresses (F XX:		-3,88E+05 YY:		-4,66E+05 ZZ:		-3,88E+05 YZ:		-2,30E+05 XZ:		-2,12E+04 XY:		-1,70E+04					
Total Strains XX:		6,69E-05 YY:		-2,21E-04 ZZ:		7,39E-06 YZ:		-6,76E-04 XZ:		-6,22E-05 XY:		-4,99E-05					

Total Displacement UX: 1,15E-05 UY: 2,47E-05 UZ: 4,77E-04

Principal Value and Direction of Total Stresses and Strains

	Normal Stress (Pa)	Normal Strain	Shear Stress (Pa)	Shear Strain	X Comp.	Y Comp.	Z Comp.
Maximum:	-1,94E+05	5,79E-04			-0,0302	-0,6439	0,7645
Minimum:	-3,66E+05	7,35E-05			0,9955	-0,0882	-0,035
Maximum:	-6,63E+05	-7,99E-04			0,09	0,76	0,6437
Maximum:			2,34E+05	6,89E-04	-0,085	-0,9927	0,0854
Minimum:	-4,28E+05				0,0423	0,0821	0,9957
Maximum:			1,48E+05	4,36E-04	0,6403	-0,5998	-0,4799
Minimum:	-5,14E+05				0,7676	0,475	0,4304
Maximum:			8,60E+04	2,53E-04	-0,7252	-0,3929	0,5654
Minimum:	-2,80E+05				0,6826	-0,5177	0,5158

Strain Energy (J) 1,95E+02
Strain Energy of 1,65E+02

Position Number 4 Layer Number: 2 X Coordinate (m): 0,00E+00 Y Coordinate (m): 2,10E-01 Z Coordinate (m): 2,50E-02

Load No.	Distance to Load Axis (m)	Theta (°)	Radial Displacement (m)	Tangential Displacement (m)	Vertical Displacement (m)	Radial Stress (Pa)	Tangential Stress (Pa)	Vertical Stress (Pa)	Rad./Tang. Stress (Pa)	Rad./Vert. Stress (Pa)	Tang./Vert. Stress (Pa)	Radial Strain	Tangential Strain	Vertical Strain	Rad./Tang. Strain	Rad./Vert. Strain	Tang./Vert. Strain
1	1,75E-01	-1,49E+02	-5,14E-06	1,87E-06	3,26E-05	-1,22E+03	-6,23E+03	3,07E+02	1,72E+02	7,15E+02	1,65E+02	3,14E-06	-1,16E-05	7,61E-06	5,04E-07	2,10E-06	4,86E-07
2	1,40E-01	-1,80E+02	-4,18E-06	-5,15E-12	-4,83E-07	1,46E+04	1,82E+03	9,75E+02	-7,71E-03	3,96E+03	-2,53E-03	2,67E-05	-1,14E-05	-1,33E-05	-2,27E-11	1,16E-05	-7,43E-12
3	1,75E-01	-2,11E+02	-5,14E-06	-1,87E-06	3,26E-05	-1,22E+03	-6,23E+03	3,07E+02	-1,72E+02	7,15E+02	-1,65E+02	3,14E-06	-1,16E-05	7,61E-06	-5,04E-07	2,10E-06	-4,86E-07
4	2,85E-01	1,84E+01	1,68E-06	-9,97E-07	3,27E-05	-1,09E+04	-7,44E+03	-3,87E+01	5,10E+01	-1,11E+03	-5,58E+01	-1,47E-05	-4,62E-06	1,71E-05	1,50E-07	-3,25E-06	-1,64E-07
5	2,80E-01	-3,67E-05	2,46E-06	1,33E-12	8,34E-07	-3,19E+03	-8,20E+02	-2,25E+01	3,01E-04	-3,03E+02	1,07E-04	-5,59E-06	1,38E-06	3,72E-06	8,84E-13	-8,90E-07	3,15E-13
6	2,85E-01	-1,84E+01	3,53E-06	9,97E-07	1,21E-06	-4,48E+03	-1,18E+03	-3,15E+01	-5,10E+01	-4,25E+02	5,58E+01	-7,82E-06	1,88E-06	5,26E-06	-1,50E-07	-1,25E-06	1,64E-07
7	1,20E-01	-9,00E+01	2,06E-10	6,90E-07	9,92E-09	-6,49E+00	-2,33E+00	-3,10E-01	2,53E+02	-1,29E+00	1,15E+02	-1,05E-08	1,72E-09	7,67E-09	7,45E-07	-3,79E-09	3,37E-07
8	3,00E-01	-9,00E+01	-5,84E-10	5,16E-07	6,98E-09	-1,68E+00	-1,73E+00	-2,01E-03	-2,99E+01	-1,83E-01	2,88E+01	-1,72E-09	-1,88E-09	3,19E-09	-8,80E-08	-5,37E-10	8,45E-08
9	2,10E-01	4,50E+01	2,29E-06	-8,59E-06	2,83E-04	-1,12E+05	-6,88E+04	-2,25E+03	8,76E+02	-1,61E+04	-3,55E+02	-1,58E-04	-3,00E-05	1,66E-04	2,57E-06	-4,73E-05	-1,04E-06
10	2,10E-01	-4,50E+01	-1,07E-06	6,55E-07	5,57E-05	-1,83E+04	-1,27E+04	-9,43E+01	2,67E+01	-2,06E+03	5,17E+01	-2,45E-05	-8,22E-06	2,90E-05	7,84E-08	-6,06E-06	1,52E-07

Total Stresses (F XX: -9,95E+04 YY: -1,39E+05 ZZ: -8,52E+02 YZ: -1,49E+04 XZ: 3,76E+02 XY: -1,08E+03
Total Strains XX: -6,73E-05 YY: -1,84E-04 ZZ: 2,23E-04 YZ: -4,37E-05 XZ: 1,10E-06 XY: -3,19E-06
Total Displacement UX: 7,31E-06 UY: -5,67E-06 UZ: 4,38E-04

Principal Value and Direction of Total Stresses and Strains

	Normal Stress (Pa)	Normal Strain	Shear Stress (Pa)	Shear Strain	X Comp.	Y Comp.	Z Comp.
Maximum:	7,28E+02	2,27E-04			0,0049	-0,1056	0,9944
Minimum:	-9,95E+04	-6,72E-05			0,9997	-0,0244	-0,0075
Maximum:	-1,41E+05	-1,89E-04			0,0251	0,9941	0,1054
Maximum:			7,08E+04	2,08E-04	-0,0143	-0,7776	0,6286
Minimum:	-7,01E+04				0,0212	0,6283	0,7777
Maximum:			5,01E+04	1,47E-04	-0,7034	-0,0574	0,7084
Minimum:	-4,94E+04				0,7103	-0,0919	0,6979
Maximum:			2,07E+04	6,09E-05	0,6892	-0,7202	-0,0788
Minimum:	-1,20E+05				0,7246	0,6857	0,0693

Strain Energy (J) 1,67E+01
Strain Energy of 1,56E+01

Position Number 5 Layer Number: 2 X Coordinate (m): 0,00E+00 Y Coordinate (m): 3,10E-01 Z Coordinate (m): 2,50E-02

Load No.	Distance to Load Axis (m)	Theta (°)	Radial Displacement (m)	Tangential Displacement (m)	Vertical Displacement (m)	Radial Stress (Pa)	Tangential Stress (Pa)	Vertical Stress (Pa)	Rad./Tang. Stress (Pa)	Rad./Vert. Stress (Pa)	Tang./Vert. Stress (Pa)	Radial Strain	Tangential Strain	Vertical Strain	Rad./Tang. Strain	Rad./Vert. Strain	Tang./Vert. Strain
1	2,66E-01	-1,60E+02	-5,36E-06	1,09E-06	3,07E-05	-1,98E+03	-5,32E+03	3,76E+01	-3,59E+01	-2,22E+02	6,63E+01	1,01E-06	-8,82E-06	6,94E-06	-1,06E-07	-6,52E-07	1,95E-07
2	2,40E-01	-1,80E+02	-2,73E-06	-4,31E-12	-7,29E-07	4,34E+03	8,87E+02	5,52E+01	-1,60E-03	5,17E+02	-4,97E-04	7,79E-06	-2,36E-06	-4,80E-06	-4,70E-12	1,52E-06	-1,46E-12
3	2,66E-01	-2,00E+02	-5,36E-06	-1,09E-06	3,07E-05	-1,98E+03	-5,32E+03	3,76E+01	3,59E+01	-2,22E+02	-6,63E+01	1,01E-06	-8,82E-06	6,94E-06	1,06E-07	-6,52E-07	-1,95E-07
4	3,81E-01	1,37E+01	7,10E-07	-6,87E-07	3,12E-05	-6,70E+03	-5,83E+03	-1,33E+01	6,90E+01	-6,42E+02	-2,33E+01	-7,81E-06	-5,56E-06	1,18E-05	2,03E-07	-1,89E-06	-6,84E-08
5	3,80E-01	-3,87E-05	2,05E-06	1,22E-12	9,72E-07	-1,82E+03	-6,68E+02	-2,55E+00	8,32E-05	-1,22E+02	4,89E-05	-3,02E-06	3,80E-07	2,34E-06	2,45E-13	-3,58E-07	1,44E-13
6	3,81E-01	-1,37E+01	3,04E-06	6,87E-07	1,44E-06	-2,69E+03	-9,89E+02	-7,67E+00	-6,90E+01	-1,82E+02	2,33E+01	-4,45E-06	5,59E-07	3,44E-06	-2,03E-07	-5,34E-07	6,84E-08
7	2,20E-01	-9,00E+01	-3,71E-10	5,58E-07	9,38E-09	-2,62E+00	-2,08E+00	-5,55E-03	2,33E+01	-2,79E-01	4,46E+01	-3,29E-09	-1,68E-09	4,41E-09	6,85E-08	-8,20E-10	1,31E-07

8	4,00E-01	-9,00E+01	-6,90E-10	4,76E-07	8,46E-09	-1,05E+00	-1,36E+00	-1,00E-03	-5,01E+01	-1,23E-01	1,52E+01	-8,27E-10	-1,73E-09	2,26E-09	-1,47E-07	-3,62E-10	4,47E-08
9	3,10E-01	4,50E+01	-8,17E-06	-7,52E-06	2,69E-04	-5,94E+04	-5,33E+04	-1,68E+02	6,17E+02	-6,22E+03	-3,42E+02	-6,85E-05	-5,06E-05	1,06E-04	1,82E-08	-1,83E-05	-1,01E-06
10	3,10E-01	-4,50E+01	-2,73E-06	5,91E-07	5,29E-05	-1,03E+04	-1,02E+04	-2,47E+01	-4,03E+01	-1,10E+03	2,97E+01	-1,10E-05	-1,07E-05	1,92E-05	-1,19E-07	-3,22E-06	8,73E-08

Total Stresses (F XX:	-8,02E+04	YY:	-8,12E+04	ZZ:	-8,57E+01	YZ:	-8,17E+03	XZ:	3,61E+02	XY:	-7,65E+02
Total Strains XX:	-8,40E-05	YY:	-8,69E-05	ZZ:	1,52E-04	YZ:	-2,40E-05	XZ:	1,06E-06	XY:	-2,25E-06
Total Displacement UX:	6,44E-06	UY:	-1,84E-05	UZ:	4,16E-04						

Principal Value and Direction of Total Stresses and Strains

	Normal Stress (Pa)	Normal Strain	Shear Stress (Pa)	Shear Strain	X Comp.	Y Comp.	Z Comp.
Maximum:	7,32E+02	1,54E-04			0,0054	-0,0993	0,995
Minimum:	-7,99E+04	-8,33E-05			0,9422	-0,333	-0,0383
Minimum:	-8,22E+04	-9,00E-05			0,3351	0,9377	0,0918
Maximum:			4,15E+04	1,22E-04	-0,2332	-0,7333	0,8387
	-4,08E+04				0,2408	0,5928	0,7685
MiniMax:			4,03E+04	1,19E-04	-0,6624	0,1652	0,7307
	-3,96E+04				0,67	-0,3057	0,6765
Minimum:			1,15E+03	3,38E-06	0,4292	-0,8985	-0,092
	-8,11E+04				0,9032	0,4276	0,0378
Strain Energy (J)	7,09E+00						
Strain Energy of	6,56E+00						

Position Number	6	Layer Number:	2	X Coordinate (m):	0,00E+00	Y Coordinate (m):	3,50E-01	Z Coordinate (m):	2,50E-02
-----------------	---	---------------	---	-------------------	----------	-------------------	----------	-------------------	----------

Load No.	Distance to Load Axis (m)	Theta (°)	Radial Displacement (m)	Tangential Displacement (m)	Vertical Displacement (m)	Radial Stress (Pa)	Tangential Stress (Pa)	Vertical Stress (Pa)	Rad./Tang. Stress (Pa)	Rad./Vert. Stress (Pa)	Tang./Vert. Stress (Pa)	Radial Strain	Tangential Strain	Vertical Strain	Rad./Tang. Strain	Rad./Vert. Strain	Tang./Vert. Strain
1	3,04E-01	-1,63E+02	-5,38E-06	9,18E-07	2,99E-05	-1,83E+03	-4,84E+03	1,94E+01	-5,89E+01	-2,79E+02	4,67E+01	8,64E-07	-7,97E-06	6,31E-06	-1,73E-07	-8,21E-07	1,37E-07
2	2,80E-01	-1,80E+02	-2,46E-06	-4,14E-12	-8,15E-07	3,19E+03	8,16E+02	2,25E+01	-9,37E-04	3,02E+02	-3,34E-04	5,58E-06	-1,38E-06	-3,72E-06	-2,76E-12	8,88E-07	-9,81E-13
3	3,04E-01	-1,97E+02	-5,38E-06	-9,18E-07	2,99E-05	-1,83E+03	-4,84E+03	1,94E+01	5,89E+01	-2,79E+02	-4,67E+01	8,64E-07	-7,97E-06	6,31E-06	1,73E-07	-8,21E-07	-1,37E-07
4	4,20E-01	1,24E+01	4,85E-07	-8,05E-07	3,05E-05	-5,63E+03	-5,38E+03	-1,01E+01	6,54E+01	-5,42E+02	-1,92E+01	-8,20E-06	-5,46E-06	1,03E-05	1,92E-07	-1,59E-06	-5,84E-08
5	4,20E-01	-3,87E-05	1,94E-06	1,18E-12	1,01E-06	-1,53E+03	-8,11E+02	-3,18E+00	4,85E-05	-9,99E+01	3,92E-05	-2,49E-06	2,21E-07	2,01E-06	1,43E-13	-2,94E-07	1,15E-13
6	4,20E-01	-1,24E+01	2,90E-06	6,05E-07	1,49E-06	-2,28E+03	-9,12E+02	-4,71E+00	-6,54E+01	-1,48E+02	1,92E+01	-3,72E-06	3,33E-07	3,00E-06	-1,92E-07	-4,34E-07	5,84E-08
7	2,60E-01	-9,00E+01	-4,83E-10	5,35E-07	9,19E-09	-2,08E+00	-1,91E+00	-2,67E-03	-1,03E+01	-2,21E-01	3,73E+01	-2,37E-09	-1,86E-09	3,75E-09	-3,03E-08	-6,50E-10	1,10E-07
8	4,40E-01	-9,00E+01	-7,15E-10	4,62E-07	8,25E-09	-8,67E-01	-1,22E+00	-1,04E-03	-5,15E+01	-1,13E-01	1,27E+01	-5,67E-10	-1,62E-09	1,96E-09	-1,51E-07	-3,33E-10	3,73E-08
9	3,50E-01	4,50E+01	-1,06E-05	-7,25E-06	2,63E-04	-4,85E+04	-4,83E+04	-9,95E+01	6,82E+02	-5,06E+03	-2,84E+02	-5,16E-05	-5,09E-05	9,08E-05	2,01E-06	-1,49E-05	-8,35E-07
10	3,50E-01	-4,50E+01	-3,11E-06	5,71E-07	5,16E-05	-8,47E+03	-9,25E+03	-1,18E+01	-5,08E+01	-9,13E+02	2,29E+01	-8,24E-06	-1,05E-05	1,66E-05	-1,49E-07	-2,69E-06	6,72E-08

Total Stresses (F XX:	-7,29E+04	YY:	-6,74E+04	ZZ:	-6,81E+01	YZ:	-7,00E+03	XZ:	2,96E+02	XY:	-8,06E+02
Total Strains XX:	-8,23E-05	YY:	-6,62E-05	ZZ:	1,32E-04	YZ:	-2,06E-05	XZ:	8,69E-07	XY:	-2,37E-06
Total Displacement UX:	6,20E-06	UY:	-2,15E-05	UZ:	4,07E-04						

Principal Value and Direction of Total Stresses and Strains

	Normal Stress (Pa)	Normal Strain	Shear Stress (Pa)	Shear Strain	X Comp.	Y Comp.	Z Comp.
Maximum:	6,53E+02	1,34E-04			0,0051	-0,1023	0,9947
Minimum:	-6,80E+04	-6,80E-05			-0,1562	0,9825	0,1019
Minimum:	-7,30E+04	-8,27E-05			0,9877	0,1559	0,011
Maximum:			3,68E+04	1,08E-04	-0,6948	-0,1826	0,6956
	-3,62E+04				0,702	0,0379	0,7111
MiniMax:			3,43E+04	1,01E-04	0,1141	-0,7671	0,6313
	-3,37E+04				-0,1068	0,6223	0,7754
Minimum:			2,50E+03	7,35E-06	-0,8089	0,5845	0,0643
	-7,05E+04				0,588	0,8049	0,0798
Strain Energy (J)	5,37E+00						
Strain Energy of	4,98E+00						

Position Number	7	Layer Number:	2	X Coordinate (m):	0,00E+00	Y Coordinate (m):	5,00E-01	Z Coordinate (m):	2,50E-02
-----------------	---	---------------	---	-------------------	----------	-------------------	----------	-------------------	----------

Load No.	Distance to Load Axis (m)	Theta (°)	Radial Displacement (m)	Tangential Displacement (m)	Vertical Displacement (m)	Radial Stress (Pa)	Tangential Stress (Pa)	Vertical Stress (Pa)	Rad./Tang. Stress (Pa)	Rad./Vert. Stress (Pa)	Tang./Vert. Stress (Pa)	Radial Strain	Tangential Strain	Vertical Strain	Rad./Tang. Strain	Rad./Vert. Strain	Tang./Vert. Strain
1	4,49E-01	-1,68E+02	-5,30E-06	5,53E-07	2,70E-05	-8,60E+02	-3,30E+03	1,12E-01	-6,18E+01	-2,41E+02	1,37E+01	1,36E-06	-5,79E-06	3,91E-06	-1,82E-07	-7,07E-07	4,02E-08

2	4.30E-01	-1.80E+02	-1.92E-06	-3.66E-12	-9.95E-07	1.47E+03	5.04E+02	5.02E-01	-1.31E-04	9.23E+01	-1.14E-04	2.38E-06	-1.95E-07	-1.94E-06	-3.86E-13	2.71E-07	-3.35E-13
3	4.49E-01	-1.92E+02	-5.30E-06	-5.53E-07	2.70E-05	-8.60E+02	-3.30E+03	1.11E-01	6.18E+01	-2.41E+02	-1.37E+01	1.38E-06	-5.79E-06	3.91E-06	1.82E-07	-7.07E-07	-4.02E-08
4	5.87E-01	9.13E+00	-1.13E-07	-4.03E-07	2.79E-05	-2.99E+03	-3.72E+03	-2.80E+00	4.57E+01	-3.14E+02	-6.37E+00	-2.48E-06	-4.82E-06	6.30E-06	1.34E-07	-9.23E-07	-1.87E-08
5	5.70E-01	-3.87E-05	1.66E-06	1.06E-12	1.05E-06	-9.07E+02	-4.26E+02	2.42E+00	-8.21E-08	-4.87E+01	1.73E-05	-1.42E-06	-1.70E-09	1.26E-06	-2.41E-16	-1.43E-07	5.10E-14
6	5.67E-01	-9.13E+00	2.51E-06	4.03E-07	1.57E-06	-1.38E+03	-6.47E+02	9.40E-01	-4.57E+01	-7.46E+01	6.37E+00	-2.15E-06	7.53E-10	1.91E-06	-1.34E-07	-2.19E-07	1.87E-08
7	4.10E-01	-9.00E+01	-6.95E-10	4.72E-07	8.41E-09	-9.91E-01	-1.31E+00	-2.17E-03	-5.02E+01	-1.17E-01	1.55E+01	-7.45E-10	-1.70E-09	2.16E-09	-1.48E-07	-3.44E-10	4.56E-08
8	5.90E-01	-9.00E+01	-7.61E-10	4.16E-07	7.45E-09	-4.04E-01	-8.34E-01	4.39E-04	-4.69E+01	-6.72E-02	4.61E+00	-2.43E-11	-1.29E-09	1.17E-09	-1.38E-07	-1.98E-10	1.36E-08
9	5.00E-01	4.50E+01	-1.53E-05	-6.47E-06	2.40E-04	-2.41E+04	-3.31E+04	-4.03E+01	7.33E+02	-2.83E+03	-1.37E+02	-1.70E-05	-4.36E-05	5.37E-05	2.16E-06	-8.31E-06	-4.04E-07
10	5.00E-01	-4.50E+01	-3.85E-06	5.10E-07	4.70E-05	-4.16E+03	-6.32E+03	-9.51E+00	-5.83E+01	-5.28E+02	1.09E+01	-2.38E-06	-8.71E-06	9.83E-06	-1.71E-07	-1.55E-06	3.21E-08

Total Stresses (F XX:	-5.01E+04 YY:	-3.39E+04 ZZ:	-4.86E+01 YZ:	-4.17E+03 XZ:	1.44E+02 XY:	-8.06E+02
Total Strains XX:	-6.81E-05 YY:	-2.08E-05 ZZ:	7.89E-05 YZ:	-1.23E-05 XZ:	4.24E-07 XY:	-2.37E-06
Total Displacement UX:	5.48E-06 UY:	-2.75E-05 UZ:	3.71E-04			

Principal Value and Direction of Total Stresses and Strains

	Normal Stress (Pa)	Normal Strain	Shear Stress (Pa)	Shear Strain	X Comp.	Y Comp.	Z Comp.
Maximum:	4.58E+02	8.03E-05				0.0048	-0.1204
Minimum:	-3.44E+04	-2.22E-05				-0.05	0.0915
Maximum:	-5.01E+04	-6.83E-05				0.9987	0.0502
Minimum:			2.53E+04	7.43E-05		-0.7028	0.1205
Maximum:	-2.48E+04					0.7096	0.0013
Minimum:			1.74E+04	5.13E-05		-0.1207	0.701
Maximum:	-1.70E+04					0.7096	0.7029
Minimum:			7.84E+03	2.31E-05		-0.0497	0.6167
Maximum:	-4.23E+04					0.0387	0.7872
Minimum:						-0.032	0.6159
Maximum:						-0.7416	0.0843
Minimum:						0.6709	0.7366

Strain Energy (J)	2.11E+00
Strain Energy of	1.97E+00

Position Number	8	Layer Number:	2	X Coordinate (m):	0.00E+00	Y Coordinate (m):	7.50E-01	Z Coordinate (m):	2.50E-02								
Load No.	Distance to Load Axis (m)	Theta (°)	Radial Displacement (m)	Tangential Displacement (m)	Vertical Displacement (m)	Radial Stress (Pa)	Tangential Stress (Pa)	Vertical Stress (Pa)	Rad./Tang. Stress (Pa)	Rad./Vert. Stress (Pa)	Tang./Vert. Stress (Pa)	Radial Strain	Tangential Strain	Vertical Strain	Rad./Tang. Strain	Rad./Vert. Strain	Tang./Vert. Strain
1	6.96E-01	-1.73E+02	-4.89E-06	3.03E-07	2.25E-05	2.35E+02	-1.74E+03	-4.25E+00	-3.15E+01	-1.12E+02	2.99E+00	2.11E-06	-3.69E-06	1.40E-06	-9.27E-08	-3.29E-07	8.80E-09
2	6.80E-01	-1.80E+02	-1.53E-06	-3.09E-12	-1.01E-06	6.60E+02	3.23E+02	-2.60E+00	1.92E-05	3.44E+01	-3.49E-05	1.02E-06	2.73E-08	-9.29E-07	5.66E-14	1.01E-07	-1.03E-13
3	6.96E-01	-1.87E+02	-4.89E-06	-3.03E-07	2.25E-05	2.35E+02	-1.74E+03	-4.25E+00	3.15E+01	-1.12E+02	2.99E+00	2.11E-06	-3.69E-06	1.40E-06	9.27E-08	-3.29E-07	-8.80E-09
4	8.15E-01	6.34E+00	-3.42E-07	-2.42E-07	2.34E-05	-9.10E+02	-1.98E+03	-5.71E+00	2.30E+01	-1.46E+02	-1.58E+00	4.17E-08	-3.09E-06	2.70E-06	6.78E-08	-4.30E-07	-4.66E-09
5	8.20E-01	-3.67E-05	1.41E-06	9.16E-13	9.70E-07	-4.61E+02	-2.29E+02	-1.20E+00	-4.91E-06	-2.41E+01	6.39E-06	-7.05E-07	-2.34E-08	6.46E-07	-1.44E-14	-7.09E-08	1.88E-14
6	8.15E-01	-6.34E+00	2.15E-06	2.42E-07	1.47E-06	-7.07E+02	-3.53E+02	-6.47E+00	-2.30E+01	-3.44E+01	1.58E+00	-1.08E-06	-3.58E-08	9.83E-07	-6.78E-08	-1.01E-07	4.66E-09
7	6.60E-01	-9.00E+01	-7.50E-10	3.98E-07	7.08E-09	-2.67E-01	-6.94E-01	-2.05E-03	-4.31E+01	-5.48E-02	4.68E+00	1.21E-10	-1.14E-09	8.99E-10	-1.27E-07	-1.61E-10	1.38E-08
8	8.40E-01	-9.00E+01	-7.02E-10	3.59E-07	6.20E-09	-3.54E-02	-4.36E-01	-2.30E-03	-3.36E+01	-2.99E-02	1.27E+00	3.41E-10	-8.36E-10	4.38E-10	-9.89E-08	-8.79E-11	3.73E-09
9	7.50E-01	4.50E+01	-1.64E-05	-5.52E-06	2.02E-04	-6.14E+03	-1.75E+04	-8.75E+00	5.51E+02	-1.28E+03	-4.43E+01	4.18E-06	-2.92E-05	2.22E-05	1.62E-06	-3.76E-06	-1.30E-07
10	7.50E-01	-4.50E+01	-3.90E-06	4.35E-07	3.94E-05	-9.35E+02	-3.33E+03	-2.63E+00	-4.34E+01	-2.34E+02	3.43E+00	1.26E-06	-5.78E-06	4.00E-06	-1.28E-07	-6.87E-07	1.01E-08

Total Stresses (F XX:	-2.65E+04 YY:	-8.09E+03 ZZ:	-3.59E+01 YZ:	-1.90E+03 XZ:	4.72E+01 XY:	-5.87E+02
Total Strains XX:	-4.53E-05 YY:	8.73E-06 ZZ:	3.24E-05 YZ:	-5.60E-06 XZ:	1.39E-07 XY:	-1.73E-06
Total Displacement UX:	4.60E-06 UY:	-2.84E-05 UZ:	3.11E-04			

Principal Value and Direction of Total Stresses and Strains

	Normal Stress (Pa)	Normal Strain	Shear Stress (Pa)	Shear Strain	X Comp.	Y Comp.	Z Comp.
Maximum:	3.93E+02	3.37E-05				0.0085	-0.2184
Minimum:	-8.50E+03	7.53E-06				-0.0313	0.9751
Maximum:	-2.65E+04	-4.54E-05				0.9995	0.0319
Minimum:			1.34E+04	3.95E-05		-0.7021	0.0005
Maximum:	-1.31E+04					0.7113	0.6895
Minimum:			8.99E+03	2.64E-05		-0.1326	0.6902
Maximum:	-1.75E+04					-0.7289	0.1548
Minimum:			4.45E+03	1.31E-05		0.6846	0.1556
Maximum:	-4.05E+03					0.0267	0.5347
Minimum:						-0.0175	0.5344

Strain Energy (J)	5.75E-01
Strain Energy of	5.51E-01

Minimum: -1,65E+03 1,66E+03 4,88E-06 -0,7079 0,0028 0,7063
0,708 0,0293 0,7076

Strain Energy (J) 8,22E-02
Strain Energy of 8,19E-02

System: 4: sys34

Layer Number	Thickness (m)	Young's Modulus (Pa)	Poisson's Ratio	Shear Spring Compliance (m ² /N)	Load Number	Normal Stress (Pa)	Shear Stress (Pa)	Radius of Loaded Area (m)	Load Position X (m)	Load Position Y (m)	Shear Direction (°)
1	0,013	3,00E+08	0,5	0,00E+00	1	4,00E+05	2,00E+05	5,26E-02	9,00E-02	6,00E-02	2,70E+02
2	0,013	5,00E+08	0,47	0,00E+00	2	1,75E+02	2,00E+05	4,26E-02	0,00E+00	7,00E-02	2,70E+02
3	0,015	8,00E+08	0,46	0,00E+00	3	4,00E+05	2,00E+05	5,26E-02	-9,00E-02	6,00E-02	2,70E+02
4	0,03	1,20E+09	0,45	0,00E+00	4	4,00E+05	2,00E+05	5,26E-02	9,00E-02	-6,00E-02	9,00E+01
5	0,03	1,52E+09	0,45	0,00E+00	5	1,75E+02	2,00E+05	4,26E-02	0,00E+00	-7,00E-02	9,00E+01
6	0,06	3,07E+09	0,45	0,00E+00	6	1,15E+02	2,00E+05	5,26E-02	-9,00E-02	-6,00E-02	9,00E+01
7	0,07	3,70E+09	0,44	0,00E+00	7	6,23E+02	1,80E+05	2,26E-02	0,00E+00	9,00E-02	1,80E+02
8	0,07	3,60E+09	0,43	0,00E+00	8	6,23E+02	1,80E+05	2,26E-02	0,00E+00	-9,00E-02	1,80E+02
9	0,25	1,00E+08	0,35	0,00E+00	9	7,50E+05	1,50E+05	1,13E-01	0,00E+00	0,00E+00	4,50E+01
10		5,00E+07	0,5		10	7,50E+05	6,00E+04	5,00E-02	0,00E+00	0,00E+00	1,35E+02

Position Number 1 Layer Number: 3 X Coordinate (m): 0,00E+00 Y Coordinate (m): 0,00E+00 Z Coordinate (m): 4,00E-02

Load No.	Distance to Load Axis (m)	Theta (°)	Radial Displacement (m)	Tangential Displacement (m)	Vertical Displacement (m)	Radial Stress (Pa)	Tangential Stress (Pa)	Vertical Stress (Pa)	Rad./Tang. Stress (Pa)	Rad./Vert. Stress (Pa)	Tang./Vert. Stress (Pa)	Radial Strain	Tangential Strain	Vertical Strain	Rad./Tang. Strain	Rad./Vert. Strain	Tang./Vert. Strain
1	1,08E-01	-4,16E+02	5,20E-06	3,78E-06	3,60E-05	-6,58E+04	-1,70E+04	-1,43E+04	-9,51E+02	-2,92E+04	-4,60E+02	-6,42E-05	2,48E-05	2,98E-05	-1,74E-06	-5,33E-05	-8,40E-07
2	7,00E-02	-3,60E+02	6,06E-06	8,28E-12	1,24E-06	-4,77E+04	-1,04E+04	-2,69E+04	3,40E-02	-3,76E+04	3,22E-02	-3,81E-05	2,98E-05	-1,94E-07	6,21E-11	-6,88E-05	5,87E-11
3	1,08E-01	-3,04E+02	5,20E-06	-3,78E-06	3,60E-05	-6,58E+04	-1,70E+04	-1,43E+04	9,51E+02	-2,92E+04	4,60E+02	-6,42E-05	2,48E-05	2,98E-05	1,74E-06	-5,33E-05	8,40E-07
4	1,08E-01	5,63E+01	5,20E-06	-3,78E-06	3,60E-05	-6,58E+04	-1,70E+04	-1,43E+04	9,51E+02	-2,92E+04	4,60E+02	-6,42E-05	2,48E-05	2,98E-05	1,74E-06	-5,33E-05	8,40E-07
5	7,00E-02	-3,67E-05	6,06E-06	2,54E-12	1,24E-06	-4,77E+04	-1,04E+04	-2,69E+04	1,05E-02	-3,76E+04	9,88E-03	-3,81E-05	2,98E-05	-1,94E-07	1,91E-11	-6,86E-05	1,80E-11
6	1,08E-01	-5,63E+01	3,94E-06	3,78E-06	6,64E-07	-2,43E+04	-3,57E+03	-6,31E+03	-9,51E+02	-1,28E+04	-4,60E+02	-2,47E-05	1,31E-05	8,13E-06	-1,74E-06	-2,33E-05	-8,40E-07
7	9,00E-02	-2,70E+02	5,95E-10	-7,97E-07	1,04E-08	-1,57E+01	-3,47E+00	-3,34E+00	-1,83E+02	-6,79E+00	-1,14E+02	-1,57E-08	6,60E-09	6,84E-09	-3,34E-07	-1,24E-08	-2,07E-07
8	9,00E-02	-9,00E+01	5,92E-10	7,97E-07	1,04E-08	-1,57E+01	-3,48E+00	-3,34E+00	1,83E+02	-6,79E+00	1,14E+02	-1,57E-08	6,58E-09	6,84E-09	3,34E-07	-1,24E-08	2,07E-07
9	0,00E+00	-4,50E+01	1,85E-05	1,85E-05	3,33E-04	-4,99E+05	-4,99E+05	-7,23E+05	0,00E+00	-7,45E+04	-7,45E+04	7,87E-05	7,87E-05	-3,30E-04	0,00E+00	-1,36E-04	-1,36E-04
10	0,00E+00	-1,35E+02	-2,05E-06	2,05E-06	8,01E-05	-2,31E+05	-2,31E+05	-5,88E+05	0,00E+00	1,29E+04	-1,29E+04	1,82E-04	1,82E-04	-4,69E-04	0,00E+00	2,35E-05	-2,35E-05

Total Stresses (F XX: -9,18E+05 YY: -9,35E+05 ZZ: -1,41E+06 YZ: -7,83E+04 XZ: -4,82E+04 XY: 1,29E+04
Total Strains XX: 2,03E-04 YY: 1,72E-04 ZZ: -7,01E-04 YZ: -1,43E-04 XZ: -8,79E-05 XY: 2,36E-05
Total Displacem UX: 1,38E-05 UY: 1,99E-05 UZ: 5,25E-04

Principal Value and Direction of Total Stresses and Strains

	Normal Stress (Pa)	Normal Strain	Shear Stress (Pa)	Shear Strain	X Comp.	Y Comp.	Z Comp.
Maximum:	-8,98E+05	2,40E-04			0,7759	0,6089	-0,1648
Minimax:	-9,39E+05	1,65E-04			-0,6245	0,7783	-0,065
Minimum:	-1,43E+06	-7,32E-04			0,0887	0,1534	0,9842
Maximum:			2,68E+05	4,86E-04	0,486	0,3221	-0,8125
	-1,16E+06				0,6114	0,539	0,5794
MiniMax:			2,46E+05	4,48E-04	-0,5043	0,4419	-0,7419
	-1,19E+06				-0,3789	0,6588	0,65
Minimum:			2,08E+04	3,79E-05	0,9903	-0,1198	-0,0706
	-9,18E+05				0,1071	0,9809	-0,1625

Strain Energy (J) 3,38E+02
Strain Energy of 1,60E+02

Position Number 2 Layer Number: 3 X Coordinate (m): 0,00E+00 Y Coordinate (m): 5,00E-02 Z Coordinate (m): 4,00E-02

Load No.	Distance to Load Axis (m)	Theta (°)	Radial Displacement (m)	Tangential Displacement (m)	Vertical Displacement (m)	Radial Stress (Pa)	Tangential Stress (Pa)	Vertical Stress (Pa)	Rad./Tang. Stress (Pa)	Rad./Vert. Stress (Pa)	Tang./Vert. Stress (Pa)	Radial Strain	Tangential Strain	Vertical Strain	Rad./Tang. Strain	Rad./Vert. Strain	Tang./Vert. Strain
1	9,06E-02	-4,44E+02	2,92E-06	5,13E-06	3,65E-05	-8,23E+04	-1,79E+04	-2,18E+04	-3,41E+03	-3,53E+04	-2,87E+03	-5,50E-05	2,60E-05	1,89E-05	-6,22E-06	-6,44E-05	-5,23E-06
2	2,00E-02	-3,60E+02	7,19E-06	1,42E-11	9,77E-07	-2,84E+04	-1,35E+04	-3,23E+04	2,05E-02	-4,52E+04	9,07E-02	-9,16E-06	1,80E-05	-1,63E-05	3,75E-11	-8,25E-05	1,66E-10
3	9,06E-02	-2,76E+02	2,92E-06	-5,13E-06	3,65E-05	-8,23E+04	-1,79E+04	-2,18E+04	3,41E+03	-3,53E+04	2,87E+03	-5,50E-05	2,60E-05	1,89E-05	6,22E-06	-6,44E-05	5,23E-06
4	1,42E-01	3,93E+01	4,71E-06	-2,46E-06	3,51E-05	-4,74E+04	-1,44E+04	-4,66E+03	-1,40E+02	-1,38E+04	-3,02E+02	-4,83E-05	1,19E-05	2,97E-05	-2,55E-07	-2,51E-05	-5,51E-07

5	1,20E-01	-3,87E-05	4,34E-06	1,78E-12	7,06E-07	-2,46E+04	-2,71E+03	-4,52E+03	4,68E-03	-1,07E+04	2,33E-03	-2,66E-05	1,34E-05	1,00E-05	8,54E-12	-1,95E-05	4,24E-12
6	1,42E-01	-3,93E+01	4,52E-06	2,46E-06	7,92E-07	-2,12E+04	-2,80E+03	-2,86E+03	1,40E+02	-7,81E+03	3,02E+02	-2,34E-05	1,06E-05	1,01E-05	2,55E-07	-1,39E-05	5,51E-07
7	4,00E-02	-2,70E+02	1,72E-09	-1,38E-06	1,26E-08	-4,81E+01	-1,44E+01	-5,77E+01	1,27E+03	-5,22E+01	2,48E+03	-1,87E-08	4,29E-08	-3,61E-08	2,32E-06	-9,52E-08	4,53E-06
8	1,40E-01	-9,00E+01	5,70E-11	6,34E-07	9,87E-09	-7,49E+00	-3,29E+00	-3,88E-01	1,83E+02	-1,59E+00	1,33E+02	-7,24E-09	4,13E-10	5,71E-09	3,33E-07	-2,90E-09	2,43E-07
9	5,00E-02	4,50E+01	2,19E-05	-1,75E-05	3,31E-04	-5,04E+05	-4,88E+05	-7,13E+05	1,02E+04	-1,19E+05	6,84E+04	6,08E-05	8,91E-05	-3,20E-04	1,87E-05	-2,17E-04	1,25E-04
10	5,00E-02	-4,50E+01	8,28E-06	1,50E-06	7,10E-05	-1,91E+05	-1,14E+05	-2,92E+05	-2,54E+03	-1,79E+05	-5,22E+03	-4,80E-06	1,36E-04	-1,90E-04	-4,63E-06	-3,27E-04	-9,53E-06

Total Stresses (F XX:	-7,78E+05	YY:	-8,33E+05	ZZ:	-1,09E+06	YZ:	-2,66E+05	XZ:	-5,69E+04	XY:	-2,13E+03
Total Strains XX:	1,35E-04	YY:	3,40E-05	ZZ:	-4,39E-04	YZ:	-4,86E-04	XZ:	-1,04E-04	XY:	-3,88E-06
Total Displacement UX:	1,38E-05	UY:	2,68E-05	UZ:	5,13E-04						

Principal Value and Direction of Total Stresses and Strains

	Normal Stress (Pa)	Normal Strain	Shear Stress (Pa)	Shear Strain	X Comp.	Y Comp.	Z Comp.	
Maximum:	-6,60E+05	3,50E-04				0,2416	0,8122	-0,531
Minimax:	-7,80E+05	1,31E-04				0,9651	-0,2583	0,044
Minimum:	-1,26E+06	-7,52E-04				0,1014	0,5231	0,8462
Maximum:			3,02E+05	5,51E-04		0,0991	0,2044	-0,9739
	-9,62E+05					0,2425	0,9442	0,2228
MiniMax:			2,42E+05	4,42E-04		0,8107	-0,5525	-0,5672
	-1,02E+06					0,7541	0,1873	0,6295
Minimum:			6,00E+04	1,10E-04		-0,5116	0,7569	-0,4066
	-7,20E+05					0,8532	0,3917	-0,3444
Strain Energy (J)	3,09E+02							
Strain Energy of	1,87E+02							

Position Number 3 Layer Number: 3 X Coordinate (m): 0,00E+00 Y Coordinate (m): 1,10E-01 Z Coordinate (m): 4,00E-02

Load No.	Distance to Load Axis (m)	Theta (°)	Radial Displacement (m)	Tangential Displacement (m)	Vertical Displacement (m)	Radial Stress (Pa)	Tangential Stress (Pa)	Vertical Stress (Pa)	Rad./Tang. Stress (Pa)	Rad./Vert. Stress (Pa)	Tang./Vert. Stress (Pa)	Radial Strain	Tangential Strain	Vertical Strain	Rad./Tang. Strain	Rad./Vert. Strain	Tang./Vert. Strain
1	1,03E-01	-1,19E+02	-2,09E-06	4,10E-06	3,50E-05	-2,24E+04	-1,05E+04	-3,60E+03	-1,44E+03	-7,02E+03	-8,80E+02	-1,99E-05	1,83E-06	1,44E-05	-2,64E-06	-1,28E-05	-1,61E-06
2	4,00E-02	-1,80E+02	-6,93E-06	-1,13E-11	-1,50E-06	4,60E+04	1,94E+04	5,04E+04	-3,42E-02	4,75E+04	-6,77E-02	1,74E-05	-3,12E-05	2,54E-05	-6,24E-11	8,68E-05	-1,24E-10
3	1,03E-01	-2,41E+02	-2,09E-06	-4,10E-06	3,50E-05	-2,24E+04	-1,05E+04	-3,60E+03	1,44E+03	-7,02E+03	8,80E+02	-1,99E-05	1,83E-06	1,44E-05	2,64E-06	-1,28E-05	1,61E-06
4	1,92E-01	2,79E+01	3,39E-06	-1,82E-06	3,43E-05	-2,96E+04	-1,27E+04	-9,94E+02	-8,28E+01	-5,69E+03	-2,50E+02	-2,92E-05	1,74E-06	2,31E-05	-1,51E-07	-1,04E-05	-4,57E-07
5	1,80E-01	-3,87E-05	3,22E-06	1,48E-12	6,97E-07	-1,12E+04	-1,44E+03	-7,28E+02	1,78E-03	-2,71E+03	6,95E-04	-1,28E-05	5,07E-06	6,38E-06	3,25E-12	-4,95E-06	1,27E-12
6	1,92E-01	-2,79E+01	4,14E-06	1,82E-06	9,68E-07	-1,33E+04	-1,93E+03	-7,49E+02	8,28E+01	-2,99E+03	2,50E+02	-1,51E-05	5,65E-06	7,81E-06	1,51E-07	-5,45E-06	4,57E-07
7	2,00E-02	-9,00E+01	1,56E-09	1,78E-06	1,49E-08	-5,92E+01	-4,07E+01	-1,85E+02	-1,74E+03	-6,48E+01	-6,93E+03	4,43E-08	7,80E-08	-1,49E-07	-3,17E-06	-1,18E-07	-1,28E-05
8	2,00E-01	-9,00E+01	-2,54E-10	5,64E-07	9,54E-09	-4,40E+00	-3,06E+00	-3,88E-02	5,01E+01	-6,85E-01	9,47E+01	-3,72E-09	-1,27E-09	4,23E-09	9,14E-08	-1,25E-09	1,73E-07
9	1,10E-01	4,50E+01	2,32E-05	-1,31E-05	3,13E-04	-4,10E+05	-3,01E+05	-4,05E+05	1,87E+04	-2,64E+05	2,90E+04	-1,06E-04	9,18E-05	-9,69E-05	3,42E-05	-4,82E-04	5,30E-05
10	1,10E-01	-4,50E+01	3,35E-06	8,56E-07	6,00E-05	-7,62E+04	-2,32E+04	-1,37E+04	-1,35E+02	-2,95E+04	-4,84E+01	-7,40E-05	2,27E-05	4,00E-05	-2,46E-07	-5,39E-05	-8,46E-08

Total Stresses (F XX:	-3,69E+05	YY:	-5,12E+05	ZZ:	-3,78E+05	YZ:	-2,81E+05	XZ:	-2,09E+04	XY:	-1,46E+04
Total Strains XX:	5,01E-05	YY:	-2,10E-04	ZZ:	3,45E-05	YZ:	-4,77E-04	XZ:	-3,81E-05	XY:	-2,67E-05
Total Displacement UX:	1,03E-05	UY:	2,18E-05	UZ:	4,78E-04						

Principal Value and Direction of Total Stresses and Strains

	Normal Stress (Pa)	Normal Strain	Shear Stress (Pa)	Shear Strain	X Comp.	Y Comp.	Z Comp.	
Maximum:	-1,75E+05	4,05E-04				-0,0389	-0,6111	0,7806
Minimax:	-3,68E+05	5,27E-05				0,9968	-0,0791	-0,0121
Minimum:	-7,16E+05	-5,84E-04				0,0699	0,7876	0,6122
Maximum:			2,71E+05	4,94E-04		-0,077	-0,989	0,1262
	-4,45E+05					0,0219	0,1248	0,9919
MiniMax:			1,74E+05	3,18E-04		0,6554	-0,6129	-0,4414
	-5,42E+05					0,7543	0,501	0,4244
Minimum:			9,65E+04	1,76E-04		-0,7324	-0,3761	0,5676
	-2,71E+05					0,6773	-0,4881	0,5505
Strain Energy (J)	1,64E+02							
Strain Energy of	1,38E+02							

Position Number 4 Layer Number: 3 X Coordinate (m): 0,00E+00 Y Coordinate (m): 2,10E-01 Z Coordinate (m): 4,00E-02

Load No.	Distance to Load Axis (m)	Theta (°)	Radial Displacement (m)	Tangential Displacement (m)	Vertical Displacement (m)	Radial Stress (Pa)	Tangential Stress (Pa)	Vertical Stress (Pa)	Rad./Tang. Stress (Pa)	Rad./Vert. Stress (Pa)	Tang./Vert. Stress (Pa)	Radial Strain	Tangential Strain	Vertical Strain	Rad./Tang. Strain	Rad./Vert. Strain	Tang./Vert. Strain
1	1,75E-01	-1,49E+02	-4,79E-06	1,84E-06	3,27E-05	-3,22E+03	-9,04E+03	7,07E+02	1,40E+02	7,16E+02	2,85E+02	7,72E-07	-9,86E-06	7,93E-06	2,55E-07	1,31E-06	5,20E-07
2	1,40E-01	-1,80E+02	-3,88E-06	-5,07E-12	-6,46E-07	1,85E+04	1,99E+03	2,37E+03	-1,04E-02	6,48E+03	-4,55E-03	2,06E-05	-9,53E-06	-8,82E-06	-1,90E-11	1,18E-05	-8,30E-12
3	1,75E-01	-2,11E+02	-4,79E-06	-1,84E-06	3,27E-05	-3,22E+03	-9,04E+03	7,07E+02	-1,40E+02	7,16E+02	-2,85E+02	7,72E-07	-9,86E-06	7,93E-06	-2,55E-07	1,31E-06	-5,20E-07
4	2,85E-01	1,84E+01	1,81E-06	-9,80E-07	3,29E-05	-1,58E+04	-1,05E+04	-1,22E+02	8,65E+01	-2,25E+03	-1,09E+02	-1,37E-05	-3,96E-06	1,50E-05	1,58E-07	-4,11E-06	-2,00E-07
5	2,80E-01	-3,67E-05	2,41E-06	1,31E-12	8,85E-07	-4,66E+03	-1,12E+03	-6,66E+01	4,63E-04	-8,06E+02	2,14E-04	-5,14E-06	1,32E-06	3,24E-06	8,45E-13	-1,11E-06	3,91E-13
6	2,85E-01	-1,84E+01	3,45E-06	9,80E-07	1,28E-06	-6,55E+03	-1,61E+03	-9,15E+01	-8,65E+01	-8,42E+02	1,09E+02	-7,21E-06	1,80E-06	4,58E-06	-1,58E-07	-1,54E-06	2,00E-07
7	1,20E-01	-9,00E+01	2,23E-10	6,78E-07	1,00E-08	-9,61E+00	-3,34E+00	-8,92E-01	2,26E+02	-2,57E+00	1,45E+02	-9,58E-09	1,87E-09	6,33E-09	4,12E-07	-4,69E-09	2,65E-07
8	3,00E-01	-9,00E+01	-5,02E-10	5,07E-07	9,03E-09	-2,45E+00	-2,47E+00	-3,92E-03	-5,00E+01	-3,69E-01	5,41E+01	-1,64E-09	-1,67E-09	2,82E-09	-9,12E-08	-6,74E-10	9,87E-08
9	2,10E-01	4,50E+01	3,17E-06	-8,43E-06	2,85E-04	-1,62E+05	-9,76E+04	-6,25E+03	1,54E+03	-3,18E+04	-5,99E+02	-1,43E-04	-2,51E-05	1,42E-04	2,82E-06	-5,79E-05	-1,09E-06
10	2,10E-01	-4,50E+01	-8,24E-07	6,45E-07	5,61E-05	-2,68E+04	-1,81E+04	-3,20E+02	1,75E+01	-4,31E+03	9,67E+01	-2,29E-05	-6,99E-06	2,54E-05	3,19E-08	-7,88E-06	1,77E-07

Total Stresses (F XX: -1,43E+05 YY: -2,07E+05 ZZ: -3,07E+03 YZ: -3,21E+04 XZ: 7,48E+02 XY: -1,62E+03
Total Strains XX: -5,77E-05 YY: -1,74E-04 ZZ: 1,97E-04 YZ: -5,86E-05 XZ: 1,37E-06 XY: -2,96E-06
Total Displacement UX: 7,11E-06 UY: -3,61E-06 UZ: 4,41E-04

Principal Value and Direction of Total Stresses and Strains

	Normal Stress (Pa)	Normal Strain	Shear Stress (Pa)	Shear Strain	X Comp.	Y Comp.	Z Comp.
Maximum:	1,89E+03	2,06E-04			0,0068	-0,1524	0,9883
Minimax:	-1,43E+05	-5,77E-05			0,9997	-0,0203	-0,01
Minimum:	-2,11E+05	-1,83E-04			0,0216	0,9881	0,1522
Maximum:			1,07E+05	1,95E-04	-0,0105	-0,8065	0,5912
	-1,05E+05				0,0201	0,5909	0,8065
MiniMax:			7,22E+04	1,32E-04	-0,7021	-0,0934	0,7059
	-7,03E+04				0,7118	-0,1221	0,6917
Minimum:			3,45E+04	6,29E-05	0,6916	-0,7131	-0,1147
	-1,77E+05				0,7222	0,6843	0,1005

Strain Energy (J) 2,37E+01
Strain Energy of 2,16E+01

Position Number 5 Layer Number: 3 X Coordinate (m): 0,00E+00 Y Coordinate (m): 3,10E-01 Z Coordinate (m): 4,00E-02

Load No.	Distance to Load Axis (m)	Theta (°)	Radial Displacement (m)	Tangential Displacement (m)	Vertical Displacement (m)	Radial Stress (Pa)	Tangential Stress (Pa)	Vertical Stress (Pa)	Rad./Tang. Stress (Pa)	Rad./Vert. Stress (Pa)	Tang./Vert. Stress (Pa)	Radial Strain	Tangential Strain	Vertical Strain	Rad./Tang. Strain	Rad./Vert. Strain	Tang./Vert. Strain
1	2,66E-01	-1,60E+02	-5,08E-06	1,07E-06	3,08E-05	-2,85E+03	-7,62E+03	9,91E+01	-7,00E+01	-5,09E+02	1,30E+02	7,60E-07	-7,94E-06	6,14E-06	-1,28E-07	-9,28E-07	2,37E-07
2	2,40E-01	-1,80E+02	-2,65E-06	-4,24E-12	-7,95E-07	6,27E+03	1,20E+03	1,57E+02	-2,40E-03	9,99E+02	-9,90E-04	7,06E-06	-2,19E-06	-4,10E-06	-4,37E-12	1,82E-06	-1,81E-12
3	2,66E-01	-2,00E+02	-5,08E-06	-1,07E-06	3,08E-05	-2,85E+03	-7,62E+03	9,91E+01	7,00E+01	-5,09E+02	-1,30E+02	7,60E-07	-7,94E-06	6,14E-06	1,28E-07	-9,28E-07	-2,37E-07
4	3,81E-01	1,37E+01	9,19E-07	-6,75E-07	3,14E-05	-9,74E+03	-8,40E+03	-3,70E+01	1,04E+02	-1,30E+03	-4,79E+01	-7,32E-06	-4,88E-06	1,04E-05	1,90E-07	-2,38E-06	-8,75E-08
5	3,80E-01	-3,67E-05	2,03E-06	1,20E-12	1,01E-06	-2,69E+03	-9,20E+02	-1,04E+01	1,43E-04	-2,50E+02	1,00E-04	-2,83E-06	4,05E-07	2,07E-06	2,60E-13	-4,56E-07	1,83E-13
6	3,81E-01	-1,37E+01	3,00E-06	6,75E-07	1,48E-06	-3,98E+03	-1,36E+03	-1,76E+01	-1,04E+02	-3,71E+02	4,79E+01	-4,18E-06	5,97E-07	3,05E-06	-1,90E-07	-6,77E-07	8,75E-08
7	2,20E-01	-9,00E+01	-3,22E-10	5,48E-07	9,44E-09	-3,83E+00	-2,94E+00	-2,15E-02	1,80E+01	-5,93E-01	8,45E+01	-3,08E-09	-1,46E-09	3,87E-09	3,47E-08	-1,08E-09	1,54E-07
8	4,00E-01	-9,00E+01	-6,17E-10	4,68E-07	8,49E-09	-1,51E+00	-1,93E+00	-5,66E-03	-7,48E+01	-2,49E-01	3,06E+01	-7,73E-10	-1,54E-09	1,97E-09	-1,36E-07	-4,54E-10	5,58E-08
9	3,10E-01	4,50E+01	-6,49E-06	-7,39E-06	2,71E-04	-8,60E+04	-7,56E+04	-4,67E+02	9,91E+02	-1,27E+04	-6,76E+02	-6,38E-05	-4,48E-05	9,23E-05	1,81E-06	-2,32E-05	-1,23E-06
10	3,10E-01	-4,50E+01	-2,36E-06	5,80E-07	5,31E-05	-1,49E+04	-1,45E+04	-4,96E+01	-6,47E+01	-2,24E+03	5,80E+01	-1,03E-05	-9,50E-06	1,88E-05	-1,18E-07	-4,09E-06	1,06E-07

Total Stresses (F XX: -1,14E+05 YY: -1,18E+05 ZZ: -2,27E+02 YZ: -1,69E+04 XZ: 7,23E+02 XY: -1,16E+03
Total Strains XX: -7,46E-05 YY: -8,14E-05 ZZ: 1,33E-04 YZ: -3,08E-05 XZ: 1,32E-06 XY: -2,12E-06
Total Displacement UX: 6,28E-06 UY: -1,56E-05 UZ: 4,18E-04

Principal Value and Direction of Total Stresses and Strains

	Normal Stress (Pa)	Normal Strain	Shear Stress (Pa)	Shear Strain	X Comp.	Y Comp.	Z Comp.
Maximum:	2,15E+03	1,37E-04			0,0076	-0,1394	0,9902
Minimax:	-1,14E+05	-7,43E-05			0,9862	-0,1626	-0,0304
Minimum:	-1,20E+05	-8,61E-05			0,1652	0,9768	0,1362
Maximum:			6,12E+04	1,12E-04	-0,1115	-0,7893	0,6039
	-5,90E+04				0,1222	0,5921	0,7965
MiniMax:			5,80E+04	1,06E-04	-0,692	0,0164	0,7217
	-5,58E+04				0,7027	-0,2135	0,6787
Minimum:			3,23E+03	5,89E-06	0,5805	-0,8057	-0,1178
	-1,17E+05				0,8142	0,5757	0,0748